

VACSIM™: A SELF-ASSEMBLING IMMUNE MATRIX THAT ENHANCES
VACCINE EFFICACY

by

EMILY-JOY FARAH SAMLI

(Under the Direction of Donald A. Harn)

ABSTRACT

Influenza is a global public health issue that results in considerable economic burden. Seasonal epidemics of this acute viral infection spread rapidly with unpredictable morbidity. The very young, the elderly and immune compromised are typically considered “high-risk” for developing severe symptoms and potentially life-threatening complications from influenza infection. Regular vaccination remains the most effective prevention, and as such, there is tremendous need for new technologies focused on improving immunogenicity and efficacy of seasonal flu vaccines that are safe for use in high-risk populations.

Vaccine Self-assembling Immune Matrix (VacSIM™) is a patent-pending delivery platform able to enhance immunogenicity and efficacy in a variety of different vaccine systems. VacSIM™ technology utilizes a synthetic hydrogel composed of a self-assembling peptide (SAP) in an aqueous solution. It is inert, biodegradable and self-assembles *in situ*. Traditional hydrogels rely on cross-linkers for self-assembly and require *ex vivo* polymerization prior to vaccine administration. VacSIM™ is a liquid *ex vivo*, providing flexibility to incorporate different vaccine components through simple

mixing. Post-injection, VacSIM™ undergoes self-assembly *in situ* encapsulating vaccine components through the formation of a temporary vaccine depot. VacSIM™ delivery was observed to enhance vaccine-specific immune responses in a murine influenza model system. Specifically, mice immunized with inactivated A/Puerto Rico/08/34 (PR8) and CpG via VacSIM™ delivery had increased vaccine-specific antibody and T cell responses, greater protection from lethal, homologous challenge and improved ability to clear virus from their lungs. Studies involving other candidate vaccine antigens suggest VacSIM™ is capable of enhancing the immunogenicity and efficacy of a wide variety of vaccines. In addition, this vaccine delivery platform provides the flexibility to rapidly incorporate various types of antigens, adjuvants or organisms for vaccine delivery and therefore VacSIM™ has potential as a true “Plug and Play” vaccine platform technology.

INDEX WORDS: Vaccine, influenza, immunize, VacSIM™, delivery

VACSIM™: A SELF-ASSEMBLING IMMUNE MATRIX THAT ENHANCES
VACCINE EFFICACY

by

EMILY-JOY FARAH SAMLI
B.S., Arizona State University, 2009

A Dissertation Submitted to the Graduate Faculty of The University of Georgia in Partial
Fulfillment of the Requirements for the Degree

DOCTOR OF PHILOSOPHY

ATHENS, GEORGIA

2015

© 2015

Emily-Joy Farah Samli

All Rights Reserved

VACSIM™: A SELF-ASSEMBLING IMMUNE MATRIX THAT ENHANCES
VACCINE EFFICACY

by

EMILY-JOY FARAH SAMLI

Major Professor:	Donald A. Harn
Committee:	Donald L. Evans
	Robert J. Hogan
	Kimberly D. Klonowski
	Wendy T. Watford

Electronic Version Approved:

Julie Coffield
Interim Dean of the Graduate School
The University of Georgia
May 2015

DEDICATION

For Kausar N. Samli

--My best friend and the love of my life.

ACKNOWLEDGEMENTS

I would like to acknowledge and express my gratitude to family, friends, and colleagues whose personal and professional contributions have made this work possible. Foremost among my colleagues is my doctoral advisor, Donald A. Harn, whose unwavering mentorship and contagious passion for inquiry and discovery has instilled in me the best aspects of my training as a scientist. Furthermore, the members of my advisory committee, Donald L. Evans, Robert J. Hogan, Kimberly D. Klonowski, and Wendy T. Watford, were critical in providing guidance, perspective, and insightful scientific discussion to enhance the significance and quality of this work in addition to expanding my scientific knowledge and expertise. I benefitted greatly from working with Lisa M. Shollenberger as my steadfast instructor and companion in navigating the complexities of my doctoral training. Without the professional contributions of these wonderful colleagues, accomplished scientists, and inspiring teachers, my doctoral training would have been incomplete. I'd like to thank all of the current and prior members of the Harn lab for their support and friendship. Rafaella Q. Grenfell for her initial experiment involving Matrigel and PuraMatrix, which was instrumental in the development of my doctoral research project. I am also thankful for the support and collaborative nature of the different research labs in the Infectious Diseases Department, specifically, members of the Watford lab, Jeff Hogan and Frank Michel, Cheryl Jones, Ralph Tripp, Mark Tompkins, the He lab, the Rada lab, Jamie Barber and the exceptional staff members in the vet school animal facility.

Prior to joining the graduate program at UGA, I was fortunate to have several inspirational friends and colleagues, including Prof. Doug Lake and members of his lab, Drs. Michelle Kilcoyne, Jared Gerlach and Mitch Magee, as well as Prof. Kelley Moremen and members of his lab. In life, in science and in all things, balance is crucial. Several dear friends helped me to maintain this balance including Sarah and Richard Chatfield, Tony Szempruch, Ryan and Brittany Stuart, the Gomezes and Kristina Buac. Thank you for always being up to grab a drink, go for a hike, or go to a painting/pottery/yoga class, and also for your encouragement, support and dog sitting services.

I'm thankful to my parents, Jim and Sue Hughes, brothers, sisters-in-law and nieces for their immeasurable love and support. Additionally, I am fortunate to have the love and unwavering encouragement of the Samli family. To Jasper and Enzo, thank you for always being there to greet me at the end of the day with those happy-waggy tails! Finally, I want to thank my husband, Kausar, who stands by my side with a kind of love that imbues strength and joy. Looking back now, it seems that together we've lived several lives, traversed several countries and faced each new adventure with courage and renewed inspiration. Adventures of the Drs. Samli – what will we do next? ☺

Thank you!

TABLE OF CONTENTS

	Page
ACKNOWLEDGEMENTS	iv
LIST OF TABLES	x
LIST OF FIGURES	xi
CHAPTER	
1 INTRODUCTION AND LITERATURE REVIEW	1
1.1 Vaccines: Historical Beginnings.....	1
1.2 Modern Vaccines and Avenues for Improvement	5
1.3 Vaccine Adjuvants	8
1.4 Vaccine Delivery Technologies	13
1.5 Influenza Virus and Host Infection.....	14
1.6 References.....	22
2 VACCINE SELF ASSEMBLING IMMUNE MATRIX (VACSIM TM)	30
2.1 The (RADA) ₄ Synthetic Oligopeptide and Commercial Product	
PuraMatrix®	30
2.2 Vaccine Delivery Conception.....	33
2.3 Developing a Vaccine Platform Technology	35
2.4 Conclusions.....	50
2.5 Materials and Methods.....	51
2.6 References.....	56

3	DELIVERY OF ADJUVANTED WHOLE INACTIVATED INFLUENZA BY VACSIM™, A THREE DIMENSIONAL VACCINE DELIVERY METHOD, IMPROVES PROTECTION FROM LETHAL HOMOLOGOUS CHALLENGE IN MICE	60
3.1	Abstract	61
3.2	Significance	62
3.3	Introduction.....	62
3.4	Results.....	65
3.5	Discussion.....	75
3.6	Materials and Methods.....	79
3.7	Acknowledgments.....	83
3.8	Supporting Information.....	83
3.9	References.....	86
4	INVESTIGATING VACSIM™ ENHANCED IMMUNE RESPONSE OF ADJUVANTED WHOLE-INACTIVATED INFLUENZA (PR8) VACCINE.....	91
4.1	Introductions	92
4.2	Results.....	94
4.3	Conclusions.....	111
4.4	Materials and Methods.....	113
4.5	References.....	117
5	VACSIM™: EVALUATING THE MECHANISM.....	121
5.1	Introductions	121

5.2 Results.....	122
5.3 Conclusions.....	136
5.4 Materials and Methods.....	138
5.5 References.....	141
6 DISCUSSION AND FUTURE DIRECTIONS	143
6.1 Discussion.....	143
6.2 References.....	154

APPENDICES

A. VACCINE SELF-ASSEMBLING IMMUNE MATRIX IS A DELIVERY PLATFORM THAT ENHANCES IMMUNE RESPONSES TO RECOMBINANT HB _s AG IN MICE	157
B. CHAPTER 2 SUPPLEMENTARY DATA	180
C. CHAPTER 4 SUPPLEMENTARY DATA	192
D. CHAPTER 5 SUPPLEMENTARY DATA	197

LIST OF TABLES

	Page
Table 1.1: Types of vaccines and their immune correlates.....	6
Table 1.2: Vaccine-triggered mechanisms of effector function and protection.....	7
Table 1.3: Compounds with known adjuvant activity	9
Table 1.4: Common vaccine adjuvants, their current regulatory status, their immune-stimulating activity and the known or hypothesized mechanism of action	12
Table 1.5: Influenza A virus genes and proteins.....	18
Table 4.1: Examples of vaccines with revaccination recommendations for general and high-risk* populations	93
Table 4.2: Summary table of percent undetectable virus in lungs by group.....	101
Table 4.3: The average cross-reactive IgG endpoint titers in sera (4 wpv)	104
Table 5.1: Phenotypic markers	134
Table 5.2: Cell-specific phenotypes for analysis by flow cytometry.....	134
Table 6.1: Summary of Chapter 2 results	145
Table 6.2: Summary of Chapter 3 results.	147
Table 6.3: Summary of Chapter 4 results	150
Table 6.4: Summary of Chapter 5 results	153
Table B.1: Lethality of influenza (A/Puerto Rico/08/34) challenge stock	184
Table B.2: Summary of strain/virus-specific peptides.....	189
Table C.1: B cell epitopes on influenza hemagglutinin	193

LIST OF FIGURES

	Page
Figure 1.1: Major milestones in the historical path of the development of vaccinology and vaccine design	2
Figure 1.2: The primary immune response and development of antigen-specific memory	4
Figure 1.3: Induction of immune responses by vaccination	6
Figure 1.4: Diagram of the lung and respiratory tract.....	16
Figure 1.5: Influenza virus infection and propagation within host cells.....	17
Figure 1.6: World Health Organization Influenza Nomenclature	20
Figure 2.1: Molecular models of the RADA16-I, RADA16-II, EAK16-I and EAK16-II self-assembling peptides	30
Figure 2.2: Schematic of design strategies (left) and assembled structures (right) for selected engineered peptide and protein materials.....	31
Figure 2.3: The self-assembling peptide scaffold	32
Figure 2.4: rHepBsAg-specific humoral responses are enhanced and sustained by VacSIM™	35
Figure 2.5: Immunization with VacSIM™ increases rHBsAg-specific antibody titers in both Th1- and Th2-biased mouse models.....	37
Figure 2.6: Immunization with VacSIM™ increases influenza protein-specific IgG endpoint titers in Th1-/Th2-biased mouse models	38

Figure 2.7: Proposed mechanism by which, VacSIM™ improves vaccine immunogenicity and efficacy.....	39
Figure 2.8: Antigen diffusion kinetics	41
Figure 2.9: Influenza A/PR/8/34-specific isotype endpoint titers from adjuvanted and unadjuvanted vaccine groups	44
Figure 2.10: Immunization with various adjuvants and their effect on specific IgG sera titers, morbidity and viral clearance from the lungs.....	46
Figure 2.11: Routes of administration vary to maximize effectiveness of vaccine	47
Figure 2.12: Route-dependent α -PR8 IgG sera levels and viral clearance from the lungs post challenge	49
Figure 3.1: Inactivated influenza vaccine delivered with CpG via VacSIM™ induces higher antibody titers in sera and mucosa.....	66
Figure 3.2: Inhibition of hemagglutination is a standard correlate of protection.....	68
Figure 3.3: Inactivated influenza vaccine delivered with CpG via VacSIM™ decreases mortality, results in the highest level of protection post challenge and increased viral clearance after lethal influenza challenge.....	71
Figure 3.4: Vaccination with PR8 and CpG by VacSIM™ delivery enhances NP-specific T cells in draining lymph nodes post challenge.....	73
Figure 3.5: Vaccine self-assembling immune matrix proposed mechanism.....	75
Figure 3.6: Inactivated influenza vaccine delivered with CpG via VacSIM™ induces higher antibody titers in sera.....	85
Figure 3.7: Low dose lethal challenge is insufficient to discriminate between protected groups	86

Figure 4.1: Immunization, viral challenge and biological sample collection schedules	95
Figure 4.2: Vaccine-induced α -PR8 IgG sera endpoint titers 4-26 weeks post vaccination.....	96
Figure 4.3: Vaccine-specific IgG endpoint titers kinetics from 1-6 months post vaccination.....	97
Figure 4.4: Immunity tapers for all vaccine groups by 6 months post influenza challenge.....	98
Figure 4.5: Vaccine groups possess marginal immunity by 1-year influenza challenge.....	100
Figure 4.6: Proportion of immunized mice with undetectable virus in lungs	102
Figure 4.7: Cross-reactive IgG endpoint titers are highly variable in sera of immunized mice	103
Figure 4.8: Alignment of hemagglutinin sequences from 6 influenza A/B viruses..	105
Figure 4.9: Heterologous and homologous antigen-specific IgG levels are similar in X:31 (WIV) immunized mice	107
Figure 4.10: Whole-inactivated X:31 immunized mice struggle to clear virus from the lungs following 100 LD ₅₀ PR8 challenge (4 wpv).....	108
Figure 4.11: Elderly mice given PR8+CpG+VacSIM™ maintain antibody levels and ability to clear virus following lethal influenza challenge	110
Figure 5.1: VacSIM™ does not induce dendritic cell (DC) activation in the absence of antigen/adjuvant.....	125

Figure 5.2: Confocal images showing VacSIM™ depots of fluorescent antigen and intercalated bone marrow derived dendritic cells (BMDCs).....	127
Figure 5.3: Vaccinating with antigen+CpG delivered in VacSIM™ leads to increased total cell counts in the draining versus non-draining lymph nodes at 1-2 days post vaccination.....	128
Figure 5.4: Fluorescently labeled BSA delivered with CpG + VacSIM™ results in an increased number of DCs that localize to the draining lymph nodes	130
Figure 5.5: BSA+ CpG delivered in VacSIM™ leads to an increased number of activated DCs, that generally localize in the draining lymph nodes	131
Figure 5.6: Increased number of T cells in the draining lymph nodes of mice vaccinated with BSA+ CpG delivered in VacSIM™ compared to the non-draining lymph nodes	132
Figure 5.7: Minimal variation between PR8(WIV) vaccine groups, in relative immune cell populations at 48 hour post influenza challenge.....	135
Figure A.1: rHBsAg-specific humoral responses are enhanced and sustained by VacSIM delivery	166
Figure A.2: Immunization with VacSIM increases rHBsAg-specific antibody titers in both Th1- and Th2-biased mouse models.....	168
Figure A.3: VacSIM delivery produces a mixed Th1/Th2 type cellular response....	169
Figure A.4: Cell-mediated immunity is induced following immunization via VacSIM™	171
Figure B.1: Vaccine-induced morbidity and viral clearance from the lungs following influenza challenge.....	180

Figure B.2: Route-dependent α -PR8 IgG sera levels and viral clearance from the lungs post challenge	181
Figure B.3: Mouse lethal $\frac{1}{2}$ dose (MLD ₅₀) determination for influenza A/Puerto Rico/08/34 challenge stock	182
Figure B.4: Plaque assays to determine influenza PR8 challenge stock titer	183
Figure B.5: Tissue culture $\frac{1}{2}$ lethal dose (TCID ₅₀) of influenza challenge stock	185
Figure B.6: Hemmagglutination unit (HAU) of influenza (PR8) challenge and vaccine stocks	185
Figure B.7: Cytokine analysis on immunized mouse spleens	186
Figure B.8: Vaccine-specific CD8 ⁺ T cells in the spleens of immunized mice	186
Figure B.9: IL-4 and IFN- γ levels in spleens of Th1- and Th2-biased, immunized mice	187
Figure B.10: Cytometric bead array (CBA) analysis on C57BL/6 spleens, naive or 28 days post vaccination (dpv)	188
Figure B.11: Representative image of IFN- γ ELISpot plates	189
Figure B.12: IFN- γ specific ELISpot results from spleens of Th2-biased immunized mice	190
Figure B.13: IFN- γ specific ELISpot results from spleens of Th1-biased immunized mice	191
Figure C.1: PR8-specific IgG endpoint titers at various time points out to 50 wpv	192
Figure C.2: Mean weight change at various heterologous (PR8) challenge doses...	193
Figure C.3: B cell epitopes from hemagglutinin of various influenza viruses.	194

Figure C.4: Dose-sparing whole-inactivated virus in saline	195
Figure C.5: Investigating low-dose vaccine-induced protection	196
Figure D.1: Gating strategy for enumerating antigen presenting cells (APCs) in the draining and non-draining lymph nodes following immunization	197
Figure D.2: Vaccine delivered in VacSIM™ may delay accumulation of antigen presenting cells (APCs) in the draining lymph nodes (d-LNs) versus the non- draining lymph nodes (nd-LNs), when compared to delivery in saline	198
Figure D.3: In the absence of antigen VacSIM™ does not induce localized cell recruitment.	197
Figure D.4: Mean fluorescent intensity (MFI) of dendritic cells (DCs) and T cells in the non-draining/draining axillary and inguinal lymph nodes at 24 hpv (n=5 per time point).....	199
Figure D.5: Mean fluorescent intensity (MFI) of dendritic cells (DCs) and T cells in the non-draining/draining axillary and inguinal lymph nodes at 48 hpv (n=5 per time point).....	200
Figure D.6: Cell counts from lymph nodes of immunized mice pre/post-challenge	202
Figure D.7: Immune cell frequencies in lymph nodes of immunized mice pre/post-challenge	203
Figure D.8: Spectral overlap using BD's fluorescence spectral viewer	204
Figure D.9: Cell population gates corresponding to Figures 5.7, C4-C5	205
Figure D.10: Cell population gates corresponding to Figure 5.1	205

CHAPTER 1

INTRODUCTION AND LITERATURE REVIEW

1.1 Vaccines: Historical Beginnings

Immunization is the process of priming the host's immune system to foreign antigens as a means of inducing protective immune responses. Thus, following pathogen exposure via immunization, there is either no infection or mild infection with limited symptoms. By 430 B.C.E. it was well known that smallpox survivors were immune to reinfection and due to their immunity, these individuals were frequently assigned to be caretakers of the sick (1). Rudimentary immunization or rather inoculation techniques were being practiced across Asia as early as the 12th century. The term 'variola' refers to the intentional inoculation, often via an intradermal (i.d.) graft on an uninfected individual (generally the arm or leg) with biological material containing live smallpox virus, which resulted in the inoculated individual developing a localized infection (survivable version) of the disease.

European records indicate that this technique left 20–60% of its survivors horribly scarred and had a case-fatality rate between 1–3% in adults (2) and 70–98% in infants (3). The high fatality associated with variolation techniques and the devastation of smallpox epidemics (400,000 smallpox-related deaths annually and 1:3 survivors left blind) continued to spread across 18th century Europe (4) and paving the way for Edward Jenner to pioneer smallpox vaccination (Figure 1.1) (5). In 1798, Jenner published the seminal smallpox vaccine paper outlining the hypothesis that exposure to vaccinia

(cowpox) a virus infecting cows but commonly known not to naturally infect humans was sufficient to provide protection from the smallpox virus (6). As evidence, Jenner outlined his findings collected over a one-year period, following his inoculation of a child with liquid residue transferred to a milkmaid's hands, which had been in contact with pustules shedding cowpox virus. Jenner's publication on vaccine inoculation against smallpox continued to be expanded and refined by innovative experimentalists like Emil Von Behring and Shibasaburo Kitasato, Jonas Salk and Albert Sabin leading to the emergence of several new scientific fields.

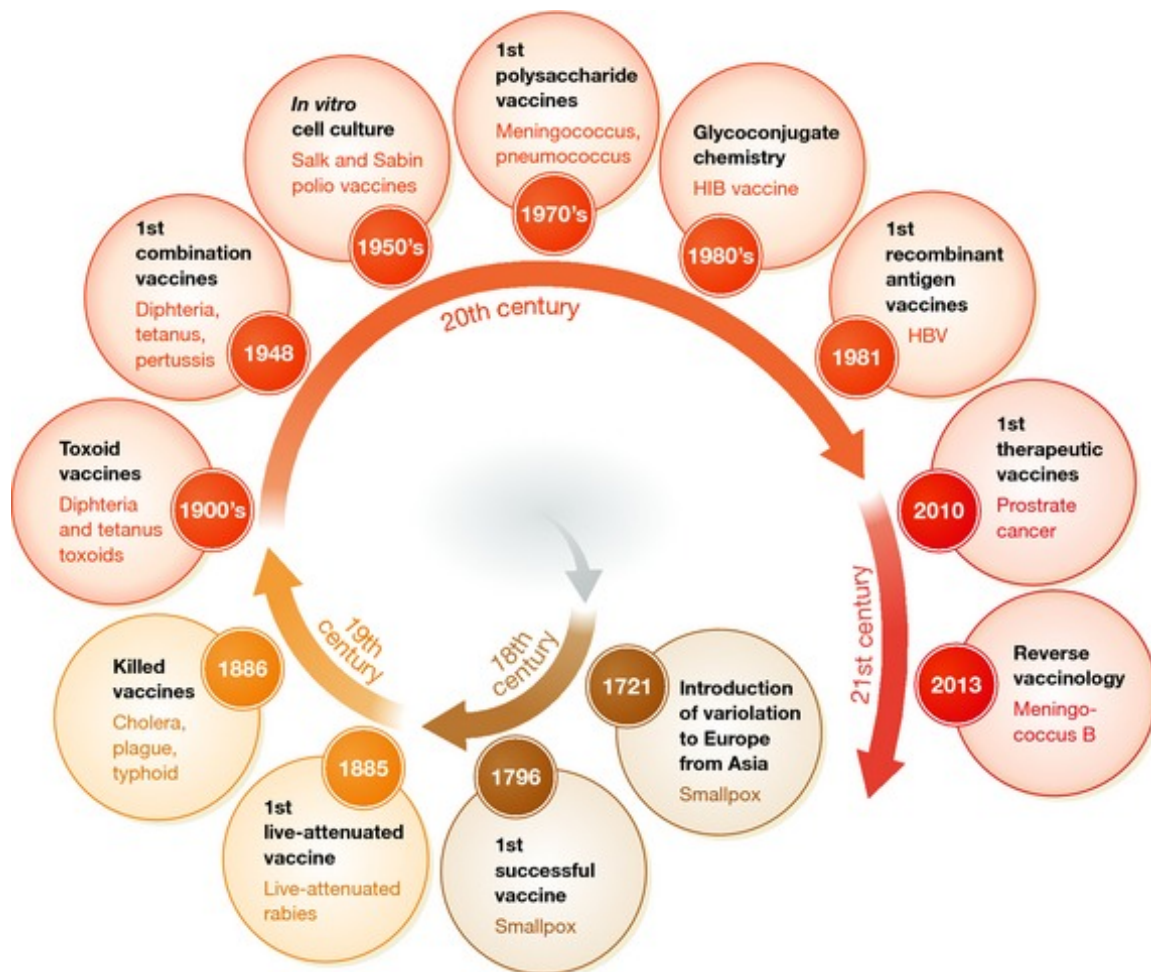


Figure 1.1: Major milestones in the historical path of the development of vaccinology and vaccine design. EMBO Molecular Medicine Volume 6, Issue 6, pages 708-720, 6 MAY 2014 DOI: 10.1002/emmm.201403876.

Figure 1.1 depicts the major milestones accomplished through numerous technological advances in the fields of molecular biology, virology, immunology, and vaccinology (7). Both the 19th and 20th century are referred to as being a golden age of vaccines (7). The first golden age was brought about by innovators such as Pasteur, Koch, Ramon, Merieux, Salmon and Smith. This century led to establishment of the germ theory and vaccines incorporating live-attenuated or inactivated (killed) pathogens as well as inactivated toxins (toxoids) (7-10). In the 20th century, a second golden age of vaccine development, was initiated by innovations in cell culture technology and scientists such Salk, Enders, Sabin, and Plotkin. The ability to propagate virus in cell cultures provided a means of attenuating viral vaccines (7, 8, 11-15).

Following establishment of the Center for Disease Control and Prevention (CDC, 1946), the World Health Organization (WHO, 1948) and mass-immunization campaigns such as the Global Smallpox Eradication Program (WHO launched in 1967), naturally occurring smallpox was eradicated. Controlling the spread of infection, towards the eventual elimination of vaccine-preventable diseases requires that the majority of the population be immune to the particular infectious disease. This immune protection can be acquired through previous exposure to an antigen associated with that particular infectious disease. Exposure is typically in the form of a prior infection or effective vaccination with a disease-associated antigen, triggering the body's immune defense systems and leading to the production of specific antibodies and antigen-specific memory cells (Figure 1.2). Immune protection requires antigen-specific effector cells, which target and clear the pathogen, as well as an effective immune memory response, derived

from long-lived antigen-specific cells capable of rapidly responding to subsequent pathogen exposures (Figure 1.3).

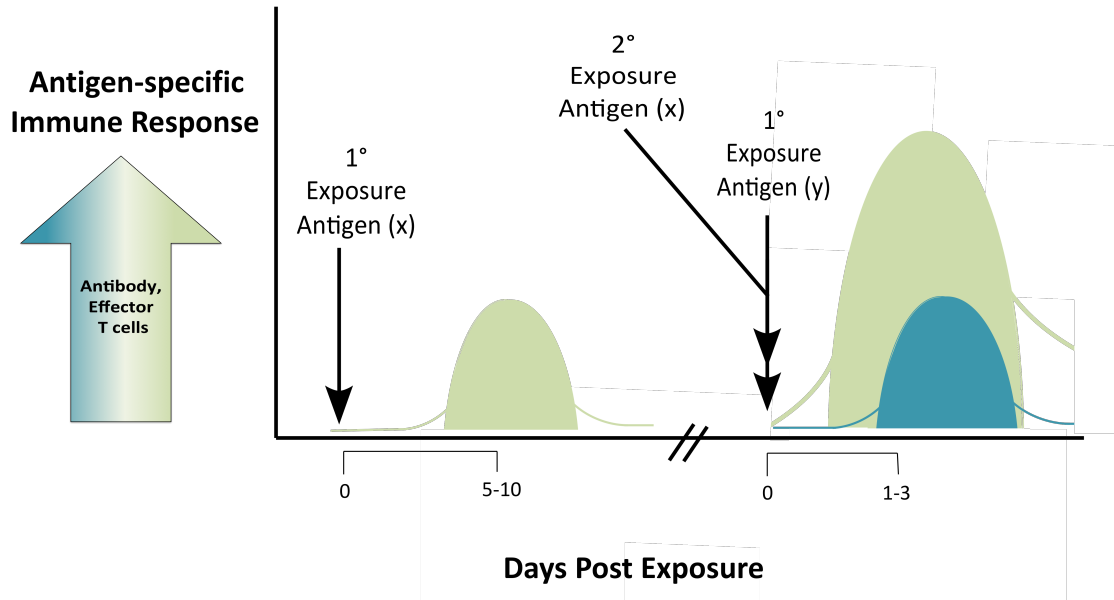


Figure 1.2: Primary immune response and development of antigen-specific memory. In the case of natural infection, exposure to an unknown pathogen, a healthy immune system begins to mount a response made up of specific antibodies and effector T cells that target and clear the unknown pathogen. This also occurs following initial exposure to vaccinating antigen (“x” or “y”) with the peak response generated after 5-10 days. Due to antigenic memory response, repeat exposure to vaccinating antigen results in an immune response that also develops more rapidly, with the response peaking after only 1-3 days. Image constructed using Perkin Elmer’s ChemBioDraw® Ultra v.13.0.2.320 and Microsoft® PowerPoint® for Mac 2011 v. 14.4.8 (150116).

When the vast majority of the population is immune to an infectious disease such as smallpox or polio for example, the likelihood of disease outbreak is significantly decreased. This concept is an essential step in the eradication of any vaccine-preventable disease and is often referred to as “herd immunity” because the population’s unvaccinated minority has a decreased risk of infection, which is correlated to the fact that the majority of the population is vaccinated. In the Spring of 1980, WHO announced

that routine vaccination had successfully eliminated the threat of smallpox, and certified the world to be free of naturally-occurring smallpox virus. Now in the 21st century, the threat of infection with polio virus has been eliminated in most countries and various global aid and mass-immunization organizations such as the United Nations Children's Fund (UNICEF), Rotary International, and the Bill and Melinda Gates Foundation are working with the CDC and WHO towards the successful eradication of polio virus and other vaccine-preventable diseases. Besides access to clean drinking water, vaccines are the most important public health tools utilized in the prevention of infectious diseases (11, 16).

1.2 Modern Vaccines and Avenues for Improvement

Through the years, researchers became increasingly aware of the complexities surrounding the various infection strategies posed by different bacterial and viral disease agents, as well as the counter-strategies being utilized by the host's immune system (Figure 1.3). Simultaneously, many different avenues for vaccine design were being explored and although some were more successful than others, these studies led to the development the various types of vaccines in use today. Table 1.1 outlines the different types of modern vaccines: 1) live-attenuated vaccines, which contain a weakened form of the infectious virus or bacteria, 2) inactivated vaccines, which contain a non-infectious protein/subunit or fragmented pieces of the whole virus or bacteria, 3) toxoid vaccines, which contain a chemical or toxin produced by the virus or bacteria and 4) biosynthetic or virus-like particle (VLP) vaccines, which contain synthetic mimics of the infectious virus or bacteria and are, therefore, noninfectious (17, 18).

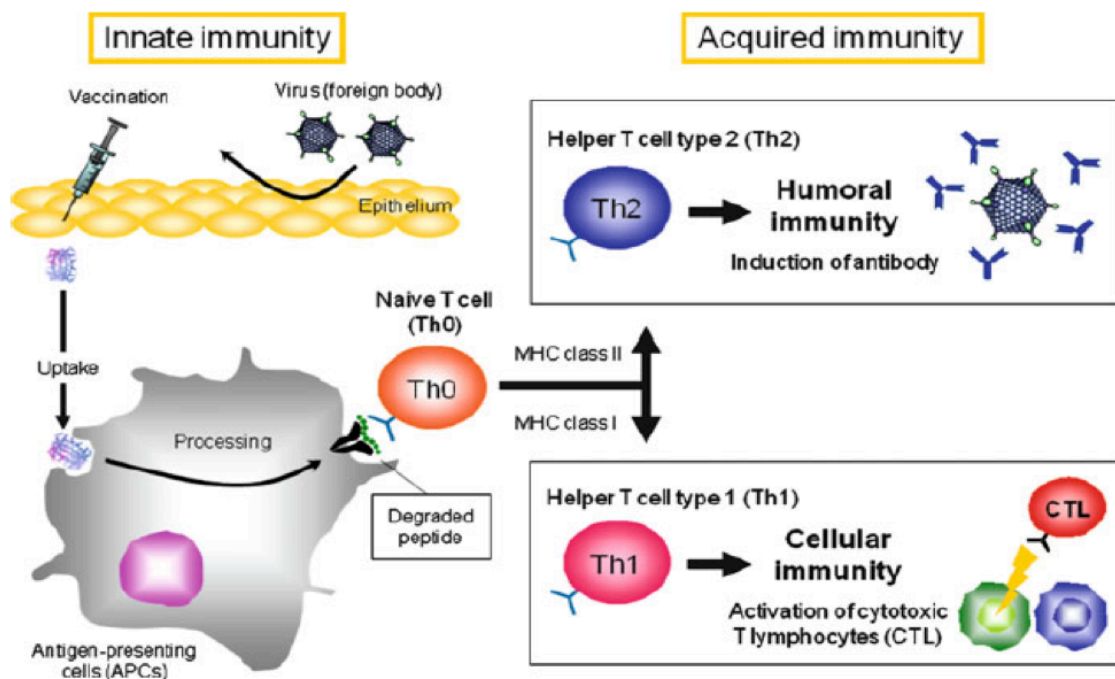


Figure 1.3: Induction of immune responses by vaccination. Reprinted with kind permission from Springer Science and Business Media: *Advances in Polymer Science* 247, 2012, 31-64, *Biodegradable Nanoparticles as Vaccine Adjuvants and Delivery Systems: Regulation of Immune Responses by Nanoparticle-Based Vaccine*, Takami Akagi, Masanori Baba, Mitsuru Akashi,(Fig.1). Copyright © 2012.

Table 1.1: Types of vaccines and their immune correlates (18).

Vaccine Type	Diseases w/ this Type of Vaccine	Vaccine-induced Immune Response
Live-attenuated	Measles	Strong serum IgG, CD8 ⁺ T cell
	Influenza (i.n.)	Strong serum IgG, mucosal IgG/IgA, CD8 ⁺ T cell
Inactivated (whole or subunit)	Influenza (subunit)	Strong serum IgG, some mucosal IgG
	Pertussis (whole-cell)	Strong serum IgG
Toxoid	Diphtheria	Strong serum IgG, some mucosal IgG
	Tetanus	Strong serum IgG
Biosynthetic, Virus-like-particle	Papillomavirus	Strong serum IgG/IgA

Effective vaccines should include adequate antigen and/or adjuvant containing pathogen-associated molecular patterns (PAMPs) for the host immune system to view as “danger signals” and trigger an innate immune response (19). The type of vaccine used typically affects the overall vaccine response due to the specific influencers being utilized to activate an innate immune response (20). In general, these “danger signals” trigger inflammatory signal cascades and recruit immune responders, also known as antigen-presenting cells (APCs). Vaccines containing inactivated (non-infectious) material can induce high levels of vaccine-specific antibodies, which may prevent or minimize infection levels as well as contribute towards clearance of extracellular pathogens through various mechanisms (Table 1.2).

Table 1.2: Vaccine-triggered mechanisms of effector function and protection. Adapted from “Vaccines” 6th ed., by Stanley Plotkin, Walter Orenstein and Paul Offit, (Chapter 2, Table 2-1).

Effectors	Vaccine-induced Action	Mechanisms Aiding in Protection
Specific antibodies	Prevent and/or reduce infection	- Bind enzymatic active sites, prevent diffusion - Inhibit binding, neutralize viral replication - Opsonophagocytosis of extracellular bacteria - Activate complement cascade
CD8 ⁺ T cells	Reduce infection, control & clear intracellular pathogens	- Kill infected cells directly by releasing granzyme/perforin - Kill infected cells via antimicrobial cytokines
CD4 ⁺ T cells	Contribute to reduction, control & clearance of extracellular & intracellular pathogens	- Produce IFN- γ , TNF- α/β , IL-2 and IL-3, support activation & differentiation of Th1-type cells (B cells, CD8 ⁺ T cells & macs) - Produce IL-4, IL-5, IL-13, IL-6 & IL-10, support activation & differentiation of Th2 cells

The majority of modern vaccines provide vaccine-induced protection through the induction of antigen-specific serum IgG (21). However, vaccine-induced specific antibody responses tend to diminish over time, thus these vaccines containing inactivated antigen typically require “boosters” and/or addition of an immune-potentiating adjuvant

or delivery system in order to maintain protection (22). Vaccines containing live-attenuated infectious material can induce CD8⁺ T cells, which assist in pathogen control and clearance in addition to inducing a robust, specific antibody response. Live-attenuated vaccines (LAV) are able to generate a more sustained specific-immune response, compared to inactivated vaccines. Although LAVs are typically the most effective at generating a protective immune response, because they contain infectious material there are many limitations, such as the type of pathogen, the route of delivery as well as the age and health status of the individual being vaccinated.

Improving vaccine formulation and delivery as well as vaccine efficacy (VE) and durability remain vital areas of research. Despite the discovery of numerous candidate antigens specific for each disease, effective vaccines have yet to be developed for many infectious diseases including HIV, TB and malaria. Additionally, in an epidemic or pandemic scenario, it is vital to have a vaccine option capable of inducing protective immune responses or enhancing weak responses after only a single vaccination.

1.3 Vaccine Adjuvants

The term “adjuvant” is broadly defined and can refer to a myriad of different compounds whether chemical or biological, naturally occurring or synthetic, so long as the addition results in an increased immune response (23). Initially, adjuvants were thought to fall into one of two categories based on their observed or hypothesized mode of action; those that functioned as immune-modulators (directly stimulating the innate immune system) or as a delivery system (inducing controlled antigen release and/or triggering the inflammasome).

Table 1.3: Compounds with known adjuvant activity (22-24).

Compounds w/ Adjuvant Activity	Example Adjuvants
synthetic ssRNA or dsDNA	Poly(I:C), CpG ODN
microbials	LPS
mineral salts	Alum
oil-in-water emulsions	MF59, IFA
cytokines	IL-12
saponin or amphipathic glycosides	ISCOMs, QS-21
liposomes	AF01, CAF01
micro/nanoparticles	protein loaded γ -PGA-Phe nanoparticles

Decades of research and clinical trials have resulted in a diverse collection of compounds with confirmed adjuvant activity (Table 1.3) (22-24). Although the precise mechanisms of many adjuvants remain at least partially unclear, decades of research has lead to a collection of hypothesized mechanisms for various immune stimulating adjuvants (23). An adjuvant or delivery system may bolster the immune response (directly/indirectly) through any one or a combination of the following methods. An adjuvant may cause formation of a depot at the injection site, which has been associated with sustained or slow-release of antigen. It may induce the transient secretion of cytokines and chemokines, inducing recruitment of immune cells back to the injection site. APCs express various pattern recognizing receptors (PRRs) intracellularly (i.e.: NLRs) and on their surfaces (i.e.: TLRs), which recognize and ligate adjuvants, leading to increased antigen uptake and presentation. An adjuvant may bolster APC activation & maturation, resulting in increased expression of major histocompatibility complex (MHC-II) as well as co-stimulatory molecules. Adjuvants may also improve the ability of APCs

to process and present antigen or increase migration of mature APCs to the draining lymph nodes (dLNs), where they are able to interact with antigen-specific B and T cells. Adjuvants may also stimulate activation of the inflammasome (Table 1.4).

In the 1920s alum became the first adjuvant licensed for use in humans. Alum refers to precipitates of either aluminum phosphate and/or aluminum hydroxide upon which the vaccinating antigens or organisms are adsorbed. This process is highly time and labor intensive (25, 26). Today, nearly a century later, alum remains the most common adjuvant in human vaccines. A track record that spans this many decades has only reinforced alum's safety; however, aspects of its immune-stimulating mechanism(s) are still being debated. It was 80 years following alum licensure before a non-aluminum salt adjuvant was approved for human vaccines (27). Adjuvant reactogenicity is a concern that continues to be relevant in the process of development and licensure of new adjuvants. Freund's adjuvant, for example, was shown to be extremely reactogenic and therefore not acceptable for licensure (28).

The mechanistic "black box" of adjuvant activity and potential reactogenicity are key factors related to vaccine adjuvant licensure, which remains a slow, tedious and frequently disappointing process. Un-methylated DNA (CpG-ODN) is an effective and frequently used adjuvant for research purposes and makes a good case-study example for the arduous process of getting vaccine adjuvants approved for use in humans. In 2013, Dynavax's Hepisilav vaccine candidate for hepatitis B completed phase-III clinical trials using CpG-ODN (1018) as an adjuvant (24, 29). Despite undergoing repetitive clinical trials, CpG/immune stimulating sequences (ISS) has not yet been approved by the United State's Food and Drug Association (FDA) following phase-III human clinical trials, due

to reactogenicity concerns (29). Dynavax's Hepislav vaccine candidate adjuvanted with ISS began a new phase-III human clinical trial shortly afterwards, and results of their most recent clinical trial should be available by the end of 2015 (ClinicalTrials.gov identifier: NCT02166671). CpG-ODN functions as a TLR-9 agonist and signals through the activation of MyD88, IRAK and TRAF-6 (24). As a vaccine adjuvant, CpG has been shown to induce DC maturation, increase antibody production as well as CD8⁺ T lymphocytes (T cells) (30, 31). By 3-hours post vaccination with CpG, pro-inflammatory cytokines, such as TNF- α , IL-1, IL-2, IL-12, IL-18 are up-regulated (30, 31).

Recent efforts to improve vaccines have led to the generation of new delivery methods in addition to traditional formulations incorporating an adjuvant (32-37). These alternative vaccine delivery methods utilize approaches such as virosomes (38-40), liposomes (41-43), layer by layer formulations and microneedle nanoparticle technology (44, 45) as well as vector-based strategies (46-48). Although still being investigated, current reports indicate drawbacks are associated with each of these delivery approaches; either associated with reactogenicity and regulatory issues, product stability or required formulation steps. Recently, there has been increasing emphasis on vaccine formulations containing a combination of adjuvants with complementary activity as well as combining traditional adjuvants with new delivery methods (23). These strategies have been employed experimentally as a means of increasing vaccine-specific immune responses, either by improving antigen stability, APC presentation, balancing adjuvant-specific immune bias or reducing reactogenicity. This combination strategy also has the potential to generate a "smart adjuvant", capable of specific targeting/activation (22, 49).

Table 1.4: Common vaccine adjuvants, their current regulatory status, their immune-stimulating activity and the known or hypothesized mechanism of action (22-24, 50).

Adjuvant	Regulatory Status	Activity & Mechanism (known or proposed)
Alum Mineral salts (aluminum hydroxide)	Common adjuvant human vaccines (ie: DTap, HepA, HepB, Flu)	--Activates compliment cascade & increases cell recruitment (eosin., mono./macs) --Promotes Ag presentation (<i>efficiency varies w/ Ag size</i>) --Increase local cytokines/chemokines (promotes an inflammatory environment at injection site) --Has a role in reducing rate of Ag degradation --Th2-type immune response
CpG-ODN Un-methylated DNA	Phase-3 Clinical trials	--TLR9 agonists: signals thru activation of MyD88, IRAK, and TRAF-6 (recruits TF's to up-regulate pro-inflammatory genes & protein expression (IL-1,IL-6,IL-12,IL-18,TNF-a)) --Induces DC maturation (enhances adaptive immunity) --Increased Ab production & CD8+ T cells --Th1-type immune response
MF59 Detergent-stabilized oil-in-water (O/W) emulsion	Certain flu vaccines (mostly in Europe)	<i>Not a Depot effect</i> --ASC-dependent (inflammasome component) --Stimulates Ab-producing plasma cells --Induces DC maturation (enhances adaptive immunity) --Promotes Ag-uptake by APCs --Increased Ag-loaded APCs in dLNs --Mixed Th1/Th2-type immune response
CFA/IFA Inactivated Mycobacteria (CFA) in water-in-oil (W/O) emulsion	Research & certain animal vaccines	--CFA → binds TLR2, TLR4 & TLR9 --Intense inflammatory response (CFA for prime, IFA for boosts) --Induces DC maturation (enhances adaptive immunity) --Stimulates production of TNF --Predominant Th1-type immune response
MPL/GLA (Monophosphoryl lipid-A, glucopyranosyl lipid adjuvant)	Few human vaccines (MPL) Clinical trials (GLA)	--TLR4 agonist --Increased Abs --Th1-type immune response
AS04 Combination of MPL & Alum (stabilizing)	HPV & HepB vaccines	--TLR4 agonist --Increased Abs --Th1-type immune response

1.4 Vaccine Delivery Technologies

In addition to combining adjuvants, a tremendous effort has focused on developing non-vector delivery methods. Hydrogels are composed predominately of water but possess both hydrophobic and hydrophilic characteristics, which allows them to alternate phases depending on environmental stimulators (51, 52). It is because of this biphasic nature that hydrogels are capable of forming highly organized, water-insoluble, 3-dimensional structures (53). This is accomplished through intricate networks of hydrated, cross-linking chains forming a lattice-based structure commonly utilized as scaffold or semi-porous barrier (54, 55). Often hydrogels existing in an aqueous phase are triggered to begin self-assembly by external stimuli, such as environmental fluctuations in light, temperature or pH (54). Although predominately composed of water, many hydrogels are excluded from being developed for clinical use because they require toxic cross-linkers for self-assembly, such as the petroleum-based polyethylene glycol (PEG)-linkers or because they contain harmful degradation products such as methacrylates or alginates resulting from hydroxyethyl methacrilates (HEMA) and various polysaccharides such as alginate, chondroitin sulfate, chitosan, and hyaluronic acid. Various natural and synthetic hydrogel constructs have been evaluated for clinical applications such as tissue engineering (56, 57), drug delivery (58) and vaccine delivery (59-61). Incorporation of short, self-assembling amino acid sequences at the C-terminal domain of certain peptide epitopes have been shown to boost immunogenicity (62). Recent studies reported that mice vaccinated with a peptide epitope conjugated to the self-assembling peptide domain Q11 led to formation of antigenic nanofibers, able to induce a vaccine-specific protective serum antibody response (63, 64).

Intradermal vaccine delivery via microneedles is an alternative to traditional intramuscular and intranasal vaccine routes that takes advantage of the unique immune environment (APC prevalence) of the skin. This approach addresses issues such as poor vaccination compliance due to trypanophobia or discomfort related to traditional immunizations, as well as reducing the amount of antigen required per dose. Vaccines delivered via microneedles can be coated onto an array of tiny metal needles, encapsulated within polymers (65) or loaded in hollow needles (66, 67).

Over the years, numerous experimental modifications to improve the influenza vaccine have been tested. These include adjuvants (32-37) as well as viral (47, 48, 68) and non-viral vectors (38-43). Unfortunately, these attempts were minimally successful and/or have limited translational appeal. Development of a flexible vaccine delivery method could be utilized with a multitude of vaccines, with particular relevance in marginally efficacious vaccines and populations of immune compromised or low-responding individuals.

1.5 Influenza Virus and Host Infection

Influenza, historically referred to as the “grippe”, is caused by successful infection of the host’s upper respiratory tract (URT) by influenza viruses. Influenza “flu” viruses contain single-stranded, negative-sense RNA and belong to the orthomyxoviridae family. There are three known influenza virus types (A, B, C). Infection with type C leads to minor symptoms and is not believed to contribute to seasonal epidemics like type A and B viruses. Influenza A viruses are the most prevalent of circulating influenza viruses, several of which are able to infect multiple species (human, avian, swine, fruit bats, etc.). Influenza A viruses have an 8-segmented genome which encode for various

viral proteins, 11 of which are described in Table 1.5 (69). Type A viruses are further classified into subtypes based on the expression of the surface glycoproteins hemagglutinin (HA) and neuraminidase (NA), which are antigenically variable. This variability is a result of antigenic shift, stemming from genetic changes occurring during viral replication, which leads to production of new viruses with alternative surface glycosylation patterns. Currently, 18 different HA and 11 different NA subtypes have been reported (70) to bind receptors on the surface of human epithelial cells.

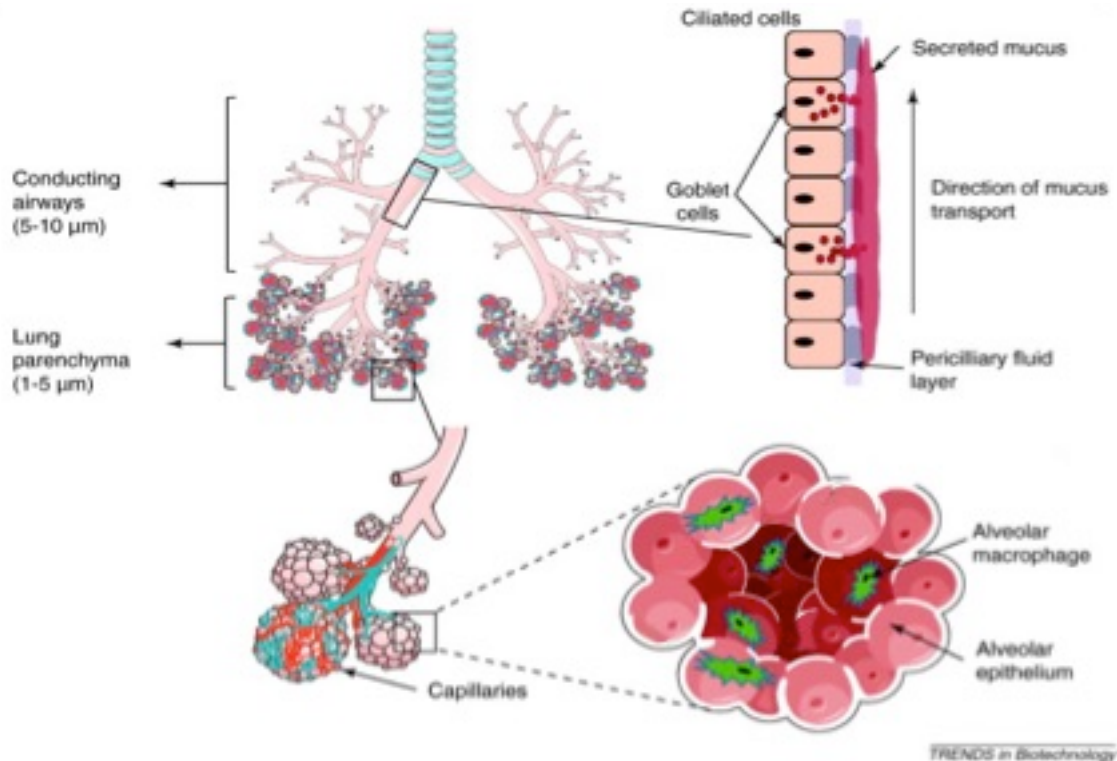


Figure 1.4: Diagram of the lung and respiratory tract. Images on the right are magnified, cartoon views of tissue structures of the conducting airways (i.e. trachea, bronchi and bronchioles) and alveoli in the parenchyma region. The mucosal tissue of the conducting airways consists of ciliated epithelium and mucus producing goblet cells which remove inhaled antigens through upwards mucociliary clearance, with the help of secretory IgA produced by local plasma cells. Blind-ended alveolar sacs are lined by a specialized, thin-walled epithelium to aid gas exchange with the underlying capillaries. Immunosuppressive alveolar macrophages and serum-derived antibodies provide a final line of protection against invading pathogens. A cellular and humoral immune response can be generated after interaction with innate immune receptors present on epithelial cells and tissue-resident dendritic cells. Image and legend have been reprinted with minor modification from Trends in Biotechnology and permission from Elsevier.

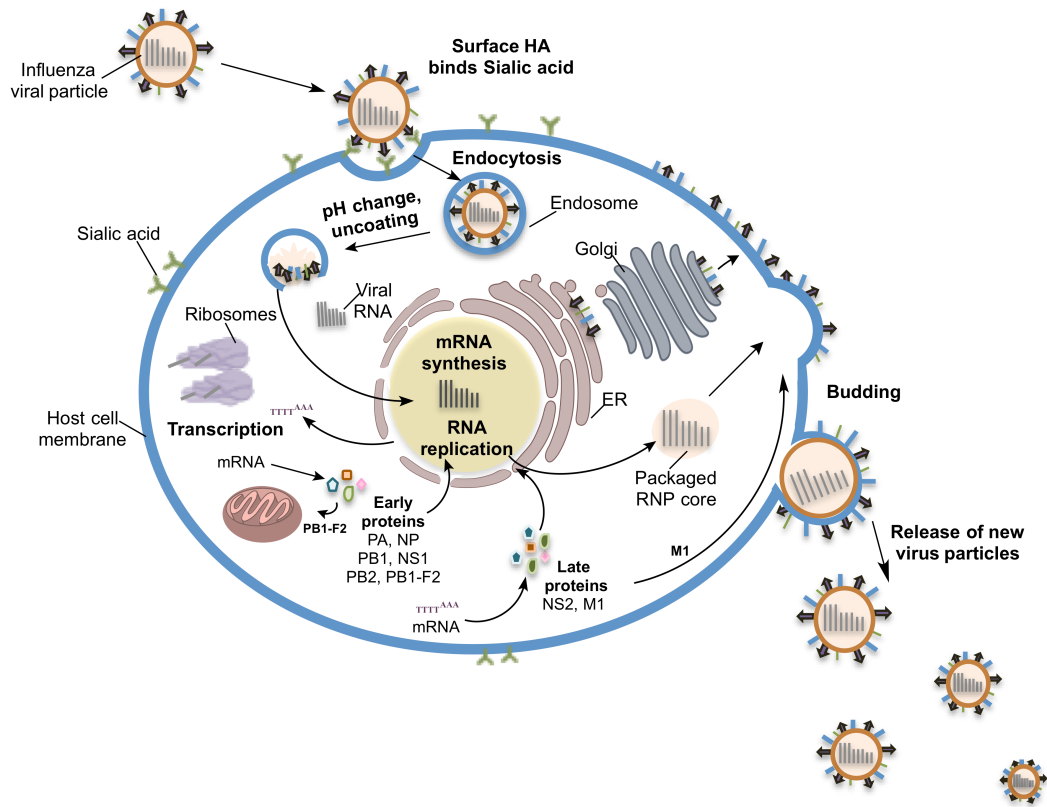


Figure 1.5: Influenza virus infection and propagation within host cells. Image constructed using Perkin Elmer's ChemBioDraw® Ultra v.13.0.2.320 and Microsoft® PowerPoint® for Mac 2011 v. 14.4.8 (150116).

The virus enters a host's URT following inhalation of infectious droplets or aerosols (Figure 1.4) (71). Upon entering the URT, virions bind to sialic acid via glycoprotein HA (Figure 1.5). Virions enter the host cell via an endosome vesicle that undergoes acidification, allowing bound HA monomers to be cleaved at the stem base by a trypsin-like enzyme into HA₁ and HA₂. Cleavage results in a conformational change, activating the membrane fusion function of HA₂, which in combination with the close proximity leads to membrane fusion of the virus envelope to the endosome. The low pH triggers the integral membrane protein, M2, to open its proton channel. As the virion becomes more acidic, due to the influx of protons, there is a dissociation/uncoating of

viral ribonucleoproteins (RNPs) from the surrounding matrix protein (M1). The combination of events leads to release of the nucleocapsid into the host cytoplasm. Viral material traffics to the nucleus due to nuclear targeting sequences present in the nucleoprotein (NP). Upon reaching the nucleus the virus hijacks the cell's production machinery to propagate more virus particles. Newly produced proteins remain in the cytoplasm, except for NP, which return to the nucleus. An infected host cell will continue virus replication and new virions are released through budding at the plasma membrane.

Table 1.5: Influenza A virus genes and proteins. Adapted from Lamb and Krug, 2001.

Gene ID	Segment	Protein Name	Protein Function
1	Polymerase B2 (PB2)	Polymerase B2 (PB2)	Internal protein, Virus replication
2	Polymerase B1 (PB1)	Polymerase B1 (PB2) PB1-F2	Internal protein, Virus replication Mitochondrial targeting and apoptosis
3	Polymerase A (PA)	Polymerase A (PA)	Internal protein, Virus replication
4	Hemagglutinin (HA)	Hemagglutinin (HA)	Surface glycoprotein, viral attachment, Antigenic determinant, Subtype specific (H1 through H16)
5	Nucleoproteins (NP)	Nucleoproteins (NP)	Nucleocapsid protein, RNA coating, Nuclear targeting, RNA transcription, Type (A,B,C) specific
6	Neuraminidase (NA)	Neuraminidase (NA)	Surface glycoprotein, antigenic determinant, Viral release from host cells, Subtype specific (N1 through N9)
7	Matrix (M)	Matrix1 (M1) Matrix 2 (M2)	Membrane protein stability, Type (A,B,C) specific Membrane protein stability & viral uncoating, Type (A,B,C) specific
8	Non-structural (NS)	Non-structural 1 (NS1) Non-structural 2 (NS2)	Internal proteins, Regulation of virus life cycle (mRNA transcription, localization of viral ribonucleic proteins)

Influenza infection is a global health concern with seasonal epidemics that rapidly spread across continents, imposing unpredictable levels of morbidity and mortality, as well as considerable economic burdens in the form of health care costs and lost productivity (72, 73). Seasonal influenza is an acute infection that hospitalizes 200-250,000 and kills approximately 36,000 persons annually in the United States alone (74). Symptoms of infection present rapidly and include high fever, headache, muscle pain, cough, sore throat and rhinitis. Infections in high-risk populations, such as those under 5 or over 65 years old and immune compromised, often lead to more severe and potentially life-threatening complications such as influenza-associated encephalitis or encephalopathy (75), and pneumonia. Pneumonia is seen as primary influenza pneumonia or secondary bacterial pneumonia, including severe community-acquired bacterial pneumonia due to MRSA (76).

Influenza vaccine effectiveness is assessed by established correlates of protection, which include seroconversion (able to generate ≥ 4 -fold higher specific antibodies than pre-vaccination) and seroprotection (capable of inducing hemagglutination inhibition (HI) antibody titers $\geq 1:40$ post-vaccination) (77). According to the package insert (www.FDA.gov) the immune mechanisms of action responsible for conferring protection following vaccination with FluMist[®] Quadravalent are still unclear; however, it is speculated that serum antibodies, mucosal antibodies, and influenza-specific T cells are involved. Vaccine-induced specific antibodies block virus binding to sialic acid receptors on epithelial cells, bind surface Fc receptors and may also be involved in intracellular virus neutralization, preventing virion egress from infected cells (78, 79). Intracellular

neutralization by flu-specific IgG is thought to require shuttling by the neonatal Fc receptor (FcRn).

Multiple virus strains are incorporated into vaccines against seasonal influenza epidemics to provide broader exposure. There are two types of influenza (A and B) known to contribute to seasonal epidemics in humans (Figure 1.6). The most effective method to prevent influenza infection is through annual vaccination. Influenza vaccines are typically effective by two weeks post immunization, but protection is variable depending on age and health status. There are numerous types of influenza vaccines available, including LAIVs (i.n.), and inactivated subunit vaccines (i.m./i.d.).

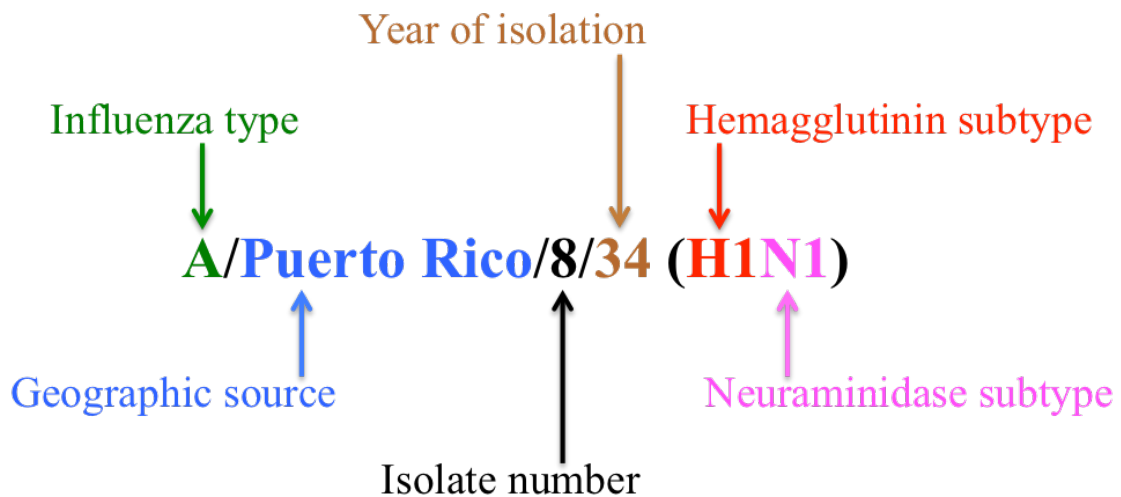


Figure 1.6: World Health Organization Influenza Nomenclature. Note: Influenza type B does not occur as subtypes. Image constructed using Microsoft® PowerPoint® for Mac 2011 v. 14.4.8 (150116).

The only seasonal vaccine recommended for high-risk populations is whole-inactivated split influenza virus. Individuals 65 years and over are recommended to receive the Fluzone high dose vaccine, which contains 4x more HA and represents a vaccine subgroup within whole-inactivated split influenza virus vaccines. A recent study

conducted in adults over the age of 65 showed the high dose vaccine to be 22% more effective than the standard seasonal vaccine (80). The CDC estimated the overall vaccine efficacy for influenza in 2013–2014 to be 61% (95% confidence interval = 52%–68%) (81), with lower efficacy in high-risk populations (81-83). Vaccine efficacy fluctuates depending on factors such as the year, virus type and population group. According to the current director of the CDC's NCIRD, Anne Schuchat, the 2013–2014 influenza vaccine was 67% effective in children aged six months–17 years, 60% effective in adults aged 18–64 years and 52% effective in seniors over the age of 65. Although 52% effectiveness may seem unacceptably low, 52% is an improvement from the 2012-2013 vaccine which was only 32% effective in seniors (84). In addition to high-risk populations being at greater risk of developing complications from influenza infection (85-87), they typically have decreased protection from vaccination. Thus, there is a tremendous need for new vaccine delivery methods and/or adjuvants capable of significantly improving immunogenicity and efficacy of seasonal influenza vaccines for use in high-risk populations (88-91).

In contrast to healthy adults under the age of 65, infections in high-risk populations, such as the elderly, the very young and the immune compromised, often lead to more severe and potentially life-threatening complications (76, 82, 83, 92, 93). Due to their heightened risk, the only seasonal vaccine recommended to these individuals is intramuscular injection of whole-inactivated virus, which is only marginally effective in high-risk populations. Regular vaccination against annual epidemics remains the most effective prevention and as such, there is tremendous need for new vaccine delivery methods and/or adjuvants, capable of significantly improving immunogenicity and

efficacy of seasonal influenza vaccines that remains safe for use in high-risk populations (73, 88-91, 94).

1.6 References

1. Gross CP & Sepkowitz KA (1998) The myth of the medical breakthrough: smallpox, vaccination, and Jenner reconsidered. *International journal of infectious diseases : IJID : official publication of the International Society for Infectious Diseases* 3(1):54-60.
2. Carrell JL (2003) *The speckled monster : a historical tale of battling smallpox* (Dutton, New York) pp xvii, 474 p.
3. Riedel S (2005) Edward Jenner and the history of smallpox and vaccination. *Proceedings* 18(1):21-25.
4. Barquet N & Domingo P (1997) Smallpox: the triumph over the most terrible of the ministers of death. *Annals of internal medicine* 127(8 Pt 1):635-642.
5. Smith KA (2011) Edward Jenner and the small pox vaccine. *Frontiers in immunology* 2:21.
6. Jenner E (1863) *On the Origin of the Vaccine Inoculation* (G. Elsie).
7. Delany I, Rappuoli R, & De Gregorio E (2014) Vaccines for the 21st century. *EMBO molecular medicine* 6(6):708-720.
8. Enders JF, Weller TH, & Robbins FC (1949) Cultivation of the Lansing Strain of Poliomyelitis Virus in Cultures of Various Human Embryonic Tissues. *Science (New York, N.Y.)* 109(2822):85-87.
9. Pasteur L (1880) De l'attenuation du virus du cholera des poules. *CR Acad. Sci. Paris* 91:673-680.
10. Sabin AB, Hennessen WA, & Winsser J (1954) Studies on variants of poliomyelitis virus. I. Experimental segregation and properties of avirulent variants of three immunologic types. *J Exp Med* 99(6):551-576.
11. Koff WC, *et al.* (2013) Accelerating Next-Generation Vaccine Development for Global Disease Prevention. *Science (New York, N.Y.)* 340(6136).
12. Hilleman MR, Buynak EB, Weibel RE, & Stokes J, Jr. (1968) Live, attenuated mumps-virus vaccine. *The New England journal of medicine* 278(5):227-232.
13. Plotkin SA, Farquhar JD, Katz M, & Buser F (1969) Attenuation of RA 27-3 rubella virus in WI-38 human diploid cells. *Am J Dis Child* 118(2):178-185.

14. Salk JE, *et al.* (1954) Formaldehyde treatment and safety testing of experimental poliomyelitis vaccines. *Am J Public Health Nations Health* 44(5):563-570.
15. Hilleman MR, *et al.* (1968) Development and evaluation of the Moraten measles virus vaccine. *Jama* 206(3):587-590.
16. D'Argenio DA & Wilson CB (2010) A decade of vaccines: Integrating immunology and vaccinology for rational vaccine design. *Immunity* 33(4):437-440.
17. Stanley Plotkin WO, Paul Offit, Susan L. Plotkin, Claire-Anne Siegrist, *et. al.*, (2012) *Vaccines* (ExpertConsult.com) 6 Ed p 1392.
18. Anonymous (Vaccines (immunizations) - overview. ed Neil K. Kaneshiro M, MHA, Clinical Assistant Professor of Pediatrics, University of Washington School of Medicine and A.D.A.M. Health Solutions, Ebix, Inc., Editorial Team: David Zieve, MD, MHA, Bethanne Black, Stephanie Slon, and Nissi Wang. (U.S. National Library of Medicine from the National Institutes of Health National Institutes of Health, MedlinePlus).
19. Hoebe K, Janssen E, & Beutler B (2004) The interface between innate and adaptive immunity. *Nature immunology* 5(10):971-974.
20. Pashine A, Valiante NM, & Ulmer JB (2005) Targeting the innate immune response with improved vaccine adjuvants. *Nat Med* 11(4 Suppl):S63-68.
21. Casadevall A (2004) The methodology for determining the efficacy of antibody-mediated immunity. *Journal of immunological methods* 291(1-2):1-10.
22. Guy B (2007) The perfect mix: recent progress in adjuvant research. *Nature reviews. Microbiology* 5(7):505-517.
23. Awate S, Babiuk LA, & Mutwiri G (2013) Mechanisms of action of adjuvants. *Frontiers in immunology* 4:114.
24. Reed SG, Orr MT, & Fox CB (2013) Key roles of adjuvants in modern vaccines. *Nat Med* 19(12):1597-1608.
25. Marrack P, McKee AS, & Munks MW (2009) Towards an understanding of the adjuvant action of aluminium. *Nature reviews. Immunology* 9(4):287-293.
26. Lambrecht BN, Kool M, Willart MA, & Hammad H (2009) Mechanism of action of clinically approved adjuvants. *Current opinion in immunology* 21(1):23-29.
27. De Gregorio E, Tritto E, & Rappuoli R (2008) Alum adjuvant activity: unraveling a century old mystery. *European journal of immunology* 38(8):2068-2071.

28. Miyaji EN, Carvalho E, Oliveira ML, Raw I, & Ho PL (2011) Trends in adjuvant development for vaccines: DAMPs and PAMPs as potential new adjuvants. *Brazilian journal of medical and biological research = Revista brasileira de pesquisas medicas e biologicas / Sociedade Brasileira de Biofisica ... [et al.]* 44(6):500-513.
29. Eng NF, Bhardwaj N, Mulligan R, & Diaz-Mitoma F (2013) The potential of 1018 ISS adjuvant in hepatitis B vaccines: HEPLISAV review. *Human vaccines & immunotherapeutics* 9(8):1661-1672.
30. Klinman DM, Yi AK, Beaucage SL, Conover J, & Krieg AM (1996) CpG motifs present in bacteria DNA rapidly induce lymphocytes to secrete interleukin 6, interleukin 12, and interferon gamma. *Proceedings of the National Academy of Sciences of the United States of America* 93(7):2879-2883.
31. Klaschik S, Tross D, Shirota H, & Klinman DM (2010) Short- and long-term changes in gene expression mediated by the activation of TLR9. *Molecular immunology* 47(6):1317-1324.
32. Principi N & Esposito S (2012) Adjuvanted influenza vaccines. *Human vaccines & immunotherapeutics* 8(1):59-66.
33. Zuccotti GV, *et al.* (2011) Long-lasting immunogenicity and safety of a 2009 pandemic influenza A(H1N1) MF59-adjuvanted vaccine when co-administered with a 2009-2010 seasonal influenza vaccine in young patients with type 1 diabetes mellitus. *Diabetic medicine : a journal of the British Diabetic Association* 28(12):1530-1536.
34. Behzad H, *et al.* (2012) GLA-SE, a synthetic toll-like receptor 4 agonist, enhances T-cell responses to influenza vaccine in older adults. *J Infect Dis* 205(3):466-473.
35. Clegg CH, *et al.* (2012) Adjuvant solution for pandemic influenza vaccine production. *Proceedings of the National Academy of Sciences of the United States of America* 109(43):17585-17590.
36. Coler RN, *et al.* (2010) A synthetic adjuvant to enhance and expand immune responses to influenza vaccines. *PloS one* 5(10):e13677.
37. Manon M.J. Cox PSC (Safety and Immunogenicity of PanBlok Influenza Vaccine in Healthy Adults. (ClinicalTrials.gov).
38. Easterbrook JD, *et al.* (2012) Protection against a lethal H5N1 influenza challenge by intranasal immunization with virus-like particles containing 2009 pandemic H1N1 neuraminidase in mice. *Virology* 432(1):39-44.
39. Deng MP, Hu ZH, Wang HL, & Deng F (2012) Developments of subunit and VLP vaccines against influenza A virus. *Virologica Sinica* 27(3):145-153.

40. Hossain MJ, *et al.* (2011) Virus-like particle vaccine containing hemagglutinin confers protection against 2009 H1N1 pandemic influenza. *Clinical and vaccine immunology : CVI* 18(12):2010-2017.
41. Rosenkrands I, *et al.* (2011) Enhanced humoral and cell-mediated immune responses after immunization with trivalent influenza vaccine adjuvanted with cationic liposomes. *Vaccine* 29(37):6283-6291.
42. Even-Or O, *et al.* (2011) A new intranasal influenza vaccine based on a novel polycationic lipid-ceramide carbamoyl-spermine (CCS). II. Studies in mice and ferrets and mechanism of adjuvanticity. *Vaccine* 29(13):2474-2486.
43. Dong L, *et al.* (2012) Cationic liposome-DNA complexes (CLDC) adjuvant enhances the immunogenicity and cross-protective efficacy of a pre-pandemic influenza A H5N1 vaccine in mice. *Vaccine* 30(2):254-264.
44. Jorquera PA, *et al.* (2013) Nanoparticle vaccines encompassing the respiratory syncytial virus (RSV) G protein CX3C chemokine motif induce robust immunity protecting from challenge and disease. *PloS one* 8(9):e74905.
45. Lee JW, Choi SO, Felner EI, & Prausnitz MR (2011) Dissolving microneedle patch for transdermal delivery of human growth hormone. *Small (Weinheim an der Bergstrasse, Germany)* 7(4):531-539.
46. Mooney AJ, Li Z, Gabbard JD, He B, & Tompkins SM (2013) Recombinant parainfluenza virus 5 vaccine encoding the influenza virus hemagglutinin protects against H5N1 highly pathogenic avian influenza virus infection following intranasal or intramuscular vaccination of BALB/c mice. *Journal of virology* 87(1):363-371.
47. Cornelissen LA, *et al.* (2012) Protective Efficacy of Newcastle Disease Virus Expressing Soluble Trimeric Hemagglutinin against Highly Pathogenic H5N1 Influenza in Chickens and Mice. *PloS one* 7(8):e44447.
48. Hashem A, *et al.* (2012) Subcutaneous immunization with recombinant adenovirus expressing influenza A nucleoprotein protects mice against lethal viral challenge. *Human vaccines & immunotherapeutics* 8(4):425-430.
49. Nkolola JP, *et al.* (Comparison of multiple adjuvants on the stability and immunogenicity of a clade C HIV-1 gp140 trimer. *Vaccine* (0).
50. Mauricio AA, *et al.* (2012) Glucopyranosyl Lipid Adjuvant (GLA), a Synthetic TLR4 Agonist, Promotes Potent Systemic and Mucosal Responses to Intranasal Immunization with HIVgp140. *PloS one* 7(7).
51. Zhang X, Wu D, & Chu CC (2004) Synthesis and characterization of partially biodegradable, temperature and pH sensitive Dex-MA/PNIPAAm hydrogels. *Biomaterials* 25(19):4719-4730.

52. Tran NQ, Joung YK, Lih E, Park KM, & Park KD (2010) Supramolecular hydrogels exhibiting fast in situ gel forming and adjustable degradation properties. *Biomacromolecules* 11(3):617-625.
53. Park KA & Joynt R (1993) Photoemission and tunneling as tests for fluctuating superconductivity above T_c in high- T_c superconductors. *Phys Rev B Condens Matter* 48(22):16833-16836.
54. Namdeo M, Bajpai SK, & Kakkar S (2009) Preparation of a magnetic-field-sensitive hydrogel and preliminary study of its drug release behavior. *J Biomater Sci Polym Ed* 20(12):1747-1761.
55. Hoffman AS (2002) Hydrogels for biomedical applications. *Advanced drug delivery reviews* 54(1):3-12.
56. Zhang L, *et al.* (2014) Preparation of novel biodegradable pHEMA hydrogel for a tissue engineering scaffold by microwave-assisted polymerization. *Asian Pacific journal of tropical medicine* 7(2):136-140.
57. Balakrishnan B & Banerjee R (2011) Biopolymer-based hydrogels for cartilage tissue engineering. *Chemical reviews* 111(8):4453-4474.
58. Zustiak SP, Pubill S, Ribeiro A, & Leach JB (2013) Hydrolytically degradable poly(ethylene glycol) hydrogel scaffolds as a cell delivery vehicle: Characterization of PC12 cell response. *Biotechnology progress* 29(5):1255-1264.
59. Sexton A, *et al.* (2009) A protective vaccine delivery system for in vivo T cell stimulation using nanoengineered polymer hydrogel capsules. *ACS nano* 3(11):3391-3400.
60. Chong SF, *et al.* (2009) A paradigm for peptide vaccine delivery using viral epitopes encapsulated in degradable polymer hydrogel capsules. *Biomaterials* 30(28):5178-5186.
61. Coeshott CM, *et al.* (2004) Pluronic F127-based systemic vaccine delivery systems. *Vaccine* 22(19):2396-2405.
62. Rudra JS, Tian YF, Jung JP, & Collier JH (2010) A self-assembling peptide acting as an immune adjuvant. *Proceedings of the National Academy of Sciences of the United States of America* 107(2):622-627.
63. Chesson CB, *et al.* (2014) Antigenic peptide nanofibers elicit adjuvant-free CD8(+) T cell responses. *Vaccine* 32(10):1174-1180.
64. Rudra JS, *et al.* (2012) Self-assembled peptide nanofibers raising durable antibody responses against a malaria epitope. *Biomaterials* 33(27):6476-6484.

65. Kim YC, Park JH, & Prausnitz MR (2012) Microneedles for drug and vaccine delivery. *Advanced drug delivery reviews* 64(14):1547-1568.
66. Alarcon JB, Hartley AW, Harvey NG, & Mikszta JA (2007) Preclinical evaluation of microneedle technology for intradermal delivery of influenza vaccines. *Clinical and vaccine immunology : CVI* 14(4):375-381.
67. Ansaldi F, *et al.* (2012) Intanza((R)) 15 mcg intradermal influenza vaccine elicits cross-reactive antibody responses against heterologous A(H3N2) influenza viruses. *Vaccine* 30(18):2908-2913.
68. Mooney AJ, Li Z, Gabbard JD, He B, & Tompkins SM (2012) Recombinant PIV5 vaccine encoding the influenza hemagglutinin protects against H5N1 highly pathogenic avian influenza virus infection following intranasal or intramuscular vaccination of BALB/c mice. *Journal of virology*.
69. Nelson MI, *et al.* (2006) Stochastic processes are key determinants of short-term evolution in influenza A virus. *PLoS Pathog* 2(12):e125.
70. Lo RY (2001) Genetic analysis of virulence factors of Mannheimia (Pasteurella) haemolytica A1. *Vet Microbiol* 83(1):23-35.
71. Sou T, *et al.* (2011) New developments in dry powder pulmonary vaccine delivery. *Trends in biotechnology* 29(4):191-198.
72. NIAID (Flu (Influenza): 2009 H1N1, Seasonal, Avian (Bird), Pandemic.
73. WHO (2003) Influenza. (WHO).
74. Goldstein E, Viboud C, Charu V, & Lipsitch M (2012) Improving the estimation of influenza-related mortality over a seasonal baseline. *Epidemiology (Cambridge, Mass.)* 23(6):829-838.
75. Steininger C, *et al.* (2003) Acute encephalopathy associated with influenza A virus infection. *Clinical infectious diseases : an official publication of the Infectious Diseases Society of America* 36(5):567-574.
76. Rothberg MB, Haessler SD, & Brown RB (2008) Complications of Viral Influenza. *The American journal of medicine* 121(4):258-264.
77. Lambert ND, Ovsyannikova IG, Pankratz VS, Jacobson RM, & Poland GA (2012) Understanding the immune response to seasonal influenza vaccination in older adults: a systems biology approach. *Expert review of vaccines* 11(8):985-994.
78. Forthal DN & Moog C (2009) Fc receptor-mediated antiviral antibodies. *Current opinion in HIV and AIDS* 4(5):388-393.

79. Bai Y, *et al.* (2011) Intracellular neutralization of viral infection in polarized epithelial cells by neonatal Fc receptor (FcRn)-mediated IgG transport. *Proceedings of the National Academy of Sciences of the United States of America* 108(45):18406-18411.
80. Izurieta HS, *et al.* (Comparative effectiveness of high-dose versus standard-dose influenza vaccines in US residents aged 65 years and older from 2012 to 2013 using Medicare data: a retrospective cohort analysis. *The Lancet Infectious Diseases* 15(3):293-300.
81. Flannery B, *et al.* (2014) Interim estimates of 2013-14 seasonal influenza vaccine effectiveness - United States, February 2014. *MMWR. Morbidity and mortality weekly report* 63(7):137-142.
82. Couch RB, *et al.* (1986) Influenza: its control in persons and populations. *J Infect Dis* 153(3):431-440.
83. Yoshikawa TT (1981) Important infections in elderly persons. *West J Med* 135(6):441-445.
84. Lowes R (2.20.2014) Flu Vaccine More Effective Than Last Year's, CDC Says. in *Medscape Medical News* (Medscape Medical News © 2014 WebMD, LLC <http://www.medscape.com/viewarticle/820908>).
85. Webster RG (2000) Immunity to influenza in the elderly. *Vaccine* 18(16):1686-1689.
86. Powers DC & Belshe RB (1993) Effect of age on cytotoxic T lymphocyte memory as well as serum and local antibody responses elicited by inactivated influenza virus vaccine. *J Infect Dis* 167(3):584-592.
87. Simonsen L, Taylor RJ, Viboud C, Miller MA, & Jackson LA (2007) Mortality benefits of influenza vaccination in elderly people: an ongoing controversy. *Lancet Infect Dis* 7(10):658-666.
88. Weinberger B & Grubeck-Loebenstien B (2012) Vaccines for the elderly. *Clinical microbiology and infection : the official publication of the European Society of Clinical Microbiology and Infectious Diseases* 18 Suppl 5:100-108.
89. Lang PO, *et al.* (2012) Effectiveness of influenza vaccine in aging and older adults: comprehensive analysis of the evidence. *Clinical interventions in aging* 7:55-64.
90. Vesikari T, Pepin S, Kusters I, Hoffenbach A, & Denis M (2012) Assessment of squalene adjuvanted and non-adjuvanted vaccines against pandemic H1N1 influenza in children 6 mo to 17 y of age. *Human vaccines & immunotherapeutics* 8(9).

91. Esposito S, *et al.* (2012) Preventing influenza in younger children. *Clinical microbiology and infection : the official publication of the European Society of Clinical Microbiology and Infectious Diseases* 18 Suppl 5:42-49.
92. Janssens JP & Krause KH (2004) Pneumonia in the very old. *Lancet Infect Dis* 4(2):112-124.
93. Stott DJ, Carman WF, & Elder AG (2001) Influenza in old age. *Age Ageing* 30(5):361-363.
94. Son J, *et al.* (2012) Immunogenicity of low-dose MF59-adjuvanted 2009 influenza A/H1N1 vaccine in dialysis patients. *Clinical and experimental nephrology*.

CHAPTER 2

VACCINE SELF-ASSEMBLING IMMUNE MATRIX (VacSIM™)

2.1 The (RADA)4 Synthetic Oligopeptide and Commercial Product PuraMatrix®

RADA-based synthetic self-assembling nanofibers scaffolds (SANS) were originally conceived and patented in 1993 by Dr. Shuguang Zhang (1-3), while a student at MIT in the lab of Dr. Alexander Rich, the esteemed biologist and Professor of Biophysics at both MIT and Harvard University (4). Synthetic (RADA)4 was designed to imitate the amphiphilic segment of naturally occurring EAKA 16-II

(EAEAKAKAEAEAKAKA), found in the yeast Zuotin protein. Known as both RADA16-I and (RADA)4, this engineered biomaterial was named for its composition

(RADARADARADARADA) of a repeating, alternatively charged, 16 amino acid (arginine=R, alanine=A, aspartic acid=D) sequence (Figure 2.1)

(5). When exposed to water, these peptides form stable beta-sheets with

distinct polar and non-polar surfaces due to the alternating ionic, hydrophilic and

hydrophobic amino acid repeats (Figure 2.2) (2, 6). Under physiologic conditions of

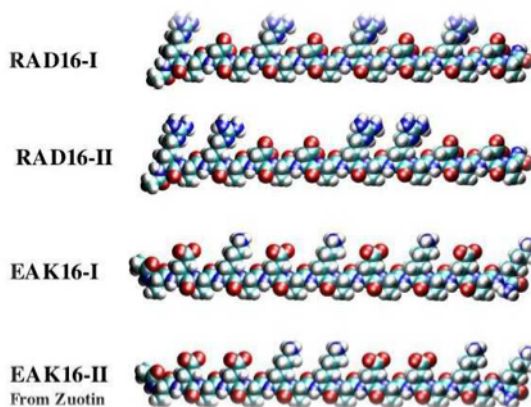


Figure 2.1: Molecular models of the RADA16-I, RADA16-II, EAK16-I and EAK16-II self-assembling peptides. Each molecule is ~5nm in length with 8 alanines on one side and 4 negative and 4 positive charge amino acids in an alternating arrangement on the other side. Reprinted (5) with permission of Taylor and Francis Group LLC, Copyright (2005).

salinity, beta-sheets continue self-assembly into hydrated nanofibers, on a scale similar to extracellular matrix, generating a highly organized and three-dimensional, porous scaffold (Figure 2.3) (7, 8). Depending on the concentration, the resulting nanofibers have a diameter range between 10-20 nm and three-dimensional scaffold pore sizes can range in diameter from 5-200 nm (5).

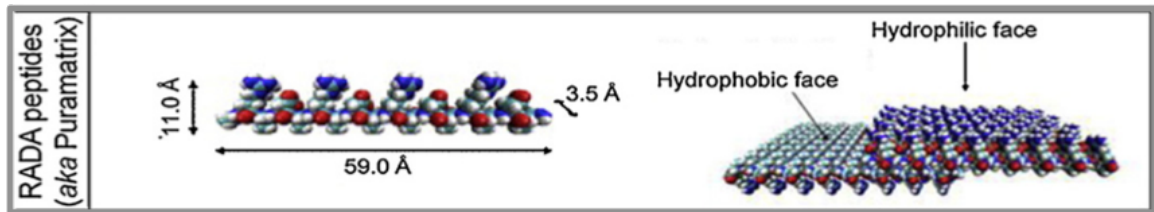


Figure 2.2: Schematic of design strategies (left) and assembled structures (right) for selected engineered peptide and protein materials. (A) Four repeats of the RADA amino acid sequence form peptides that self-assemble based on electrostatic and hydrophilic/hydrophobic interactions to form a 3D hydrogel. Originally published in the *Journal of Controlled Release* (2) copyright (2006) and modified for *Neuroscience letters*, (6) Copyright (2012). Reprinted with permission from Elsevier.

In 2002 the RADA-based patents (US 5,670,483, US 5,955,343, US 2002/0160471, WO 02/062969) were acquired by 3-D Matrix Inc., and the synthetic (RADA)₄ self-assembling peptide (SAP) was further developed and commercialized. The product known as PuraMatrix™ Peptide Hydrogel was initially marketed to researchers as a synthetic matrix for use in cell culture experiments requiring defined three-dimensional microenvironments both *in vivo* and *ex vivo* (9) (Corning® Inc., product no. 354250). PuraMatrix™ Peptide Hydrogel is produced and quality tested by 3-D Matrix Inc. according to proprietary protocols, which incorporate F-MOC solid-phase peptide synthesis, aseptic fill-finish, liquid formulation and sterile filtration. The final product is available as a transparent, 1% solution of aqueous peptide, which is both biocompatible

and resorbable. Solutions of the (RADA)4 oligopeptide have undergone third party testing, demonstrating no reactogenicity or toxicity (10), leading to clinical trials for multiple applications including, wound healing, tissue repair (11) and as scaffolding for dental implants (12, 13). 3D Matrix Inc. has expanded their product line and now includes PuraStat® Synthetic Surgical Hemostatic Agent (2.5% semi-viscous aqueous peptide) and a clinical-grade version of the original peptide hydrogel, sold as PuraMatrix GMP®.

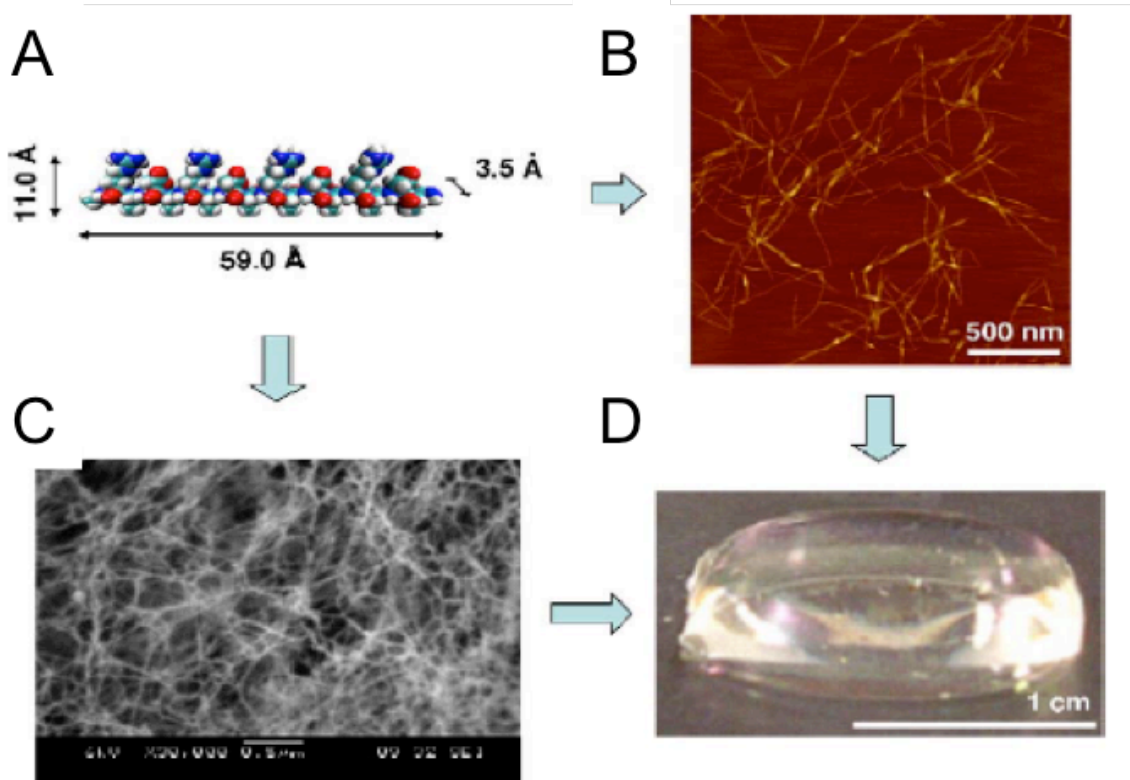


Figure 2.3: The self-assembling peptide scaffold. (A) Molecular model of RADA16, the dimensions of which are 59.0 Å x 11.0 Å x 3.5 Å. For the representation the VMD software was used: cyan, carbons; red, oxygen; blue, nitrogen; white, hydrogen. (B) AFM image of the RADA16 nanofibers. (C) SEM image of the RADA16 hydrogel. (D) Image of the RADA16 hydrogel with high water content, i.e., N99.5% w/v (photograph by Dr. Hidenori Yokoi). Reprinted from the Journal of Controlled Release (2) with permission from Elsevier.

2.2 Vaccine Delivery Conception

The base-concept that initiated and eventually led to development of the vaccine delivery platform technology, VacSIM™, was proposed as a strategy to increase antigen presenting cell activation and maturation via presentation of vaccine components as particulates, or a porous 3D scaffold. Particulate vaccine components and/or 3D porous scaffold presentation of vaccine components should increase vaccine antigen persistence, and antigen persistence is thought to contribute to the duration of immune memory. Initially, a semi-viscous commercial extracellular matrix (ECM) material known as Matrigel (BD™ Matrigel™ Basement Membrane Matrix (currently available as Corning® Matrigel® matrix) was obtained and tested, in an attempt to enhance vaccine immunogenicity. Matrigel is a preparation of solubilized basement membrane originating from Engelbreth-Holm-Swarm (EHS) mouse sarcoma. According to the manufacturer, the Matrigel™ preparation contains laminin, collagen IV, heparan sulfate proteoglycans, nitrogen, TGF-β and various growth factors including epidermal, insulin-like and fibroblast.

The first vaccine study employing this strategy, utilized a purified, recombinant *Schistosoma mansoni* circulating cathodic antigen (CCA) as vaccine antigen delivered to mice in the BD™ cell culture product, Matrigel™ Basement Membrane Matrix to produce monoclonal antibodies to CCA (14). The Grenfell study demonstrated the superiority of Matrigel to deliver schistosome CCA as compared to other vaccine delivery methods/adjuvants. A separate experiment was designed to test Matrigel® delivery of recombinant Hepatitis B surface antigen (rHepBsAg). As hypothesized, Matrigel™ was an effective adjuvant delivery system, inducing potent antigen specific

antibody responses, not seen in mice vaccinated with rHepBsAg in Complete Freund's Adjuvant (CFA)(15).

Concerned that the basement membrane matrix molecules, contained in Matrigel™ would prevent further development of this 3D porous matrix approach of vaccine delivery for use in human vaccines, a synthetic alternative was preferable. Additionally, it was unclear whether the components within Matrigel™ could be responsible for the adjuvanted response, rather than the physical properties of the membrane-matrix leading to persistence of antigen. The BD™ available product, PuraMatrix™ Peptide Hydrogel was proposed as a possible alternative to Matrigel. PuraMatrix™ is simply a 1% solution of the (RADA)4 synthetic oligopeptide in sterile solution and thus represented a far less complicated delivery system. The results indicated that in Th2-biased BALB/c mice, inclusion of PuraMatrix™ increased specific antibody levels in the sera and were maintained out to five weeks post prime, compared to mice receiving rHBsAg alone, in combination with Matrigel™ or adjuvanted with Alum, CFA or CpG-ODN (Figure 2.4) (15) (full text in Appendix A).

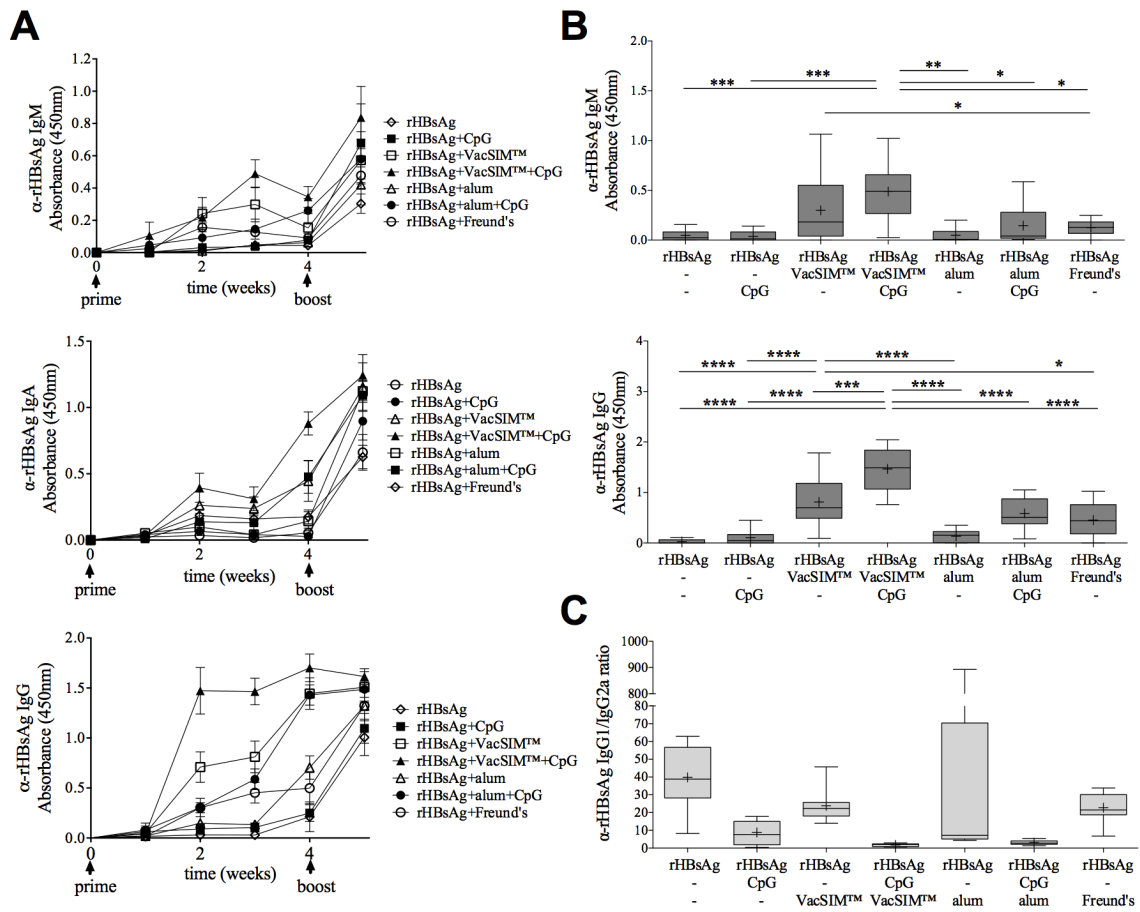


Figure 2.4: rHepBsAg-specific humoral responses are enhanced and sustained by VacSIMTM. (A) Kinetic evaluation of rHBsAg-specific IgA, IgM and IgG antibodies in sera of immunized BALB/c mice (n=10, pooled from 2 independent experiments) were determined by ELISA. Immunization times are indicated by arrowheads. (B) rHBsAg-specific IgM (upper panel) and IgG (lower panel) levels from sera collected 21 days post-immunization. (C) The IgG1:IgG2a ratio was determined at 35 days post-immunization. Statistical differences (*p<0.05, **p<0.01, ***p<0.001, ****p<0.0001) were determined by two-way ANOVA with Bonferroni post-test. Copyright © American Society for Microbiology (15) full text in Appendix A.

2.3 Developing a Vaccine Platform Technology

The use of PuraMatrix® to deliver vaccines was not an anticipated application by 3D-Matrix Inc., and is therefore an innovative application of this technology. The trademarked name “VacSIMTM” stands for Vaccine Self-assembling Immune Matrix and

refers to the vaccine delivery method (patents-pending) being evaluated. VacSIM™ is comprised of a 1.0% solution of PuraMatrix®, which is easily combined with other vaccine components through simple mixing. The results presented in this dissertation outline the initial experiments utilized for evaluation and development of VacSIM™ as a vaccine delivery platform, with specific emphasis on assessing its ability to improve immunogenicity and vaccine efficacy (VE) of a whole-inactivated influenza vaccine, in a murine model.

Additional experiments were necessary to evaluate whether a similar immune effect could be generated with an alternative antigen and ultimately, whether this new method could be further developed and broadly utilized as a vaccine delivery platform. Immunized mice were vaccinated with either rHBsAg or influenza recombinant nucleoprotein (rNP), via subcutaneous (s.c.) injection, following the previous schedule (boost 3 weeks after prime) and utilizing both Th1- and Th2-biased mouse models (C57BL/6 and BALB/c). Protein-specific IgG and IgA endpoint titers from sera collected 3 weeks post prime were used to compare naïve and vaccinated (Ag+Alum, Ag+CpG, Ag+CpG+VacSIM™). The results from these experiments confirmed that immunizing mice with rHBsAg+CpG in VacSIM™ generates increased production of rHBsAg-specific antibodies (Figure 2.5) (15) (full text in Appendix A).

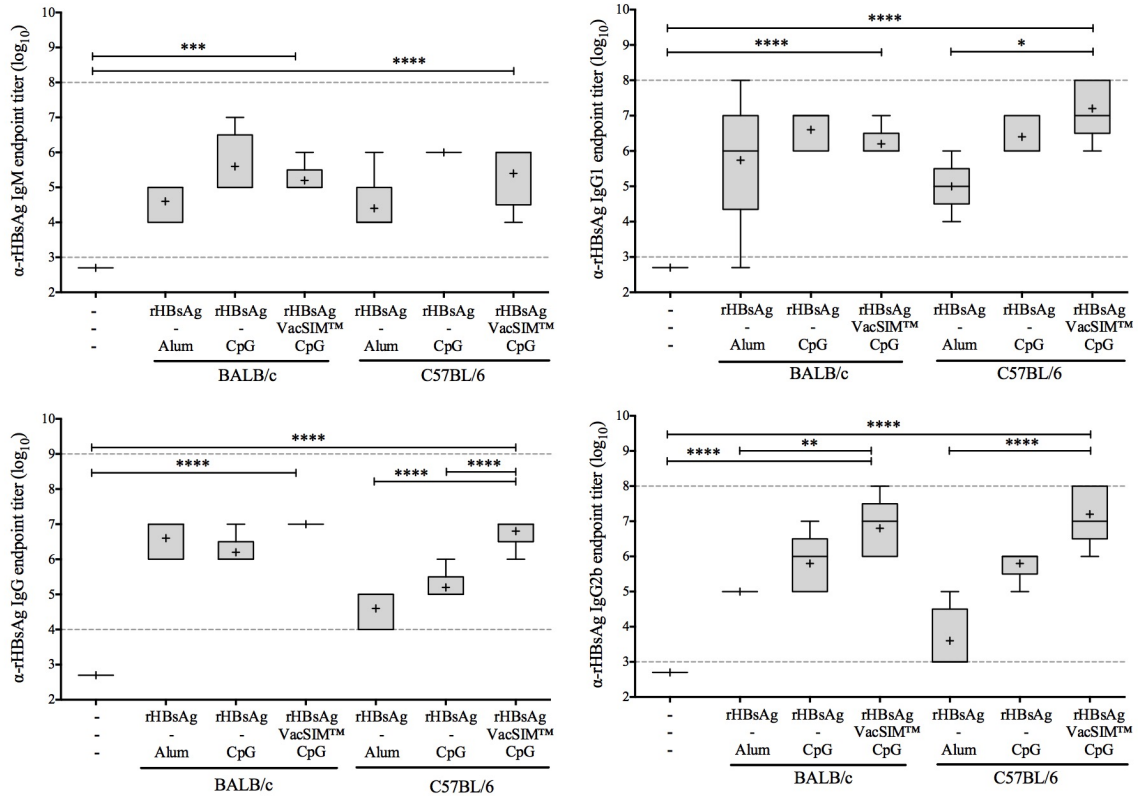


Figure 2.5: Immunization with VacSIM™ increases rHBsAg-specific antibody titers in both Th1- and Th2-biased mouse models. Comparison of rHBsAg-specific antibodies induced in mice immunized three weeks apart. There are 5 or 4 mice per group for immunized or naïve, respectively. There are only 3 IgM values for rHBsAg + CpG immunized C57BL/6 mice, as sera were limited. Sera was collected 3 weeks post boost and rHBsAg-specific IgM, IgG, IgG₁ and IgG_{2b} endpoint titers were determined by indirect ELISA. Dashed lines indicate detection limits of the assay. Statistical differences (*p<0.05, **p<0.01, ****p<0.0001) were determined by one-way ANOVA with Bonferroni post-test. Copyright © American Society for Microbiology (15) full text in Appendix A.

Elevated rNP-specific endpoint titers in mice vaccinated with rNP+CpG in

VacSIM™ indicates the immunogenicity effect is not confined to rHBsAg (Figure 2.6).

Additionally, because elevated titers are visible (Ag+CpG+VacSIM™) in both Th1- and

Th2-biased mouse models, the effect does not appear to be limited to either a Th1- or

Th2-predominant immune response (15). Taken together, these findings confirm that

VacSIM™, composed of the synthetic (RADA)4 oligopeptide PuraMatrix™, has the

potential for development as a vaccine delivery method. Figures 2.4-2.6 demonstrate successful delivery of recombinant protein antigen vaccines using VacSIM™. A vaccine delivery platform technology would require the flexibility to easily incorporate multiple different types of antigens (Table 1.1) and/or adjuvants (Table 1.4). In addition to recombinant protein antigens (rHBsAg, rNP, Ch.2) it was necessary to evaluate VacSIM™ delivery of live-attenuated antigens and inactivated virus particles (influenza, whole-inactivated PR8, X-31, Chapters 2-5).

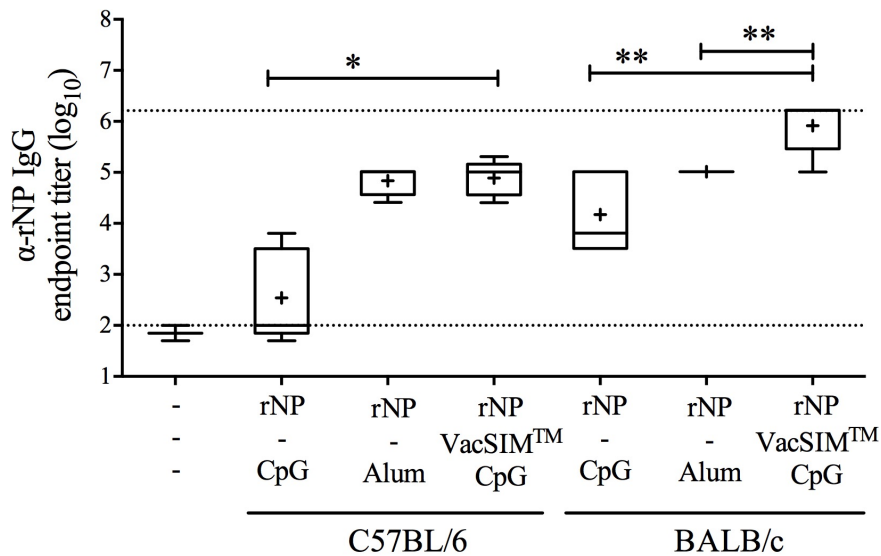


Figure 2.6: Immunization with VacSIM™ increases influenza protein-specific IgG endpoint titers in Th1-/Th2-biased mouse models. Comparison of rNP-specific antibodies induced in mice immunized three weeks apart (n=5 vaccine, n=4 naive). Sera were collected 3 weeks after boost and rNP-specific IgG endpoint titers were determined via indirect ELISA. Dashed lines indicate dilution thresholds of the assay. Representative of 2 independent experiments. Statistical differences (*p<0.05, **p<0.01) were determined by one-way ANOVA with Bonferroni post-test.

The precise mechanism by which VacSIM™ delivered vaccine components induce an immune response is still being investigated and will be discussed in more detail in Chapter 5. Numerous studies have found PuraMatrix®, when compared to other biodegradable hydrogels, to be less immunogenic and inflammatory and more biocompatible overall (3, 16-20). Additionally, in-house experiments (Chapter 3) indicate that VacSIM™ does not have inherent immunostimulatory activity. It is hypothesized that a key component of the mechanism to be the *in situ* construction of the vaccine gel matrix depot via hydrated nanofibers of the (RADA)4 oligopeptides. (Figure 2.7). Post-injection, under physiological conditions, VacSIM™ self-assembles, forming a porous and biodegradable gel-matrix depot of concentrated vaccine components. In addition to sustained antigen egress, the VacSIM™ depot may provide a stabilizing effect, delaying systemic degradation of vaccine components.

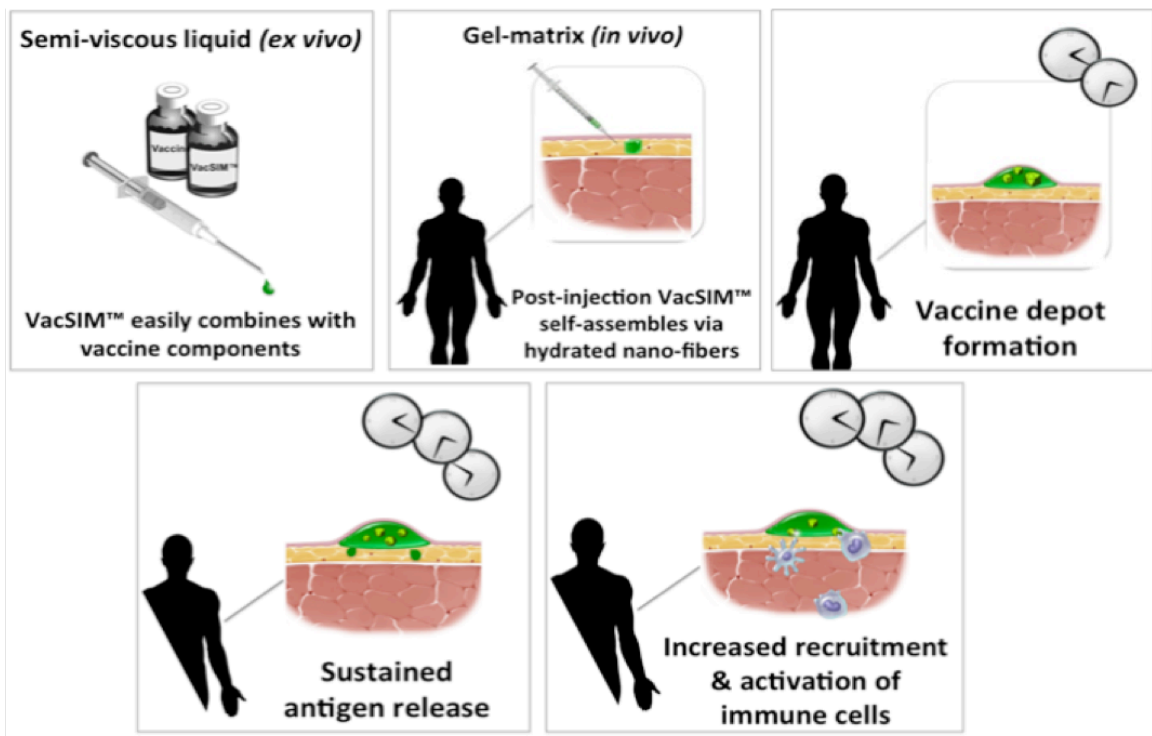


Figure 2.7: Proposed mechanism by which, VacSIM™ improves vaccine immunogenicity and efficacy.

As previously mentioned (Section 2.1), pore sizes of the assembled gel-matrix depot can be adjusted, simply by varying the (RADA)4 oligopeptide concentration in the vaccine. Therefore, depending on the overall size of vaccine antigens, the range of pore sizes in the VacSIM™ gel-matrix can be increased or made smaller by reducing or increasing the concentration of (RADA)4 respectively. Further, though not discussed here in detail, two alternative versions of the (RADA)4 oligopeptide exist to function more effectively with increased/decreased hydrophobic molecules (5). A recent study demonstrated *in situ*, that insulin delivered in PuraMatrix® led to the slow release of insulin over time (21). In regards to varying the pore sizes of the VacSIM gel-matrix, Figure 2.8 shows the varying diffusion results over time, comparing two different concentrations of VacSIM™, combined with a protein antigen (OVA) or WIV (PR8). In this study, a 1% and 0.5% concentration of VacSIM™ was compared to evaluate any effects of pore size on the two alternative antigens. In contrast to OVA, which diffused differentially at both VacSIM™ concentrations, WIV was unable to diffuse at either concentration (Figure 2.8). These results are consistent with *in vivo* results discussed in Chapter 3, showing ineffective protection after immunization of unadjuvanted PR8 (WIV) via VacSIM™ delivery. One explanation for why PR8 did not egress from the gel-matrix may involve PR8 being a formalin-inactivated whole virus preparation, thus viral antigens/particles/virions may be too large to diffuse through the gel-matrix pores. If the lack of diffusion of PR8 and other WIV preparations is a general phenomena, then whole inactivated preparations will require use of an adjuvant, such as CpG, which will diffuse through the gel-matrix pores, to recruit APCs to the localized vaccine depot.

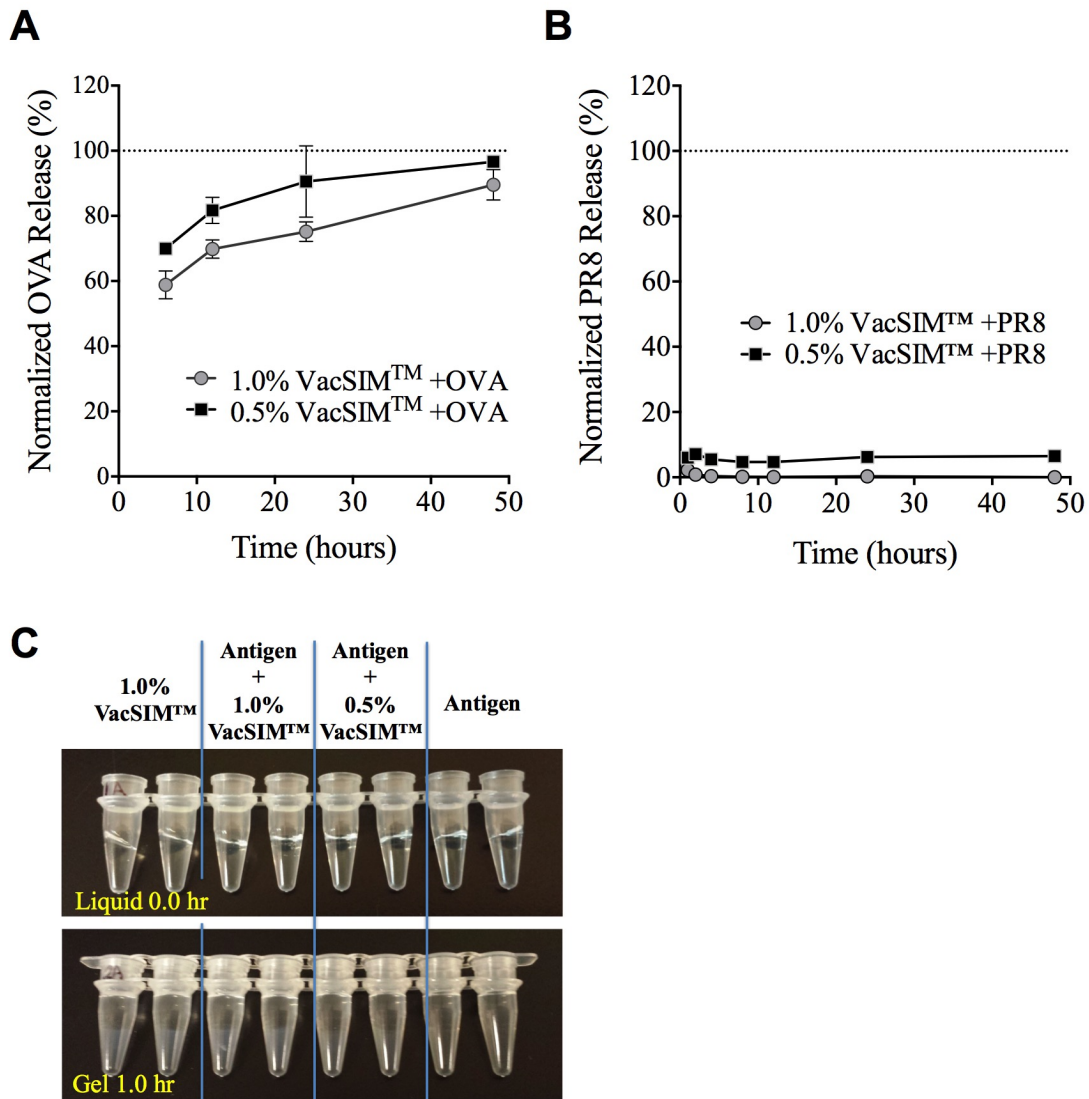


Figure 2.8: Antigen diffusion kinetics. Diffusion of ovalbumin (OVA) protein and influenza A/PR/8/34 (PR8) whole-inactivated virus (WIV) from a 0.5% or 1% VacSIM™ gel matrix, assembled *in vitro* (A-B). Supernatant samples were collected from PBS overlay out to 48 hours, and antigen diffusion was detected through α -OVA or α -PR8 indirect ELISA. Photographs show that following preparation, all samples remain liquid and appear more or less identical. After 1hr incubation, the VacSIM™ containing samples have transitioned to a gel phase, while the antigen-only samples remain liquid (C). Representative of 2 independent experiments.

The majority of influenza vaccines contain inactivated virus. Additionally this is the only type of vaccine recommended to populations with increased risk of developing

potentially life-threatening complications with influenza infection. Therefore, inactivated virus represents a crucial type of antigen to be further evaluated for increased immunogenicity and improved vaccine efficacy through VacSIM™ delivery. The following experiments were designed to evaluate the effect of incorporating various adjuvants with a whole-inactivated PR8 vaccine delivered in VacSIM™ by a single (s.c.) immunization. Antibody endpoint titers (IgM, IgA, IgE, IgG, IgG1, IgG2a, IgG2b, IgG3) were determined in sera harvested 4 weeks post vaccination (wpv), utilizing the C57/BL/6 mouse model (Figure 2.9), via indirect EILSA. Comparisons were made between groups receiving a PR8 (WIV) vaccine delivered in saline or in VacSIM™, unadjuvanted or in combination with CpG, or GLA variant prepared as aqueous solution (AQ501) or emulsion (EM582). The mentioned vaccine groups were also compared to relevant controls, including naïve and a group immunized with a vaccine containing PR8 and the emulsion vehicle used in EM582 delivered in VacSIM™ (EM081). All mice receiving adjuvanted vaccines had minimal levels of antigen specific IgM (naïve antibody) and IgE (allergic antibody). Unadjuvanted PR8 whether delivered in VacSIM™ or saline resulted in similar levels of specific antibody, except in the case of IgA (increased in VacSIM™) and total IgG (increased in saline). Among the adjuvants compared in combination with PR8 and VacSIM™ delivery, CpG was the most effective. The mean endpoint titers for mice receiving PR8+CpG in VacSIM™ showed increased, PR8-specific IgG, IgA and IgG3, compared to all other groups (Figure 2.9).

A separate experiment was designed to confirm that CpG was an ideal adjuvant for VacSIM™ delivery of whole-inactivated PR8 (Figure 2.9, A.4). Three new groups were added in addition to the vaccine groups described in Figure 2.9, in order to compare

mice immunized with PR8+Alum delivered in VacSIM™ or in saline and PR8+CpG+Alum delivered in saline (Figure 2.10). The combination of adjuvants CpG+Alum has been shown to be quite effective in a research setting (22, 23). Serum samples were collected from C57BL/6 mice at 4 wpv and anti-PR8 IgG endpoint titers were determined by indirect ELISA. Mice receiving an immunization of whole-inactivated PR8 and CpG delivered in VacSIM™ had significantly elevated antigen-specific antibody titers compared to all other vaccine groups (Figure 2.10A).

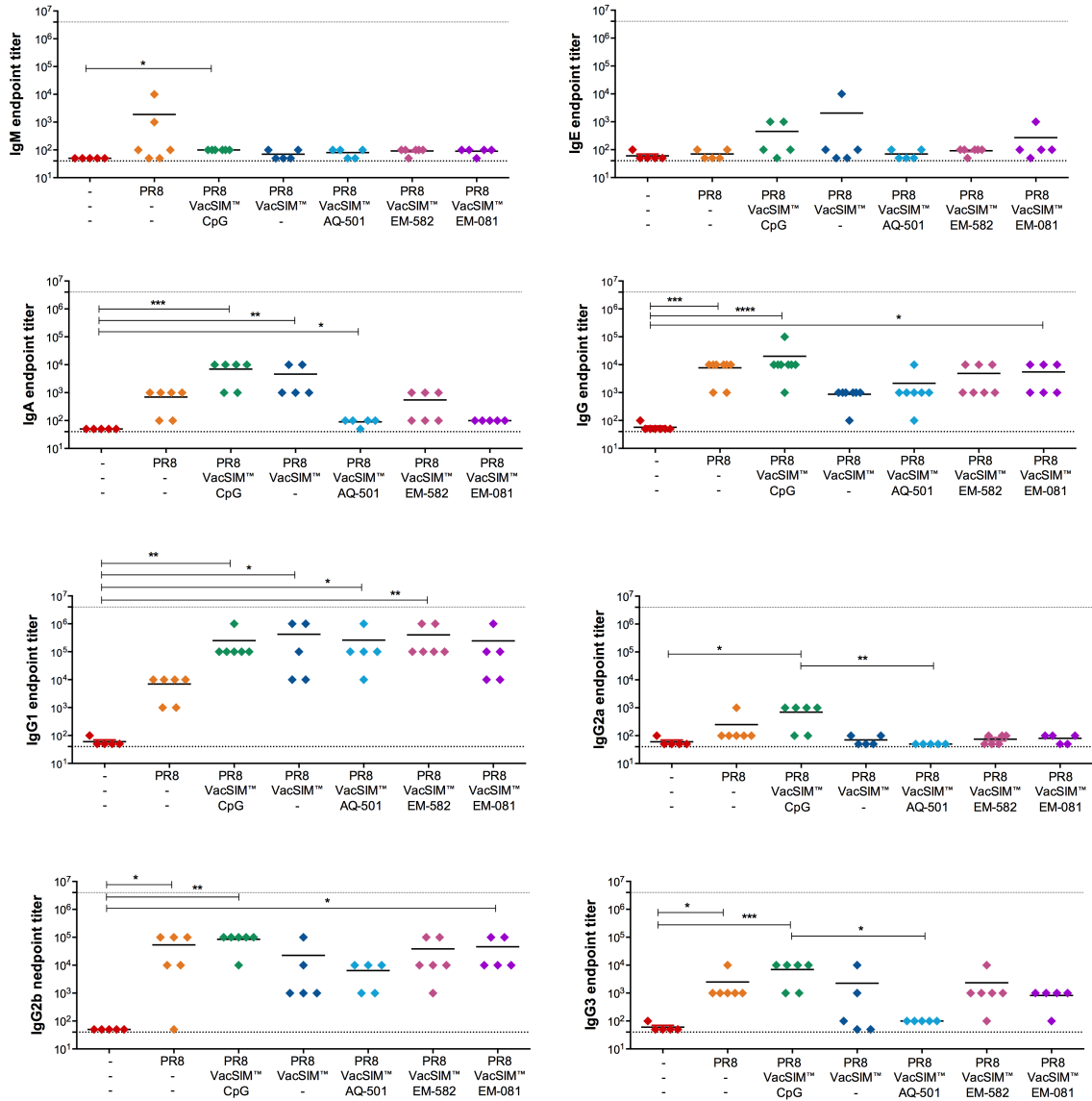


Figure 2.9: Influenza A/PR/8/34-specific isotype endpoint titers from adjuvanted and unadjuvanted vaccine groups. Sera were collected 4 weeks following a single s.c. vaccination and A/PR/8/34 (PR8)-specific IgM, IgE, IgA, IgG, IgG1, IgG2a, IgG2b and IgG3 endpoint titers determined by indirect ELISA. Dashed lines indicate detection thresholds of the experiment. Representative of 2 independent experiments. Statistical significance (*p<0.05, **p<0.01, ***p<0.001, ****p<0.0001) between vaccination groups was determined by 1-way ANOVA and Dunn's multiple comparisons test

Measuring antigen-specific antibodies provides vital information regarding antigen-specific vaccine immunogenicity and reactogenicity. Ideally, the increase in specific antibodies seen mice immunized with PR8+CpG delivered in VacSIM™ (Figure

2.10A) would correlate to a decrease in symptom severity (morbidity) as well as virus levels present in the lungs, following influenza challenge, compared to other vaccine groups. To determine whether antibody levels did in fact correlate to improved protection, all mice received an intranasal (i.n.) challenge with a lethal dose (1,000 LD₅₀) of homologous influenza virus (A/PR/8/34) at 4 wpv. Following challenge, mice were monitored daily to evaluate variations in symptom severity between vaccine groups. In addition to monitoring changes in weight, a daily morbidity score was determined for each individual, which represented their cumulative symptoms for each day post-challenge (Figure 2.10B). The results indicated a clustering of four different vaccine groups, which maintained minimal weight loss and morbidity out to 4 days post challenge (dpc). These groups receiving PR8+CpG delivered in VacSIM™ and PR8, PR8+Alum, or PR8+Alum+CpG all delivered in saline. Finally, to determine whether decreased weight loss and morbidity would correlate to viral clearance and as a measure of vaccine efficacy, individual viral lung titers were evaluated by plaque assay at 4 dpc (Figure 2.10C). The clearance results indicated that mice immunized with whole-inactivated PR8+CpG delivered in VacSIM™ were more effective at clearing virus than naïve mice and those receiving unadjuvanted PR8, regardless of whether it was delivered in saline or VacSIM™. All of the mice in the PR8+Alum and PR8+Alum+CpG in saline had undetectable levels of virus and are clearly performing as effective adjuvants to the whole-inactivated PR8 vaccine. However, when comparing all of the adjuvanted vaccines that were delivered using VacSIM™, CpG remains the preferred adjuvant with all but one of the mice showing undetectable levels of virus in the lungs at 4 dpc (Figure 2.10C).

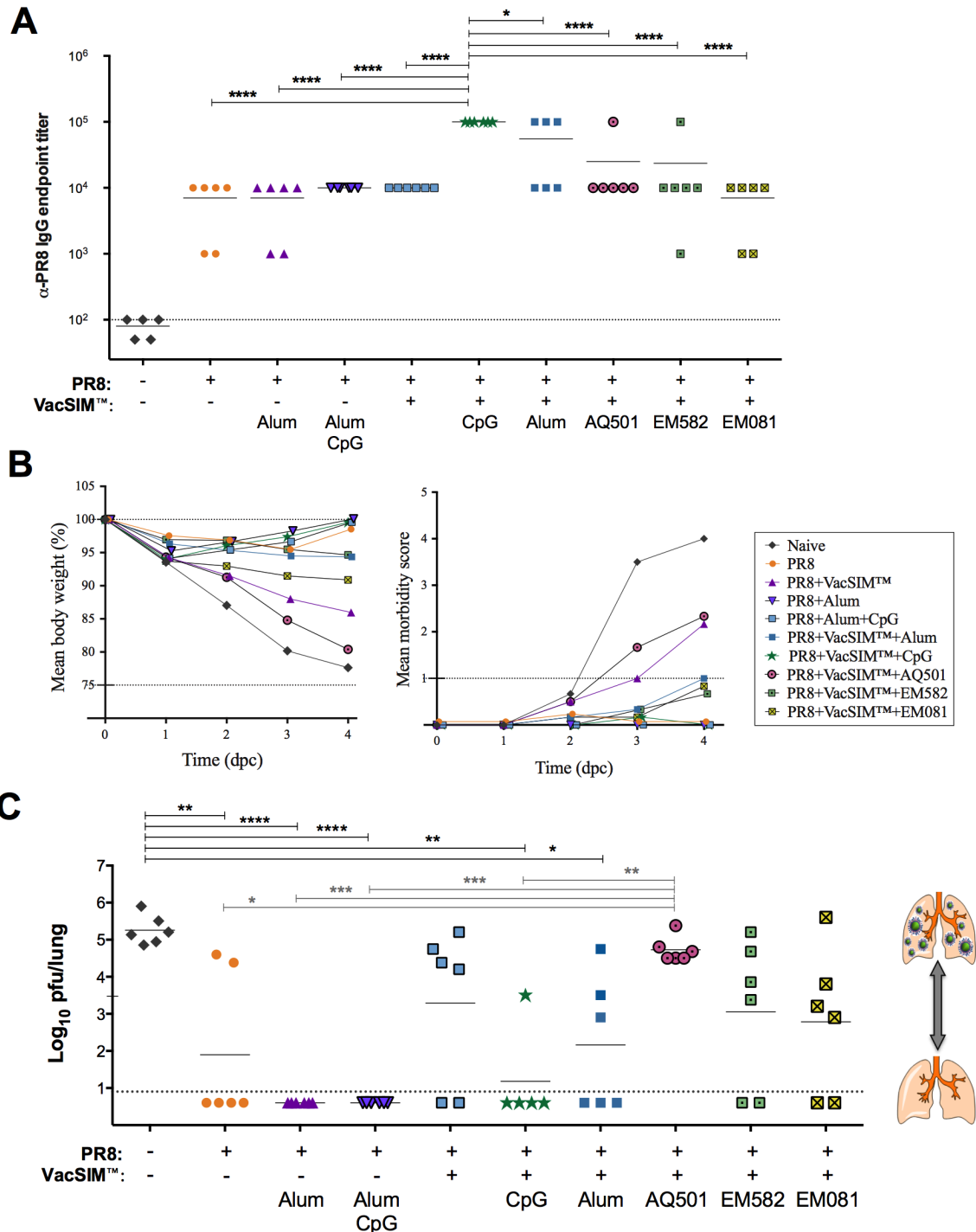


Figure 2.10: Immunization with various adjuvants and their effect on specific IgG sera titers, morbidity and viral clearance from the lungs. Sera collected prior to vaccination (baseline) and 4wpv was used to determine A/PR/8/34-specific IgG endpoint titers via indirect ELISA (A). Mice were challenged at 4wpv with $1,000_{\text{LD50}}$ PR8 and monitored daily for weight changes and morbidity post-challenge (B). Lungs were harvested 4dpc and viral clearance determined (C). Statistical significance (* $p < 0.05$, ** $p < 0.01$, *** $p < 0.001$, **** $p < 0.0001$) compared to PR8+VacSIMTM+CpG determined by one-way ANOVA and Dunnett's post-test (A) or between vaccine groups by one-way ANOVA and Tukey's post-test on log-transformed data (C). Dashed lines indicate detection thresholds. Results representative of ≥ 2 separate experiments (n=5-6).

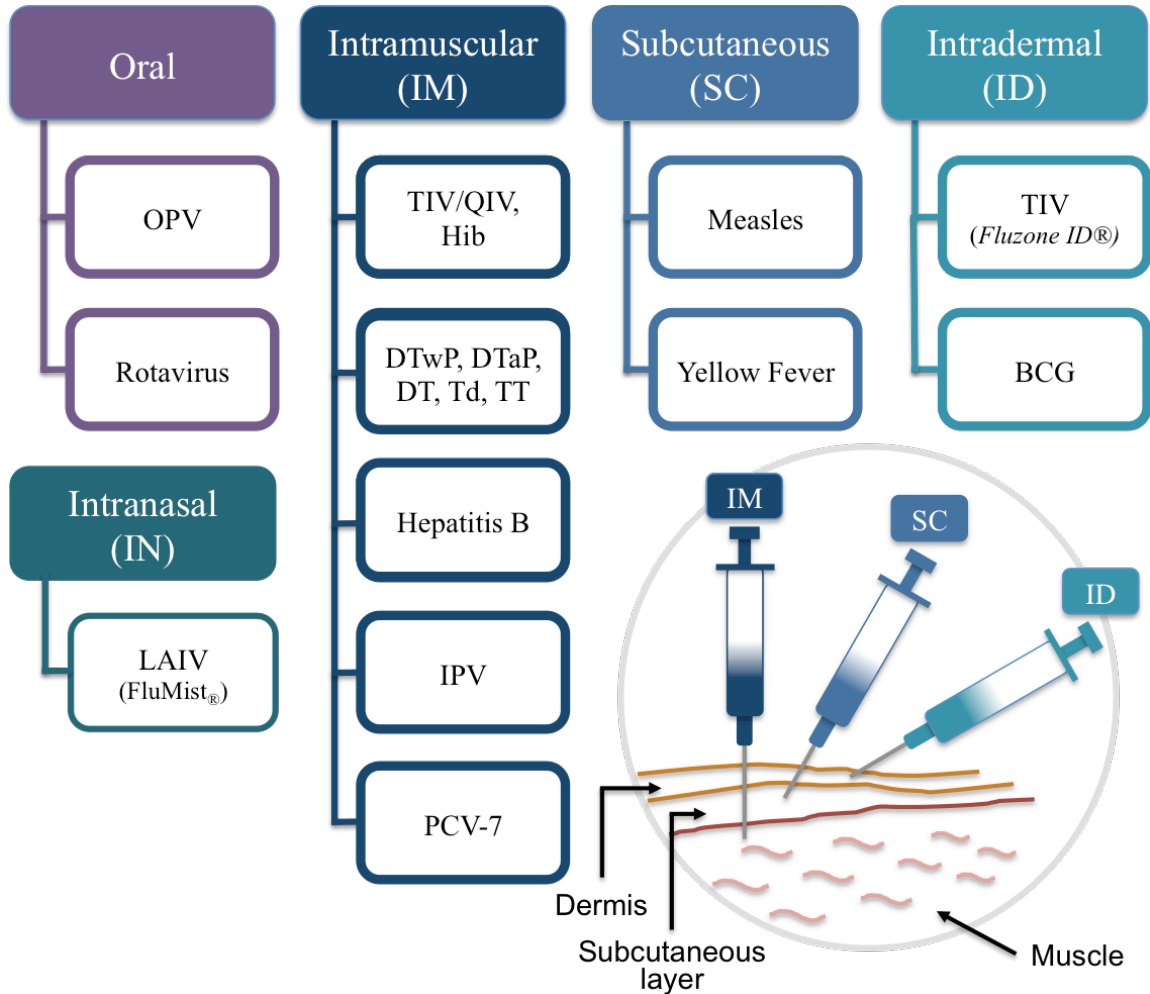


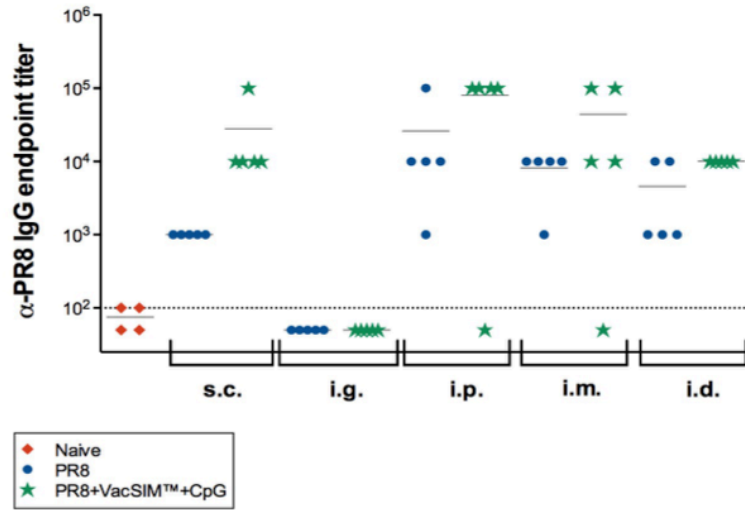
Figure 2.11: Routes of administration vary to maximize effectiveness of vaccine. Acronyms top to bottom and left to right: oral polio virus (OPV), live attenuated influenza virus (LAIV), trivalent/quadrivalent inactivated influenza virus (TIV/QIV), Haemophilus influenza type B (Hib), diphtheria tetanus toxoids (TT)(DT/Td) and whole-cell pertussis (DTwP), diphtheria tetanus toxoids and acellular pertussis (DTaP), inactivated polio vaccine (IPV), pneumococcal conjugate vaccine (PCV-7) and Bacillus Calmette–Guérin (BCG). Adapted from World Health Organization (<http://vaccine-safety-training.org/route-of-administration.html>).

Depending on the vaccine, the route of delivery will vary (Figure 2.11). Some common routes include intramuscular (i.m.), as with the inactivated seasonal influenza vaccines, intranasal (i.n.), as with the live-attenuated seasonal influenza vaccines and

oral, as with specific Polio vaccines. Additionally, the measles vaccine is delivered via a subcutaneous (s.c.) injection, and the tuberculosis vaccine (BCG) is administered via intradermal (i.d.) injection. In order to be truly effective as a vaccine delivery platform technology, VacSIM™ must be versatile enough to enable incorporation with multiple immunization routes.

Given the route variability amongst current vaccines, the following experiment was designed to evaluate whether the improved antigen-specific immunogenicity and vaccine efficacy were specific to the s.c. vaccination route, or if similarly improved vaccine responses could be generated with alternative routes. In this vaccine study unvaccinated mice were compared to mice that received either whole-inactivated PR8 in saline or PR8+CpG in VacSIM™. For both vaccines, five alternative routes were explored, including s.c., i.d., i.m., intraperitoneal (i.p.) as well as intragastric (i.g.). As previously described, antigen-specific immunogenicity was evaluated by comparing α -PR8 IgG levels in the sera, at 4 wpv by indirect ELISA, and vaccine efficacy was evaluated by comparing viral lung loads at 2 dpc via plaque assay (Figure 2.12). Overall, when comparing the PR8+CpG in VacSIM™ vaccines across different routes, the results indicate successful immunization in four out of the five tested routes. Immunization by the i.g. route was ineffective in the case of either vaccine. It is possible, given the hostile environment, that VacSIM™ assembly was delayed or all together disrupted, allowing the vaccinating antigen to be rapidly degraded. The combination of route and vaccine, which generated the most variable response, was in i.m. immunization of PR8+CpG in VacSIM™. Of the five routes evaluated, i.p., followed closely by s.c. were the most effective immunization routes for delivery of PR8+CpG in VacSIM™ (Figure 2.12).

A



B

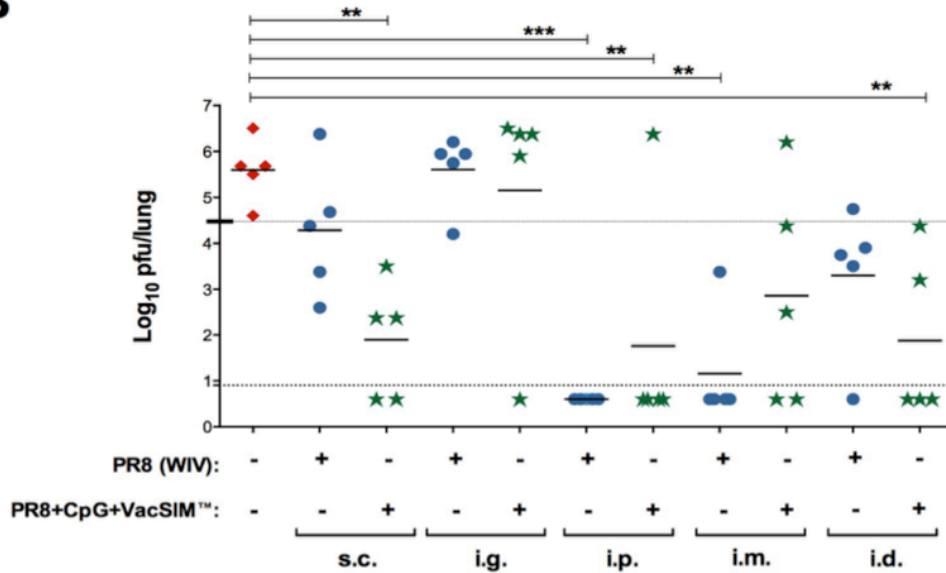


Figure 2.12: Route-dependent α -PR8 IgG sera levels and viral clearance from the lungs post challenge. All mice were bled prior to vaccination (baseline) with either PR8 in saline or PR8+CpG in VacSIM™ and again 4 wpv, when α -PR8 IgG levels in the sera were detected by indirect ELISA (A). Viral clearance from the lungs was assessed 2 days post challenging with 1,000 LD₅₀ live PR8, via plaque assay (B). Dotted lines indicate assay detection limits. Statistical significance (* p <0.05, ** p <0.01, *** p <0.001, **** p <0.0001) of vaccine groups compared to naive was determined by one-way ANOVA and Dunnet's multiple comparisons test, on log-transformed data (B). Results representative of 2 separate experiments.

2.4 Conclusions

Vaccine Self-assembling Immune Matrix (VacSIM™) is a patent-pending vaccine delivery system incorporating a sterile solution of the synthetic (RADA)4 self-assembling oligopeptides. A liquid *ex vivo*, VacSIM™ can easily be utilized for vaccine delivery through simple mixing with vaccine components prior to vaccination. Unlike traditional hydrogels, which tend to rely upon toxic cross-linkers for self-assembly, this rapid and straightforward preparation suggests VacSIM™ would be amenable to rapid formulation changes, the likes of which would be essential in a pandemic situation. Additionally, because VacSIM™ self-assembles *in vivo*, triggered by physiological levels of pH and salinity, VacSIM™ is readily set apart from alternative vaccine delivery methods, which typically involve *ex vivo* polymerization (24-29). Immediately following delivery, there is a rapid formation of a porous gel-matrix, which is inert, biocompatible and resorbable (16, 17). When these (RADA)4 oligopeptides are utilized for vaccine delivery, as proposed by VacSIM™, the resulting gel matrix assembles in and around the aqueous vaccine components, generating a localized depot of concentrated vaccine.

The results presented in Figures 2.4-2.6, 2.8-2.10 and 2.12 indicate that VacSIM™ delivery is capable of enhancing immunogenicity and vaccine efficacy by multiple delivery routes, as well as delivery of different types of antigens and antigen-adjuvant combinations. Taken together these results suggest that VacSIM™ delivery is flexible and has potential to be developed as a vaccine delivery platform that is able to enhance immunogenicity and efficacy in a variety of different vaccine systems. Combined, this work has lead to the inventors and The University of Georgia jointly filing applications for the following provisional patents: (61/476,431) “Vaccine Delivery

Method” filed on April 18th, 2011 (30) and (61/968,531) “Reduction of Reactogenicity of Adjuvants” filed on March 21st, 2014.

2.5 Materials and Methods

2.5.1 Experimental Design

To evaluate VacSIM™ delivery of an influenza vaccine in a mammalian model system controlled laboratory experiments were conducted in C57BL/6 mice (Harlan). Also utilized was the Madin-Darby Canine Kidney (MDCK) epithelial cell line (ATCC). Analyses of vaccine-specific immune responses were conducted according to standard protocols with slight modifications (33). Endpoint titers were calculated for antibodies specific to inactivated virus (PR8) or recombinant proteins (rNP, rHBsAg) in the sera by indirect ELISA. Protection from lethal challenge was assessed *in vivo* in accordance with IACUC guidelines and clearance of the virus was assessed by viral lung titers determined from plaque assay.

Group size for significant statistical power was determined by consultation with collaborating scientists, who have substantial experience with influenza infection in mice. In general, a sample size of at least four mice per treatment group was utilized. Animals within a group were not pooled during analysis and unless otherwise stated, data from individual mice were graphed. Following influenza challenge, mice were monitored daily and symptoms were recorded, including changes in weight, behavior, activity, posture, grooming and respiratory rate. Each animal was given a daily morbidity score, calculated from the assigned values of each symptom: hunched back or ruffed fur (1), lethargy (2), head tilt (3), weight loss >20% (3), weight loss >25% (4), weight loss >30% (5), cyanosis (5), paralysis (5), seizure (5) and severe dyspnea (5). Animals were immediately sacrificed (CO₂ inhalation followed by cervical dislocation) if they received a total score

of ≥ 5 and said to have reached their humane endpoint. Mice could be excluded from the final analysis if there was evidence of its difference prior to employing the experimental manipulation (i.e.: physical or behavioral abnormality recorded prior to vaccination or challenged). No outliers have been excluded.

2.5.2 Animals - rHBsAg and rNP Experiments

Five to seven week old female BALB/c or C57BL/6 mice were purchased from Harlan Laboratories, housed in specific pathogen-free conditions and allowed to acclimate for one week prior to manipulation. All animal work was performed in accordance with all applicable policies and approved by the institutional animal care and use committee.

2.5.3 Animals - PR8 (WIV) Experiments

Female C57BL/6 mice (Harlan) aged 5-7 weeks were obtained from Harlan laboratories and housed in pathogen-free conditions. Mice were acclimated for one week prior to manipulations. All animal handling was conducted in accordance with applicable regulations and with the approval of the institutional animal care and use committee.

2.5.4 Cell Culture

Madin-Darby Canine Kidney (MDCK) epithelial cells were cultured in 1:1 ratio of Dulbecco's Modified Eagle Medium (DMEM) and Eagle's minimal essential medium (MEM) supplemented with 1% L-glutamine and 5% fetal bovine serum (FBS) at 37 °C and 5% CO₂.

2.5.5 Vaccination - rHBsAg and rNP Experiments

Mice were vaccinated subcutaneously with recombinant Hepatitis B surface antigen (rHBsAg) adw subtype (5 µg, Fitzgerald Industries, Inc. Massachusetts, USA) or human recombinant influenza-A nuclear protein (10 µg, rNP, Imgenex, clone 2F205) ±

CpG (50 µg ODN 1826, InvivoGen, Inc. California, USA), via alhydrogel (250 µg, Inject Alum, Thermo Fisher Scientific, Inc., Pittsburgh, PA, USA) ± CpG, by VacSIM™ (PuraMatrix™, BD) ± CpG, or in Freund's (13 µL, Sigma-Aldrich Co. Missouri, USA), at a maximum volume of 200 µL per injection site. For most experiments, mice were primed then boosted four weeks later in an identical manner. For the endpoint titer experiments, mice were primed and boosted three weeks apart and the endpoint titers were determined three weeks post boost.

2.5.6 Vaccination - PR8 (WIV) Experiments

For the route optimizing experiments (Figure 2.12, Appendix Figure A.2), 6-8 week old mice (n=4-8) were vaccinated with 200 uL, a single time, by a subcutaneous (s.c.), intraperitoneal (i.p.) or intragastric (i.g.) route. Mice that were vaccinated by an intradermal (i.d.) or intramuscular (i.m.) route received two injections, of 50uL each (for i.d. one injection in the right and left side flank and for i.m. one injection in the thigh muscle of each leg). A 28^{5/8} G needle with 1mL syringe was used for s.c. and i.p. routes. A 30 G insulin syringe was used for both i.d. and i.m. routes and a 20x1½ G feeding needle with 1mL syringe was used for the i.g. route. Regardless of route and whether receiving a total vaccine volume of 100 uL or 200 uL, all mice were immunized, in accordance to their groups, with identical amounts of antigen, adjuvant and/or VacSIM™.

In all other experiments, 6-8 week old mice received a single, subcutaneous (s.c.) vaccination of 200 µL to their right flank. Vaccinations contained sterile saline, PR8 whole-inactivated virus (WIV) (15 µg, Charles River Laboratories), CpG (50 µg, ODN1826, InvivoGen), Alum (250 µg, Inject Alum, Thermo Scientific), AQ501 (10 µg,

aqueous formulated TLR-4 agonist, Infectious Disease Research Institute), EM582 (10 µg, oil-in-water formulated TLR-4 agonist, Infectious Disease Research Institute), EM081 (1:5 dilution, oil-in-water formulation, Infectious Disease Research Institute), or equal volumes VacSIM™ (PuraMatrix, BD), as indicated by group.

2.5.7 Viral Challenge

Influenza challenge virus (A/Puerto Rico/08/34, H1N1) was mouse-adapted through serial passage prior to propagation in embryonated chicken eggs (Appendix Figure A.) and lethality was determined by MLD₅₀ (Appendix Figure A.), as described previously (31). Four weeks post-vaccination, age-matched mice were challenged intranasally (i.n.) with a lethal dose (1,000 LD₅₀, as indicated) of mouse-adapted homologous PR8 virus, while under temporary sedation with tribromoethanol. Mice were monitored daily for weight change and symptom severity (subsection 2.5.1). In a minimum of two mice, lungs were harvested 6-12 hours post challenge (hpc) to confirm infection via plaque assay.

2.5.8 Antibody Endpoint Titers

Serum samples were collected from mice prior to vaccination (pre-bleed) and four weeks following vaccination. Briefly, ELISA plates were coated with whole A/Puerto Rico/08/34 (H1N1) inactivated/purified virus (4 µg/ml) at 4 °C overnight. Plates were washed five times with wash buffer (160 mM NaCl, 0.5 mM EDTA and 0.05% Tween 20), then blocked in 1X PBS containing 5% non-fat milk powder and 1% BSA for at least two hours. Plates were decanted, incubated for 2-24 hours with samples serially diluted in blocking buffer, then washed five times. Detection antibodies (HRP-conjugated α-mouse IgG₁, IgA and IgM from Santa Cruz, IgG₃, IgG_{2a} and IgG_{2b} from Invitrogen, IgE from Southern Biotech or total IgG from BioLegend) were diluted in blocking buffer and

incubated for one hour. After five washes, plates were developed in the dark using SureBlue 1 component TMB substrate (KPL Laboratories) and the reaction was stopped with 2 N sulfuric acid. Absorbance was measured at 450 nm with 570 nm background correction.

Figure 2.4 only: Blood samples were collected from all vaccinated and control mice weekly, beginning week -1 prior to primary immunization. rHBsAg-specific antibodies in sera were analyzed by ELISA. Briefly, plates were coated with 4 µg/ml rHBsAg and sera antibodies specific for rHBsAg were detected by HRP-conjugated secondary antibodies (α -IgA, α -IgM, and α -IgG from Santa Cruz; α -IgG₁ and IgG_{2a} from Invitrogen).

2.5.9 Plaque Assays for Viral Quantitation

Briefly, serially diluted lung homogenates were incubated with MDCK lawns under a 2.4% Avicel (FMC BioPolymer) overlay (Appendix Figure A.4). After incubation for 2-3 days, cells were fixed with methanol/acetone and stained with crystal violet (Acros Organics) for enumeration of plaque forming units (pfu). Lung samples with undetectable virus were graphed as four pfu per lung, which is a value equal to ½ of the detection threshold of the assay.

2.5.10 ELISpots – Data in Appendix B

Splenocytes were obtained three weeks post-prime or three weeks post-boost, then stimulated for 20 hours to evaluate HBsAg-/NP-specific cell-mediated vaccine responses using IFN γ ELISpot, according to the manufacturer's instructions (BD Biosciences, San Francisco, CA, USA). Briefly, single cell suspensions (3 and 1.5×10^5 cells per well) were cultured at 37 °C with 5% CO₂ for 20 hours in complete medium [RPMI-1640 (Hyclone, Thermo Scientific, Utah, USA) supplemented with 10% FBS, 100 U/ml penicillin, 100 µg/ml streptomycin, antimycotic, non-essential amino acids and

β -mercaptoethanol (Sigma-Aldrich, St. Louis, MO, USA)] and stimulated with either 1 μ g/ml Concanavalin A (ConA), 20 μ M specific peptide (Appendix Table A.2), or synthesized at greater than 95% purity (Biosynthesis Inc., Lewisville, TX, USA) and dissolved in DMSO prior to dilution in culture media, 10 μ g/ml recombinant protein] or left unstimulated. ELISpot plates were developed with AEC substrate and spot forming units (SFU) were counted using an Immunospot Analyzer (C.T.L.). The SFU value was expressed as mean of the triplicate cultures per mouse (Appendix Figures A.11-A.12).

2.5.11 Cytometric bead array – Data in Appendix B

Splenocytes were harvested, plated at 1.5 million cells per well in 48-well plates, and stimulated with 20 μ M peptide, 25 μ g/ml SEA, or 1 μ g/ml ConA or left unstimulated for 72 hours. Cytokine levels in supernatant were measured using a Th1/Th2/Th17 cytometric bead array (CBA) kit according to the manufacturer's instructions (BD).

2.5.12 Statistical Analyses

Statistical analyses were performed using GraphPad Prism version 6.0. Statistical methods and significant differences between vaccination groups include one-way ANOVA or two-way ANOVA followed by either Dunn's, Tukey's, Dunnett's or Bonferroni test for multiple comparisons. The specific statistical method(s) as well as the alpha level (0.05 or 0.01) have been specified in each figure legend.

2.6 References

1. Koutsopoulos S, Unsworth LD, Nagai Y, & Zhang S (2009) Controlled release of functional proteins through designer self-assembling peptide nanofiber hydrogel scaffold. *Proceedings of the National Academy of Sciences of the United States of America* 106(12):4623-4628.

2. Nagai Y, Unsworth LD, Koutsopoulos S, & Zhang S (2006) Slow release of molecules in self-assembling peptide nanofiber scaffold. *Journal of controlled release : official journal of the Controlled Release Society* 115(1):18-25.
3. Zhang S, *et al.* (1995) Self-complementary oligopeptide matrices support mammalian cell attachment. *Biomaterials* 16(18):1385-1393.
4. Kresge N, Simoni RD, & Hill RL (2009) The Discovery of Z-DNA: the Work of Alexander Rich. *The Journal of Biological Chemistry* 284(51):e23-e25.
5. Xiaojun Z, Shuguang Z, & Lisa S (2005) PuraMatrix. *Scaffolding In Tissue Engineering*, (CRC Press), pp 217-238.
6. Lampe KJ & Heilshorn SC (2012) Building stem cell niches from the molecule up through engineered peptide materials. *Neuroscience letters* 519(2):138-146.
7. Zhang S, Holmes T, Lockshin C, & Rich A (1993) Spontaneous assembly of a self-complementary oligopeptide to form a stable macroscopic membrane. *Proceedings of the National Academy of Sciences of the United States of America* 90(8):3334-3338.
8. Ye Z, *et al.* (2008) Temperature and pH effects on biophysical and morphological properties of self-assembling peptide RADA16-I. *Journal of peptide science : an official publication of the European Peptide Society* 14(2):152-162.
9. Zhang S, Gelain F, & Zhao X (2005) Designer self-assembling peptide nanofiber scaffolds for 3D tissue cell cultures. *Seminars in cancer biology* 15(5):413-420.
10. Zhang S ZX, Spirio L. (2010) *PuraMatrix: Self-Assembling Peptide Nanofiber Scaffolds* (CRC Press, Scaffolding In Tissue Engineering) 2 Ed pp 217-240.
11. Kondo Y, Nagasaka T, Kobayashi S, Kobayashi N, & Fujiwara T (2014) Management of peritoneal effusion by sealing with a self-assembling nanofiber polypeptide following pelvic surgery. *Hepato-gastroenterology* 61(130):349-353.
12. Rosa V, Zhang Z, Grande RH, & Nor JE (2013) Dental pulp tissue engineering in full-length human root canals. *Journal of dental research* 92(11):970-975.
13. Dissanayaka WL, Hargreaves KM, Jin L, Samaranayake LP, & Zhang C (2014) The Interplay of Dental Pulp Stem Cells and Endothelial Cells in an Injectable Peptide Hydrogel on Angiogenesis and Pulp Regeneration In Vivo. *Tissue engineering. Part A*.
14. Grenfell RF, *et al.* (2014) Newly Established Monoclonal Antibody Diagnostic Assays for *Schistosoma mansoni* Direct Detection in Areas of Low Endemicity. *PloS one* 9(1):e87777.

15. Grenfell RF, Shollenberger LM, Samli EF, & Harn DA (2015) Vaccine Self-assembling Immune Matrix is a new delivery platform that enhances immune responses to rHBsAg in mice. *Clinical and Vaccine Immunology* 22(3):337-343.
16. Semino CE, Kasahara J, Hayashi Y, & Zhang S (2004) Entrapment of migrating hippocampal neural cells in three-dimensional peptide nanofiber scaffold. *Tissue engineering* 10(3-4):643-655.
17. Meng H, Chen L, Ye Z, Wang S, & Zhao X (2009) The effect of a self-assembling peptide nanofiber scaffold (peptide) when used as a wound dressing for the treatment of deep second degree burns in rats. *Journal of biomedical materials research. Part B, Applied biomaterials* 89(2):379-391.
18. Yoshida D & Teramoto A (2007) The use of 3-D culture in peptide hydrogel for analysis of discoidin domain receptor 1-collagen interaction. *Cell adhesion & migration* 1(2):92-98.
19. Spencer NJ, Cotanche DA, & Klapperich CM (2008) Peptide- and collagen-based hydrogel substrates for in vitro culture of chick cochleae. *Biomaterials* 29(8):1028-1042.
20. Kyle S, Aggeli A, Ingham E, & McPherson MJ (2009) Production of self-assembling biomaterials for tissue engineering. *Trends in biotechnology* 27(7):423-433.
21. Nishimura A, *et al.* (2012) Controlled release of insulin from self-assembling nanofiber hydrogel, PuraMatrix: application for the subcutaneous injection in rats. *European journal of pharmaceutical sciences : official journal of the European Federation for Pharmaceutical Sciences* 45(1-2):1-7.
22. Siegrist CA, *et al.* (2004) Co-administration of CpG oligonucleotides enhances the late affinity maturation process of human anti-hepatitis B vaccine response. *Vaccine* 23(5):615-622.
23. Kim SK, Ragupathi G, Cappello S, Kagan E, & Livingston PO (2000) Effect of immunological adjuvant combinations on the antibody and T-cell response to vaccination with MUC1-KLH and GD3-KLH conjugates. *Vaccine* 19(4-5):530-537.
24. Ingavle GC, Gehrke SH, & Detamore MS (2014) The bioactivity of agarose-PEGDA interpenetrating network hydrogels with covalently immobilized RGD peptides and physically entrapped aggrecan. *Biomaterials* 35(11):3558-3570.
25. Browning MB, Cereceres SN, Luong PT, & Cosgriff-Hernandez EM (2014) Determination of the in vivo degradation mechanism of PEGDA hydrogels. *Journal of biomedical materials research. Part A.*

26. Jose S, Hughbanks ML, Binder BY, Ingavle GC, & Leach JK (2014) Enhanced trophic factor secretion by mesenchymal stem/stromal cells with Glycine-Histidine-Lysine (GHK)-modified alginate hydrogels. *Acta biomaterialia*.
27. Xiong Y, *et al.* (2014) Compartmentalized multilayer hydrogel formation using a stimulus-responsive self-assembling polysaccharide. *ACS applied materials & interfaces* 6(4):2948-2957.
28. Zustiak SP, Pubill S, Ribeiro A, & Leach JB (2013) Hydrolytically degradable poly(ethylene glycol) hydrogel scaffolds as a cell delivery vehicle: Characterization of PC12 cell response. *Biotechnology progress* 29(5):1255-1264.
29. Zhang L, *et al.* (2014) Preparation of novel biodegradable pHEMA hydrogel for a tissue engineering scaffold by microwave-assisted polymerization. *Asian Pacific journal of tropical medicine* 7(2):136-140.
30. Harn DA, Queiroz R, & McEwen L (2013) WO/2012/145355 .
31. Webster R CN, Stohr K (2002) WHO Manual on Animal Influenza Diagnosis and Surveillance in *WHO Global Influenza Program*, ed Webster R CN, Stohr K (World Health Organization, Geneva, Switzerland), p 105.

CHAPTER 3

DELIVERY OF ADJUVANTED WHOLE INACTIVATED INFLUENZA BY VACSIM™, A THREE DIMENSIONAL VACCINE DELIVERY METHOD, IMPROVES PROTECTION FROM LETHAL HOMOLOGOUS CHALLENGE IN MICE¹

¹ E. Farah Samli, Lisa M. Shollenberger, Donald A. Harn,
Resubmitted to *Proceedings of the National Academy of Sciences*.

3.1 Abstract

Human and Veterinary vaccines remain the best public health measures to prevent infectious diseases, second only to clean drinking water. As effective as vaccines have been in preventing disease, for many diseases the current vaccines afford only marginal protection. For example, overall efficacy for the seasonal influenza vaccine varies, with efficacy from 50-67%. This relatively low level of efficacy is further decreased in the very young, the elderly and immune compromised. Therefore, improving vaccine efficacy remains a high priority for influenza and many other diseases. One approach to enhance vaccine efficacy is to find delivery methods that provide antigen persistence, leading to increased activation and maturation of antigen presenting cells. Here we describe a new platform vaccine delivery system that provides antigen persistence. VacSIM™ (Vaccine Self-assembling Immune Matrix) is an inert, synthetic (RADA)₄ oligopeptide liquid that self-assembles to form hydrated nanofibers *in vivo*. When delivered in combination with a vaccine, the hydrated nanofibers immediately self-assemble, forming a porous gel-depot, encompassing aqueous vaccine components and allowing gradual egress from the gel. VacSIM™ provides the flexibility to rapidly incorporate various vaccine components without requiring *ex vivo* polymerization.

Here, we describe how gradual exposure to antigen, as a result of VacSIM™ delivery, enhances influenza-specific immune responses, which may be driven by increased activation of antigen presenting cells. Mice immunized with inactivated A/Puerto Rico/08/34 (PR8) and CpG in VacSIM™ had increased PR8-specific antibody responses as well as greater protection and improved viral clearance following lethal, homologous challenge, compared to mice immunized with PR8 and CpG in the absence

of VacSIM™. Surprisingly, although we vaccinated with inactivated virus, VacSIM™ delivery of inactivated PR8 and CpG generated PR8-specific T cell responses. VacSIM™ as a new vaccine platform technology has the potential to enhance efficacy of numerous current and future vaccines, with advantages over earlier hydrogel based methods.

3.2 Significance

VacSIM™, is a new vaccine delivery method that produces a three dimensional gel depot *in situ*, providing vaccine antigen persistence as a means to enhance vaccine efficacy. Because VacSIM™ can be used to deliver subunit or whole organism vaccines as well as vector based vaccines, and increases both cellular and humoral responses, VacSIM™ technology should have wide applicability to enhance vaccine efficacy.

3.3 Introduction

Vaccines remain one of the greatest public health tools to reduce morbidity and mortality caused by infectious diseases. As powerful as vaccination has been to prevent infection and reduce morbidity, there are numerous human and veterinary diseases for which no vaccines exist, or that are only marginally effective. For some vaccines, notably pneumonia and influenza, vaccine efficacy is further reduced in low responder populations such as the very young, the elderly and immune compromised. Therefore tremendous effort has been devoted to discovery and development of new adjuvants and/or vaccine delivery methods that can safely improve vaccine efficacy (VE). Our long-term approach to increase vaccine immunogenicity and efficacy has been to deliver vaccines as particulates, to enhance antigen persistence and activation of antigen presenting cells (APC). Toward this goal, we wanted a method that allowed for simple mixing of vaccine components without the need to precipitate or polymerize *ex vivo*, such

that a “Plug and Play” vaccine platform is realized. This led us to develop a new vaccine delivery method named VacSIM™ (Vaccine Self-Assembling Immune Matrix) (1), which is based on the properties of the synthetic (RADA)4 oligopeptide and other biopolymers (2-6). Created by Zhang (6), the (RADA)4 synthetic oligopeptide was commercialized by 3-D Matrix Inc., as a cell scaffold for 3D cell cultures *in vivo* and *ex vivo* (7). Solutions of the (RADA)4 oligopeptide have undergone third party testing, demonstrating no reactogenicity or toxicity (8), which had led to clinical trials for wound healing (PuraStat®), tissue repair (9) and as scaffolding for dental implants (PuraMatrix™) (10, 11).

VacSIM™, composed of the (RADA)4 oligopeptide solution remains liquid *ex vivo*, allowing for easy incorporation of vaccine subunit or whole antigens, organisms and adjuvants. Under physiological conditions, hydrated nanofibers self-assemble to form an inert and biodegradable, gel-matrix. The VacSIM™ gel- matrix depot concentrates vaccine components in the aqueous phase of the gel-matrix enabling gradual egress of these components through the gel-matrix pores (1). This gel-matrix depot, in addition to providing slow egress of vaccine components, may also provide protection from systemic degradation. Therefore, VacSIM™ is a flexible, vaccine delivery method with wide applicability in terms of the types of vaccines that can be delivered.

Recently, we demonstrated that VacSIM™ delivery of recombinant Hepatitis B surface antigen (rHBsAg) induced superior vaccine-specific responses compared to delivery of the same antigen in aluminum hydroxide (alum) or complete Freund’s adjuvant (CFA) (1). Having demonstrated that VacSIM™ delivery enhances vaccine immunogenicity, our next goal was to determine its ability to enhance VE. To test this we

evaluated immunogenicity and VE in a murine influenza model prior to and after challenge infection. Influenza is a highly infectious virus, responsible for seasonal epidemics and occasional pandemics. Infection is a global health concern, imposing often-unpredictable levels of morbidity, mortality and considerable economic burden in the form of health care costs and lost productivity (12, 13). Seasonal influenza is an acute infection that hospitalizes 200-250,000 and kills approximately 36,000 persons annually in the United States alone (14, 15). Infections in low-responding or high-risk populations, such as the elderly, the very young and the immune compromised, often lead to more severe and potentially life-threatening complications such as pneumonia (16-18).

Annual vaccination is the most effective method to prevent infection from seasonal influenza epidemics. Several of the influenza vaccines contain more than one strain of inactivated viruses, and are trivalent or quadrivalent vaccines that function by generating flu-specific antibodies. However, the live attenuated influenza vaccine (LAIV) option (FluMist®) is most effective because it induces a T cell response in addition to generating flu-specific antibodies. The only seasonal influenza vaccine recommended for high-risk populations is intramuscular injection of either tri or quadrivalent vaccines. For the most recent 2013-2014 influenza season, the CDC estimated the overall VE to be 61% (95% confidence interval = 52–68%) (19), with lower efficacy in high-risk populations (16, 17, 19). In addition to exhibiting lower VE, high-risk populations have greater morbidity/mortality (18, 20, 21). Thus, development of safe vaccine delivery methods and/or adjuvants to significantly improve immunogenicity and efficacy of seasonal influenza vaccines is a high priority, especially for high-risk populations (22-25).

In this study we evaluated whether VacSIM™ delivery of an influenza vaccine would enhance immunogenicity and efficacy from challenge infection in C57BL/6 mice. We utilized the whole inactivated virus (WIV), influenza A/Puerto Rico/08/34 (PR8), for its high immunogenicity and reputation as a standard in the field. Because PR8 is known to be highly effective when the vaccine is administered by the intramuscular (i.m.) route, we chose a sub-optimal vaccination route, subcutaneous (s.c.), to better assess effects of VacSIM™ and differences between functional vaccine groups. To be consistent with how the seasonal influenza vaccine is administered, mice received a single immunization.

3.4 Results

3.4.1 Delivery of WIV PR8 and CpG by VacSIM™ Increases Vaccine-Specific Antibody Titers

Vaccine-specific endpoint titers of sera collected 4 weeks post vaccination (wpv) from each vaccination group were determined for multiple antibody classes and isotypes (Figure 3.1, S3.6). Total IgG endpoint titers were significantly higher in sera from mice vaccinated with PR8 + CpG via VacSIM™ delivery compared to all other vaccine groups: 1) naïve mice and mice vaccinated with 2) un-adjuvanted PR8, 3) PR8 + Alum, 4) PR8 in VacSIM™, 5) PR8 adjuvanted with Alum + CpG and 6) PR8 + Alum in VacSIM™. For IgG isotypes, vaccine-specific IgG₁ endpoint titers were significantly higher in mice receiving PR8 + CpG in VacSIM™ compared to naïve, unadjuvanted PR8 in saline, PR8 + Alum and PR8 + CpG in saline groups. Sera quantity was limited from the group receiving unadjuvanted PR8 in VacSIM™ and only three of five mice were assayed for IgG₁ and IgG_{2a} endpoint titers. This group (PR8 in VacSIM™) was excluded from statistical analysis due to low sample size (Figure 3.1). Mice vaccinated with PR8 + CpG in VacSIM™ consistently had the highest vaccine-specific IgG isotype endpoint

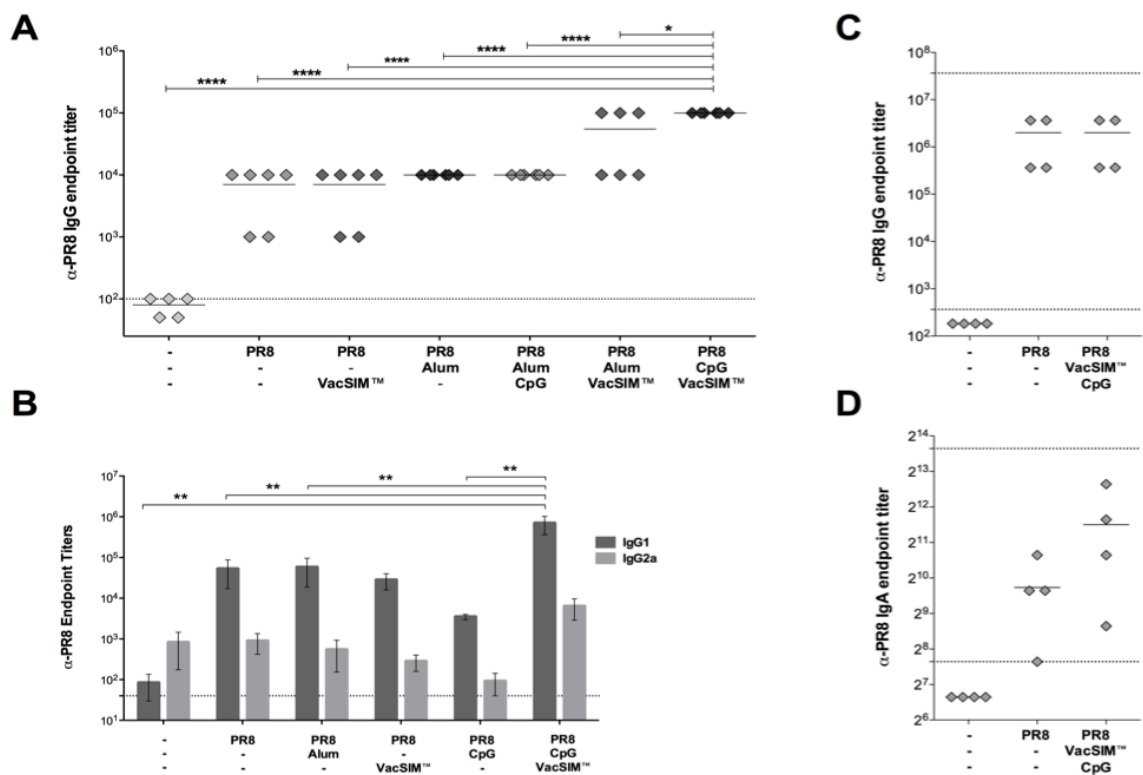


Figure 3.1: Inactivated influenza vaccine delivered with CpG via VacSIM™ induces higher antibody titers in sera and mucosa. Sera collected 4 wpv and A/PR/8/34-specific IgG, IgG1 and IgG2a endpoint titers determined by indirect ELISA (A-B). A/PR/8/34-specific IgG and IgA endpoint titers determined from the lungs of immunized mice, 4 wpv and 1 dpc with 1000 LD₅₀ of live virus (A/PR/8/34) (C-D). Dashed lines indicate detection thresholds of the experiment. Results were replicated, for each vaccine group (A-B), in a minimum of 3 separate experiments (n=5-16). Statistical significance (*p<0.05, **p<0.01, ***p<0.001, ****p<0.0001) between vaccination groups was determined from the log transformed isotype titers using 1-way ANOVA and Tukey’s multiple-comparisons post-test (A-B). Data is representative (C-D) of 2 independent experiments (n=4-5) with no significant differences (p < 0.05) between groups by 1-way ANOVA and Bonferroni’s multiple comparisons post-test.

titers, with significantly increased levels of vaccine-specific IgG₁ and IgG_{2b}, and decreased levels of IgG_{2a} and IgG₃ suggesting a mixed Th1/Th2 immune response. The IgG_{2a} endpoint titers were the lowest for all vaccine groups (Figure 3.1, S3.6.).

To evaluate mucosal antibody responses, we determined IgA and IgG endpoint titers from lungs one-day post challenge (dpc). We compared the PR8 + CpG in VacSIM™ group to PR8 in saline group, with naïve mice as controls. Both of the

vaccinated groups had high IgG endpoint titers in lung tissue. However, the PR8 + CpG in VacSIM™ group had increased levels of IgA, compared to the PR8 vaccinated group (Figure 3.1).

3.4.2 Hemagglutination Inhibition (HI) Titers Do Not Correlate with Endpoint Titers

HI titers are one parameter employed to evaluate VE and immunogenicity (26, 27). HI titers ranging between 15 and 65 have been associated with 50% reduced risk of infection with influenza A-H1N1, A-H2N2, A-H3N2, and B strains in humans (28). The CDC defines the standard protective titer to be ≥ 40 (29). We performed HI assays for vaccine-specific antibodies present in sera 4 wpv (Figure 3.2). The average HI titers of both naïve mice and those vaccinated with PR8 in VacSIM™ were below our detection threshold. Average HI titers of the remaining four vaccine groups (PR8, PR8 + Alum, PR8 + CpG, and PR8 + CpG in VacSIM™) all met the CDC standard of ≥ 40 HI titer. Surprisingly, although sera from mice immunized with PR8 + CpG via VacSIM™ had consistently high vaccine-specific antibodies (Figure 3.1), their ability to inhibit hemagglutination varied greatly (Figure 3.2).

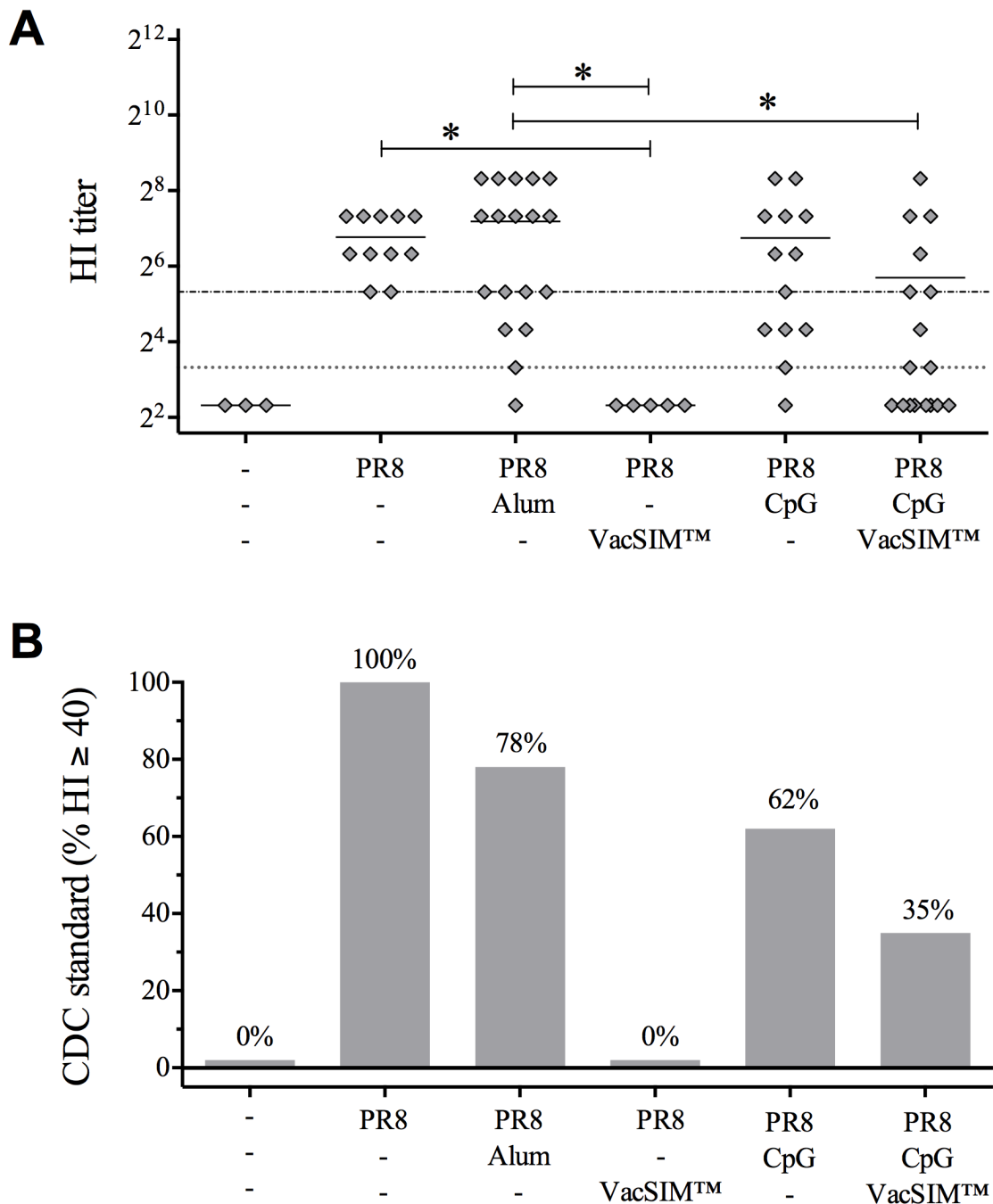


Figure 3.2: Inhibition of hemagglutination is a standard correlate of protection. Hemagglutination inhibition (HI) titers relative to baseline-corrected, vaccine-specific sera collected at 4 wpv from immunized mice (A) and the percent of samples, relative to each vaccine group, with an HI titer ≥ 40 (B) were determined. Graph represents pooled data from three identical experiments (n= 5-16). Dashed lines indicate detection thresholds of the 2. Statistical significance (* $p < 0.05$, ** $p < 0.01$) between vaccination groups was determined via the Kruskal-Wallis test followed by Dunn's multiple-comparisons post-test.

3.4.3 PR8 and CpG Delivered by VacSIM™ Protects Vaccinated Mice from Lethal Challenge

Mice vaccinated with PR8 + CpG in VacSIM™ had increased humoral responses, but not greater HI titers (Figure 3.1, 3.2). To assess VE as protection from infection, we initially challenged vaccinated mice at 4 wpv with a lethal dose (30 LD₅₀) of homologous live virus via intranasal challenge (S3.7). As expected, based on flu-specific antibody levels, the naïve group and mice vaccinated with PR8 via VacSIM™ suffered weight loss and increased morbidity scores, indicative of symptom severity. Each of the other vaccine groups showed no morbidity or mortality at this challenge dose. Due to poor protection, the PR8 via VacSIM™ group was excluded from subsequent challenge studies, where we increased the challenge dose to 1000 LD₅₀, to distinguish differences among protected groups.

As shown in Figure 3.3, the higher dose (1000 LD₅₀) challenge resulted in all unvaccinated mice having high composite morbidity scores indicating their humane endpoint by day seven post challenge. In contrast, mice vaccinated with PR8 alone or PR8 + CpG had similar weight loss and overall morbidity scores, resulting in identical levels of protection (87.5% survival at 14 dpc). Mice vaccinated with PR8 in alum had lower protection (75% survival at 14 dpc). Consistent with antibody endpoint titer data, the group vaccinated with PR8 + CpG in VacSIM™ had minimal weight loss, low morbidity scores and was the only group fully protected from the 1000 LD₅₀ challenge (100% survival at 14 dpc) (Figure 3.3). These results suggest the increased VE seen in the PR8 + CpG in VacSIM™ group may correlate with high, vaccine-specific endpoint titers in both the sera and lungs (Figure 3.1, S3.1). Only the HI titer data were inconsistent with VE against a 1000 LD₅₀ challenge (Figure 3.2).

To further examine vaccine-induced protection to lethal challenge, we evaluated clearance of challenge virus from the lungs of control and vaccinated mice. Lung viral loads were measured at 1, 2, 3, and 5 dpc via plaque assay. We compared the group with the highest antibody response and protection (PR8 + CpG in VacSIM™) to the group vaccinated with PR8 alone. Naïve mice were included as controls for viral replication *in vivo*. The naïve mouse group maintained high lung viral loads at all time points post challenge infection, whereas mice vaccinated with PR8 had approximately two logs lower viral titers at 1 dpc and began clearing the infection at 5 dpc, evidenced by undetectable virus levels in two mice at this time (30). Correlating with the 100% survival to challenge infection, we observed several mice in the PR8 + CpG in VacSIM™ group that had undetectable levels of virus, at each time point. The PR8 + CpG in VacSIM™ group had approximately two logs lower lung viral loads than PR8 vaccinated mice on days 1-3 post-challenge, demonstrating a significant improvement in viral clearance (Figure 3.3). To determine whether mice receiving PR8 + CpG in saline rather than in VacSIM™ would have similarly enhanced viral clearance, we repeated the vaccination and challenge study with an expanded set of groups and a single time point. Mice receiving PR8 + CpG in Saline or in VacSIM™ were compared to groups vaccinated with PR8 alone, VacSIM™ alone (containing no antigen) as well as naïve mice, three days following a 1000 LD₅₀ influenza challenge (Figure 3.3). Not surprisingly, the delivery of VacSIM™ in the absence of antigen provided no protection and resulted in a group mean similar to naïve mice post challenge. However, the addition of CpG in saline (PR8 + CpG) was unable to reproduce the viral clearance efficacy seen in mice vaccinated with PR8 + CpG in VacSIM™. Further, the observation that several

mice in this group had undetectable virus at 1 dpc, suggests that PR8 + CpG in VacSIM™.

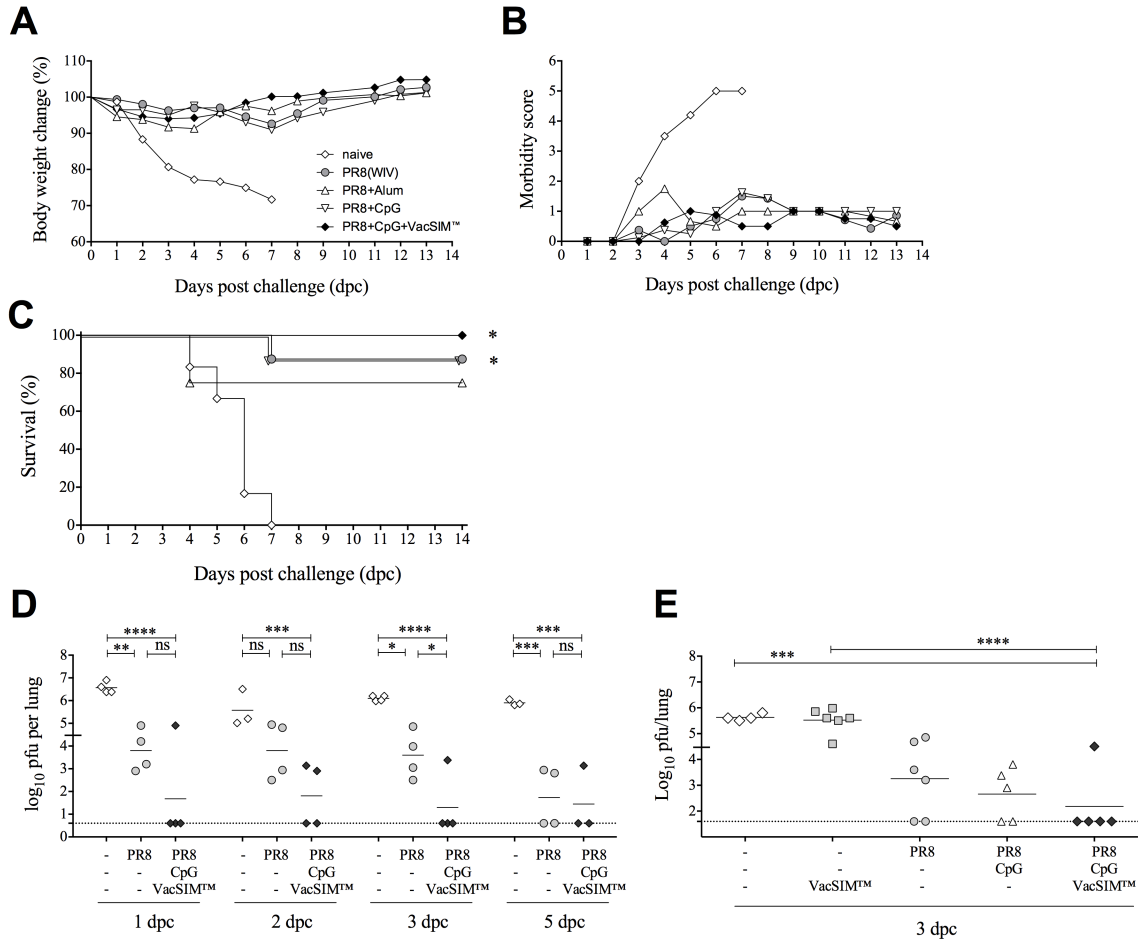


Figure 3.3: Inactivated influenza vaccine delivered with CpG via VacSIM™ decreases mortality, results in the highest level of protection post challenge and increased viral clearance after lethal influenza challenge. Immunization with PR8+VacSIM™+CpG leads to sterilizing immunity and improved viral clearance from the lungs. Presented are post-challenge weight (A), morbidity scores (B) and survival (C) of mice following lethal (1,000 LD₅₀) challenge administered at 4 wpv, as well as virus levels in lungs of immunized mice harvested between 1-5 days (D) and 3 days (E) post lethal (1,000 LD₅₀) challenge. Dashed lines indicate detection threshold. Representative of 3 independent experiments (n=5-9). Statistical significance (*p<0.05) of survival (C) was determined relative to unvaccinated mice using the Log-rank (Mantel-Cox) test with multiple comparisons. Statistical significance of the log-transformed values (*p<0.05, **p<0.01, ***p<0.001, ****p<0.0001) was determined by two-way ANOVA and Bonferroni's multiple comparisons post test (D) or compared to PR8+CpG+VacSIM by one-way ANOVA and Dunnett's post-test (E).

Virus-Specific T Cell Responses are Enhanced in Mice Vaccinated with PR8 and CpG via VacSIM™

Previously we noted that sera HI titers from mice vaccinated with PR8 + CpG via VacSIM™ were not a predictive correlate of VE, as measured by 100% survival and increased lung viral clearance upon lethal challenge. To examine another potential anti-viral mechanism as a correlate of protection, we examined T cell responses. We compared the PR8 + CpG in VacSIM™ group, which had the highest antibody responses and levels of protection, to the PR8 only group and naïve mice, which were included as controls for basal T cell levels *in vivo* (Figure 3.4). Fewer than half of the mice in the PR8 only vaccine group had higher percentages of tetramer-specific T cells in draining lymph nodes than in the non-draining lymph nodes at 2 dpc. In comparison, all animals in the PR8 + CpG in VacSIM™ group had increased levels of NP-specific CD8⁺ T cells in the draining lymph nodes, which were also elevated compared to non-draining lymph nodes. This finding suggests that VacSIM™ delivery is able to drive T cell responses to an internal protein present in formalin-inactivated virus delivered to a distant site.

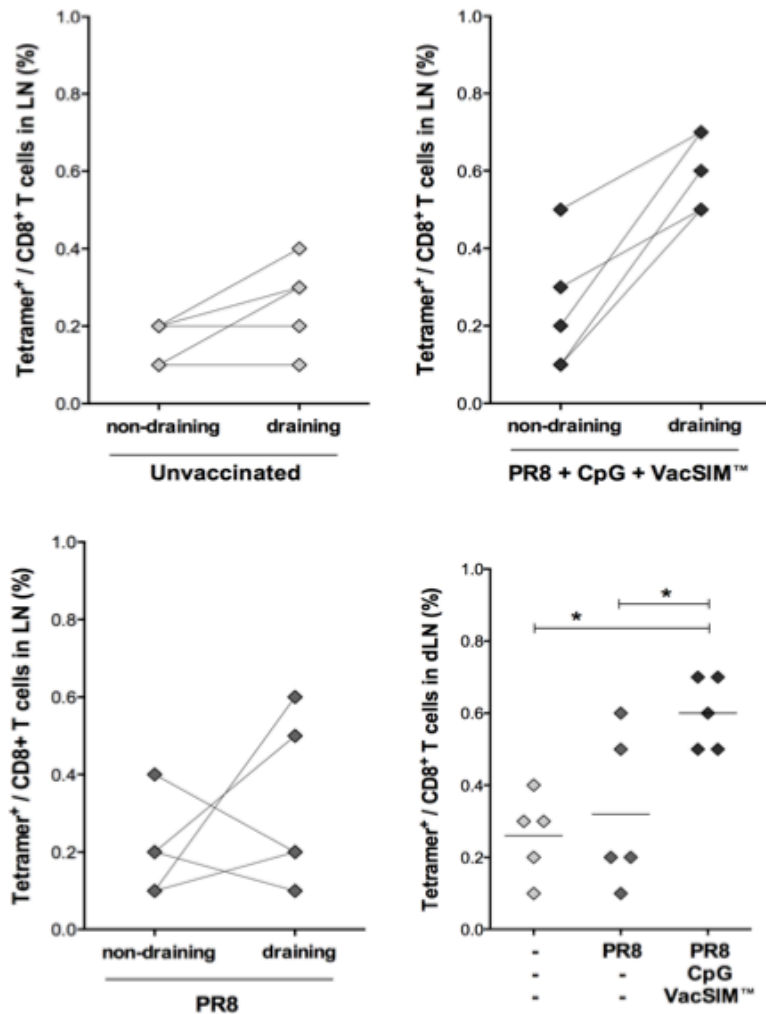


Figure 3.4: Vaccination with PR8 and CpG by VacSIM™ delivery enhances NP-specific T cells in draining lymph nodes post challenge. Levels of NP-specific CD8+ T cells in draining and non-draining lymph nodes of mice 2 days post lethal (1000 LD50) challenge are shown (A-D). Statistical significance (*p<0.05) was determined by one-way ANOVA and Bonferroni's multiple comparisons test.

3.4.4 Proposed Mechanism for VacSIM™ Improving Vaccine Responses

We hypothesize that combining VacSIM™ with vaccine ± adjuvant prior to immunizing, leads to localized formation of a porous gel-matrix depot, which allows gradual egress of vaccine components (Figure 3.5). To investigate whether VacSIM™

enhanced immunogenicity (1) (Figures 3.1, 3.4, S3.7) and vaccine efficacy (Figures 3.3, S3.7) was a result of inherent immune-stimulating factors associated with VacSIM™, we compared its ability to induce activation of bone marrow derived dendritic cells (BMDCs). Results indicate that unlike alternative vaccine components such as PR8 or CpG, the level of DC activation following incubation with VacSIM™ was comparable to media and human serum albumin (HSA). Therefore, in the absence of antigen or adjuvant, VacSIM™ fails to initiate an immune response through DC activation.

We next wanted to investigate gradual egress of antigen from the gel-matrix depot and the effects of altering concentrations of the oligopeptide within VacSIM™, which has been shown to affect the pore size range (31). The diffusion of two alternative antigens from the *in vitro* assembled vaccine depot was measured over time and incorporation of either 0.5% or 1% VacSIM™. In contrast to whole-inactivated PR8, which did not diffuse at either concentration, the protein antigen ovalbumin (OVA) differentially diffused over time in a VacSIM™ concentration-dependent manner.

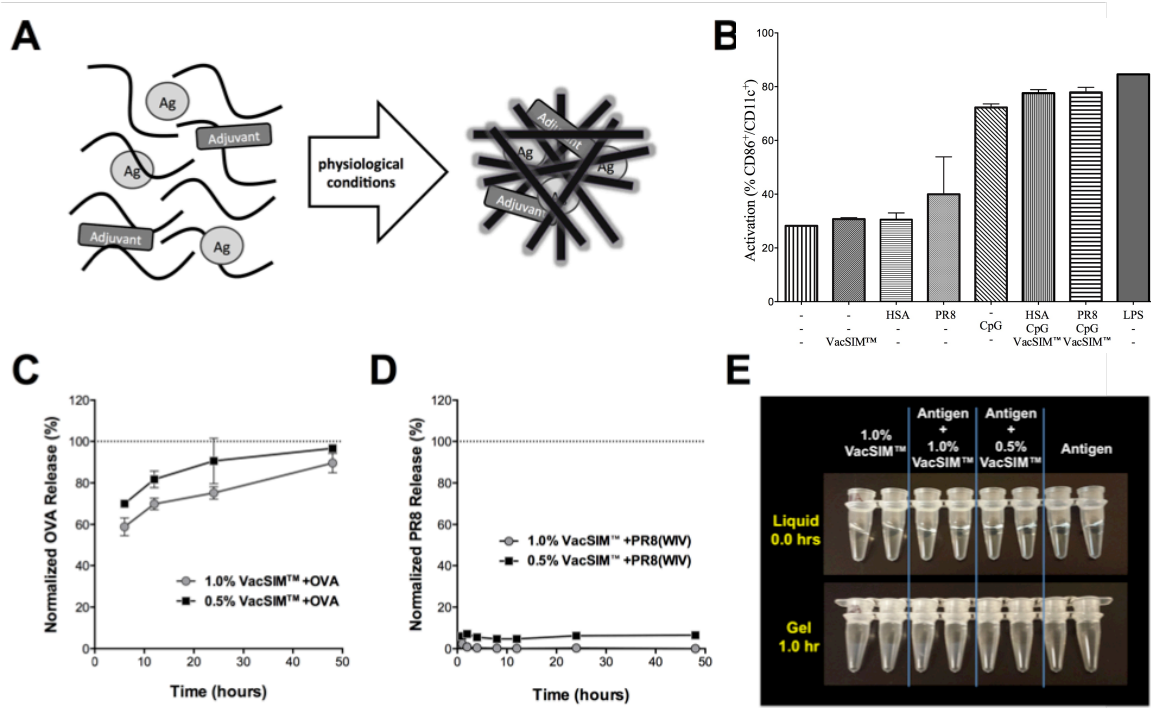


Figure 3.5: Vaccine self-assembling immune matrix proposed mechanism. Schematic of antigen and adjuvant vaccine components being delivered in VacSIM™, which under physiological conditions begins to self-assemble generating a porous vaccine-matrix depot localized to vaccination site (A). In the absence of antigen, VacSIM™ did not induce dendritic cell (DC) activation in bone marrow derived dendritic cells (BMDCs). BMDC cultures were incubated 24-hours with either VacSIM™, human serum albumin (HSA), PR8 (WIV), CPG, combinations of antigen + adjuvant + VacSIM™ and either media, or lipopolysaccharide (LPS) prior to staining. Activated DCs (CD86⁺/CD11c⁺) were determined by flow (B). Diffusion over time of ovalbumin (OVA) protein (C) and influenza A/PR/8/34 (PR8) whole-inactivated virus (D) from *in vitro* assembled vaccine-gel depots incorporating a 0.5% or 1% VacSIM™ solution. Samples were collected from PBS overlay out to 48 hours, and antigen diffusion was detected via α -OVA or α -PR8 indirect ELISA. Photographs depict VacSIM™ \pm antigen in the initial liquid phase maintained during preparation and the gel phase induced by incubation under physiological conditions (E).

3.5 Discussion

Until a universal influenza vaccine is developed, annual vaccination for seasonal influenza epidemics will be necessary to reduce infection related morbidity and mortality. Production of annual influenza vaccines is dependent on global surveillance and a “best

guess” for which circulating influenza A and B strains should be incorporated into the vaccine. This results in fluctuating VE from year to year and represents an added variable to producing effective seasonal influenza vaccines. Due to population-biased VE disparity, a major goal for seasonal influenza vaccines is to increase efficacy in high-risk populations, such as the very young, the elderly and immune compromised, who are limited to the less-potent inactivated vaccines. In the current study, we demonstrated that delivery of whole-inactivated influenza in VacSIM™ led to enhancement of multiple aspects of vaccine immunogenicity and overall efficacy to challenge when the adjuvant CpG was also incorporated into the vaccine. Specifically, we showed that VacSIM™ delivery of the inactivated influenza vaccine plus CpG to mice, significantly increased production of flu-specific antibodies, protection from lethal challenge and significantly increased viral clearance from the lungs compared to other PR8 delivery methods.

Delivery in VacSIM™ is flexible enough to incorporate a variety of different vaccine components and as such, represents a new vaccine delivery platform, capable of enhancing VE, and is amenable to rapid formulation changes and immediate deployment. Composed of the (RADA)₄ synthetic oligopeptide, VacSIM™ is not analogous to first or second generation hydrogels, which were based on polyethylene glycol (PEG), hydroxyethyl methacrilates (HEMA), polysaccharides (such as alginate, chondroitin sulfate, chitosan, and hyaluronic acid) or polyaminoacids (32-35) that require *ex vivo* polymerization. Similarly, vaccine alternatives involving nanoengineering, such as layer-by-layer assembly of hydrogel vesicles and dermal microneedle patch technologies, are unlike VacSIM™ and require polymerization prior to administration (36, 37). In addition to the (RADA)₄ oligopeptide, various other natural and synthetic hydrogel constructs

have been evaluated for clinical applications such as tissue engineering (38, 39), drug delivery (40) and vaccine delivery (41-43). In regards to vaccine delivery, incorporation of short, self-assembling amino acid sequences at the C-terminal domain of certain peptide epitopes have been shown to boost immunogenicity (44). Further, direct coupling of vaccine antigen peptide epitope(s) to the self-assembling peptide (SAP) domain Q11, induced vaccine-specific antibody responses in mice (45, 46).

Although the precise mechanism is still being evaluated, we hypothesize a key component to be *in situ* construction of the vaccine gel matrix depot via hydrated nanofibers of the (RADA)₄ oligopeptides. This formation immediately following injection, allows gradual egress of aqueous vaccine components from the porous gel matrix depot, providing antigen persistence and increasing activation of APCs. In this regard, one formulation of the (RADA)₄ oligopeptide, PuraMatrix™, has been shown to gradually release insulin over time *in vivo* (47). Initial mechanistic studies are consistent with *in vivo* challenge results (Figure 3.3) indicating that VacSIM™ itself does not poses immune stimulating characteristics (Figure 3.5). In addition to sustained antigen egress, which was demonstrated *in vitro* using the protein antigen OVA (Figure 3.5), the VacSIM™ gel matrix depot may also help stabilize vaccine components by delaying systemic degradation. These findings are consistent with reports on other SAPs and Q11 nanofibers to be non-immunogenic (45).

The results presented here show that a single vaccination of PR8 + CpG via VacSIM™ in mice, was sufficient to drive increased systemic and mucosal humoral responses, including increased vaccine-specific antibody titers in sera and vaccine-specific mucosal titers from the lungs (Figure 3.1). Importantly, mice vaccinated with

PR8 + CpG in VacSIM™ had increased protection from lethal influenza challenge and improved viral clearance from the lungs (Figure 3.3). The HI titers however, were lower (Figure 3.2). Thus, HI titers alone may not always be an appropriate correlate of protection or indicator of VE in this mouse model (48). Interestingly, VacSIM™-induced protection correlates with increases in influenza-specific T cells in the draining lymph nodes (Figure 3.4), an observation that warrants further exploration. Antigen persistence is thought to contribute to the duration of immune memory responses (49) and the concept that antigen persistence increases vaccine-specific immune responses, notably antigen-specific CD4⁺ and CD8⁺ T cell responses, has been gaining traction for some time (50).

Taken together, our results suggest there is a synergistic effect between CpG and VacSIM™ delivery of WIV PR8 vaccine. Why simple mixing of WIV PR8 in VacSIM™ did not drive enhanced responses remains to be determined. However, simple mixing of recombinant protein subunit vaccines, including Hepatitis B Surface Antigen show dramatic enhancement of vaccine-specific responses without addition of other adjuvants (1). Additionally, the protein antigen OVA diffused gradually from in situ assembled vaccine depots, whereas whole-inactivated PR8 was unable to diffuse (Figure 3.5). One explanation is that WIV PR8 is a formalin-inactivated whole virus preparation, whose particle sizes may hinder subunits from diffusing through the VacSIM™ gel matrix depot as easily as single recombinant protein subunit vaccines. The lack of diffusion through the gel matrix, therefore, increases reliance on use of an adjuvant such as CpG to recruit APCs directly to the VacSIM™ gel depot. This could explain the lower overall VE seen in mice vaccinated with PR8 via VacSIM™ versus elevated levels when PR8 was

delivered in saline and how addition of CpG to PR8 in VacSIM™ was sufficient to increase overall levels of anti-influenza antibodies and VE beyond the levels observed in PR8 or PR8 + CpG vaccinated mice (Figure 3.1, 3.3).

Regardless, adjuvants might be necessary to improve VE in high-risk populations, who have increased potential to develop severe complications. In this regard, we predict that another advantage of the VacSIM™ gel matrix depot will be the ability to reduce adjuvant reactogenicity through gradual egress of adjuvant from the vaccine depot. This attribute of reducing adjuvant reactogenicity while retaining the ability to increase APC activation would represent a major advance in adjuvant development and broaden the use of adjuvants in vaccines.

In summary, VacSIM™ enables flexibility to incorporate various types of antigens/organisms plus or minus adjuvants in a straightforward and time-effective manner, prior to injection. We believe VacSIM™ delivery can be applied to the majority of vaccines that have been or are currently being developed and represents a true “Plug and Play” vaccine delivery method that can be utilized for the rapid development and administration of vaccines for biodefense and against emerging and pandemic diseases.

3.6 Materials and Methods

3.6.1 Animals

Female C57BL/6 mice (Harlan) aged 5-7 weeks were obtained from Harlan laboratories and housed in pathogen-free conditions. Mice were acclimated for one week prior to manipulations. All animal handling was conducted in accordance with applicable regulations and with the approval of the institutional animal care and use committee.

3.6.2 Cell Culture

Madin-Darby Canine Kidney (MDCK) epithelial cells (ATCC) were cultured in 1:1 ratio of Dulbecco's Modified Eagle Medium (DMEM) and Eagle's minimal essential medium (MEM) supplemented with 1% L-glutamine and 5% fetal bovine serum (FBS) at 37°C and 5% CO₂.

3.6.3 Bone marrow derived dendritic cells

Femurs and tibias were collected from C57BL/6 mice and sterilized by sequentially submerging bones in 70% EtOH (1x), 1x PBS (2x), after which marrow was isolated in RPMI-1640 serum-free media. Suspended lymphocyte precursor cells were separated and adherent cells were retained for continued culture in complete media [RPMI-1640, 10% FBS, 1% antibiotic/antimycotic, non-essential amino acids, 1000 U/ml granulocyte macrophage colony stimulating factor (GM-CSF) and 1000 U/ml IL-4] at 37 °C and 5% CO₂. After six days, DC cultures were confirmed by incubating 2E6 cells in 2ml complete media ± 100ng/mL LPS for 16-20 hours (differentiate activated/resting DCs). Cells were treated with Fc Block (BD) and stained with CD86-FITC (BD) and CD11c-PE (BD).

3.6.4 Vaccination

Six to eight week old mice (n=4-8) were vaccinated via a single, subcutaneous (s.c.) vaccination. Vaccinations contained sterile saline, PR8 whole-inactivated virus (WIV) (15 µg, Charles River Laboratories), CpG (50 µg, ODN1826, InvivoGen), alum (250 µg, Imject Alum, Thermo Scientific), or equal volumes VacSIM™ (PuraMatrix™, BD), as indicated, with a total injection volume of 200 uL.

3.6.5 Viral Challenge

Influenza challenge virus (A/Puerto Rico/08/34, H1N1) was mouse-adapted through serial passage prior to propagation in embryonated chicken eggs and lethality was determined by MLD₅₀, as described previously (51). Four weeks post-vaccination, age-matched mice sedated with tribromoethanol, were challenged intranasally (i.n.) with a lethal dose (30 or 1000 LD₅₀, as indicated) of mouse-adapted homologous PR8 virus. Immediately post-challenge, lungs were harvested from minimally 2 control mice, to confirm infection by plaque assay. Mice were monitored daily for weight change and symptom severity in accordance with IACUC guidelines. Following challenge each animal was given a daily morbidity score, calculated from the sum of the assigned values of each symptom: hunched back or ruffled fur (1), lethargy (2), head tilt (3), weight loss >20% (3), weight loss >25% (4), weight loss >30% (5), cyanosis (5), paralysis (5), seizure (5) and severe dyspnea (5). Animals were immediately sacrificed (CO₂ inhalation followed by cervical dislocation) if they received a total score of ≥ 5 indicating they reached their humane endpoint.

3.6.6 Antibody Endpoint Titers

Humoral responses were measured by indirect ELISA. Sera were collected from mice prior to vaccination (pre-bleed) and four weeks following vaccination. In addition, lungs were collected to evaluate vaccine-specific mucosal IgA and IgG levels. Briefly, ELISA plates were coated with whole A/Puerto Rico/08/34 (H1N1) inactivated/purified virus (4 μ g/ml) at 4 °C overnight. Plates were washed five times with wash buffer (160 mM NaCl, 0.5 mM EDTA and 0.05% Tween 20), then blocked in 1X PBS containing 5% non-fat milk powder and 1% BSA for at least two hours. Plates were decanted, incubated for 2-24 hours with samples serially diluted in blocking buffer, then washed five times.

Detection antibodies (HRP-conjugated α -mouse IgG₁, IgA and IgM from Santa Cruz, IgG₃, IgG_{2a} and IgG_{2b} from Invitrogen, IgE from Southern Biotech or total IgG from BioLegend) were diluted in blocking buffer and incubated for one hour. After five washes, plates were developed in the dark using SureBlue 1 component TMB substrate (KPL Laboratories) and the reaction was stopped with 2N sulfuric acid. Absorbance was measured at 450 nm with 570 nm background correction.

3.6.7 Hemagglutination Inhibition (HI) Assay

Sera samples were heat-inactivated for 30 minutes at 56 °C, and then pre-absorbed with 1% turkey RBCs for 30 minutes at 4 °C. Sera were diluted two-fold and incubated with 4HAU/25 μ L mouse-adapted PR8 virus, at equal volumes and room temperature for 30 minutes. Plates were developed with 0.05% turkey RBCs for 30-60 minutes at 4 °C and immediately imaged. Samples with an undetectable HI titer were assigned an arbitrary value of 5, which is equal to one half the assay detection limit.

3.6.8 Plaque Assays for Viral Quantitation

Briefly, serially diluted lung homogenates were incubated with MDCK lawns under a 2.4% Avicel (FMC BioPolymer) overlay. After incubation for two days, cells were fixed with methanol/acetone and stained with crystal violet (Acros Organics) for enumeration of plaque forming units (pfu). Lung samples with undetectable virus were graphed as four pfu per lung, which is a value equal to $\frac{1}{2}$ of the detection threshold of the assay.

3.6.9 Flow Cytometry for T Cell Enumeration

Draining and non-draining (contra-lateral) axillary and inguinal lymph nodes were harvested 2 dpc. Tissues were macerated and single cell suspensions were stained for flow cytometry with α -CD16/CD32, α -CD3-V500, and α -CD8a-Pacific Blue

antibodies (BD), APC-conjugated NP (ASNENMETM) tetramer (NIH Tetramer Core Facility), and Live/Dead fixable green viability dye (Invitrogen), using standard methods. Samples were acquired on a BD LSRII running FACSDiva software (BD). Tetramer-positive CD3+CD8+ viable singlets were analyzed using FlowJo vX (10.0.6) software.

3.6.10 Statistical Analyses

In general, a sample size of at least 4 mice per treatment group was utilized. Animals within a group were not pooled during analysis and unless otherwise stated, data from individual mice were graphed. No outliers were excluded. Statistical analyses were performed using GraphPad Prism version 6.0. Statistical methods and significant differences between vaccination groups include one-way ANOVA, two-way ANOVA, Kruskal-Wallis test, Log-rank (Mantel-Cox) test, Dunn's post-test, Tukey's post-test and Bonferroni post-test. The statistical method(s) used and alpha level (0.05 or 0.01) has been specified in each figure legend.

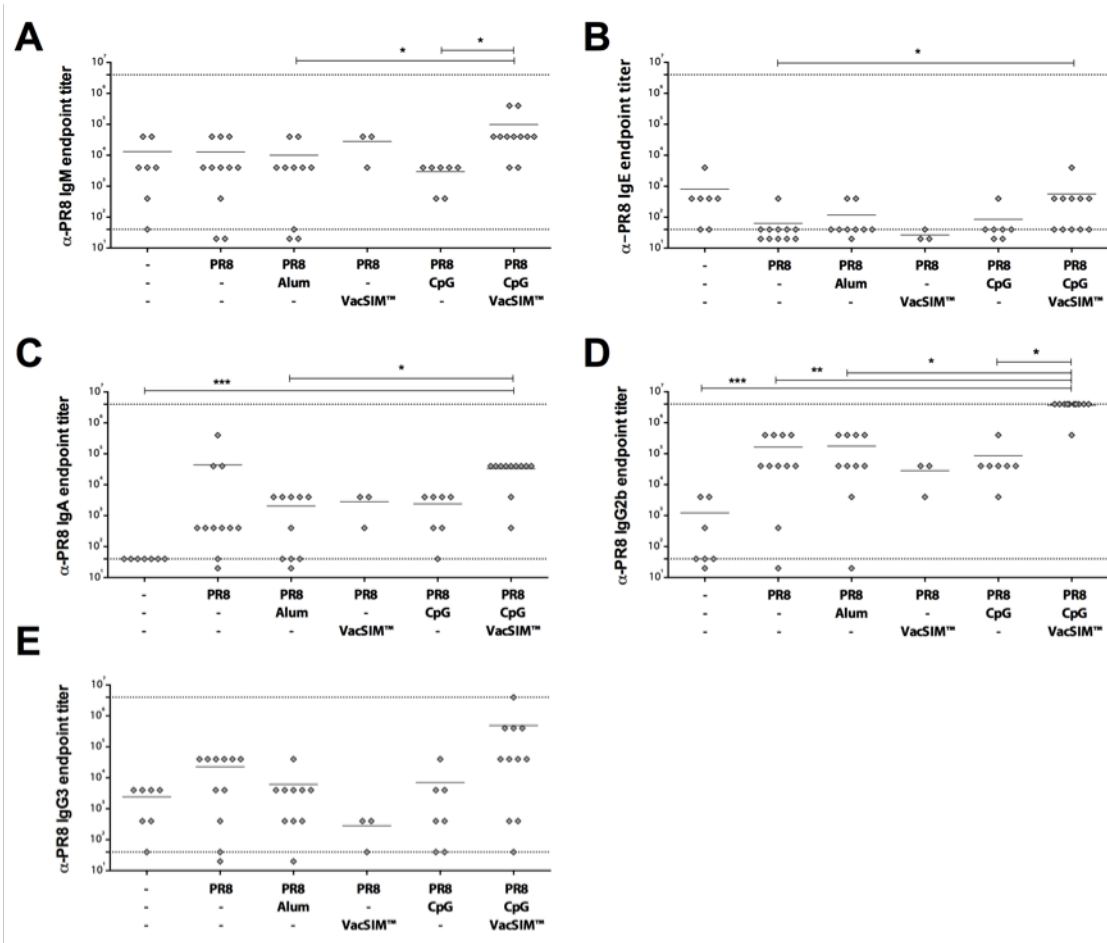
3.7 Acknowledgments

The authors thank Lindsay Nyhoff, Cac Bui and Mai Himedan for technical assistance. The authors also thank the UGA College of Veterinary Medicine Cytometry Core Facility and the NIH Tetramer Core Facility. This work was supported by NIH grants AI-071883 and AI-078787, awarded to DAH. Two patent applications have been filed on behalf of the authors. Experiments were designed by EFS, LMS and DAH and performed by EFS and LMS. Results were interpreted by EFS, LMS and DAH. The manuscript was written and edited by EFS, LMS and DAH.

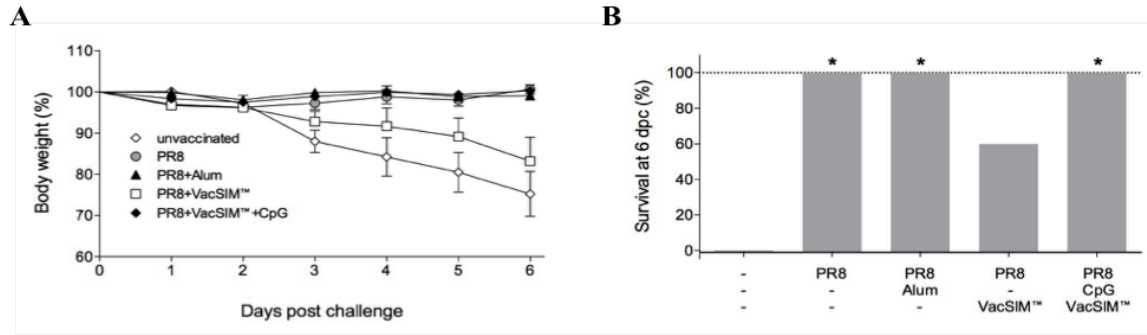
3.8 Supporting Information

Four out of five vaccine groups had PR8-specific IgM titers comparable to naïve mice. Mice vaccinated with PR8 in VacSIM™ containing CpG had slightly increased

IgM endpoint titers. For IgE, all vaccine groups maintained low PR8-specific IgE titers, with the group vaccinated with PR8 + CpG in VacSIM™ having IgE titers that while low, were significantly increased compared to mice vaccinated with PR8 alone. Analysis of IgA showed that mice vaccinated with PR8 + CpG in VacSIM™ had the highest PR8-specific sera IgA endpoint titers, significantly increased over other vaccine groups. Sera quantity was limited from the group vaccinated with PR8 via VacSIM™, so only three of five mice were assayed. The vaccine-specific endpoint titers from this group (PR8 via VacSIM™) were excluded from statistical analysis due to low sample size, however, their levels of IgG and IgA were lower compared with mice vaccinated with PR8 + Alum or CpG.



Supplementary Figure 3.6: Inactivated influenza vaccine delivered with CpG via VacSIM™ induces higher antibody titers in sera. Sera was collected 4 wpv and A/PR/8/34-specific IgM, IgE, IgA, IgG2b and IgG3 endpoint titers were determined by indirect ELISA (A-E). Dashed lines indicate detection thresholds of the experiment. Results were replicated, for each vaccine group, in a minimum of 3 separate experiments (n=5-16). Statistical significance (*p<0.05, **p<0.01, ***p<0.001, ****p<0.0001) between vaccination groups was determined using the Kruskal-Wallis test and followed by Dunn's multiple-comparisons post-test.



Supplementary Figure 3.7: Low dose lethal challenge is insufficient to discriminate between protected groups. Presented are post-challenge weight (A) and survival (B) of mice following lethal (30 LD₅₀) challenge administered at 4 wpv. Dashed lines indicate detection thresholds of the experiment. Representative of a single experiment (n=5). Statistical significance (*p<0.05) of survival was determined relative to unvaccinated mice using the Log-rank (Mantel-Cox) test with multiple comparisons.

3.9 References

1. Grenfell RF, Shollenberger LM, Samli EF, & Harn DA (2015) Vaccine Self-assembling Immune Matrix is a new delivery platform that enhances immune responses to rHBsAg in mice. *Clinical and Vaccine Immunology* 22(3):337-343.
2. Kisiday J, *et al.* (2002) Self-assembling peptide hydrogel fosters chondrocyte extracellular matrix production and cell division: implications for cartilage tissue repair. *Proceedings of the National Academy of Sciences of the United States of America* 99(15):9996-10001.
3. Iwai Y, Matsuda Y, Nakatsuka M, Mikami Y, & Kumabe S (2012) A preliminary study of the dental implant therapy--initial osteogenesis of human mesenchymal stem (HMS0014) cells on titanium discs with different surface modifications. *Okajimas folia anatomica Japonica* 88(4):133-140.
4. Horii A, Wang X, Gelain F, & Zhang S (2007) Biological designer self-assembling peptide nanofiber scaffolds significantly enhance osteoblast proliferation, differentiation and 3-D migration. *PloS one* 2(2):e190.
5. Henriksson H, Hagman M, Horn M, Lindahl A, & Brisby H (2011) Investigation of different cell types and gel carriers for cell-based intervertebral disc therapy, in vitro and in vivo studies. *Journal of tissue engineering and regenerative medicine*.
6. Zhang S (2003) Fabrication of novel biomaterials through molecular self-assembly. *Nature biotechnology* 21(10):1171-1178.

7. Zhang S, Gelain F, & Zhao X (2005) Designer self-assembling peptide nanofiber scaffolds for 3D tissue cell cultures. *Seminars in cancer biology* 15(5):413-420.
8. Zhang S ZX, Spirio L. (2010) *PuraMatrix: Self-Assembling Peptide Nanofiber Scaffolds* (CRC Press, Scaffolding In Tissue Engineering) 2 Ed pp 217-240.
9. Kondo Y, Nagasaka T, Kobayashi S, Kobayashi N, & Fujiwara T (2014) Management of peritoneal effusion by sealing with a self-assembling nanofiber polypeptide following pelvic surgery. *Hepato-gastroenterology* 61(130):349-353.
10. Rosa V, Zhang Z, Grande RH, & Nor JE (2013) Dental pulp tissue engineering in full-length human root canals. *Journal of dental research* 92(11):970-975.
11. Dissanayaka WL, Hargreaves KM, Jin L, Samaranayake LP, & Zhang C (2014) The Interplay of Dental Pulp Stem Cells and Endothelial Cells in an Injectable Peptide Hydrogel on Angiogenesis and Pulp Regeneration In Vivo. *Tissue engineering. Part A*.
12. NIAID (Flu (Influenza): 2009 H1N1, Seasonal, Avian (Bird), Pandemic.
13. WHO (2003) Influenza. (WHO).
14. Goldstein E, Viboud C, Charu V, & Lipsitch M (2012) Improving the estimation of influenza-related mortality over a seasonal baseline. *Epidemiology (Cambridge, Mass.)* 23(6):829-838.
15. McLean HQ, Meece JK, & Belongia EA (2014) Influenza vaccination and risk of hospitalization among adults with laboratory confirmed influenza illness. *Vaccine* 32(4):453-457.
16. Couch RB, *et al.* (1986) Influenza: its control in persons and populations. *J Infect Dis* 153(3):431-440.
17. Yoshikawa TT (1981) Important infections in elderly persons. *West J Med* 135(6):441-445.
18. Webster RG (2000) Immunity to influenza in the elderly. *Vaccine* 18(16):1686-1689.
19. Flannery B, *et al.* (2014) Interim estimates of 2013-14 seasonal influenza vaccine effectiveness - United States, February 2014. *MMWR. Morbidity and mortality weekly report* 63(7):137-142.
20. Powers DC & Belshe RB (1993) Effect of age on cytotoxic T lymphocyte memory as well as serum and local antibody responses elicited by inactivated influenza virus vaccine. *J Infect Dis* 167(3):584-592.

21. Simonsen L, Taylor RJ, Viboud C, Miller MA, & Jackson LA (2007) Mortality benefits of influenza vaccination in elderly people: an ongoing controversy. *Lancet Infect Dis* 7(10):658-666.
22. Weinberger B & Grubeck-Loebenstien B (2012) Vaccines for the elderly. *Clinical microbiology and infection : the official publication of the European Society of Clinical Microbiology and Infectious Diseases* 18 Suppl 5:100-108.
23. Lang PO, *et al.* (2012) Effectiveness of influenza vaccine in aging and older adults: comprehensive analysis of the evidence. *Clinical interventions in aging* 7:55-64.
24. Vesikari T, Pepin S, Kusters I, Hoffenbach A, & Denis M (2012) Assessment of squalene adjuvanted and non-adjuvanted vaccines against pandemic H1N1 influenza in children 6 mo to 17 y of age. *Human vaccines & immunotherapeutics* 8(9).
25. Esposito S, *et al.* (2012) Preventing influenza in younger children. *Clinical microbiology and infection : the official publication of the European Society of Clinical Microbiology and Infectious Diseases* 18 Suppl 5:42-49.
26. Beyer WEP, Palache AM, Lüchters G, Nauta J, & Osterhaus ADME (2004) Seroprotection rate, mean fold increase, seroconversion rate: which parameter adequately expresses seroresponse to influenza vaccination? *Virus Research* 103(1-2):125-132.
27. Hobson D, Curry RL, Beare AS, & Ward-Gardner A (1972) The role of serum haemagglutination-inhibiting antibody in protection against challenge infection with influenza A2 and B viruses. *The Journal of hygiene* 70(4):767-777.
28. de Jong JC, *et al.* (2003) Haemagglutination-inhibiting antibody to influenza virus. *Developments in biologicals* 115:63-73.
29. Zanoni I, *et al.* (2009) CD14 regulates the dendritic cell life cycle after LPS exposure through NFAT activation. *Nature* 460(7252):264-268.
30. Quan FS, Compans RW, Nguyen HH, & Kang SM (2008) Induction of heterosubtypic immunity to influenza virus by intranasal immunization. *Journal of virology* 82(3):1350-1359.
31. Xiaojun Z, Shuguang Z, & Lisa S (2005) PuraMatrix. *Scaffolding In Tissue Engineering*, (CRC Press), pp 217-238.
32. Ingavle GC, Gehrke SH, & Detamore MS (2014) The bioactivity of agarose-PEGDA interpenetrating network hydrogels with covalently immobilized RGD peptides and physically entrapped aggrecan. *Biomaterials* 35(11):3558-3570.

33. Browning MB, Cereceres SN, Luong PT, & Cosgriff-Hernandez EM (2014) Determination of the in vivo degradation mechanism of PEGDA hydrogels. *Journal of biomedical materials research. Part A*.
34. Jose S, Hughbanks ML, Binder BY, Ingavle GC, & Leach JK (2014) Enhanced trophic factor secretion by mesenchymal stem/stromal cells with Glycine-Histidine-Lysine (GHK)-modified alginate hydrogels. *Acta biomaterialia*.
35. Xiong Y, *et al.* (2014) Compartmentalized multilayer hydrogel formation using a stimulus-responsive self-assembling polysaccharide. *ACS applied materials & interfaces* 6(4):2948-2957.
36. Jorquera PA, *et al.* (2013) Nanoparticle vaccines encompassing the respiratory syncytial virus (RSV) G protein CX3C chemokine motif induce robust immunity protecting from challenge and disease. *PloS one* 8(9):e74905.
37. Lee JW, Choi SO, Felner EI, & Prausnitz MR (2011) Dissolving microneedle patch for transdermal delivery of human growth hormone. *Small (Weinheim an der Bergstrasse, Germany)* 7(4):531-539.
38. Zhang L, *et al.* (2014) Preparation of novel biodegradable pHEMA hydrogel for a tissue engineering scaffold by microwave-assisted polymerization. *Asian Pacific journal of tropical medicine* 7(2):136-140.
39. Balakrishnan B & Banerjee R (2011) Biopolymer-based hydrogels for cartilage tissue engineering. *Chemical reviews* 111(8):4453-4474.
40. Zustiak SP, Pubill S, Ribeiro A, & Leach JB (2013) Hydrolytically degradable poly(ethylene glycol) hydrogel scaffolds as a cell delivery vehicle: Characterization of PC12 cell response. *Biotechnology progress* 29(5):1255-1264.
41. Sexton A, *et al.* (2009) A protective vaccine delivery system for in vivo T cell stimulation using nanoengineered polymer hydrogel capsules. *ACS nano* 3(11):3391-3400.
42. Chong SF, *et al.* (2009) A paradigm for peptide vaccine delivery using viral epitopes encapsulated in degradable polymer hydrogel capsules. *Biomaterials* 30(28):5178-5186.
43. Coeshott CM, *et al.* (2004) Pluronic F127-based systemic vaccine delivery systems. *Vaccine* 22(19):2396-2405.
44. Rudra JS, Tian YF, Jung JP, & Collier JH (2010) A self-assembling peptide acting as an immune adjuvant. *Proceedings of the National Academy of Sciences of the United States of America* 107(2):622-627.
45. Chesson CB, *et al.* (2014) Antigenic peptide nanofibers elicit adjuvant-free CD8(+) T cell responses. *Vaccine* 32(10):1174-1180.

46. Rudra JS, *et al.* (2012) Self-assembled peptide nanofibers raising durable antibody responses against a malaria epitope. *Biomaterials* 33(27):6476-6484.
47. Nishimura A, *et al.* (2012) Controlled release of insulin from self-assembling nanofiber hydrogel, PuraMatrix: application for the subcutaneous injection in rats. *European journal of pharmaceutical sciences : official journal of the European Federation for Pharmaceutical Sciences* 45(1-2):1-7.
48. Co MD, Cruz J, Takeda A, Ennis FA, & Terajima M (2012) Comparison of complement dependent lytic, hemagglutination inhibition and microneutralization antibody responses in influenza vaccinated individuals. *Human vaccines & immunotherapeutics* 8(9):1218-1222.
49. Gray D & Skarvall H (1988) B-cell memory is short-lived in the absence of antigen. *Nature* 336(6194):70-73.
50. Sacks DL (2014) Vaccines against tropical parasitic diseases: a persisting answer to a persisting problem. *Nature immunology* 15(5):403-405.
51. Webster R CN, Stohr K (2002) WHO Manual on Animal Influenza Diagnosis and Surveillance in *WHO Global Influenza Program*, ed Webster R CN, Stohr K (World Health Organization, Geneva, Switzerland), p 105.

CHAPTER 4

INVESTIGATING THE VACSIM™ ENHANCED IMMUNE RESPONSE OF ADJUVANTED WHOLE-INACTIVATED INFLUENZA (PR8) VACCINE²

² Samli EF, Shollenberger LM, & Harn DA (2015). To be submitted to Vaccine.

4.1 Introduction

Vaccine effectiveness is typically defined as a percent reduction in the incidence or severity of disease. Effectors, such as CD8⁺ cytotoxic T cells (CTLs) and antigen-specific antibodies directed to activate the immune response as a result of immunization, are typically what cause efficiency variations among different vaccines (1, 2). The vast majority of vaccines in use today rely on inducing immune responses that mimic those elicited as a result of a natural infection. Specifically, generating strong antigen-specific B cell responses that produce high titers of vaccine-specific IgG antibodies along with the eventual development of memory B cells, allowing for an efficient immune recall response to infection (3, 4). Research efforts focused on developing vaccines to elicit CD8⁺ effector CTLs increased dramatically as a result of HIV/AIDs. However, thus far there remains a singular example vaccine that utilizes a predominately CD8⁺ immune response and has been licensed for human use. The Bacillus Calmette–Guérine (BCG) vaccine utilizes T cell induced cytokine production, contributing to macrophage activation as the means to control *M. tuberculosis* (5, 6). The most effective vaccines are those that employ live/attenuated or killed, bacterial or virus (3). Whole organism vaccines generally induce strong CD4⁺ T cell responses that promote B cell maturation and vaccine-specific antibody production. For some whole organism vaccines, CD8⁺ T cell responses, including vaccine-specific CTL are also induced (3).

Table 4.1: Examples of vaccines with revaccination recommendations for general and high-risk* populations. *In this table “high-risk” includes those at continued risk due to environment or occupational hazards, in addition to immune compromised and >65years.

Vaccine	Semi-regular revaccination (booster shot)	
	General	High-risk
Seasonal influenza	1 dose / 1 year	3 doses / 1 year
Tetnus, diphtheria, acellular pertussis (Tdap)	(Td) 1 dose /10 years	(Td) 1 dose / 10 years
Rabies	-	1 dose / 6-24 months if serum Ab level drops

One unfortunate drawback of vaccines that rely predominately on generation of strong antibody responses is the need for vaccine booster shots, as a means of maintaining sufficiently high titers of vaccine-specific antibodies (7). Thus, many current vaccines result in waning protection over time necessitating a one-time series or in some cases recurrent booster vaccines to maintain immunity. Not surprisingly, waning of vaccine-specific responses is more pronounced in high-risk populations (Table 4.1). The seasonal influenza vaccine is a good example of this, with infants and the elderly having difficulty mounting sufficient immune responses to the vaccine (8-15). Additionally, individuals with compromised immune responses, such as those with asthma or other respiratory-related and unrelated illnesses, as well as those undergoing certain anti-cancer therapies, generate less effective vaccine responses.

This chapter focuses on several complicating factors of seasonal influenza vaccines, such as waning protection, cross-protection between alternative virus subtypes and age-specific variability in vaccine efficacy. Insufficient vaccine-induced immunity is affected by the vaccine-induced immune response durability (i.e.: how rapidly the immune response wanes over time). Another significant factor affecting seasonal

influenza vaccine efficacy is the frequent changes in viral strain that require vaccine manufacturers to rely on annual predictions for the following season's infectious strains. The experiments outlined in this chapter were designed to evaluate whether VacSIM™ delivery of CpG adjuvanted whole-inactivated virus (PR8), would enhance immunogenicity and protection in an elderly population, affect the response durability (protection over time) and/or the breadth (cross-reactivity/cross-protection) of vaccine-induced immunity, compared to alternative vaccine groups.

4.2 Results

4.2.1 Durability of the Vaccine-Induced Immune Response

To evaluate the durability of immune protection in mice after a single vaccination (s.c.) of whole-inactivated PR8+CpG delivered in VacSIM™, two vaccine studies were designed (Figure 4.1) that would challenge mice at four different time points, out to one year post immunization. In this study (see vaccination schedule in Panel A of Figure 4.1), unvaccinated and mice immunized with PR8 in saline were included, as standard control groups for comparison to PR8+CpG delivered in VacSIM™. Additionally, PR8+CpG delivered in saline as well as PR8+CpG+Alum vaccine groups were included for comparison. Sera were collected from individual mice in each group (n=5-8) prior to vaccination, to establish a baseline and again at 4, 10, 18, and 26 weeks post vaccination (wpv). PR8-specific IgG endpoint titers were determined from individual mice sera at each time point, prior to challenge, via indirect ELISA (Figure 4.2).

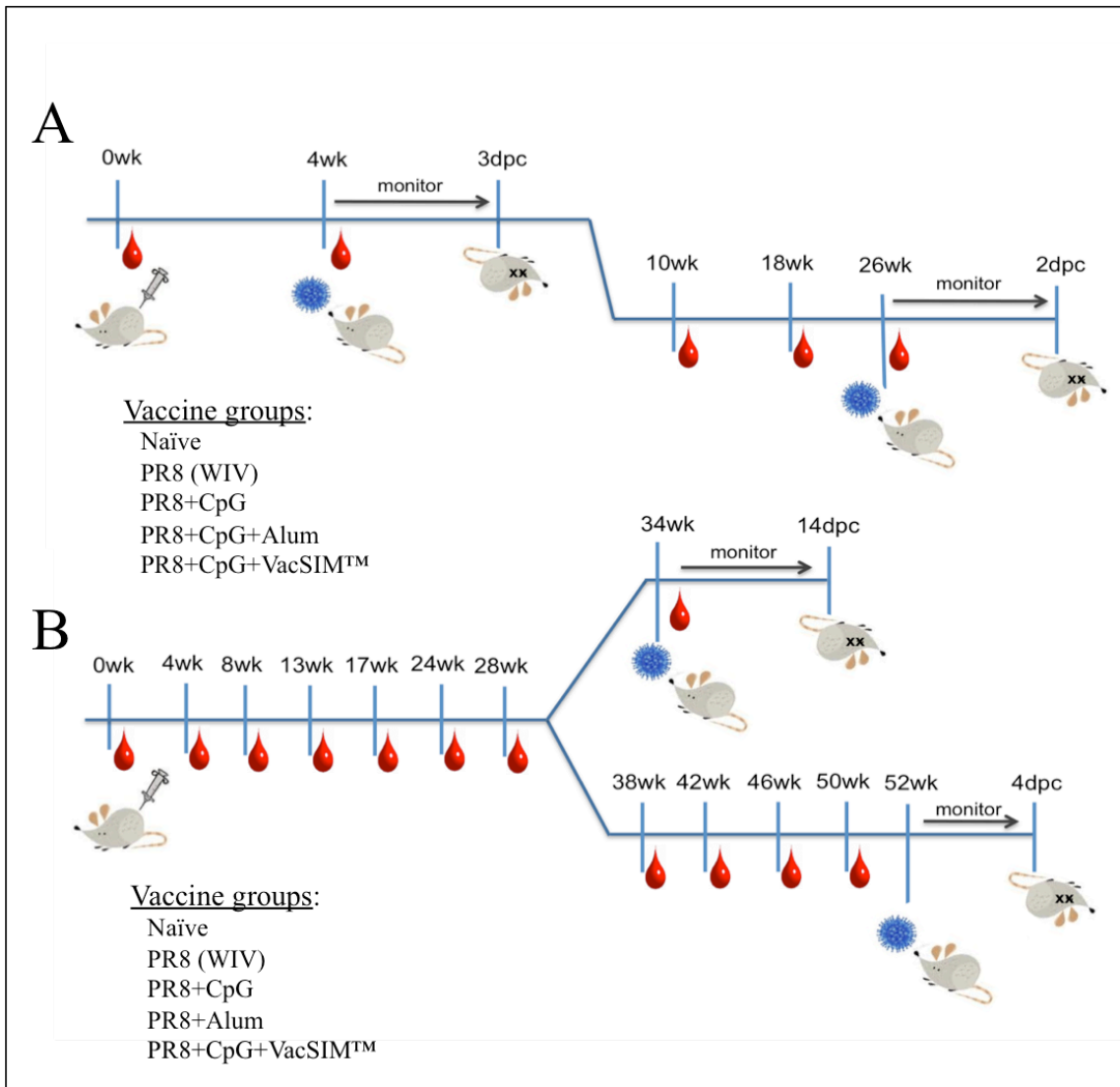


Figure 4.1: Immunization, viral challenge and biological sample collection schedules. Sera were collected from all mice, as a baseline, prior to receiving a single, subcutaneous vaccination. As presented here, subsequent serum samples were collected between 4-50 wpv and prior to lethal challenge. Mice received a single, intranasal challenge at 4, 26, 34, or 52 wpv, after which they were monitored daily until either the experiment completion and sample harvest or until the individual reached a level of post challenge weight loss and morbidity equal to or greater than its predefined humane endpoint. Image constructed in combination with Perkin Elmer's ChemBioDraw® Ultra v.13.0.2.320 and Microsoft® PowerPoint® for Mac 2011 v. 14.4.8 (150116).

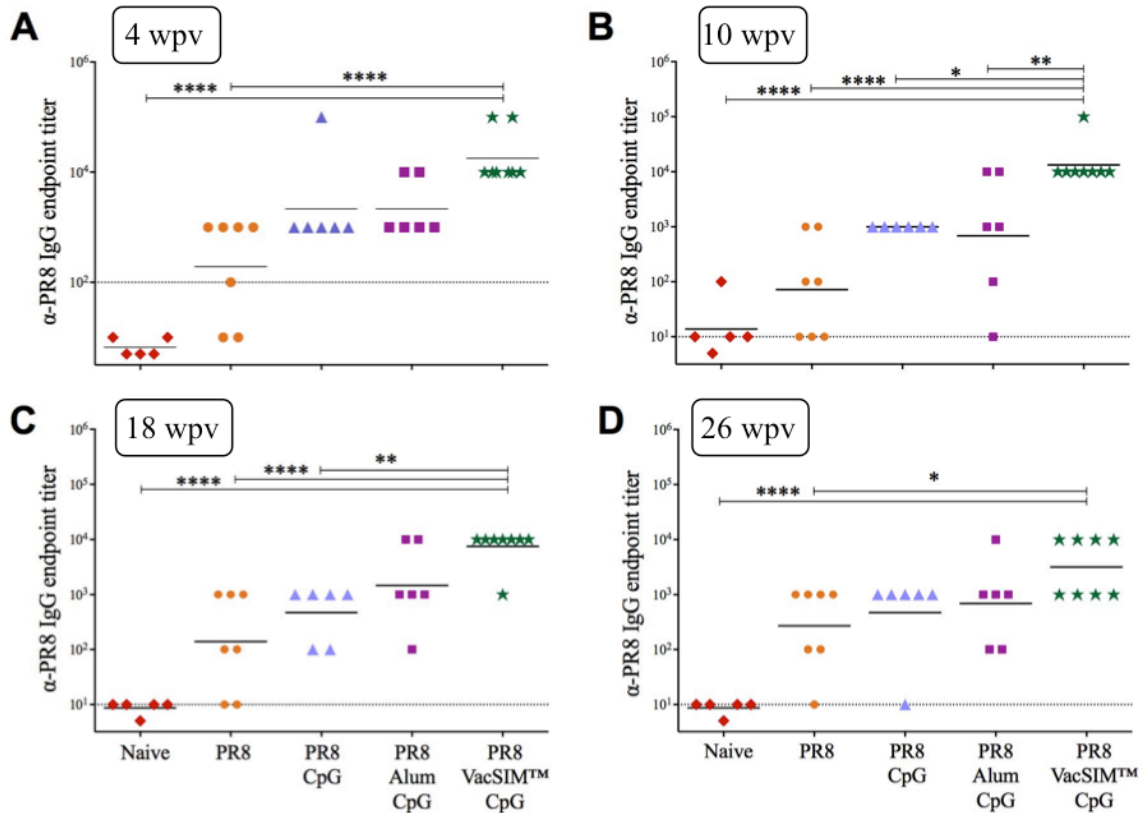


Figure 4.2: Vaccine-induced α -PR8 IgG sera endpoint titers 4-26 wpv. All mice were bled prior to vaccination, as a baseline and again at 4 wks (A), 10 wks (B), 18 wks (C), 26 wks (D), when α -PR8 IgG levels in the sera were detected by indirect ELISA. Dashed lines indicate detection thresholds of the experiment. Results are representative of 2 separate experiments (n=5-8). Statistical significance (*p<0.05, **p<0.01, ***p<0.001, ****p<0.0001) compared to the PR8+VacSIMTM+CpG vaccine group was determined using one-way ANOVA and Dunnett's test for multiple comparisons (A-D).

Mice receiving a single vaccination of PR8+CpG in VacSIMTM showed significantly elevated PR8-specific IgG endpoint titers compared to mice immunized with PR8 in saline or PR8+CpG in saline at 4, 10, and 18 wpv. After 6 months or 26 wpv mice that had been immunized with PR8+CpG in VacSIMTM maintained significantly increased levels of PR8-specific IgG in the sera, compared to mice that received PR8 in saline. In addition to comparing the individual endpoint titers at each time point, the mean endpoint titers for each vaccine group, across all time points post vaccination was

graphed in Figure 4.3 to more effectively visualize the kinetic response variations between vaccine groups. Unvaccinated mice maintain background levels of PR8-specific IgG in the sera samples collected across all time points. Likely due to the oscillating trend and range of individual responses at each time point (mean \pm SD), no significant change over time could be determined for the vaccine groups including PR8, PR8+CpG or PR8+Alum+CpG delivered in saline. Mice that were immunized with PR8+CpG in VacSIM™ had the highest endpoint titers at each time point and their kinetic response shows a trend of gradually decreasing PR8-specific IgG levels in the sera (Figure 4.3).

As part of this same study, a cohort of mice from each vaccine group (n=5-8) was challenged at 4 wpv and a second, equal cohort was challenged at 26

wpv. Following lethal PR8 challenge, individual morbidity scores were determined through daily monitoring for changes in weight and influenza-related symptoms. After a total of 2 or 3 days post challenge (dpc),

depending on the cohort, lungs were harvested and viral clearance efficiency was elucidated from the lungs via plaque assay (Figure 4.4).

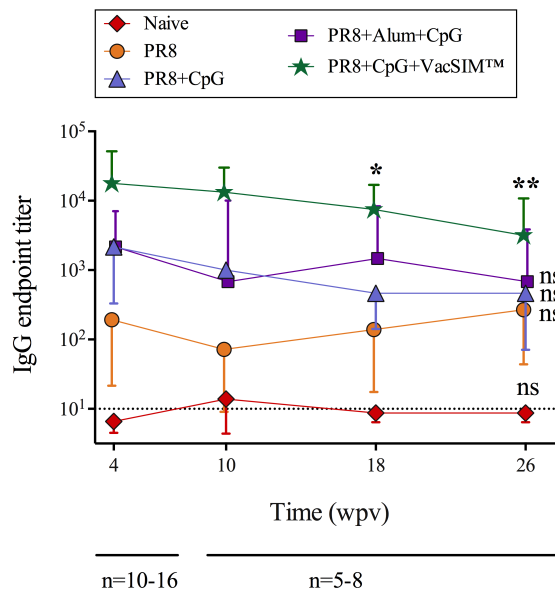


Figure 4.3: Vaccine-specific IgG endpoint titers kinetics from 1-6 months post vaccination. Sera mean endpoint titers of α -PR8 IgG at 4, 10, 18 and 26 weeks post vaccination (wpv). Error bars above or below indicate standard deviation. Statistically significant (*p<0.05, **p<0.01) change in IgG endpoint titer over time was evaluated within each vaccine group by two-way ANOVA and Tukey's multiple comparisons test.

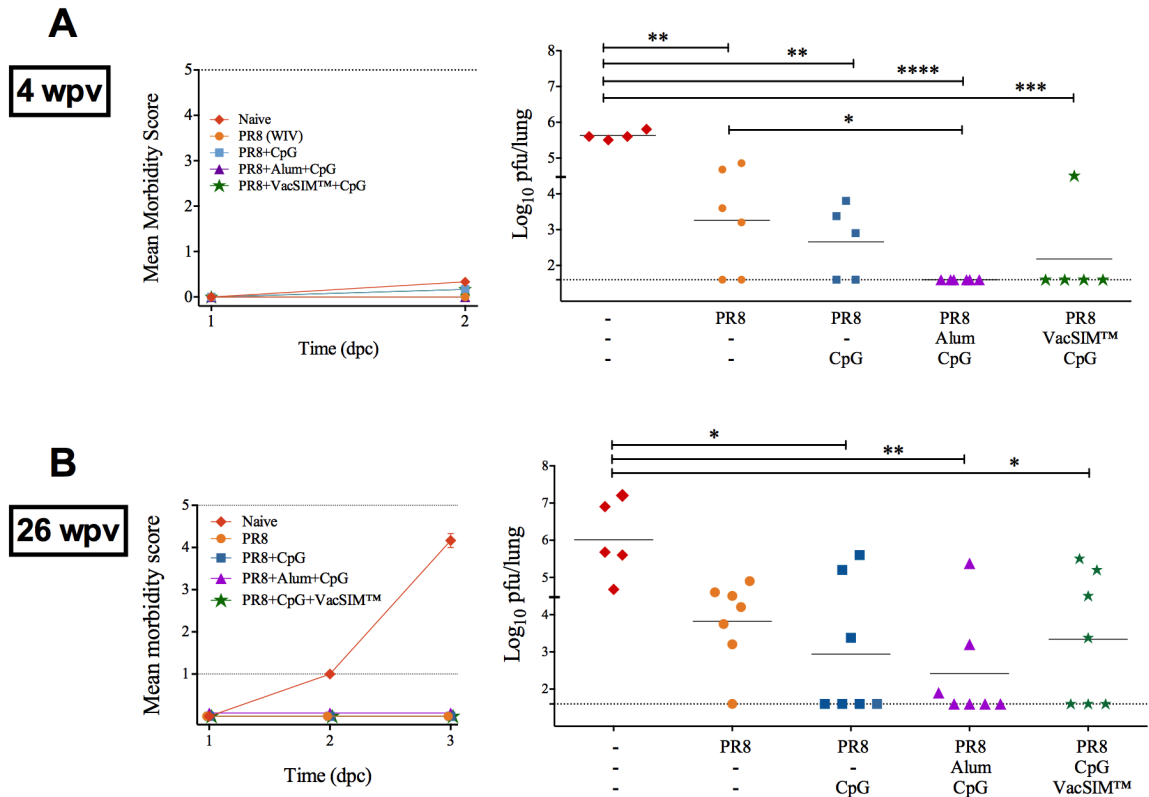


Figure 4.4: Immunity tapers for all vaccine groups by 6 months influenza challenge. Immunized mice received a single vaccination (s.c.) at 4 (A) or 26 (B) weeks prior to lethal challenge (n=5-8). Immunized and naïve mice, were challenged with 1000 LD₅₀ PR8 (influenza A/PR/8/34), following which, mice were monitored daily for 2-3 days, recording weight change and overall symptom severity (morbidity scores) post-challenge. Dashed lines at 1 and 5 indicate the minimal symptom/morbidity score (asymptomatic = 0) and the humane endpoint (individual with morbidity score of 5), respectively. Vaccine efficiency was evaluated by viral clearance from the lungs at 2 (A), 3 (B) days post challenge. Statistical significance (*p<0.05, **p<0.01, ***p<0.001, ****p<0.0001) between groups was determined by one-way ANOVA and Tukey's multiple comparisons test (A-B).

Following lethal challenge at 4wpv, both naïve and immunized mice showed insignificant morbidity at 1 and 2 dpc. The lack of morbidity this soon after challenge is consistent with previous challenge studies using C57BL/6 mice and this particular PR8 challenge virus (16, 17). Typically, naïve challenged mice show signs of morbidity around the third day post challenge and frequently have a score equal to their humane

endpoint no later than the sixth day. Viral clearance from the lungs at 2 dpc, of the cohort challenged 4 wpv indicates that vaccines containing an adjuvant provided better sterilizing immunity compared to naïve mice or mice immunized with unadjuvanted PR8 in saline. Even when incorporating outliers (one out of five mice unable to clear the virus effectively at 2 dpc time point) in the PR8+CpG in VacSIM™ group, this delivery regimen was among the most efficient tested, along with PR8+CpG+Alum, at inducing immunity to homologous challenge. Results from the cohort challenged six months post-vaccination (26 wpv) shows a decrease in vaccine efficacy across all vaccine groups, except for mice vaccinated with PR8+CpG in saline, which shows a greater proportion of challenged mice with undetectable virus levels in the lung at 3 dpc (Table 4.2).

An additional vaccine durability experiment was performed utilizing the vaccine groups and immunization/challenge schedule outlined in panel B of Figure 4.1, in which the durability of each vaccine-induced immune response was compared out to 12 months post vaccination. As previously described, serum samples were collected from all mice prior to vaccination and at various times post vaccination to determine vaccine-specific IgG endpoint titers (Appendix B, Figure 1). The durability of vaccine-induced protection was evaluated through lethal challenge of a cohort of mice from each vaccine group (n=8 immunized, n=5 naive) at 34 wpv (~ 8 months) and lethal challenge of a second, equal cohort at 52 wpv (12 months). Following PR8 challenge at 34 wpv, individual morbidity scores were determined daily, out to 14 dpc, for comparing morbidity trends and percent survival among vaccine groups. Following the PR8 challenge at 52 wpv, individual morbidity scores were determined out to 4 dpc, at which point lungs were harvested and viral clearance efficiency was elucidated (Figure 4.5) and summarized in Table 4.2.

Somewhat surprisingly, the two vaccine groups with less than 100% survival 14 days post 1,000 LD₅₀ PR8 challenge (34 wpv), were PR8 in saline (87.5% survival) and

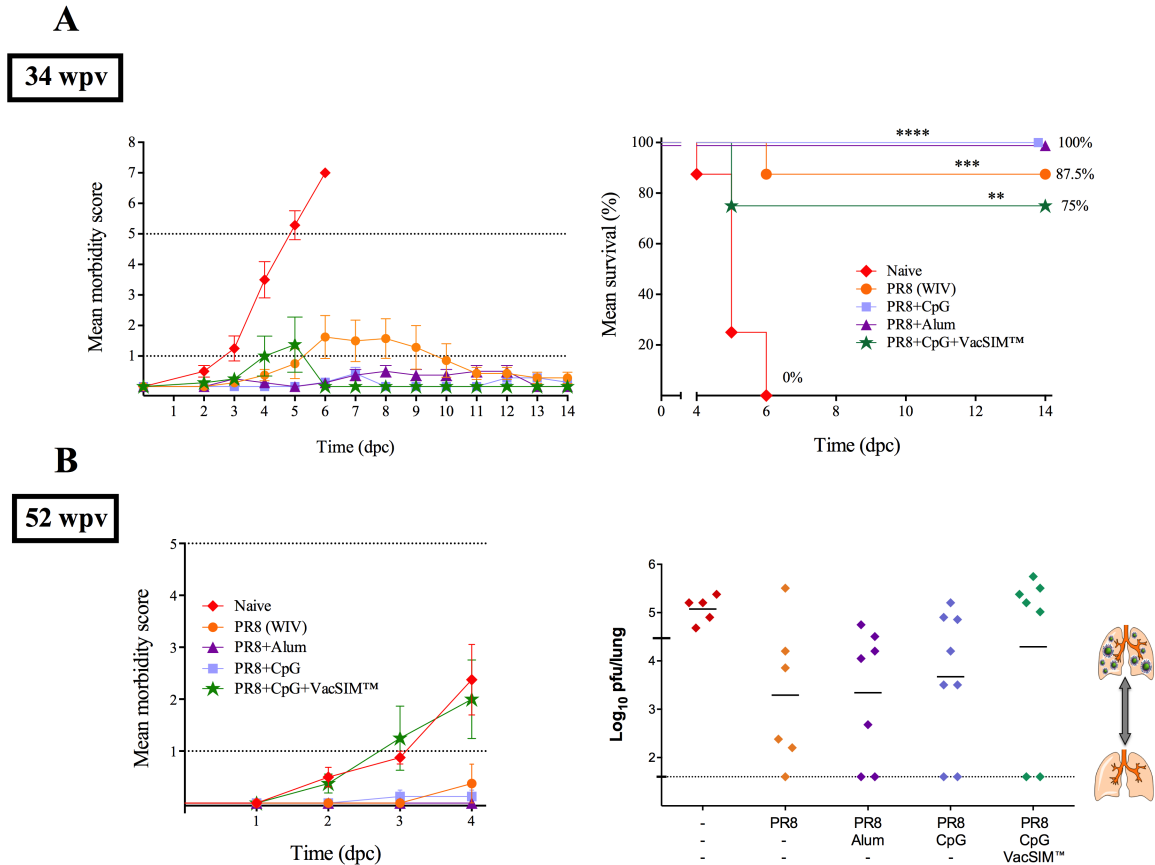


Figure 4.5: Vaccine groups possess marginal immunity by 1-year influenza challenge. Immunized mice received a single vaccination (s.c.), 34 (A) or 52 (B) weeks prior to lethal challenge (n=5-8). All mice, were challenged (i.n.) with 1,000_{LD50} PR8 (influenza A/PR/8/34) and monitored daily for either 14 (A) or 4 (B) days post challenge (dpc), recording individual weight change and overall symptom severity (morbidity scores) post-challenge. Error bars indicate standard deviation. Dashed lines at 1 and 5 indicate the minimal symptom/morbidity score (asymptomatic = 0) and the humane endpoint (individual with morbidity score of 5), respectively. Vaccine efficiency was evaluated by percent mean survival out to 14 dpc (A) and viral clearance from the lungs at 4 dpc (B). Dashed line at 1.6pfu represents detection threshold (a value of 1.6 was given samples with 0 plaques at lowest detection). Statistical significance (**p=0.0029, ***p=0.0002, ****p<0.0001) of survival (A) was determined relative to unvaccinated mice using the Log-rank (Mantel-Cox) test with multiple comparisons.

PR8+CpG in VacSIM[™] (75% survival). By comparing the percent survival of these two

groups with their associated morbidity scores over time post challenge (mean \pm SD) provides further context for interpreting survival results. The morbidity and survival results for PR8+CpG in VacSIM™, indicates that only two of the eight mice developed symptoms and/or lost weight post challenge. Further, two of these mice developed symptoms on the 4th day, one day after onset in the unvaccinated (naïve) group, and rapidly hit their humane endpoint morbidity score on day 4-5. This is in contrast to morbidity and survival results for the PR8 in saline group, in which several mice experienced weight loss and/or symptoms for a prolonged time period post challenge (days 5-10), yet only a single mouse reached its humane morbidity threshold.

Table 4.2: Summary table of percent undetectable virus in lungs by group. Proportion of immunized mice with undetectable virus level in the lungs (2, 3 or 4 dpc) following lethal challenge (4, 26 or 52 wpv). Data represents two independent experiments (n=5-8) described in subsection 4.1.1.

Challenged at 4, 26 or 52 weeks post vaccination (wpv) Viral load detected at 2, 3 or 4 days post challenge (dpc)			
Vaccine	4 wpv, 2 dpc	26 wpv, 3 dpc	52 wpv, 4 dpc
PR8	33%	14%	17%
PR8 + CpG	40%	67%	29%
PR8 + Alum	NA	NA	29%
PR8 + CpG + Alum	100%	57%	NA
PR8 + CpG + VacSIM™	80%	43%	29%

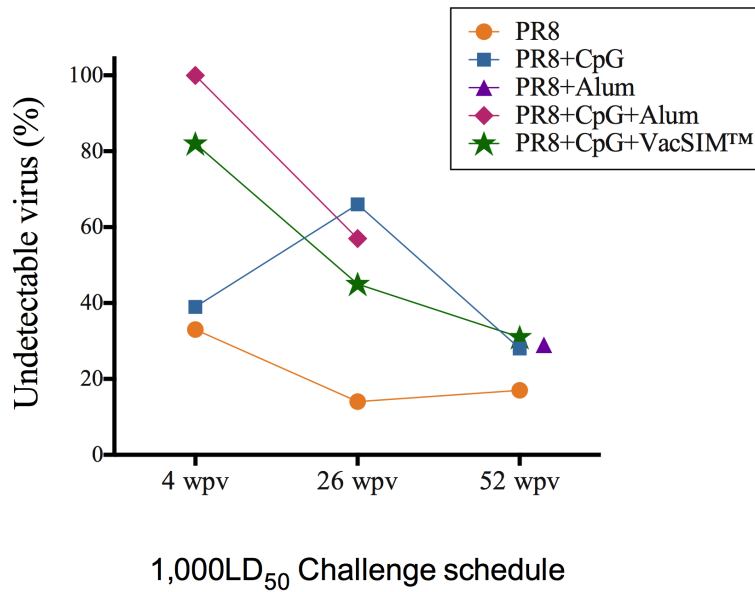


Figure 4.6: Proportion of immunized mice with undetectable virus in lungs. Data was pooled from 2 independent experiments (n=5-8), described in subsection 4.1.1 and Table 4.2.

4.2.2 Breadth of the Vaccine-Induced Immune Response

Sera collected from naïve and immunized mice were evaluated to determine if vaccination with PR8+CpG delivered in VacSIM™ led to increased levels of cross-reactive antibodies, compared to mice immunized with PR8 in saline. The presence of cross-reactive IgG antibodies in sera (4 wpv) was detected via indirect ELISA. Plates were coated with a standard concentration (200 ng/50 μ L/well) of recombinant hemagglutinin (HA) proteins from various influenza-A subtypes as well as influenza-B strains (Table 4.3). Cross-reactive antibodies were detected, specific for rHA from 2 different influenza-A subtypes, H1N1 (A/CA/07/09) and H5N1 (A/HK/156/97). Additionally, sera from mice vaccinated with PR8+CpG in VacSIM™ had increased IgG sera endpoint titers, compared to mice given PR8 in saline (Figure 4.7A).

In an expanded strain analysis, rHA surface proteins from two different influenza-B strains and one additional H1N1 strain were tested for cross-reactivity with serum samples from immunized and naïve mice. Additionally we included the conserved internal protein, recombinant nucleoprotein (rNP) and whole-inactivated PR8 as a baseline and a positive control (PR8-WIV). However, despite the promising results seen in panel A, the results of

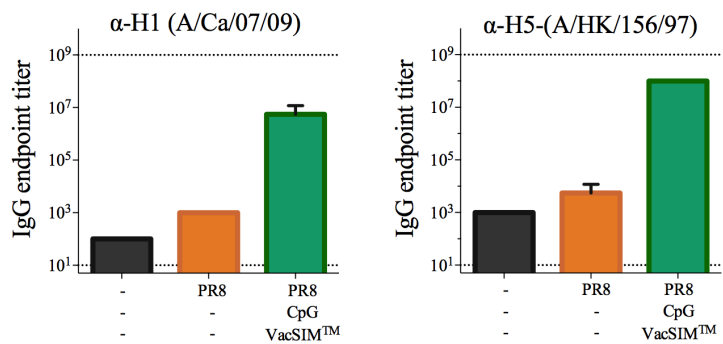
this expanded study (Figure

4.7B) do not show a detectable level of cross-reactive IgG antibodies in the serum samples tested.

Additionally, a hemagglutinin sequence alignment was done to compare the alternative influenza viruses (Table 4.3) to hemagglutinin from the vaccinating PR8 strain (Figure 4.8). This sequence

alignment showed that the H1 from A/CA/07/09 and A/BR/59/07 had the highest percent identity to H1 from

A



B

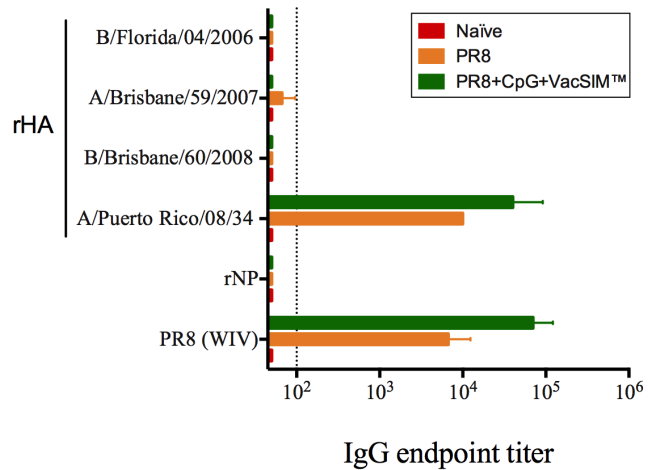


Figure 4.7: Cross-reactive IgG endpoint titers are highly variable in sera of immunized mice. Serum samples were collected prior to vaccination (baseline) and 4 wpv of PR8 in saline or PR8+CpG in VacSIM™. Naïve mice received an equivalent volume of saline. Antigen-specific IgG in mice sera was detected by indirect ELISA. Dashed line indicate detection threshold.

A/PR/8/34 (81.27% and 82.38%, respectively), followed by H5 from A/HK/156/97 (65.22%) and finally the two B-viruses B/Brisbane/60/2008 and B/Florida/04/2006 (18.97% and 18.34%, respectively). Appendix Table C.1 and Figure C.3 show a second alignment of these hemagglutinin sequences (all amino acids shown), which indicates the published locations of certain B cell epitopes (18, 19).

Table 4.3: The average cross-reactive IgG endpoint titers in sera (4 wpv).

ELISA coating antigen	Antigen type	IgG endpoint titer PR8 (WIV) in Saline	IgG endpoint titer PR8(WIV)+CpG in VacSIM™
A/California/07/09, (H1N1)	rHA	1,000	5,500,000
A/Hong Kong/156/97, (H5N1)	rHA	5,500	100,000,000
A/Brisbane/59/2007, (H1N1)	rHA	66.667	50
B/Brisbane/60/2008	rHA	50	50
B/Florida/04/2006	rHA	50	50
A/ Puerto Rico//08/34, (H1N1)	rHA	10,000	40,000
A/ Puerto Rico//08/34, (H1N1)	rNP	50	50
A/Puerto Rico/08/34, (H1N1)	WIV	6,700	70,000

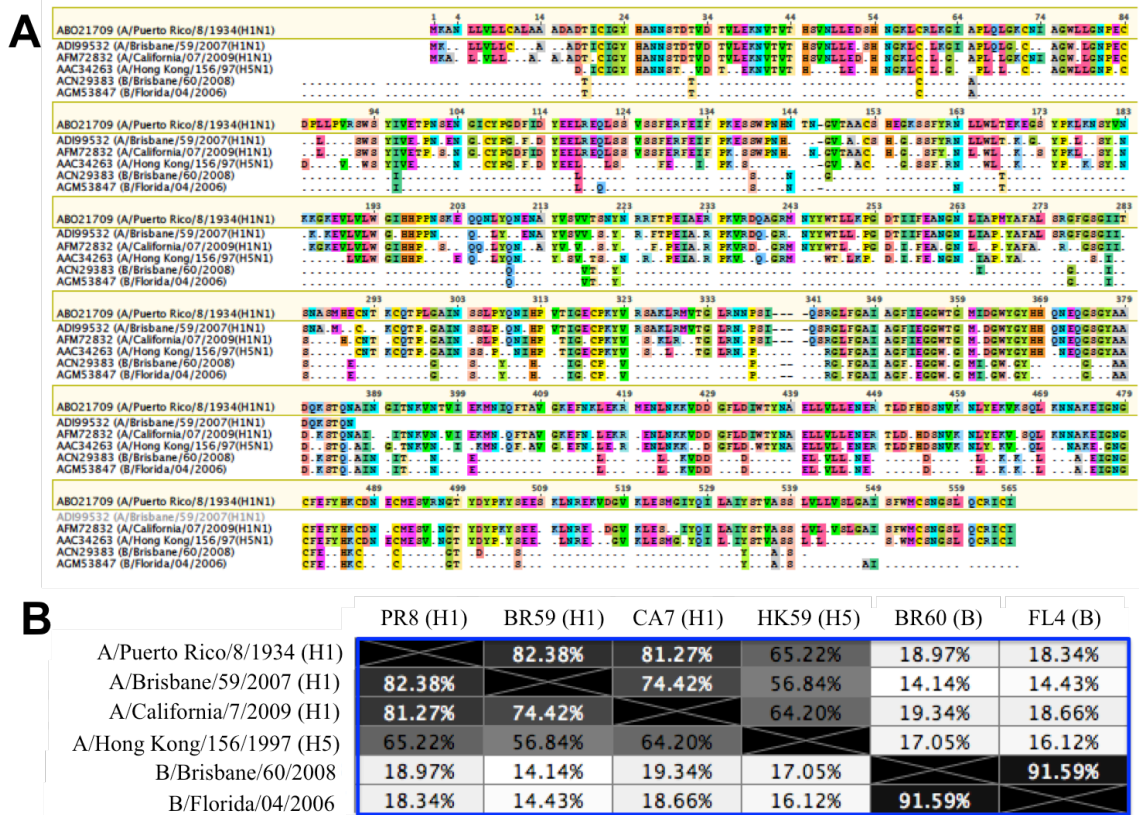


Figure 4.8: Alignment of hemagglutinin sequences from 6 influenza A/B viruses. The sequence information for 6 different (Figure 4.7, Table 4.3) influenza viruses (ABO21709, ADI99532, AFM72832, AAC34263, ACN29383, AGM53847) were obtained from the Immune Epitope Database (IEDB) version 3.0 (www.iedb.org). Hemagglutinin sequence alignment (A) was generated using Geneious® version 8.1.4 and shows the similarity to influenza H1N1 (A/PR/08/34). The percent identity between cross-reacting influenza strains is provided in the far-left heat map column (B).

A heterologous vaccine and challenge study was designed to compare the heterosubtypic immune responses between vaccine groups. In this study, mice were immunized with whole-inactivated X:31 virus (20) delivered either in saline or in VacSIM™. Additionally the following adjuvanted vaccine groups were examined: X:31+CpG in saline or in VacSIM™, X:31+Alum in saline or in VacSIM™, X:31+Alum+CpG and X:31+VacSIM™+Alum. Serum samples were collected as previously described and IgG endpoint titers were determined via indirect ELISA,

specific for the vaccinating antigen (whole-inactivated X:31) as well as an alternative (whole-inactivated PR8) antigen (Figure 4.9). Vaccine-specific antibody responses from mice immunized with X:31 were lower across all groups, compared to the vaccine-specific IgG endpoint titers obtained following vaccination with WIV PR8 or protein subunit antigens (rHBsAg, rNP) (Chapters 2-4). Virus-specific antibodies were significantly increased in two X:31 vaccine groups over naïve levels. These were X:31 adjuvanted with Alum and X:31 adjuvanted with Alum+CpG (Figure 4.9A). Evaluation of PR8-specific IgG endpoint titers confirmed that X:31 functioned best when adjuvanted with Alum (Figure 4.9B). In fact, X:31 in the absence of Alum or Alum combinations including Alum+CpG and Alum delivered in VacSIM™, appear to have a negative effect on X:31 antibody titers.

Four weeks post whole-inactivated X:31 vaccination, mice were challenged with 100 LD₅₀ PR8 to compare morbidity and viral clearance following heterologous challenge between vaccine groups. Challenge dose was determined following a pilot study involving an unvaccinated and X:31 vaccinated cohort (n=3) at 4 different challenge doses (1 LD₅₀, 10 LD₅₀, 100 LD₅₀, 500 LD₅₀). Morbidity and viral clearance were examined in an attempt to determine a challenge dose that would overwhelm all naïve mice and induce symptoms in a portion of the vaccinated mice but not overwhelm them (Appendix Figure B.2). Unfortunately, no variations could be elucidated post-challenge, using these parameters (Figure 4.10).

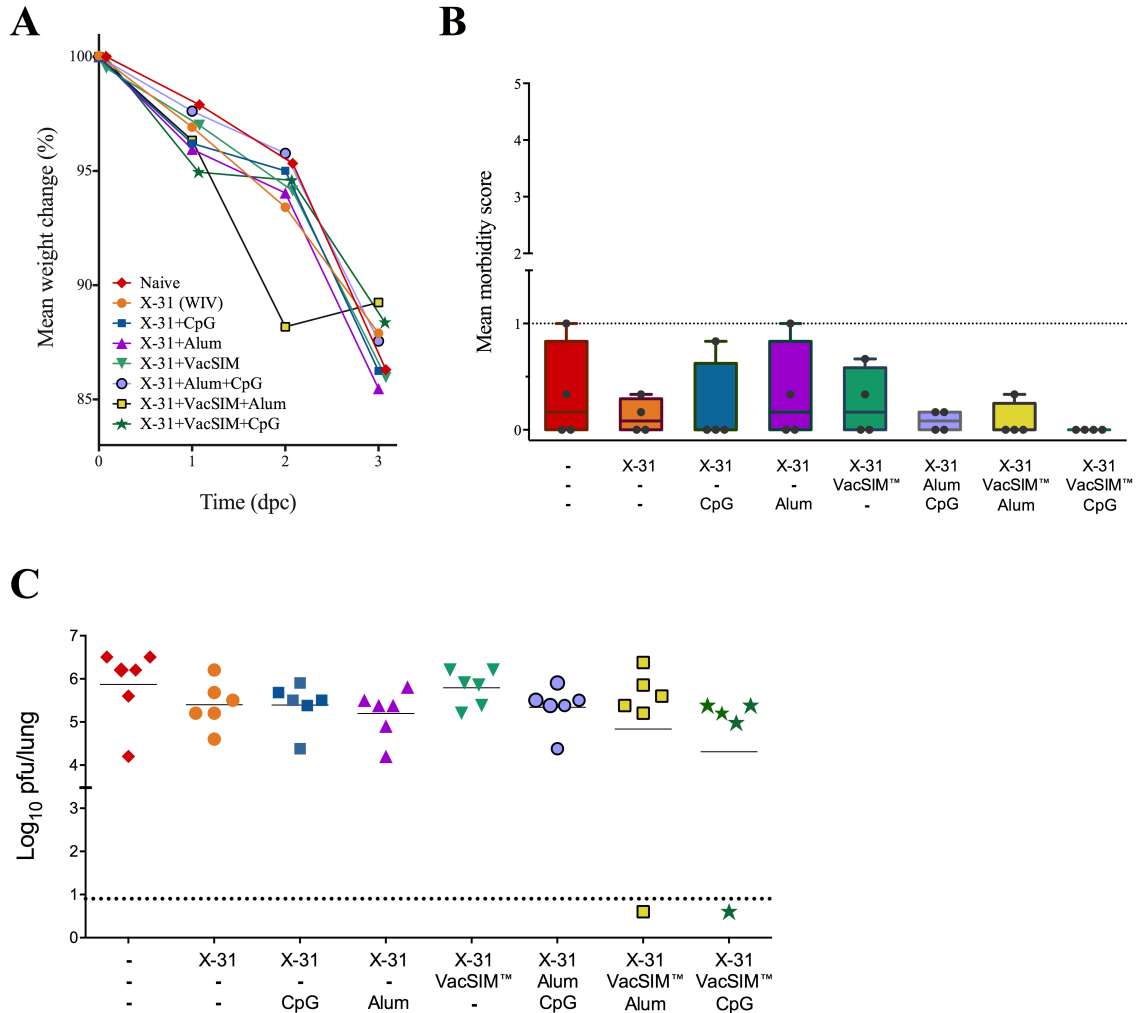


Figure 4.10: Whole-inactivated X:31 immunized mice struggle to clear virus from the lungs following 100 LD₅₀ PR8 challenge (4 wpv). Mean change in weight of vaccine groups over time post challenge (A). Viral clearance from the lungs at 3 days post challenge (dpc) from naïve and immunized mice. Vaccine group mean morbidity scores (B) graphed as box and whiskers showing all points. Dashed line on y-axis designates viral challenge dose (C) and dotted line indicates minimal morbidity score (asymptomatic=0) (B) or assay detection threshold (C).

4.2.3 Population-Biased Vaccine-Induced Immunity

Population-bias within this thesis, specifically refers to age-related variation in vaccine-induced immunity. Therefore, population bias was examined using two alternatively aged populations (young vs. elderly). In accordance with previously

published age-specific mouse studies (10, 21), a “young” population, consisting of 8-week old female BALB/c mice were compared to an “elderly” population, consisting of 12-month old female BALB/c mice. Unvaccinated mice were compared to the following vaccine groups: whole-inactivated PR8 delivered in saline or in VacSIM™ and PR8+CpG delivered in saline or in VacSIM™. Sera were collected, as previously described, for evaluating α -PR8 IgG endpoint titers in sera of naïve and vaccinated mice at 4 wpv (Figure 4.11A). In the young mice, vaccine-specific IgG levels were significantly increased over naïve and all other vaccine groups. In comparison, elderly mice immunized with PR8+CpG in VacSIM™ had a similar group mean to young mice, and was statistically increased over naïve and all vaccine groups except PR8+CpG delivered in VacSIM™. As previously described, both young and elderly cohorts were challenged intranasally (i.n.) after 4 wpv with a lethal (1000 LD₅₀) dose of homologous virus (PR8). Following challenge, mice were monitored daily for 2 days, and lungs were harvested for virus enumeration via plaque assay (Figure 4.11B). The cohort of young mice was able to clear virus as anticipated from results in prior vaccine studies (PR8-WIV antigen, 1000 LD₅₀ homologous challenge at 4 wpv, C57BL/6 mice). The cohort of elderly mice had more difficulty clearing the virus at 2 days post challenge across all vaccine groups. Mice vaccinated with PR8+CpG in VacSIM™ were the only vaccine group with undetectable virus levels (two out of five mice). Statistics were not attempted for viral clearance data in the elderly cohort since two out of the five mice in three different groups (naïve, PR8 in saline and PR8+CpG in saline) reached their humane morbidity score prior to harvesting lungs on 2 dpc and therefore could not be included.

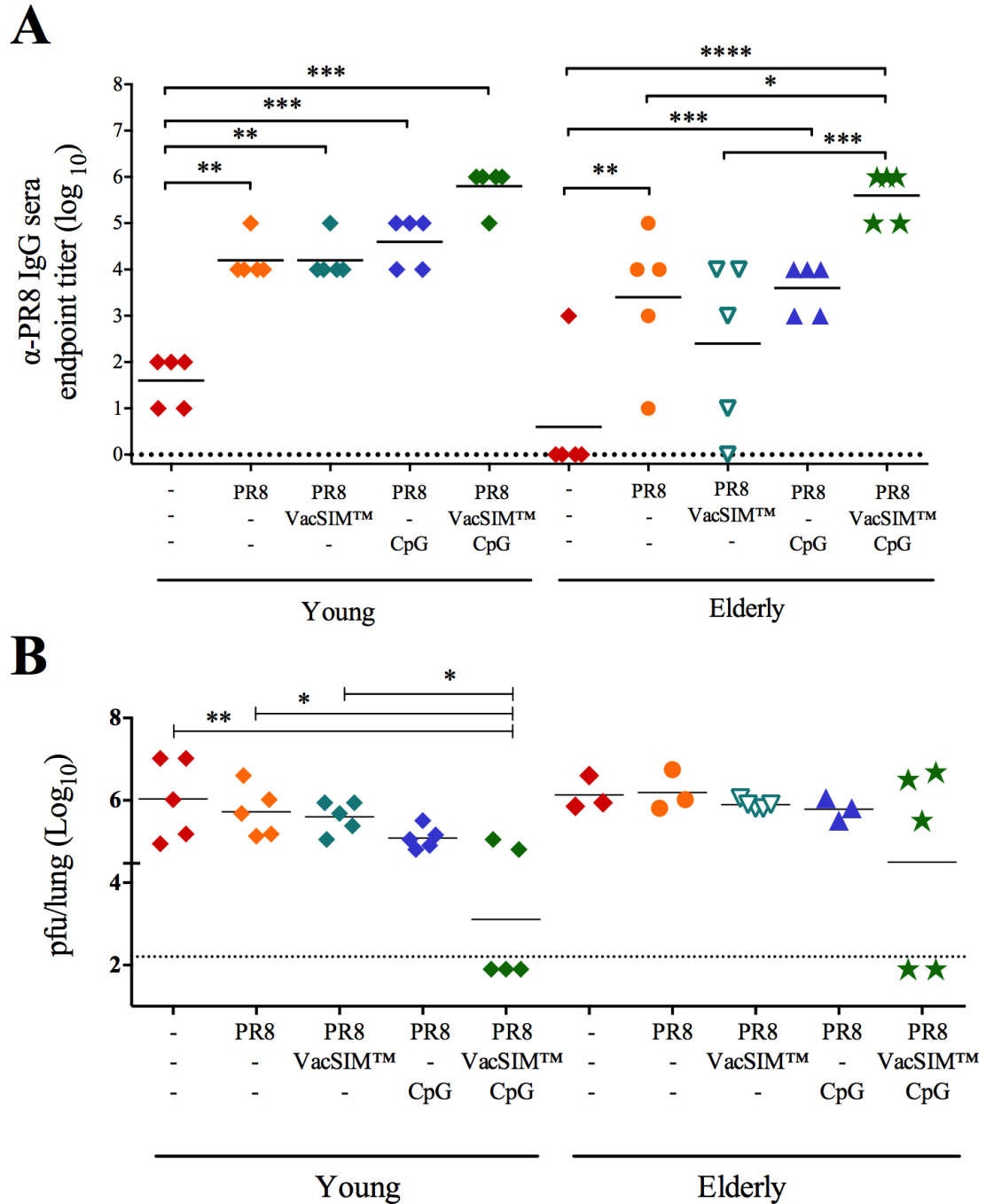


Figure 4.11: Elderly mice given PR8+CpG+VacSIMTM maintain antibody levels and ability to clear virus following lethal influenza challenge. Dashed line on y-axis designates viral challenge dose (B) and dotted line indicates assay detection threshold. Statistical significance (* $p < 0.05$; ** $p < 0.01$; *** $p < 0.001$; **** $p < 0.0001$) was determined by 1 way ANOVA of log-transformed data and Bonferroni's multiple comparisons test (A). Statistical significance (* $p < 0.05$; ** $p < 0.01$; *** $p < 0.001$) was determined by 1 way ANOVA of log-transformed data and Tukey's multiple comparisons test (B).

4.3 Conclusions

There remains a critical need for development and availability of safe and effective adjuvants and/or delivery systems that can provide increased vaccine-induced protection that remains intact for extended durations (22). In the case of influenza, there are additional needs for vaccine improvement arising from the inherent complications of immunizing against zoonotic viruses with ever evolving subtypes (antigenic shift/drift). Additionally, seasonal influenza vaccines have been shown to be less effective in specific populations, such as children under 5 years and adults over 65 years (11, 23-27). Vaccine delivery by VacSIM™ as proposed in this dissertation, is a method inducing antigen-persistence that is subsequently hypothesized to result in enhanced immunity and increased vaccine efficacy.

The improved vaccine efficacy and immunogenicity, consistently demonstrated in earlier time points post vaccination, were not seen in the long-term vaccine/challenge studies. Specifically, using a prime-only vaccination schedule, the results from both long-term studies (Figure 4.1) indicate that immunizing (s.c.) with whole-inactivated PR8 + CpG delivered in VacSIM™, leads to a gradual reduction in protection (indicated by viral clearance) following a 1000 LD₅₀ homologous challenge (Figures 4.4, 4.5). However, this gradual decrease seen in mice immunized with PR8 + CpG in VacSIM™ was in contrast to the sporadic trends seen in mice receiving PR8 + CpG in saline. Mice given unadjuvanted PR8 delivered in saline showed minimal levels of protection (33%) compared to some of the other groups (80-100%) at the earlier time points (4 wpv-26 wpv, Figure 4.4). The reduced viral clearance in mice vaccinated with PR8 in saline may be due to the suboptimal route being used (optimal protection via i.m.). More expansive

evaluation will be necessary before direct correlations can be made regarding the effects of VacSIM™ on the durability of vaccine-induced protection, particularly with regard to the human experience.

Seasonal influenza vaccines typically contain 3-4 different strains as a means of increasing the breadth of vaccine protection. This is necessary because protection is generally not transferable between influenza subtypes. Therefore, until a universal influenza vaccine (28-30) is successfully designed, annual immunizations will be necessary to ensure some level of protection (31). Formulation of seasonal influenza vaccines involves an international consensus of which infectious strains are predicted to be in circulation (32-34). When the predicted strains align with those in circulation, vaccine efficacy improves. Vaccine effectiveness in the case of seasonal influenza vaccines indicates the probability that vaccinated individuals will avoid clinical symptoms of acute respiratory illness (ARI), which require treatment by a healthcare professional, resulting in laboratory confirmation of infection. The predicted and circulating strains were poorly aligned for the 2014-2015 influenza season and the CDC estimated overall vaccine efficacy to be 19% (95% CI: 7%-29%) (24). This, in combination with the ever-present threat of a new pandemic provides impetus for researchers to improve heterosubtypic immunity and cross-protection from newly emerging viruses. Unfortunately, VacSIM™ delivery of whole-inactivated PR8 + CpG seems to induce variably cross-reactive serum IgG levels. Further heterologous vaccine/challenge investigation may elucidate whether the increase in cross-reactive antibodies (Figure 4.7A) are also cross protective.

The need to improve seasonal influenza vaccine efficacy is particularly relevant in high-risk populations (22, 26, 35-39). Individuals who are over the age of 65, for example, are at an increased risk for influenza related complications, which can become life threatening (12, 14, 15). A preliminary vaccine study was designed to compare vaccine efficacies between alternatively aged cohorts of mice and determine whether VacSIM™ delivery is able to improve immunogenicity and vaccine efficacy of adjuvanted (CpG) whole-inactivated PR8 vaccine. The results showed that mice vaccinated with PR8+CpG via VacSIM™ had higher levels of specific IgG in sera, regardless of age. Age was a more significant factor for viral clearance. In the elderly cohort, all vaccine groups struggled to clear virus, but mice immunized with PR8+CpG in VacSIM™ appeared to be more successful, given that two out of five mice challenged had undetectable levels of virus in the lungs at 2 dpc.

In conclusion, VacSIM™ delivery of adjuvanted-PR8 (WIV) effectively increases immunogenicity and vaccine efficacy to lethal homologous challenge at 4-6 wpv (Th1 and Th2 biased mouse models), with immune responses steadily decreasing by 6 months. The potential of VacSIM™ delivery inducing a cross-reactive and cross-protective immune response remains unclear from the results of X:31/PR8 heterologous challenge study and require further evaluation. Results from the initial age-bias vaccine study suggest that PR8+CpG delivered in VacSIM™ improves vaccine-specific immune responses in elderly mice.

4.4 Materials and Methods

4.4.1 Experimental Design

To evaluate VacSIM™ delivery of an influenza vaccine in a mammalian model system controlled laboratory experiments were conducted in C57BL/6 mice (Harlan).

Also utilized was the Madin-Darby Canine Kidney (MDCK) epithelial cell line (ATCC). Analyses of vaccine-specific immune responses were conducted according to standard protocols with slight modifications (33). Endpoint titers were calculated for antibodies specific to inactivated virus (PR8, X:31) or recombinant proteins (rNP, rHA) in the sera by indirect ELISA. Protection from lethal challenge was assessed *in vivo* in accordance with IACUC guidelines and clearance of the virus was assessed by viral lung titers determined from plaque assay.

Group size for significant statistical power was determined by consultation with collaborating scientists, who have substantial experience with influenza infection in mice. In general, a sample size of at least four mice per treatment group was utilized. Animals within a group were not pooled during analysis and unless otherwise stated, data from individual mice were graphed. Following influenza challenge, mice were monitored daily and symptoms were recorded, including changes in weight, behavior, activity, posture, grooming and respiratory rate. Each animal was given a daily morbidity score, calculated from the assigned values of each symptom: hunched back or ruffed fur (1), lethargy (2), head tilt (3), weight loss >20% (3), weight loss >25% (4), weight loss >30% (5), cyanosis (5), paralysis (5), seizure (5) and severe dyspnea (5). Animals were immediately sacrificed (CO₂ inhalation followed by cervical dislocation) if they received a total score of ≥ 5 and said to have reached their humane endpoint. Mice could be excluded from the final analysis if there was evidence of its difference prior to employing the experimental manipulation (i.e.: physical or behavioral abnormality recorded prior to vaccination or challenged). No outliers have been excluded.

4.4.2 Animals

Six to eight week old, female, C57BL/6 or BALB/c mice were purchased from Harlan Laboratories and housed in specific pathogen-free conditions and allowed to acclimate for one week prior to manipulation. All animal work was performed in accordance with all applicable policies and approved by the institutional animal care and use committee.

4.4.3 Cell Culture

Madin-Darby Canine Kidney (MDCK) epithelial cells were cultured in 1:1 ratio of Dulbecco's Modified Eagle Medium (DMEM) and Eagle's minimal essential medium (MEM) supplemented with 1% L-glutamine and 5% fetal bovine serum (FBS) at 37°C and 5% CO₂.

4.4.4 Vaccination

Six to eight week old mice were received a single, subcutaneous (s.c.) vaccination of 200 µL to their right flank. Vaccinations contained sterile saline, PR8 whole-inactivated PR8 (A/PR/8/34 (H1N1) influenza, 15 µg, Charles River Laboratories, Cat. No. 10100782), whole-inactivated X:31 (A/Aichi/68 (H3N2) influenza, 15 µg, Charles River Laboratories, Cat. No. 10100784) CpG (50 µg, ODN1826, TriLink BioTechnologies, 5' TCC ATG ACG TTC CTG ACG TT 3'), Alum (250 µg, Imject Alum, Thermo Scientific, Cat. No. 77161), or equal volumes VacSIM™ (PuraMatrix, BD Biosciences, Cat. No. 354250), as indicated.

4.4.5 Viral Challenge

Influenza challenge virus (A/Puerto Rico/08/34, H1N1) was mouse-adapted through serial passage prior to propagation in embryonated chicken eggs and lethality was determined by MLD₅₀ (Appendix Figure A.), as described previously (40). Four

weeks post-vaccination, age-matched mice were challenged intranasally (i.n.) with a lethal dose (100-1000 LD₅₀, as indicated) of mouse-adapted homologous PR8 virus under temporary sedation with tribromoethanol. Mice were monitored daily for weight change and symptom severity (subsection 4.4.1). Lungs were harvested 6-12 hours following challenge from minimally two control mice, to confirm infection by plaque assay.

4.4.6 Antibody Endpoint Titers

Sera samples were collected from mice prior to vaccination (pre-bleed) and 4 weeks following vaccination. Briefly, ELISA plates were coated (4 µg/mL) with desired antigen at 4 °C overnight. ELISA coating antigens included whole A/Puerto Rico/08/34 (H1N1) inactivated/purified virus (Charles River Laboratories, Cat. No. 10100782), recombinant HNP-A (A/Puerto Rico/8/34/Mount Sinai (H1N1), Imgenex, Cat. No. IMR-274) or recombinant hemagglutinin (rHA) proteins from the following influenza strains: A/Puerto Rico/08/34 (H1N1, Protein Sciences Corp., Cat. No. 3006), B/Brisbane/60/2008 (Protein Sciences Corp., Cat. No. 3006), A/Brisbane/59/2007 (H1N1, BEI Resources, Cat. No. NR-15477, gifted by Professor R. Jeff Hogan) or B/Florida/04/2006 (BEI Resources, Cat. No. NR-15482, gifted by Professor R. Jeff Hogan). Plates were washed five times with wash buffer (160 mM NaCl, 0.5 mM EDTA, and 0.05% Tween 20), then blocked in 1X PBS containing 5% non-fat milk powder and 1% BSA for at least two hours. Plates were decanted, incubated for 2-24 hours with samples serially diluted in blocking buffer, then washed five times. Detection antibodies (HRP-conjugated α-mouse IgG₁, IgA and IgM from Santa Cruz, IgG₃, IgG_{2a} and IgG_{2b} from Invitrogen, IgE from Southern Biotech or total IgG from BioLegend) were diluted in blocking buffer and incubated for one hour. After five washes, plates were developed in the dark using SureBlue 1 component TMB substrate (KPL Laboratories) and the reaction was stopped

with 2 N sulfuric acid. Absorbance was measured at 450 nm with 570 nm background correction.

4.4.7 Plaque Assays for Viral Quantitation

Briefly, serially diluted lung homogenates were incubated with MDCK lawns under a 2.4% Avicel (FMC BioPolymer) overlay. After incubation for 2-3 days, cells were fixed with methanol/acetone and stained with crystal violet (Acros Organics) for enumeration of plaque forming units (pfu). Lung samples with undetectable virus were graphed as 4 pfu per lung, which is a value equal to ½ of the detection threshold of the assay.

4.4.8 Statistical Analyses

Statistical analyses were performed using GraphPad Prism version 6.0. Statistical methods and significant differences between vaccination groups include one-way ANOVA, two-way ANOVA, followed by Tukey or Bonferroni's test for multiple comparisons. Mean survival was calculated using Log-rank (Mantel-Cox) test. The statistical method(s) used and alpha level (0.05 or 0.01) have been specified in each figure legend.

4.5 References

1. Ross PJ, *et al.* (2013) Relative contribution of Th1 and Th17 cells in adaptive immunity to *Bordetella pertussis*: towards the rational design of an improved acellular pertussis vaccine. *PLoS Pathog* 9(4):e1003264.
2. Pashine A, Valiante NM, & Ulmer JB (2005) Targeting the innate immune response with improved vaccine adjuvants. *Nat Med* 11(4 Suppl):S63-68.
3. Stanley Plotkin WO, Paul Offit, Susan L. Plotkin, Claire-Anne Siegrist, *et. al.*, (2012) *Vaccines* (ExpertConsult.com) 6 Ed p 1392.
4. Weintraub A (2003) Immunology of bacterial polysaccharide antigens. *Carbohydrate research* 338(23):2539-2547.

5. Hanekom WA (2005) The immune response to BCG vaccination of newborns. *Annals of the New York Academy of Sciences* 1062:69-78.
6. Derrick SC, Kolibab K, Yang A, & Morris SL (2014) Intranasal administration of Mycobacterium bovis BCG induces superior protection against aerosol infection with Mycobacterium tuberculosis in mice. *Clinical and vaccine immunology : CVI* 21(10):1443-1451.
7. Lee CJ, Lee LH, Lu CS, & Wu A (2001) Bacterial polysaccharides as vaccines--immunity and chemical characterization. *Advances in experimental medicine and biology* 491:453-471.
8. Yoshikawa TT (1981) Important infections in elderly persons. *West J Med* 135(6):441-445.
9. Bender BS, Johnson MP, & Small PA (1991) Influenza in senescent mice: impaired cytotoxic T-lymphocyte activity is correlated with prolonged infection. *Immunology* 72(4):514-519.
10. Bender BS, Taylor SF, Zander DS, & Cottey R (1995) Pulmonary immune response of young and aged mice after influenza challenge. *J Lab Clin Med* 126(2):169-177.
11. Couch RB, *et al.* (1986) Influenza: its control in persons and populations. *J Infect Dis* 153(3):431-440.
12. Webster RG (2000) Immunity to influenza in the elderly. *Vaccine* 18(16):1686-1689.
13. Powers DC, Sears SD, Murphy BR, Thumar B, & Clements ML (1989) Systemic and local antibody responses in elderly subjects given live or inactivated influenza A virus vaccines. *J Clin Microbiol* 27(12):2666-2671.
14. Powers DC & Belshe RB (1993) Effect of age on cytotoxic T lymphocyte memory as well as serum and local antibody responses elicited by inactivated influenza virus vaccine. *J Infect Dis* 167(3):584-592.
15. Simonsen L, Taylor RJ, Viboud C, Miller MA, & Jackson LA (2007) Mortality benefits of influenza vaccination in elderly people: an ongoing controversy. *Lancet Infect Dis* 7(10):658-666.
16. Hai R, Garcia-Sastre A, Swayne DE, & Palese P (2011) A reassortment-incompetent live attenuated influenza virus vaccine for protection against pandemic virus strains. *Journal of virology* 85(14):6832-6843.
17. Xue FS, Liu JH, Yuan YJ, & Liao X (2011) Comments on comparison of the combined Airtraq(R) laryngoscope and a fiberoptic bronchoscope with the Airtraq(R) alone for tracheal intubation. *J Anesth* 25(3):465-466.

18. Sun J, *et al.* (2014) Large-scale analysis of B-cell epitopes on influenza virus hemagglutinin - implications for cross-reactivity of neutralizing antibodies. *Frontiers in immunology* 5:38.
19. Morris GE (2001) Epitope Mapping. *eLS*, (John Wiley & Sons, Ltd).
20. Newell DH (1991) The role of the prosthodontist in restoring root-resected molars: a study of 70 molar root resections. *J Prosthet Dent* 65(1):7-15.
21. Parzych EM, *et al.* (2013) Influenza virus specific CD8(+) T cells exacerbate infection following high dose influenza challenge of aged mice. *Biomed Res Int* 2013:876314.
22. Flannery B, *et al.* (2014) Interim estimates of 2013-14 seasonal influenza vaccine effectiveness - United States, February 2014. *MMWR. Morbidity and mortality weekly report* 63(7):137-142.
23. Thompson WW, *et al.* (2004) Influenza-associated hospitalizations in the United States. *Jama* 292(11):1333-1340.
24. CDC (2015) Fluview. 2014–2015 influenza season ending January 30, 2015 (CDC.gov).
25. Rothberg MB, Haessler SD, & Brown RB (2008) Complications of Viral Influenza. *The American journal of medicine* 121(4):258-264.
26. Jules A, *et al.* (2015) Influenza-Related Hospitalization and ED Visits in Children Less Than 5 Years: 2000–2011. *Pediatrics* 135(1):e66-e74.
27. Lambert ND, Ovsyannikova IG, Pankratz VS, Jacobson RM, & Poland GA (2012) Understanding the immune response to seasonal influenza vaccination in older adults: a systems biology approach. *Expert review of vaccines* 11(8):985-994.
28. Paddock C (2013) Universal flu vaccine closer after natural immunity study. in *Medical News Today* (MedicalNewsToday.com).
29. Cohen J (2013) Immunology. A once-in-a-lifetime flu shot? *Science (New York, N.Y.)* 341(6151):1171.
30. Margine I, *et al.* (2013) Hemagglutinin stalk-based universal vaccine constructs protect against group 2 influenza A viruses. *Journal of virology* 87(19):10435-10446.
31. Dilillo DJ, Tan GS, Palese P, & Ravetch JV (2014) Broadly neutralizing hemagglutinin stalk-specific antibodies require FcγR interactions for protection against influenza virus in vivo. *Nat Med* 20(2):143-151.

32. Sexton A, *et al.* (2009) A protective vaccine delivery system for in vivo T cell stimulation using nanoengineered polymer hydrogel capsules. *ACS nano* 3(11):3391-3400.
33. Chong SF, *et al.* (2009) A paradigm for peptide vaccine delivery using viral epitopes encapsulated in degradable polymer hydrogel capsules. *Biomaterials* 30(28):5178-5186.
34. Coeshott CM, *et al.* (2004) Pluronic F127-based systemic vaccine delivery systems. *Vaccine* 22(19):2396-2405.
35. Weinberger B & Grubeck-Loebenstien B (2012) Vaccines for the elderly. *Clinical microbiology and infection : the official publication of the European Society of Clinical Microbiology and Infectious Diseases* 18 Suppl 5:100-108.
36. Lang PO, *et al.* (2012) Effectiveness of influenza vaccine in aging and older adults: comprehensive analysis of the evidence. *Clinical interventions in aging* 7:55-64.
37. Vesikari T, Pepin S, Kusters I, Hoffenbach A, & Denis M (2012) Assessment of squalene adjuvanted and non-adjuvanted vaccines against pandemic H1N1 influenza in children 6 mo to 17 y of age. *Human vaccines & immunotherapeutics* 8(9).
38. Esposito S, *et al.* (2012) Preventing influenza in younger children. *Clinical microbiology and infection : the official publication of the European Society of Clinical Microbiology and Infectious Diseases* 18 Suppl 5:42-49.
39. Steininger C, *et al.* (2003) Acute encephalopathy associated with influenza A virus infection. *Clinical infectious diseases : an official publication of the Infectious Diseases Society of America* 36(5):567-574.
40. Webster R CN, Stohr K (2002) WHO Manual on Animal Influenza Diagnosis and Surveillance in *WHO Global Influenza Program*, ed Webster R CN, Stohr K (World Health Organization, Geneva, Switzerland), p 105.

CHAPTER 5

VACSIM™: EVALUATING THE MECHANISM

5.1 Introduction

There remains a critical need to engineer more effective prophylactic and therapeutic vaccines that have the ability to induce effector CD4⁺ and CD8⁺ T lymphocytes in addition to inducing strong vaccine-specific antibody responses (1-3). The proposed mechanism by which VacSIM™ delivery leads to increased immunogenicity was initially discussed in Chapter 2. To reiterate, VacSIM™ enhances vaccine immunogenicity and efficacy based on its ability to produce a three-dimensional vaccine depot, which provides for antigen persistence (4). To recap, VacSIM™ is simply a solution of the synthetic (RADA)4 oligopeptides in solution. Under physiological conditions, the (RADA)4 synthetic oligopeptide self-assembles into a hydrated nanofiber gel-depot with vaccine components present in the aqueous phase. Over time, vaccine components in the aqueous phase egress via pores, out of the gel-matrix. The three-dimensional vaccine-matrix depot, is resorbable, non-toxic and non-reactogenic (5, 6). This chapter describes early mechanistic experiments designed to further investigate characteristics innate to VacSIM™.

Coinciding with published results (4, 6, 7) and the hypothesized slow release or delayed antigen egress, the *in vitro* antigen release experiments discussed in Chapters 2 and 3, indicated that protein subunit vaccines, differentially diffuse from the three-dimensional vaccine-matrix depot based on pore size, which itself is governed by the

concentration of (RADA)₄ oligopeptides in solution. Cell recruitment experiments were designed to evaluate whether the gradual egress of antigen due to VacSIM™ delivery, caused enhanced maturation of antigen presenting cells (APCs), resulting in maturation/activation of vaccine-specific CD4⁺ and CD8⁺ T cells. Antigen release experiments (Chapters 2 and 3) also demonstrated that vaccines comprised of formalin-inactivated whole virus, were unable to diffuse from the *in vitro* assembled vaccine-matrix depots. Thus, for whole inactivated vaccines, the addition of adjuvants, such as CpG, appears necessary for enhanced vaccine immunogenicity and efficacy. It is likely that this molecular adjuvant plays a role in recruitment of APCs to the vaccine depot, such that immune responding cells may encounter and uptake vaccine antigen. In addition, experiments were designed to evaluate the total cell numbers in draining versus non-draining lymph nodes at 1-2 days post vaccination, as well as the total and vaccine-specific cell populations (DCs, CD4⁺ and CD8⁺ T cells). For comparison between vaccine groups, total cell numbers and relative percentages (of live) were determined from a pool of draining and non-draining lymph nodes (1 pool/mouse) harvested 48 hours post challenge. In addition, pre-challenge lymph nodes were collected from a cohort of mice, previously (4 wpv) vaccinated with PR8+CpG in VacSIM™, so that cell population variations pre- and post-challenge could be evaluated.

5.2 Results

5.2.1 VacSIM™-Induced Activation of APCs

Various cells can function as antigen presenting cells (APCs), including B cells, macrophages and dendritic cells (DCs), however DCs are considered as professional APCs (8-10). Therefore *in vitro* experiments were performed utilizing bone-marrow derived dendritic cells (BMDCs) to evaluate immune activating properties of VacSIM™.

These studies compared VacSIM™ in the presence or absence of antigen/adjuvant (Figure 5.1). BMDCs were isolated from the femurs of C57BL/6 mice and cultured for 6-7 days. Flow cytometry was used to validate 6 and 7-day cultures of BMDCs. Specifically, looking for the presence of a defined DC population that when incubated with lipopolysaccharide (LPS) 24 hours prior to staining, underwent a clear shift in phenotype from CD11c⁽⁺⁾,CD86⁽⁻⁾ to CD11c⁽⁺⁾, CD86⁽⁺⁾ (Figure 5.1). Fluorescently conjugated activation markers (CD86, CD11c) and live/dead indicator were used to distinguish live cells that were activated DCs.

The ability of mitogens and vaccine antigens alone, or in combination with VacSIM™, were evaluated for their ability to stimulate day 6-7 BMDCs *in vitro* (Figure 5.1). Specifically, vaccine components (human serum albumin, HSA) or whole-inactivated virus (influenza A/Puerto Rico/8/34, PR8), or the adjuvants LPS and CpG (ODN-1826) plus or minus VacSIM™, were incubated with 2x10⁵ cells per 200uL in complete media. Vaccine components were used at 1/10th the standard vaccination concentrations, whether incubated with BMDCs individually or in combination. Positive and negative controls were culture of BMDCs in complete media alone (negative), or with LPS (positive) for DC activation. Figure 5.1 shows that in the absence of antigen or adjuvant, VacSIM™ by itself does not induce DC activation, supporting the hypothesis that VacSIM™ functions as a delivery method that lacks inherent adjuvant activity. Further, in regards to VacSIM™ being non-immunostimulatory, a preliminary (n =2) *in vivo* study was conducted to determine if injection of VacSIM™ alone would give rise to increased cell recruitment in the draining lymph nodes (Appendix Figure C.3). In this study, mice received a single, subcutaneous (s.c.) vaccination of saline or VacSIM™ ±

CpG. The draining and non-draining lymph nodes were collected at 24 and 48 hours post-vaccination (hpv), and total cell counts were determined and compared between groups. Results from this pilot study showed that injection of VacSIM™ in the absence of antigen/adjuvant does not alter cell numbers in the draining and non-draining lymph nodes and was comparable to mice injected with sterile saline.

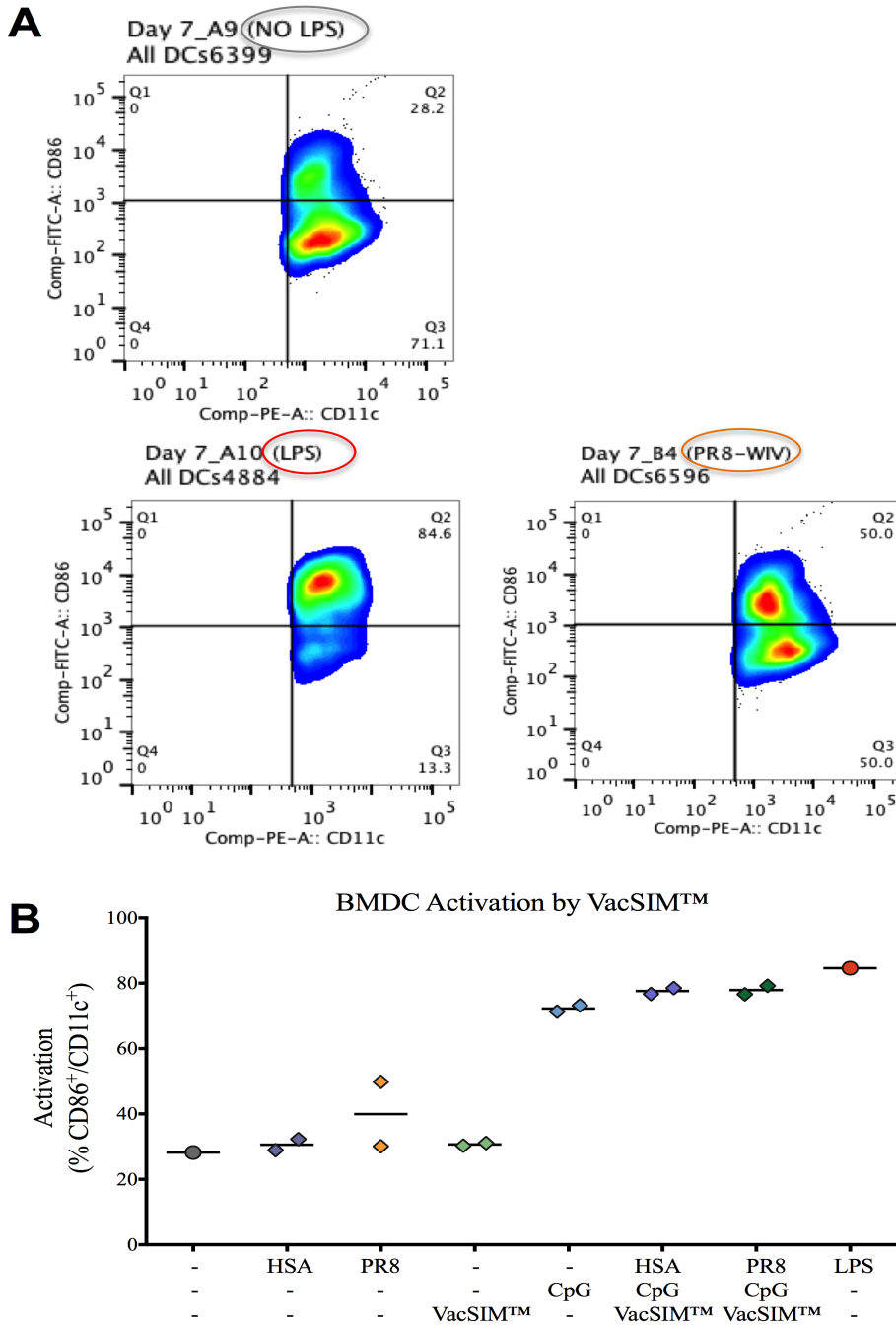


Figure 5.1: VacSIM™ does not induce dendritic cell (DC) activation in the absence of antigen/adjuvant. Six day BMDCs were incubated with the various vaccine components singly and in combination as shown in Panel B. DCs were considered activated CD11⁺, CD86⁺.

5.2.2 *In vitro* Assembled Antigen-Incorporating Depots and Antigen Uptake by DCs

A preliminary confocal study was conducted in an attempt to visualize antigen uptake by dendritic cells (DCs). The antigen selected was human serum albumin (HSA) fluorescently conjugated to DyLight-488, DyLight-405 or DyLight-680 (DL-405 not shown due to inadequate fluorescence at the time of imaging). Fluorescently conjugated HSA was premixed with VacSIM™ at a 1:5 ratio. This mixture was added without mixing, into a single well (12-well plate) containing BMDCs (7-day culture) in sterile 1x PBS. Imaging began immediately following addition of labeled HSA and VacSIM™ mixture. Images recorded by fluorescent and light microscopy and collected in the minutes following incubation with BMDCs provide visual confirmation of *in vitro* induce 3-dimensional gel-matrix depots incorporating and containing fluorescent antigen (blue arrows). After some time, there is the appearance of individual fluorescent cells, possibly indicating uptake of fluorescent antigen (white arrows) by the DCs in culture (Figure 5.2).

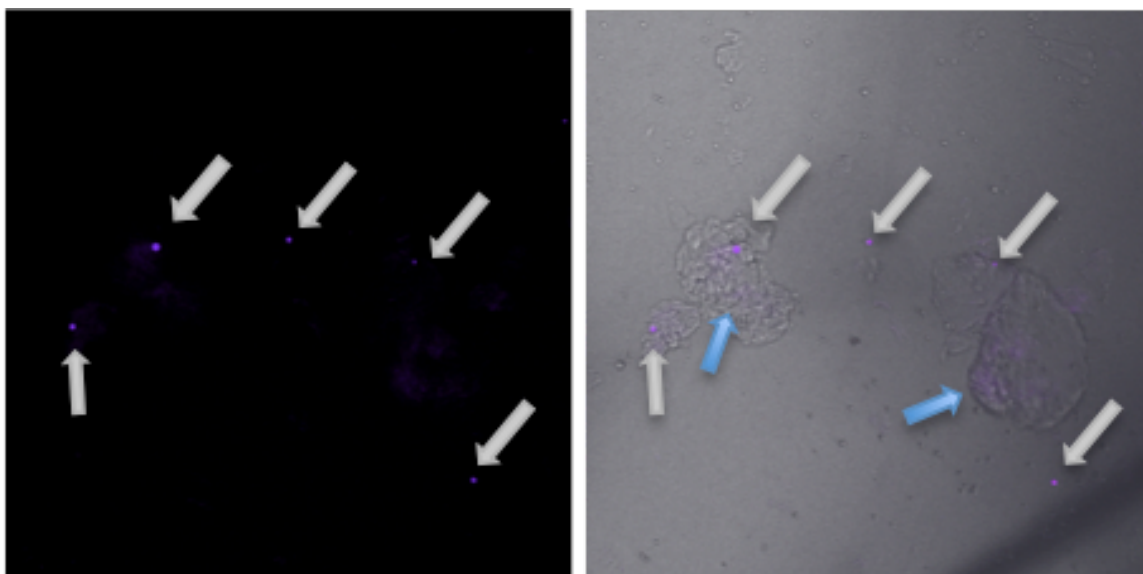


Figure 5.2: Confocal images showing VacSIM™ depots of fluorescent antigen and intercalated bone marrow derived dendritic cells (BMDCs). Fluorescently conjugated antigen (DL680 in top panels or DL488 in bottom panels) and VacSIM™ induced to self-assemble upon incubation with bone marrow derived dendritic cells (BMDCs). Conjugated antigen was pre-mixed with VacSIM™ immediately prior to being added to 6-7 day BMDC culture. Confocal images were taken immediately following addition to antigen+VacSIM™ to BMDC culture. White arrows in top panels indicate fluorescent cells. Blue arrows in bottom panels indicate fluorescent HSA within VacSIM™ *in vitro* self-assembled gel depot.

5.2.3 VacSIM™ Delivery of Antigen/Adjuvant Leads to the Localized Increase of Immune Cells

A more expansive *in vivo* study was conducted to further explore whether the persistence of antigen, as a result of VacSIM™ delivery, would affect cell recruitment to draining and/or non-draining lymph nodes. Mice were vaccinated (s.c.) with bovine serum albumin (BSA) delivered in saline or in VacSIM™, with or without the adjuvants CpG and alum (alone or in combination). The axillary and inguinal lymph nodes (draining /non-draining) were harvested at 24 and 48 hpv. Total cell counts were determined for each lymph node at both time points following immunization. Figure 5.3 shows that mice vaccinated with BSA+CpG in VacSIM™ consistently had an increased number of cells in their draining lymph nodes compared to non-draining lymph nodes.

This trend is maintained in this particular vaccine group, regardless of time point (24 or 48 hpv) or specific lymph node (axillary or inguinal). In general, when comparing the six different vaccine groups, the mice who received BSA adjuvanted with CpG showed an increased accumulation of cells by the 48 hpv time point, which appeared most striking in the inguinal lymph nodes.

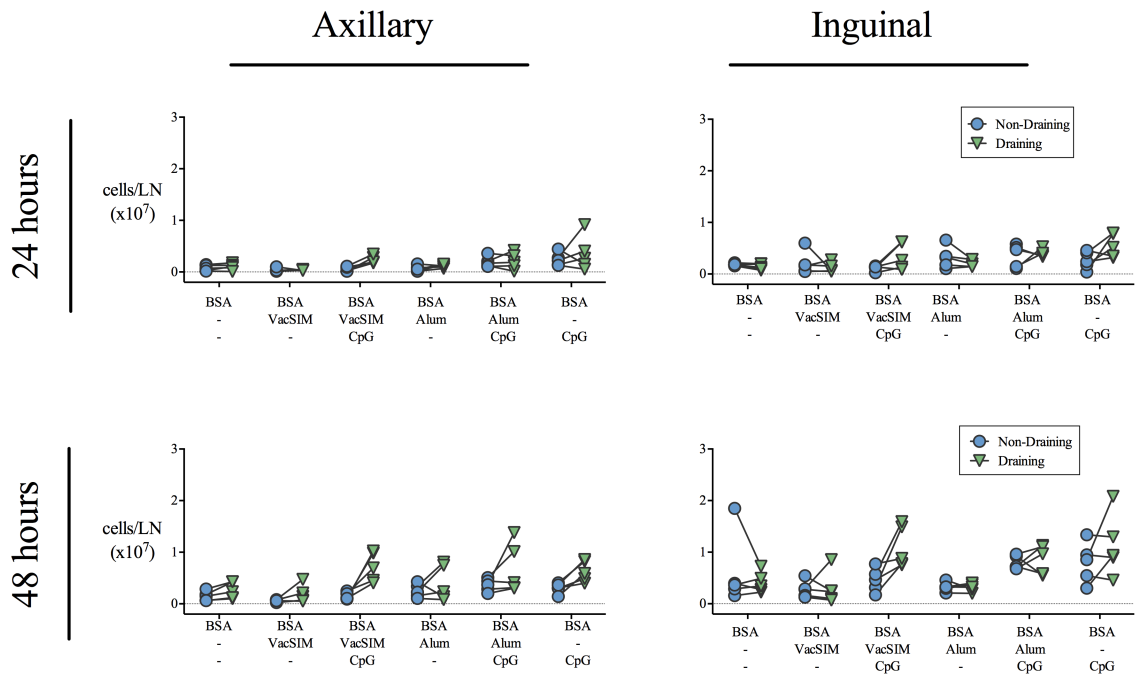


Figure 5.3: Vaccinating with antigen+CpG delivered in VacSIM™ leads to increased total cell counts in the draining versus non-draining lymph nodes at 1-2 days post vaccination. Mice receive a single vaccination (s.c.) 24 or 48 hours prior to harvesting lymph nodes (n=4-5/time point). Cell counts determined using a 1:1 dilution with trypan blue viability dye on a TC-10 automatic cell counter available from Bio-rad.

In addition to total cell counts, the type of immune cells present in the lymph nodes at 24 and 48 hpv was assessed by flow cytometry. Mice were vaccinated with fluorescently conjugated BSA (BSA:DyLight-680) ± adjuvant and delivered in saline or VacSIM™. Lymph nodes were harvested at 24 and 48 hpv, processed and resulting cells stained with specific cell markers to detect DCs and T cells (CD11b, CD11c, CD86,

CD3) following live/dead discrimination. The following phenotypes were used to distinguish cell populations present in the lymph nodes at 24 and 48 hpv: T cells were defined CD3⁺ and DCs were defined as CD11c⁺ and either CD86⁻ (resting) or CD86⁺ (activated). Consistent with the total cell counts (Figure 5.3), cell type analysis by flow cytometry showed that mice vaccinated with BSA+CpG in VacSIM™ had increased numbers of total DCs (Figure 5.4), activated DCs (Figure 5.5) and T cells (Figure 5.6) in the draining lymph nodes compared to non-draining lymph nodes. In contrast, lymph nodes that were harvested from mice vaccinated with BSA adjuvanted with Alum and/or CpG delivered in saline, were far more variable. Although there were occasions when these vaccine groups had increased cell numbers in the draining lymph nodes compared to non-draining lymph nodes, particularly by the 48 hpv time point, this was often accompanied by a systemic increase in specific cell numbers. The mean fluorescent intensity (MFI) specific for these three cell populations at both 24/48 hpv was also determined, although the results were far more variable and no clear trend emerged (Appendix Figures C.3-C.4).

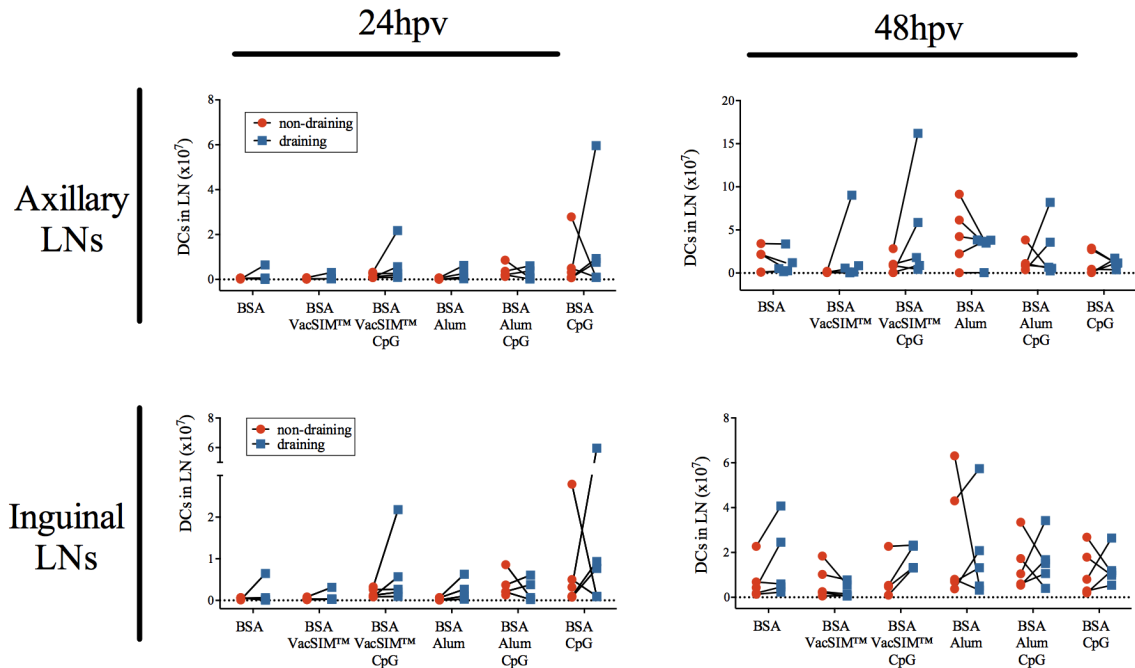


Figure 5.4: Fluorescently labeled BSA delivered with CpG + VacSIM™ results in an increased number of DCs that localize to the draining lymph nodes. Shown here are the cell counts of total DCs per draining or non-draining lymph node (axillary and inguinal) at 24 or 48 hours following a single vaccination (s.c.) with fluorescently conjugated bovine serum albumin (BSA) ± adjuvant (CpG, Alum) delivered in saline or VacSIM™ (n=4-5 per time point). Total DC counts were determined by flow cytometry, discriminating for live CD11c⁺, CD86^{+/-} lymph node cells.

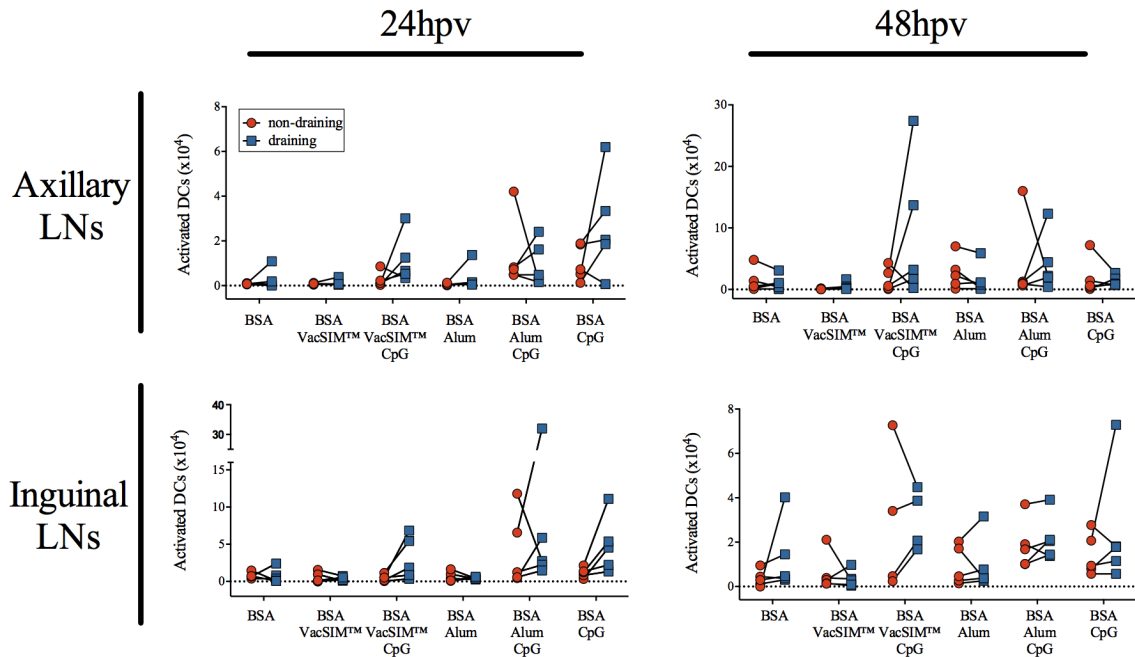


Figure 5.5: BSA+ CpG delivered in VacSIM™ leads to an increased number of activated DCs, that generally localize in the draining lymph nodes. Shown here are the cell counts of activated DCs (live, CD11c⁺, CD86⁺) per draining or non-draining lymph node (axillary and inguinal) at 24 or 48 hours following a single vaccination (s.c.) with fluorescently conjugated bovine serum albumin (BSA) ± adjuvant (CpG, Alum) delivered in saline or VacSIM™ (n=4-5 per time point). Activated DC counts per lymph node were determined by flow cytometry, discriminating for live CD11c⁺, CD86⁺ lymph node cells.

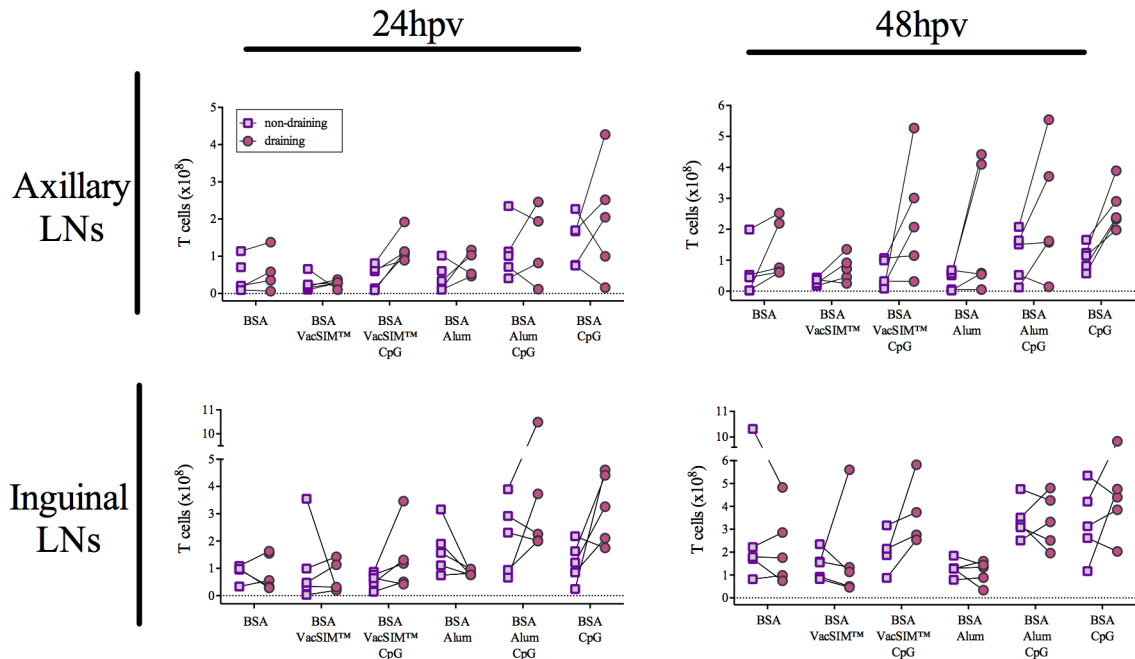


Figure 5.6: Increased number of T cells in the draining lymph nodes of mice vaccinated with BSA+ CpG delivered in VacSIM™ compared to the non-draining lymph nodes. Shown here are the T cell counts per draining or non-draining lymph node (axillary and inguinal) at 24 or 48 hours following a single vaccination (s.c.) with fluorescently conjugated bovine serum albumin (BSA) ± adjuvant (CpG, Alum) delivered in saline or VacSIM™ (n=4-5 per time point). T cells were discriminated as live CD3⁺ lymph node cells by flow cytometry.

5.2.4 Cells Present in Pooled Lymph Nodes of Vaccinated Mice 48 Hours Following Intranasal Challenge

The following study was conducted to provide a more complete picture of the mechanism behind VacSIM™ delivery and its ability to improve vaccine efficacy. Specifically this study focused on obtaining a more detailed understanding of underlying factors enabling VacSIM™ delivery of CpG-adjuvanted, whole-inactivated PR8 to induce more effective viral clearance as well as the production of vaccine-specific mucosal antibodies in the lungs, following homologous challenge (discussed in Chapters 2-4). Mice received a single vaccination (s.c.) containing whole-inactivated PR8 ± CpG, delivered in either saline or VacSIM™. Four weeks later these same mice received an

intranasal (i.n.) challenge with a lethal dose (1,000 LD₅₀) of homologous virus (A/Puerto Rico/8/34). Following challenge, mice were monitored daily for weight loss and symptoms of illness as described previously (Chapters 2-4). At 48 hours post challenge (hpc) lymph nodes were harvested, processed and stained for cell-specific analysis via flow cytometry. A pool of six lymph nodes was collected from each mouse, including the mediastinal, brachial and axillary draining lymph nodes and non-draining lymph nodes. Therefore, the cell counts per mouse, indicate the pool of six lymph nodes, harvested from an individual mouse. Table 5.1 lists the fluorescent markers used in this study and the spectral overlap has been included in the appendix (Figure C.8). In this and all other flow experiments described in this dissertation, live cells were initially selected using live/dead discrimination, after which population gates were determined according to fluorescence minus one (FMO) controls. Compensation controls included single-stained cell samples, an unstained cell sample as well as a sample containing all fluorophores being used.

Cell counts per mouse were determined for eight distinct immune cell populations, including activated/naive CD8⁺ and CD4⁺ T cells, influenza-specific NP-tetramer⁺ CD8⁺ T cells (activated/naïve), natural killer cells (NKs) or a population defined as “other”, which indicated cells that were neither CD8⁺/CD4⁺ T cells or NKs (Figure 5.7A). The phenotypes used to discriminate distinct cell populations from total live cells are listed in Table 5.2. In addition to cell counts, the relative populations were determined, with respect to total live cells (Figure 5.7B). The group vaccinated with PR8+CpG delivered in VacSIM™ had a slight increase in the relative proportion of NK

cells compared to all other vaccine groups, however neither the population counts nor the relative percentages showed statistically significant differences.

Table 5.1: Phenotypic markers.

Marker : Fluorophore
CD8a : Pacific Blue (PB)
CD3 : V500
CD44 :FITC
NK1.1 : PE
NP-Tetramer : APC

Table 5.2: Cell-specific phenotypes for analysis by flow cytometry. Live cells were initially selected using live/dead discrimination and population gates were determined according to fluoresce minus one (FMOs) controls.

Immune cell type	Population phenotype
Naive CD8 T cells	CD3 ⁺ , CD8 ⁺ , CD44 ⁻
Activated CD8 T cells	CD3 ⁺ , CD8 ⁺ , CD44 ⁺
Naive CD8 T cells with NP-tetramer	CD3 ⁺ , CD8 ⁺ , NP-tet. ⁺ , CD44 ⁻
Activated CD8 T cells with NP-tetramer	CD3 ⁺ , CD8 ⁺ NP-tet. ⁺ , CD44 ⁺
Naive CD4 T cells	CD3 ⁺ , CD4 ⁺ , CD44 ⁻
Activated CD4 T cells	CD3 ⁺ , CD4 ⁺ , CD44 ⁺
Natural Killer cells (NKs)	CD3 ⁻ , CD8 ⁻ , CD4 ⁻ NK1.1 ⁺
“Other” cells	CD3 ⁻ , CD8 ⁻ , CD4 ⁻ , NK1.1 ⁻

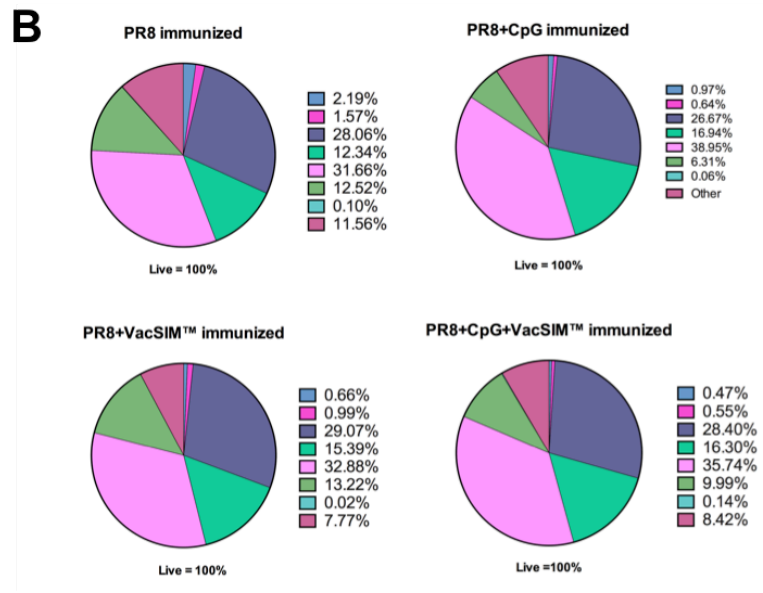
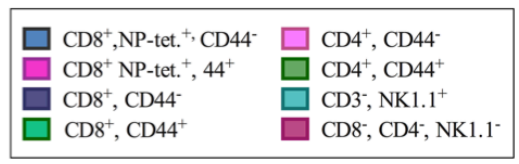
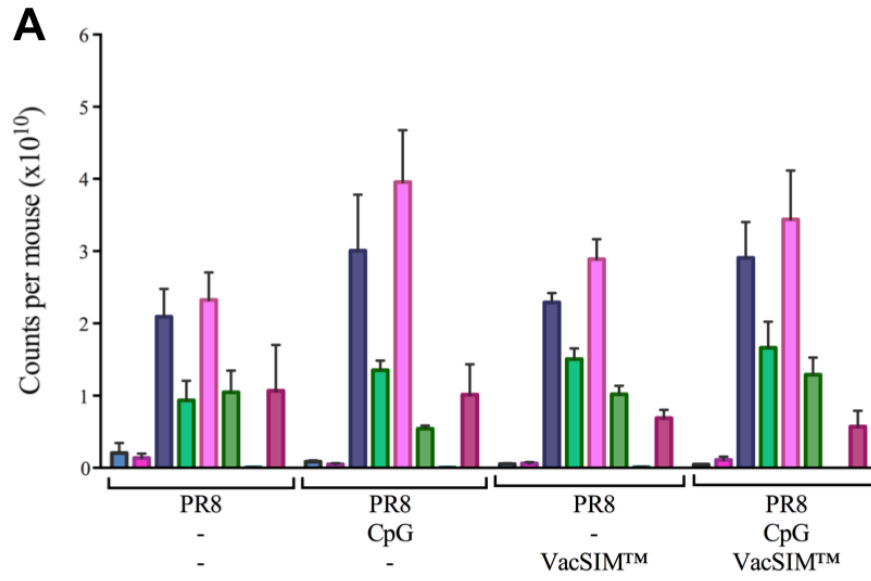


Figure 5.7: Minimal variation between PR8(WIV) vaccine groups, in relative immune cell populations at 48 hour post influenza challenge. Immune cell population counts per mouse and population frequencies were determined from pooled lymph node samples, at 48 hour post influenza challenge. Data was shown to be not significant by 2-way ANOVA and Bonferroni's multiple comparisons test.

5.3 Conclusions

VacSIM™ delivery provides improved immunogenicity (4) and vaccine efficacy. However in the absence of antigens and/or adjuvants, VacSIM™ lacks immunostimulatory characteristics (Figure 5.1, Figure 5.3). The (RADA)4 oligopeptides within VacSIM™ have previously been shown, *in vitro* and *in vivo*, to provide an effective porous barrier and facilitate slow release of molecules such as insulin (7, 11). All of which is consistent with the hypothesized mechanism and preliminary results discussed in this chapter. This dissertation proposes that delivery of vaccine antigens and/or adjuvants in VacSIM™ allows for an extended (Figure 5.3) and gradual exposure to antigens/adjuvants to the immune system (Figure 5.1, Figure 5.2).

The confocal experiments showing DCs infiltrating the VacSIM™ gel-matrix and taking up fluoresceinated HSA are limited in nature and need to be extended to determine if DCs enter the porous vaccine-gel structure to retrieve antigen/adjuvant components, and how this is influenced by the addition of adjuvants, and/or altering the concentration of the (RADA)4 synthetic oligopeptide in VacSIM™ to reduce/increase the gel-matrix pore size. Similar evaluations with model antigens of small, medium and high molecular weights to gain further understanding on how vaccine antigen size may influence egress from the gel-matrix, as well as DC migration into the gel-matrix. Future imaging experiments should utilize time-lapse microscopy to monitor DC entry and exit from the gel-matrix *in vitro*. Ultimately, the use of whole animal imaging coincident with cytometry, to monitor migration of APCs and labeled antigen trafficking to and from the VacSIM™ gel-matrix depot and lymph nodes over time.

The cell recruitment experiments (Figures 5.3–5.6) presented in this chapter show that VacSIM™ delivery of antigen/adjuvant leads to a non-systemic increase of immune cells in the draining lymph nodes compared to the non-draining lymph nodes. This trend is visible in total cell counts as well as DC and T cell populations, and is most impressive by 48 hours post vaccination. This trend of cell recruitment being localized to the draining lymph nodes at 48 hours post vaccination remains consistent for mice receiving antigen + CpG delivered in VacSIM™, with the exception of one non-draining lymph node with more activated DCs than the corresponding draining lymph node. Mice that received antigen in the presence or absence of antigen showed increased cell recruitment to the draining and/or the non-draining lymph nodes by 48 hours post vaccination, particularly with CpG.

Taken together, these results suggest that in addition to increasing immunogenicity and vaccine efficacy, VacSIM™ may also be able to minimize vaccine adverse events that can arise due to incorporation of highly reactogenic/immunostimulating vaccine components, through “controlled” release or gradual exposure. This potential added benefit to immunizing in VacSIM™ could enable the incorporation of vaccine components, historically considered too potent and therefore otherwise excluded from clinical development due to reactogenicity concerns. Additional reactogenicity studies are currently ongoing, funded through a Georgia Research Alliance (GRA) Ventures seed grant. The forthcoming results should provide additional evidence necessary to move forward or reevaluate this hypothesis.

Immune cell phenotype analysis was conducted by flow cytometry to investigate specific cell populations present in pooled lymph node samples of draining and non-

draining lymph nodes harvested 1 day prior or 2 days following homologous influenza challenge (Figure 5.7- Figure 5 .10). As previously discussed, there were no significant variations in cell populations (counts/mouse or frequency with respect to live) between vaccine groups post challenge. Similarly, there was no significant variation in immune populations when comparing 1 day prior to challenge with 2 days following challenge. Due to the extended time post vaccination (4-weeks), it was determined that pooling the lymph nodes would ensure a sufficient number of cells were collected. It is possible that had draining and non-draining lymph nodes been treated individually rather than being pooled, a similar trend of increasing immune cells localized to the draining versus the non-draining lymph nodes would be visible. Should a similar experiment be conducted in the future, it may be interesting to include lung washes (bronchoalveolar lavage), comparing between the various vaccine groups.

5.4 Materials and Methods

5.4.1 Animals

Female C57BL/6 mice (Harlan) aged 5-7 weeks were obtained from Harlan laboratories and housed in pathogen-free conditions. Mice were acclimated for one week prior to manipulations. All animal handling was conducted in accordance with applicable regulations and with the approval of the institutional animal care and use committee. Animals within a group were not pooled during analysis and unless otherwise stated, data from individual mice were graphed. Mice could be excluded from the final analysis if there was evidence of its difference prior to employing the experimental manipulation (i.e.: physical or behavioral abnormality recorded prior to vaccination or challenged).

5.4.2 Bone marrow derived dendritic cells

Femurs and tibias were collected from C57BL/6 mice and sterilized by sequentially submerging bones in 70% EtOH (1x), 1x PBS (2x), after which marrow was isolated in RPMI-1640 serum-free media. Suspended lymphocyte precursor cells were separated and adherent cells were retained for continued culture in complete media [RPMI-1640, 10% FBS, 1% antibiotic/antimycotic, non-essential amino acids, 1000 U/mL granulocyte macrophage colony stimulating factor (GM-CSF) and 1000 U/mL IL-4] at 37°C and 5% CO₂. After 6 days, DC cultures were confirmed by incubating 2 x 10⁶ cells in 2ml complete media ± 100 ng/mL LPS for 16-20 hours (differentiate activated/resting DCs). Cells were treated with Fc Block (BD) and stained with CD86-FITC (BD) and CD11c-PE (BD).

5.4.3 Vaccination

Six to eight week old mice (n=4-8) received a single vaccination of 200 µL for subcutaneous (s.c.) to their right flank. Vaccinations consisted of sterile saline, PR8 whole-inactivated PR8 (A/PR/8/34 (H1N1) influenza, 15 µg, Charles River Laboratories, Cat. No. 10100782), whole-inactivated X:31 (A/Aichi/68 (H3N2) influenza, 15 µg, Charles River Laboratories, Cat. No. 10100784), BSA (add), HSA (add), CpG (50 µg, ODN1826, TriLink BioTechnologies, 5' TCC ATG ACG TTC CTG ACG TT 3'), Alum (250 µg, Imject Alum, Thermo Scientific, Cat. No. 77161), or equal volumes VacSIM™ (PuraMatrix, BD Biosciences, Cat. No. 354250), as indicated.

5.4.4 Challenge

Influenza challenge virus (A/Puerto Rico/08/34, H1N1) was mouse-adapted through serial passage prior to propagation in embryonated chicken eggs and lethality was determined by MLD₅₀, as described previously (12). Four weeks post-vaccination, age-matched mice were challenged intranasally (i.n.) with 1000 LD₅₀ of mouse-adapted

homologous PR8 virus under temporary sedation with tribromoethanol. Lungs were harvested immediately following challenge from minimally two control mice, to confirm infection by plaque assay. Mice were monitored daily for weight change and symptom severity including changes in weight, behavior, activity, posture, grooming and respiratory rate. Each animal was given a daily morbidity score, calculated from the assigned values of each symptom: hunched back or ruffed fur (1), lethargy (2), head tilt (3), weight loss >20% (3), weight loss >25% (4), weight loss >30% (5), cyanosis (5), paralysis (5), seizure (5) and severe dyspnea (5). Animals were immediately sacrificed (CO₂ inhalation followed by cervical dislocation) if they received a total score of ≥ 5 and said to have reached their humane endpoint.

5.4.5 Flow Cytometry

Draining and/or non-draining (contra-lateral) axillary, inguinal, mediastinal or brachial lymph nodes were harvested at 12, 24, 36 or 48 hours post vaccination, 4 weeks post vaccination and prior to challenge or 4 weeks post vaccination and 2 days following challenge. Tissues were macerated and single cell suspensions were stained for flow cytometry with α -CD344-FITC, α -NK1.1-PE, α -CD16/CD32, α -CD3-V500, and α -CD8a-Pacific Blue antibodies (BD), APC-conjugated NP (ASNENMETM) tetramer (NIH Tetramer Core Facility), and Live/Dead fixable green/NIR viability dye (Invitrogen). Following live/dead discrimination, population gates were determined according to fluoresce minus one (FMOs) controls. Compensation controls included single-stained cell samples (or bead samples), an unstained cell sample as well as a sample containing all fluorophores being used in the particular staining experiment. When an experiment contained multiple time points, resulting in multiple staining sessions, all FMO and compensation controls were remade, during subsequent sample

staining. Samples were acquired on a BD LSRII running FACSDiva software (BD). CD3+, CD86+CD11c+, CD86+CD11c-, CD3+CD11c+CD86+, CD3-CD11c+CD86-, CD3+ CD8+CD44-, CD3+ CD8+CD44+, CD3+CD8+Tetramer+CD44-, CD3+CD8+Tetramer+CD44-, CD3+CD4+CD44-, CD3+CD4+CD44+, CD3-CD8-CD4-NK1.1+, or CD3-CD8-CD4-NK1.1- viable singlets were analyzed using either FlowJo version X (10.0.6) or FACSDiva software (BD).

5.4.6 Statistical Significance

In general, a sample size of at least four mice per treatment group was utilized. Animals within a group were not pooled during analysis and unless otherwise stated, data from individual mice were graphed. No outliers were excluded. Statistical analyses were performed using GraphPad Prism version 6.0. Statistical methods and significant differences between vaccination groups were determined using two-way ANOVA and Bonferroni's multiple comparisons test.

5.5 References

1. Berzofsky JA, *et al.* (2004) Progress on new vaccine strategies against chronic viral infections. *J Clin Invest* 114(4):450-462.
2. Koff WC, *et al.* (2013) Accelerating Next-Generation Vaccine Development for Global Disease Prevention. *Science (New York, N.Y.)* 340(6136).
3. Delany I, Rappuoli R, & De Gregorio E (2014) Vaccines for the 21st century. *EMBO molecular medicine* 6(6):708-720.
4. Grenfell RF, Shollenberger LM, Samli EF, & Harn DA (2015) Vaccine Self-assembling Immune Matrix is a new delivery platform that enhances immune responses to rHBsAg in mice. *Clinical and Vaccine Immunology* 22(3):337-343.
5. Zhang S ZX, Spirio L. (2010) *PuraMatrix: Self-Assembling Peptide Nanofiber Scaffolds* (CRC Press, Scaffolding In Tissue Engineering) 2 Ed pp 217-240.
6. Xiaojun Z, Shuguang Z, & Lisa S (2005) *PuraMatrix. Scaffolding In Tissue Engineering*, (CRC Press), pp 217-238.

7. Nishimura A, *et al.* (2012) Controlled release of insulin from self-assembling nanofiber hydrogel, PuraMatrix: application for the subcutaneous injection in rats. *European journal of pharmaceutical sciences : official journal of the European Federation for Pharmaceutical Sciences* 45(1-2):1-7.
8. Steinman RM & Banchereau J (2007) Taking dendritic cells into medicine. *Nature* 449(7161):419-426.
9. Banchereau J & Steinman RM (1998) Dendritic cells and the control of immunity. *Nature* 392(6673):245-252.
10. Gamvrellis A, *et al.* (2004) Vaccines that facilitate antigen entry into dendritic cells. *Immunol Cell Biol* 82(5):506-516.
11. Nagai Y, Unsworth LD, Koutsopoulos S, & Zhang S (2006) Slow release of molecules in self-assembling peptide nanofiber scaffold. *Journal of controlled release : official journal of the Controlled Release Society* 115(1):18-25.
12. Webster R CN, Stohr K (2002) WHO Manual on Animal Influenza Diagnosis and Surveillance in *WHO Global Influenza Program*, ed Webster R CN, Stohr K (World Health Organization, Geneva, Switzerland), p 105.

CHAPTER 6

DISCUSSION AND FUTURE DIRECTIONS

6.1 Discussion

Natural infection can be sufficient for a host to generate extended or even lifelong immunity to re-infection; such is the case in polio, measles or rubella infections. It is through this same concept that many successful vaccines utilize pathogen mimicry or provide a low-level infection as a means of inducing host immunity. However, there still remains a critical need to develop effective vaccines targeting pathogens that are unable to induce sterilizing immunity following natural infection, such as malaria or respiratory syncytial virus (RSV) to list just two such diseases. Similarly, pathogens inducing latent or persistent infections, such as human immunodeficiency virus (HIV) represent further complicated vaccine targets (1, 2). In addition, several current vaccines, as well as numerous candidate vaccine antigens induce sub-optimal immune responses and thus fail to induce good levels of protection. Therefore, availability of safe and effective adjuvants and/or delivery systems that will allow increased vaccine-induced protection remains a crucial goal (3, 4).

Chapter 2 introduces the patent pending delivery system, VacSIM™ (vaccine self-assembling immune matrix), the development of which has been the focus of this dissertation. The results outlined in this chapter (summarized in Table 6.1), provide the foundation on which is built a framework for investigating the potential of VacSIM™ as a three-dimensional vaccine delivery platform. VacSIM™ is solely comprised of a 1.0%

solution of the synthetic (RADA)4 self-assembling oligopeptide in aqueous buffer. Immediately post-injection, the (RADA)4 synthetic oligopeptides self-assemble into hydrated fibers that form a gel-matrix with vaccine components found in the aqueous phase. We hypothesize that the egress of vaccine components through the pores in the gel-matrix provides antigen persistence and improved vaccine responses. The RADA-based self-assembling nanofibers scaffolds (SANS) were originally conceived and designed by Zhang and colleagues (5-7). The (RADA)4 synthetic oligopeptide was commercialized by 3-D Matrix Inc. as the product PuraMatrix™ for use in 3-D cell culture experiments. The (RADA)4 oligopeptides contained in VacSIM™ are triggered to self-assemble, shifting from a semi-viscous liquid to a gel phase, upon exposure to physiological conditions of salinity and pH (6, 8-10). Vaccine delivery in VacSIM™ is possible through simple mixing with the desired vaccine antigen and/or adjuvant prior to immunizing. Immediately after being injected, the oligopeptide, which make up the VacSIM™ portion of this vaccine, begin self-assembling into a porous a gel-matrix depot of concentrated vaccine components, which is hypothesized to provide antigen persistence and improve vaccine efficacy. Thus, VacSIM™ enables rapid and straightforward preparation, making it an ideal candidate for pandemic scenarios as well as vaccines that may require rapid formulation changes.

Table 6.1: Summary of Chapter 2 results.

Figure(s)	Chapter 2: Results Overview	Timeline
2.4	Humoral responses (α -rHBsAg) are enhanced by VacSIM™ out to 5 wpv in BALB/c mice	1-5 wpv (prime+boost)
2.5, 2.6	Enhanced α -rHBsAg/ α -rNP humoral responses (antigen+CpG+VacSIM™) in Th1-/Th2-biased mouse models	3 wk post-boost (prime+boost)
2.8, 3.5	Protein subunit antigen (OVA) but not whole-inactivated virus (PR8) results in differential diffusion from <i>in vitro</i> assembled depots (0.5% vs. 1% VacSIM™)	<i>in vitro</i>
2.9, 2.10	CpG ODN 1826 was the most effective adjuvant tested, at enhancing immune responses to PR8 in VacSIM™. (IgG, IgG subtypes, IgA, IgE, IgM)	4 wpv (prime only)
2.12	VacSIM™ is able to enhance vaccine efficacy of whole-inactivated PR8+CpG via multiple routes.	4 wpv, 2 dpc (prime only)

Results described in Chapters 2, 3 and 4 of this dissertation indicate that VacSIM™ is flexible enough to be successfully used with different types of vaccine antigens, including protein subunits and inactivated viruses (Figures 2.4-2.5, 2.9, Figure 4.9). Specifically, these results demonstrate that immunizing Th1- and/or Th2-biased mice with various protein subunit antigens (rHBsAg, rNP), provides increased antigen-specific immunogenicity that can be further improved by addition of an adjuvant, such as CpG (Figures 2.4-2.6). Results discussed in both Chapters 2 and 3 showed that VacSIM™ is not limited to improving protein subunit vaccines, but also improved immunogenicity and vaccine efficacy with adjuvanted whole-inactivated viruses (PR8). Specifically, demonstrating that VacSIM™ delivery of CpG adjuvanted PR8 (WIV) provides improved protection from lethal challenge (1,000 LD₅₀, homologous, 4 wpv), determined by increased viral clearance from the lungs as well as reduced morbidity and mortality (Figures 2.10, 2.11, Figures 3.3, S3.7). Results shown in Figure 2.10 demonstrate VacSIM™ is also flexible enough to incorporate alternative types of

adjuvants, including unmethylated CpG-ODN that signals through toll-like receptor 9 (TLR-9), inorganic aluminum salts (Alum, Al(OH)₃) that induce activation of multiple complement cascades (11) as well as candidate adjuvant formulations of a glucopyranosyl lipid adjuvant (GLA)-variant, which function as TLR-4 agonists (12).

Mice that received a single vaccination of whole-inactivated PR8+CpG in VacSIM™ had increased tetramer-specific CD8⁺ T cells in the lungs at two days post challenge (dpc), compared to naïve mice or those vaccinated with PR8 in saline. Whole-inactivated PR8 utilized in this comparison due to its high immunogenicity and reputation as a research standard in the field (Figure 3.4). In addition to enhanced influenza-specific CD8⁺ T cells, this vaccine group (PR8+CpG in VacSIM™) also had increased vaccine-specific mucosal antibodies in the lungs compared to naïve mice or those vaccinated with PR8 in saline after 1 dpc (Figure 3.1D). This finding is particularly intriguing since inactivated vaccines are not typically capable of inducing a mucosal antibody response.

Table 6.2: Summary of Chapter 3 results.

Figure(s)	Chapter 3: Results Overview (Mice receiving PR8+CpG in VacSIM™)	Timeline
3.1A	α -PR8 IgG endpoint titers significantly > all other groups	4 wpv
3.1B, S3.6	Suggests a mixed Th1-/Th-2 type immune response (Significantly increased IgG ₁ , IgG _{2b} and decreased IgG _{2a} , IgG ₃)	4 wpv
3.1D	Mucosal IgA endpoint titers in lungs > naïve, PR8 in saline	4-5 wpv, 1 dpc
3.2	Variable ability to inhibit hemagglutination	4 wpv
3.3A-C, S3.7	Decreased morbidity/mortality out to 14 days following 30LD ₅₀ or 1,000LD ₅₀ PR8 challenge	5-6 wpv, 6-14 dpc
3.3D	More efficient viral clearance from the lungs as early as 1 dpc	5 wpv, 1-3,5 dpc
3.4	Tetramer-specific CD8 ⁺ T cells in lungs > naïve, PR8 in saline	4-5 wpv, 2 dpc
Figure(s)	Chapter 3: Results Overview	Timeline
3.3E	Vaccinating without antigen/adjuvant in VacSIM™ results in viral clearance from the lungs that is identical to naïve	4-5 wpv, 5 dpc
3.5B	Without antigen/adjuvant VacSIM™ is not immunostimulating (does not induce DC activation in 6d BMDC cultures)	<i>in vitro</i>
3.5C	OVA diffuses differentially at 0.5 and 1% VacSIM™	<i>in vitro</i>
3.5D	PR8 (WIV) fails to diffuse at either 0.5 or 1% VacSIM™	<i>in vitro</i>

VacSIM™ has been used successfully with multiple vaccination routes, including subcutaneous (s.c.), intradermal (i.d.), intramuscular (i.m.) and intraperitoneal (i.p.) (Figure 2.12). Myself, Professor Harn and Dr. Shollenberger hypothesize that VacSIM™ will also be effective when delivered directly to mucosal sites such as the gastrointestinal, genitourinary and the respiratory tract, which are infection ground zero for a many different pathogens (13). Mucosal vaccines activate mucosal B and T lymphocytes and induce secretory IgA responses (14) that assists in cell-mediated toxicity and preventing colonization of mucosal barrier cells by infectious pathogens (15). There are several

advantages to vaccine delivery via mucosal surfaces, but relatively few approved vaccines do so. Those that have been approved include orally delivered vaccines against polio, rotavirus, cholera, typhoid and the intranasal delivered seasonal influenza vaccine (13). One of the main complicating factors associated with mucosal vaccines is poor immunogenicity, as a result of ineffective antigen uptake and/or presentation, which may be exacerbated by enzymatic degradation (13, 16). A major component in the proposed VacSIM™ mechanism involves generation of a vaccine depot. Thus, it is possible that another advantage of VacSIM™ is that the gel-matrix provides a stabilizing effect to vaccine components and in the case of mucosal environments may delay and/or reduce enzymatic or systemic degradation. Therefore, mucosal delivery of vaccines using VacSIM™ presents an approach, which may overcome some, if not all of the above-mentioned complications typically associated with delivery to mucosal sites.

In the case of seasonal influenza vaccines, efficacy varies from year to year, depending on the alignment of predicted and circulating viral strains. Experts at the Center for Disease Control (CDC) recommend that all persons older than six months receive an annual influenza vaccination, particularly those with increased risk of developing more severe complications as a result of infection. As discussed in Chapter 4, vaccine effectiveness in the case of seasonal influenza, refers to probability that vaccinated individuals will avoid clinical symptoms of acute respiratory illness (ARI) that require treatment by a healthcare professional that results in laboratory confirmation of virus infection. A recent publication, spanning five influenza seasons (November-April) between 2006 and 2012 (data from 2009-2010 was excluded) indicated seasonal trivalent inactivated vaccines to be 58.4% effective (95% CI, 7.9%–81.1%) in those aged

65 years and over (17). Seasonal influenza vaccines are typically less effective in those under the age of 5 and over the age of 65 (18, 19). In the most recent influenza season (2014-2015) the predicted virus strains were not aligned with the circulating strains, as a result of drifted influenza A H3N2 circulating virus strains. For the 2014-2015 season the CDC has estimated overall vaccine efficacy to be 19% (95% CI: 7%– 29%) (20). As there are still several weeks before the close of this season, the age-specific vaccine efficacy estimations are not yet available. However, a recent modeling study conducted by the CDC suggests that during a moderately severe influenza season (i.e.: 2012-2013) a vaccine efficacy for adults over the age of 65 that is only 10%, would translate to preventing ~13,000 hospital visits due to influenza related illness (IRI) by adults ≥ 65 in the United States (21). These hypothetical modeling studies suggest that even minor improvement in seasonal influenza vaccine efficacy would provide significant health and socioeconomic benefits. The preliminary results described in chapter 4 and summarized in Table 6.3 indicate that VacSIM™ delivery of an adjuvanted, inactivated influenza vaccine leads to improved vaccine-specific immune responses and viral clearance, compared to delivery in saline (Figure 4.10).

Unfortunately, under the experimental conditions outlined in Chapter 4, VacSIM™ did not appear to extend the duration of vaccine efficacy (Figures 4.4-4.5) or induce cross-reactive immunity to alternative influenza A subtypes (Figures 4.6, 4.8-4.9). However, the inability to extend the duration of vaccine-induced protection (under these conditions) is not by any means a fatal flaw in the case of seasonal influenza vaccines. The influenza season is typically ≤ 6 months and annual vaccination against seasonal viruses will continue to be the recommendation at least until there is a viable “universal”

influenza vaccine option. Additionally, the results presented in this thesis were derived from studies using naïve mice and thus these results cannot be expected to translate directly to outcomes within a non-naïve human population. Further, based on the results presented here, it is likely that VacSIM™ delivery would provide enhanced immunogenicity for a broad spectrum of influenza subtypes, if combined with one or more universal vaccine antigen candidates, which are notoriously poor immune stimulators.

Table 6.3: Summary of Chapter 4 results.

Figure(s)	Chapter 4: Results Overview	Timeline
4.2, 4.3, (Appendix B.1)	A single (s.c.) immunization of whole-inactivated PR8 and CpG delivered in VacSIM™ leads to enhanced α -PR8 IgG levels in the sera, which are maintained out to 6 and 12 months	4, 10, 18, 26 wpv
4.4, 4.5, (Table 4.2)	Whole-inactivated PR8 and CpG delivered in VacSIM™ via a single s.c. vaccination provides gradually decreasing level of protection from lethal challenge out to 6 and 12 months.	4, 26, 34, 52 wpv 2, 3, 14, 4 dpc
4.6, 4.7 (Table 4.3)	The cross-reactive α -IgG levels in sera of mice immunized with PR8 (WIV) are variable depending on the recombinant hemagglutinin (rHA) being evaluated	4 wpv
4.8, 4.9	The α -PR8 and α -X:31 specific IgG levels in sera of mice immunized with X:31(WIV) are quite similar. Unfortunately (likely due to challenge dose) there was no variation in protection between groups.	4 wpv, 3 dpc
4.10	Initial study indicates that VacSIM™ is also able to improve vaccine-specific immune responses and induced protection of an adjuvanted whole-inactivated vaccine (PR8+CpG) in elderly mice.	4 wpv 3 dpc

The precise mechanism by which VacSIM™ provides improved vaccine responses is still under investigation. The results from several early studies were presented in Chapter 5 and summarized in Table 6.4. Overall, VacSIM™ is hypothesized to allow antigen persistence through generation of a porous gel-matrix, resulting in a

depot of vaccine components localized at the site of delivery. All *in vitro* and *in vivo* studies, which included VacSIM™ in the absence of an antigen or adjuvant, indicate that VacSIM™ does not itself possess immunostimulatory activity (Figures, 5.1, 5.3, Figure 3.3E). Specifically, VacSIM™ alone was insufficient to induce DC activation. However, in combination with CpG and either a protein subunit antigen (HSA) or inactivated virus (PR8), DC activation was not only achieved, but increased over levels of either antigen or adjuvant component individually (Figure 5.1). Immunization with VacSIM™, in the absence of an antigen or adjuvant resulted in no protection from influenza challenge (Figure 3.3E) and did not induce cell recruitment to the draining or non-draining lymph nodes at 12, 24 or 36 hours post vaccination (h_{pv}) (Appendix Figure C.3). Given that the (RADA)₄ oligopeptides contained in VacSIM™ are resorbable, non-toxic and non-reactogenic (22, 23), the results included in this dissertation, showing that VacSIM™ is not immunostimulating are not surprising. Again, further studies on the mechanism of VacSIM delivery need to be performed, including repetitive immunizations using VacSIM over time to insure that VacSIM is not reactogenic when used repeatedly. Lastly, such “repeat” vaccine experiments would also be able to show if local or systemic immune alterations occur simply as a result of environmental disturbances due to physical changes on a nanoscale level, instigated by VacSIM™ self-assembly and depot formation.

As shown in these studies, model antigens diffuse out of the VacSIM™ gel-depot over time, thus generating antigen persistence (Figure 2.8/Figure 3.5). This slow egress from the depot provides an extended window of opportunity for early responding antigen presenting cells (APCs) to become activated by the available vaccinating

antigen/adjuvant (24). Chapter 5 describes the results from several studies investigating the effects on cell recruitment to the lymph nodes after immunization with or without VacSIM™. Mice that received a vaccine containing antigen + CpG in VacSIM™, showed an increased number of total cells localized to the draining lymph nodes compared to the non-draining lymph nodes at 24 hpv and increased further at 48 hpv (Figure 5.3). In addition to total cell counts, flow cytometry was used to discriminate between immune cell population phenotypes and determine population counts as well as relative frequencies. The DC, activated DC and T-cell populations present in the individual draining and non-draining lymph nodes were evaluated across six alternative vaccine groups (n= 4-5) and at two time points (24, 48hpv). Intriguingly, the trend of increased cell recruitment being localized to the draining lymph nodes in the antigen + CpG + VacSIM™ cohort, was maintained consistently (Figures 5.4-5.6). However, results from fluor-conjugated antigens used to calculate the mean fluorescent intensity (MFI) were not clearly defined and require further optimization of fluorescent conjugates including, the dose per mouse of labeled protein as well as investigating multiple times post vaccination (Appendix Figures C.4 and C.5).

Table 6.4: Summary of Chapter 5 results.

Figure(s)	Chapter 5: Results Overview	Timeline
5.1	VacSIM™ in the absence of antigen/adjuvant is not sufficient to induce DC activation (6-day BMDC cultures)	<i>in vitro</i>
5.2	Confocal image depicts in vitro assembled depots containing/incorporating fluorescent antigen.	<i>in vitro</i>
5.2	Confocal image suggests incorporation of fluorescent antigen by BMDCs, after interacting with gel-vaccine depot	<i>in vitro</i>
Appendix (5.3A)	Mice give VacSIM™ in the absence of antigen/adjuvant, show no differences in cell recruitment to the draining or non-draining lymph nodes (similar trend as saline)	5 wpv, 12, 24, 36 hpc
5.7, 5.8	Pooled LNs (d/nd from axillary, mediastinal, brachial) show no significant differences between vaccine groups in total counts or frequency of immune cell population / total live	5 wpv, 48 hpc
Figure(s)	Chapter 5: Results Overview (Mice receiving PR8+CpG in VacSIM™)	Timeline
5.3	Consistent trend of increased total cells in the draining lymph nodes (d-LNs) compared to nd-LNs (axillary & inguinal)	4-5 wpv, 24, 48 hpc
5.4, 5.5, 5.6	Similar trend shows increases DCs, activated DCs and T cells localized to the draining lymph nodes	4-5 wpv, 24, 48 hpc
5.7 Appendix (C-6, C-7)	No statistically significant differences in immune cell populations (cell counts or frequency) pre/post-challenge	5wpv, -24, 48 dpc

The results presented in this dissertation suggest that VacSIM™ delivery provides a localized immune response, in contrast to the systemic response seen in non-VacSIM™ cohorts. These findings remain to be validated with additional subunit antigens and adjuvants. Because VacSIM™ provides gradual egress of vaccine components; these results suggest that in addition to increasing immunogenicity and vaccine-induced protection, VacSIM™ may also represent an avenue for reducing reactogenicity from vaccine-incorporated antigens/adjuvants. Therefore, through

“controlled” release of the highly immune-stimulating vaccine component(s), VacSIM™ could provide for more physiologically acceptable exposure to the highly immune-stimulating vaccine component(s). This potential new benefit to immunizing in VacSIM™ could lead to re-evaluation of promising vaccine antigens/adjuvants, which historically have been considered too potent and excluded due to reactogenicity concerns from clinical development. One such adjuvant class is the CpG-ODNs. Additional reactogenicity studies funded through a Georgia Research Alliance (GRA) Ventures seed grant are currently ongoing and these forthcoming results will hopefully provide the additional evidence necessary to move forward or reevaluate this new hypothesis.

6.2 References

1. Kim HW, *et al.* (1969) Respiratory syncytial virus disease in infants despite prior administration of antigenic inactivated vaccine. *American journal of epidemiology* 89(4):422-434.
2. Delany I, Rappuoli R, & De Gregorio E (2014) Vaccines for the 21st century. *EMBO molecular medicine* 6(6):708-720.
3. Flannery B, *et al.* (2014) Interim estimates of 2013-14 seasonal influenza vaccine effectiveness - United States, February 2014. *MMWR. Morbidity and mortality weekly report* 63(7):137-142.
4. Manon M.J. Cox PSC (Safety and Immunogenicity of PanBlok Influenza Vaccine in Healthy Adults. (ClinicalTrials.gov).
5. Koutsopoulos S, Unsworth LD, Nagai Y, & Zhang S (2009) Controlled release of functional proteins through designer self-assembling peptide nanofiber hydrogel scaffold. *Proceedings of the National Academy of Sciences of the United States of America* 106(12):4623-4628.
6. Zhang S, Holmes T, Lockshin C, & Rich A (1993) Spontaneous assembly of a self-complementary oligopeptide to form a stable macroscopic membrane. *Proceedings of the National Academy of Sciences of the United States of America* 90(8):3334-3338.
7. Zhang S, *et al.* (1995) Self-complementary oligopeptide matrices support mammalian cell attachment. *Biomaterials* 16(18):1385-1393.

8. Ye Z, *et al.* (2008) Temperature and pH effects on biophysical and morphological properties of self-assembling peptide RADA16-I. *Journal of peptide science : an official publication of the European Peptide Society* 14(2):152-162.
9. Zhang S, Lockshin C, Cook R, & Rich A (1994) Unusually stable beta-sheet formation in an ionic self-complementary oligopeptide. *Biopolymers* 34(5):663-672.
10. Kisiday J, *et al.* (2002) Self-assembling peptide hydrogel fosters chondrocyte extracellular matrix production and cell division: implications for cartilage tissue repair. *Proceedings of the National Academy of Sciences of the United States of America* 99(15):9996-10001.
11. Guven E, Duus K, Laursen I, Hojrup P, & Houen G (2013) Aluminum hydroxide adjuvant differentially activates the three complement pathways with major involvement of the alternative pathway. *PloS one* 8(9):e74445.
12. Mauricio AA, *et al.* (2012) Glucopyranosyl Lipid Adjuvant (GLA), a Synthetic TLR4 Agonist, Promotes Potent Systemic and Mucosal Responses to Intranasal Immunization with HIVgp140. *PloS one* 7(7).
13. Srivastava A, Gowda DV, Madhunapantula SV, Shinde CG, & Iyer M (2015) Mucosal vaccines: a paradigm shift in the development of mucosal adjuvants and delivery vehicles. *APMIS : acta pathologica, microbiologica, et immunologica Scandinavica*.
14. Ogra PL, Faden H, & Welliver RC (2001) Vaccination strategies for mucosal immune responses. *Clin Microbiol Rev* 14(2):430-445.
15. Macpherson AJ, McCoy KD, Johansen FE, & Brandtzaeg P (2008) The immune geography of IgA induction and function. *Mucosal immunology* 1(1):11-22.
16. Holmgren J & Svennerholm AM (2012) Vaccines against mucosal infections. *Current opinion in immunology* 24(3):343-353.
17. Chen Q, *et al.* (2015) Influenza vaccine prevents medically attended influenza-associated acute respiratory illness in adults aged ≥ 50 years. *J Infect Dis* 211(7):1045-1050.
18. Thompson WW, *et al.* (2004) Influenza-associated hospitalizations in the United States. *Jama* 292(11):1333-1340.
19. Steininger C, *et al.* (2003) Acute encephalopathy associated with influenza A virus infection. *Clinical infectious diseases : an official publication of the Infectious Diseases Society of America* 36(5):567-574.
20. CDC (2015) Fluview. 2014–2015 influenza season ending January 30, 2015 (CDC.gov).

21. Fry AM, *et al.* (2014) Modeling the effect of different vaccine effectiveness estimates on the number of vaccine-prevented influenza-associated hospitalizations in older adults. *Clinical infectious diseases : an official publication of the Infectious Diseases Society of America* 59(3):406-409.
22. Zhang S ZX, Spirio L. (2010) *PuraMatrix: Self-Assembling Peptide Nanofiber Scaffolds* (CRC Press, Scaffolding In Tissue Engineering) 2 Ed pp 217-240.
23. Xiaojun Z, Shuguang Z, & Lisa S (2005) PuraMatrix. *Scaffolding In Tissue Engineering*, (CRC Press), pp 217-238.
24. Zhang XQ, *et al.* (2007) Potent antigen-specific immune responses stimulated by codelivery of CpG ODN and antigens in degradable microparticles. *Journal of immunotherapy* 30(5):469-478.

APPENDIX A

VACCINE SELF-ASSEMBLING IMMUNE MATRIX IS A NEW DELIVERY
PLATFORM THAT ENHANCES IMMUNE RESPONSES TO RECOMBINANT
HB_SAG IN MICE³

³Grenfell RF*, Shollenberger LM*, Samli EF, & Harn DA (2015), *Clinical and Vaccine Immunology*, 22(3): 336-343. *Authors have contributed equally. Copyright © American Society of Microbiology.

Reprinted here with permission from publisher.

A.1 Abstract

Vaccination remains the most effective public health tool to prevent infectious diseases. Many vaccines are marginally effective and need enhancement for immunocompromised, elderly, and very young populations. To enhance immunogenicity, we exploited the biphasic property of the (RADA)₄ synthetic oligopeptide to create VacSIM (vaccine self-assembling immune matrix), a new delivery method. VacSIM solution can easily be mixed with antigens, organisms, and adjuvants for injection. Postinjection, the peptides self-assemble into hydrated nanofiber gel matrices, forming a depot with antigens and adjuvants in the aqueous phase. We believe the depot provides slow release of immunogens, leading to increased activation of antigen-presenting cells that then drive enhanced immunogenicity. Using recombinant hepatitis B virus surface antigen (rHBsAg) as a model immunogen, we compared VacSIM delivery to delivery in alum or complete Freund's adjuvant (CFA). Delivery of the rHBsAg antigen to mice via VacSIM without adjuvant elicited higher specific IgG responses than when rHBsAg was delivered in alum or CFA. Evaluating IgG subtypes showed a mixed Th1/Th2 type response following immunization with VacSIM, which was driven further toward Th1 with addition of CpG as the adjuvant. Increased specific IgG endpoint titers were observed in both C57BL/6 and BALB/c mice, representative of Th1 and Th2 environments, respectively. Restimulation of splenocytes suggests that VacSIM™ does not cause an immediate proinflammatory response in the host. Overall, these results suggest that VacSIM, as a new delivery method, has the potential to enhance immunogenicity and efficacy of numerous vaccines.

A.2 Introduction

Vaccines remain the single greatest public health tool to combat infectious diseases. Vaccine formulation and delivery are key to the ability of vaccines to induce the desired immune responses. One goal of vaccine delivery is to present vaccine antigens in a manner that enhances antigen-presenting-cell (APC) activation, leading to antigen/organism uptake and processing of vaccine antigen(s). Delivery methods or adjuvants that safely enhance vaccine immunogenicity/efficacy are desirable for vaccines that are marginally effective and for vaccines administered to low responders or immunocompromised populations. Additional goals are to reduce the number of doses required to induce effective, vaccine responses and to reduce the amount of vaccine/dose, especially when a single dose of vaccine is administered, as with annual influenza vaccines. Lastly, in pandemics, a vaccine that produces high titers after a single administration would be beneficial. Recent advances in the understanding of how innate mechanisms influence adaptive immunity have led to more rational design in the development of new vaccine adjuvants and delivery systems.

Aluminum salts were the first adjuvants licensed for human vaccines in the 1920s. The licensure of non-aluminum salt adjuvants took an additional 80 years (1). One reason for this long gap is that the principles of adjuvant activity were largely unknown; thus, the development of adjuvants was empirical. Moreover, many adjuvants, including Freund's adjuvant, were reactogenic and not acceptable for licensure (2). Recent methods to improve vaccine delivery have taken several approaches, including the use of virosomes (3–5), vector-based methods (6–8), liposome-based methods (9–11), and the use of more traditional formulation with adjuvants (12–17). Each of these methods has

some drawbacks, in terms of reactogenicity, regulatory issues, product stability, or time required for formulation; however, each of these methods focuses on presenting the vaccine as a particulate.

To enhance vaccine immunogenicity over that seen when conventional alum-based delivery methods are used, we focused on identifying ways to deliver vaccines such that vaccine antigens are released over time. This led to our development of a new vaccine delivery method we call VacSIM (vaccine self-assembling immune matrix). VacSIM is based on the unique properties of the (RADA)₄ synthetic oligopeptide and other biopolymers (18–22). The (RADA)₄ synthetic oligopeptide was created by Zhang (22) and commercialized by 3-D Matrix Inc. for cell scaffolding and is currently in clinical trials for wound healing (PuraStat), tissue repair (23), and dental implant scaffolding (PuraMatrix) (24). As such, it has already undergone third-party reactogenicity and toxicity testing (25). VacSIM is composed solely of the (RADA)₄ synthetic oligopeptide. Thus, it is biocompatible and biodegradable. Ex vivo, a 1.0% VacSIM solution is in liquid phase, resulting in the flexibility to mix virtually any antigen, organism, and adjuvant. Upon injection into tissue, VacSIM self-assembles into hydrated nanofibers (26), forming a gel matrix depot, which entraps and concentrates vaccine components in the aqueous phase at the injection site (27). We hypothesize that the vaccine depot allows slow egress of antigen out of the gel pores, leading to persistent release of antigen, which is considered to be important in the development of robust adaptive immunity and memory responses (28, 29). We theorize that slow release of antigen and possible cellular infiltration of the VacSIM gel depot increases activation

and maturation of antigen-presenting cells, which then drive more robust adaptive responses. Further, it is possible that the gel depot protects vaccine components from degradation.

VacSIM is different from other hydrogels, such as alginates and methacrylates, as well as microneedle and layer-by-layer technology, as all of these require polymerization *ex vivo* (30–35). Further, it is different from other self-assembling peptide (SAP) technologies, such as the Q11 peptide, where the antigenic motif must be directly conjugated to the SAP (36–38). In contrast, VacSIM is prepared by simply mixing SAP and antigens prior to administration.

The biphasic property of VacSIM, coupled with the inert nature of the resultant vaccine gel depot, provides novel technology that can be translated for use in a multitude of vaccines. In this study, we tested the ability of VacSIM to enhance specific immune responses to the recombinant hepatitis B virus surface antigen.

A.3 Materials and Methods

Immunizations. Five- to seven-week-old female BALB/c or C57BL/6 mice were purchased from Harlan Laboratories, housed under specific-pathogen-free conditions, and allowed to acclimate for 1 week prior to manipulation. All animal work was performed in accordance with all applicable policies and approved by the University of Georgia institutional animal care and use committee. Mice were immunized subcutaneously with recombinant hepatitis B virus surface antigen (rHBsAg), subtype adw (5 µg; Fitzgerald Industries, Inc., North Acton, MA, USA), with or without CpG (50 µg; ODN 1826; InvivoGen, Inc., San Diego, CA, USA), via alhydrogel (250 µg; Inject Alum; Thermo Fisher Scientific, Inc., Pittsburgh, PA, USA) with or without CpG, by VacSIM with or

without CpG, or in Freund's (13 μ l; Sigma-Aldrich Co., St. Louis, MO, USA) or sham immunized with VacSIM or phosphate-buffered saline (PBS), at a maximum volume of 200 μ l per injection site. Three or four weeks later, as indicated in the figures, mice were administered a second, identical immunization.

Antibody responses. For the kinetic experiments, blood samples were collected from all immunized and control mice weekly, beginning at week 1 prior to primary immunization. rHBsAg-specific antibodies in sera were analyzed by enzyme-linked immunosorbent assay (ELISA). Briefly, plates were coated with 4 μ g/mL rHBsAg before singly diluted serum (1:800 for IgA and IgG2a and 1:1,200 for IgM, IgG, and IgG1) was added. Antibodies specific for rHBsAg were detected by horseradish peroxidase (HRP)-conjugated secondary antibodies (1:2,000 anti-IgA, 1:2,500 anti-IgM, and 1:2,500 anti-IgG from Santa Cruz; 1:1,000 anti-IgG1 and 1:1,000 IgG2a from Invitrogen). Plates were developed with SureBlue TMB (3,3',5,5'-tetramethylbenzidine) 1-component substrate (KPL), and the reaction was stopped by the addition of 2 N sulfuric acid. To evaluate the IgG1/IgG2a ratio, we multiplied the absorbance values by the dilution factors of the sera to normalize prior to dividing. For nonkinetic studies, all methods remained the same except that mice were bled prior to immunization and after each subsequent immunization. Each sample of serum was diluted serially for endpoint titer antibody analysis, and samples with undetectable antibody were assigned a value below the detection limit.

ELISpots. Splenocytes were obtained 3 weeks postprime or 2 weeks postboost and then stimulated for 20 h to evaluate HBsAg-specific cell-mediated

responses using gamma interferon (IFN- λ) enzyme-linked immunospot assay (ELISpot), according to the manufacturer's instructions (BD Biosciences, San Francisco, CA, USA). Briefly, single-cell suspensions (3×10^5 and 1.5×10^5 cells per well) were cultured at 37°C with 5% CO₂ for 20 h in complete medium (RPMI 1640 [HyClone, Thermo Scientific, Logan, UT, USA] supplemented with 10% fetal bovine serum [FBS], 100 U/mL penicillin, 100 μ g/mL streptomycin, antimycotic, nonessential amino acids, and β -mercaptoethanol [Sigma-Aldrich, St. Louis, MO, USA]). Cells were stimulated with 1 μ g/mL concanavalin A (ConA), 20 μ M HBs-specific peptide [S28-39; IPQSLDSWWTSL (synthesized at more than 95% purity [Biosynthesis Inc., Lewisville, TX, USA] and dissolved in dimethyl sulfoxide [DMSO] prior to dilution in culture medium) or left unstimulated. ELISpot plates were developed with 3-amino-9-ethylcarbazole (AEC) substrate, and spot-forming units (SFU) were counted using an immunospot analyzer (Cellular Technology Limited). The SFU value was expressed as the mean for triplicate cultures per mouse.

Flow cytometry. Splenocytes collected at 3 weeks postprime and 2 weeks postboost were stimulated for 3 days with 5 μ M HBs S28-39 peptide and 40 U/mL recombinant interleukin 2 (rIL-2) (Peprotech) for assessment of molecular specificity. Briefly, HBs peptide was bound with H2-Ld DimerX reagent (BD) at 37°C overnight and incubated with secondary antibody (A85-1-PE; BD) and isotype control (mouse IgG1 λ [mIgG1 λ]; BD). Two million restimulated splenocytes were stained with DimerX-HB reagent, anti-CD8 Pacific Blue antibody (BD), and viability dye (live/dead near-infrared

fixable dye; Invitrogen). Live cells were acquired using a BD LSRII flow cytometer and analyzed with FACSDiva software (BD).

Cytokine responses. Splenocytes were isolated 2 weeks postboost and tested for rHBsAg-specific cytokine production. Single-cell suspensions (1.5×10^6 /mL) were cultured at 37°C with 5% CO₂ in complete medium and stimulated with 1 µg/mL ConA or 5 µg/mL rHBsAg or left unstimulated. Levels of tumor necrosis factor alpha (TNF- α) and IFN- γ were quantified after 24 and 48 h culture, IL-5 after 48 h, IL-4 at 48 and 72 h, and IL-10 after 72 h, each in triplicate, by ELISA, according to the manufacturer's instructions (BD).

Statistical analyses. Except for the kinetic studies whose results are shown in Fig. 1A, all data are represented by box-and-whisker plots, ranging from the minimum value to the maximum, with the mean displayed as a plus sign. Statistical analyses (one- or two-way analyses of variance [ANOVAs] with Bonferroni posttests) were performed using Prism 5 (GraphPad, La Jolla, CA, USA). Differences were considered statistically significant when P values were ≤ 0.05 , as indicated by asterisks in the figures.

A.4 Results

Using recombinant hepatitis B surface antigen (rHBsAg) as a model immunogen, we compared the VacSIM delivery to that of rHBsAg in alum or Freund's, with or without CpG as a model adjuvant for use with VacSIM and alum.

A.4.1 VacSIM enhances and sustains specific humoral immunity.

To assess humoral immunity, total rHBsAg-specific IgA, IgM, and IgG titers were quantified at various times postimmunization and are presented in Fig. 1A. Mice immunized with VacSIM-delivered rHBsAg had higher specific IgM levels than CFA-

delivered antigen (Fig. 1B, top) ($P < 0.05$) 21 days after a single injection. When mice were given rHBsAg administered with CpG adjuvant and delivered by VacSIM, IgM levels were higher than those in all other groups except those receiving antigen by VacSIM without CpG adjuvant. Mice immunized with rHBsAg in VacSIM developed anti-rHBsAg IgG antibody within 2 weeks postprime. At 21 days postprime (Fig. 1B, bottom), mice receiving rHBsAg in VacSIM had significantly higher levels of rHBsAg-specific IgG antibodies than mice immunized with rHBsAg alone ($P < 0.0001$) or rHBsAg with the standard adjuvant/delivery methods, CpG ($P < 0.0001$), alum ($P < 0.0001$), or Freund's ($P < 0.05$).

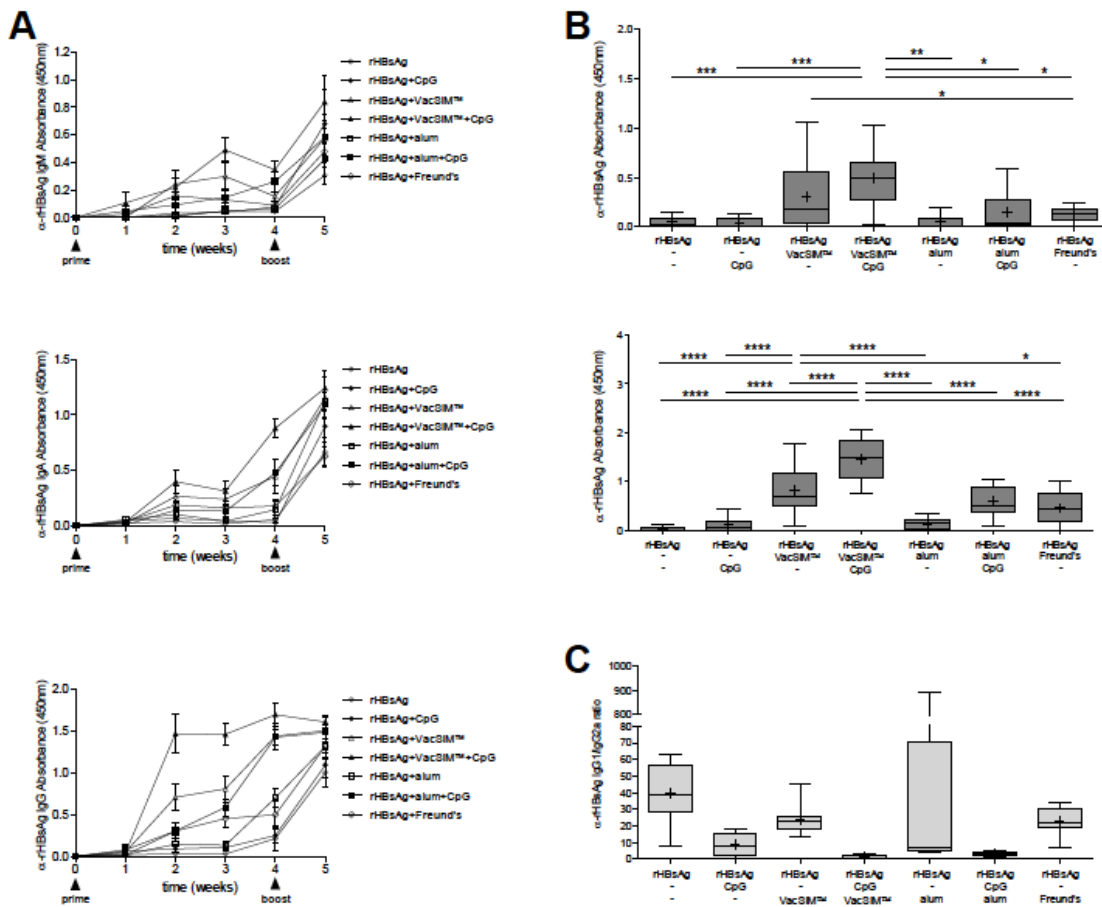


Figure A.1: rHBsAg-specific humoral responses are enhanced and sustained by VacSIM delivery. (A) Kinetic evaluation of rHBsAg-specific IgA, IgM, and IgG antibodies in sera of immunized BALB/c mice (n10, pooled from 2 independent experiments) were determined by ELISA. Immunization times are indicated by arrowheads. (B) rHBsAg-specific IgM (top) and IgG (bottom) levels from sera collected 21 days postimmunization. (C) The IgG1:IgG2a ratio was determined at 35 days postimmunization. Statistical differences (*, $P < 0.05$; **, $P < 0.01$; ***, $P < 0.001$; ****, $P < 0.0001$) were determined by two-way ANOVA with Bonferroni post test.

When rHBsAg was delivered by CpG-adjuvanted VacSIM, the IgG levels postprime were higher than those obtained with CpG-adjuvanted alum delivery of rHBsAg ($P < 0.0001$) and all other groups ($P < 0.0001$). One week postboost (Fig. 1A), levels of antibodies were similar between groups, with the exception that the group immunized with rHBsAg in VacSIM plus CpG had higher specific IgA levels than mice immunized

with rHBsAg in Freund's. Immunization via VacSIM, compared to immunization with CpG, alum, or Freund's adjuvant, generated higher levels of specific antibody responses after only a single injection, which remained elevated postboost.

To determine if immunization using VacSIM would alter rHBsAg-specific IgG isotype responses, we measured rHBsAg-specific IgG1 and IgG2a levels in mice after the prime and boost. As shown in Fig. 1C, the IgG1/IgG2a ratio elicited in vivo shows that VacSIM delivery drove a mixed Th1/Th2 response, which could be skewed further toward the Th1 type by the inclusion of CpG. As expected, mice immunized with Freund's trended toward a Th1 response, and those immunized with alum trended toward a Th2 response, which could be driven toward Th1 by addition of CpG. Overall, these data show that single immunization with VacSIM™ enhances specific antibody responses over that seen with single immunization in the absence of adjuvants or with conventional adjuvants such as alum or Freund's.

To determine if host Th1/Th2 bias would alter the effect of VacSIM, both C57BL/6 and BALB/c mice (Th1 and Th2 biased, respectively) were immunized in a prime-boost manner, 3 weeks apart, and serum was collected 3 weeks postboost. Ten-fold serial dilutions of the serum were analyzed by ELISA, as described in Materials and Methods. The reciprocal value of the last dilution showing a positive value after baseline correction was recorded as the endpoint titer. As shown in Fig. 2, rHBsAg delivered by VacSIM and CpG had high titers of all antibody types tested. Evaluating specific antibodies in serum showed high IgM, IgG, IgG1, and IgG2b endpoint titers in both C57BL/6 and BALB/c mice.

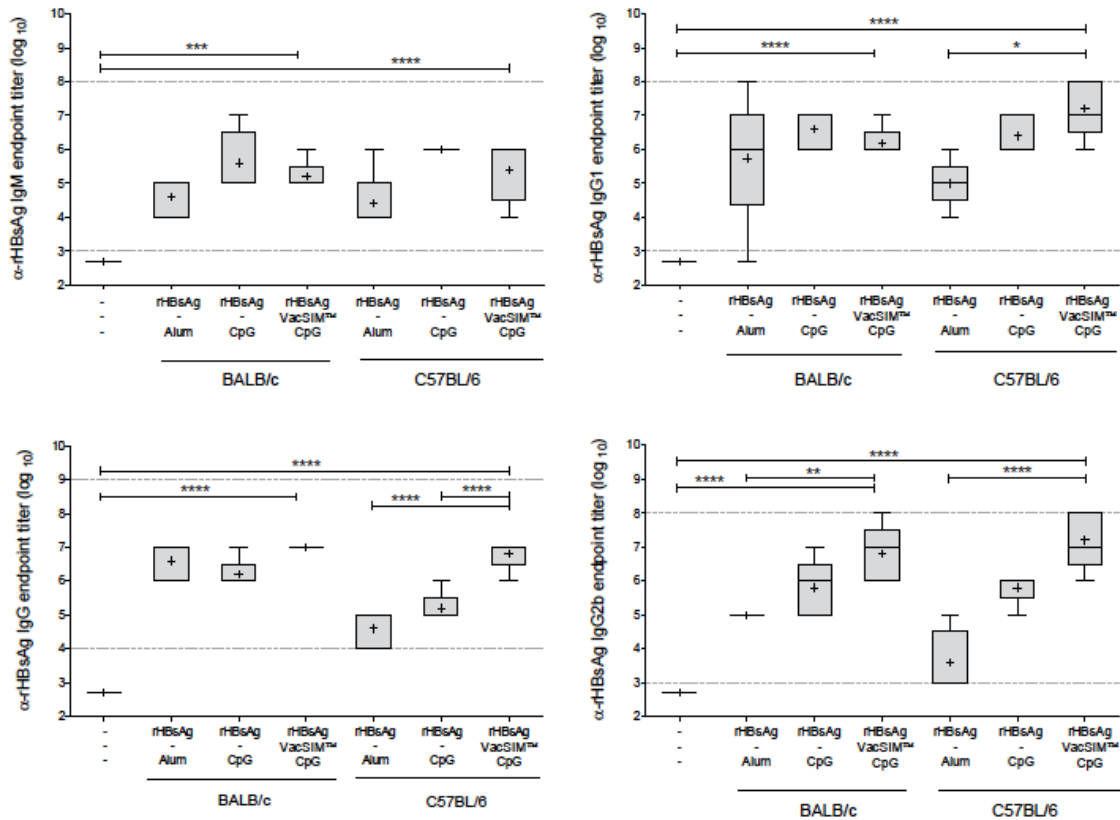


Figure A.2: Immunization with VacSIM increases rHBsAg-specific antibody titers in both Th1- and Th2-biased mouse models. Comparison of rHBsAg-specific antibodies induced in mice immunized 3 weeks apart. The immunized and naïve groups had 5 and 4 mice per group, respectively. There are only 3 IgM values for rHBsAg _ CpG-immunized C57BL/6 mice, as sera were limited. Serum was collected 3 weeks postboost, and rHBsAg-specific IgM, IgG, IgG1 and IgG2b endpoint titers were determined by indirect ELISA. Dashed lines indicate detection limits of the assay. Statistical differences (*, $P < 0.05$; **, $P < 0.01$; ***, $P < 0.001$; ****, $P < 0.0001$) were determined by one-way ANOVA with the Bonferroni posttest.

Together, these results indicate that immunization of mice with rHBsAg using VacSIM substantially improves and sustains humoral immunity while requiring fewer doses and that it can be used in a variety of host environments.

A.4.2 VacSIM induces rHBsAg-specific cellular responses.

rHBsAg-specific cytotoxic-T-lymphocyte (CTL) responses were evaluated after the prime and boost by IFN- γ ELISpot and flow cytometry upon restimulation of

splenocytes with the dominant CD8-restricted peptide epitope (Fig. 3). All delivery methods tested resulted in specific IFN- γ ELISpot responses. Responses in groups administered rHBsAg via VacSIM with and without CpG were not significantly higher than those in other groups. When molecular specificity of the CTL was examined by flow cytometry, all groups showed an increase in percentage of CD8⁺ T cells with T cell

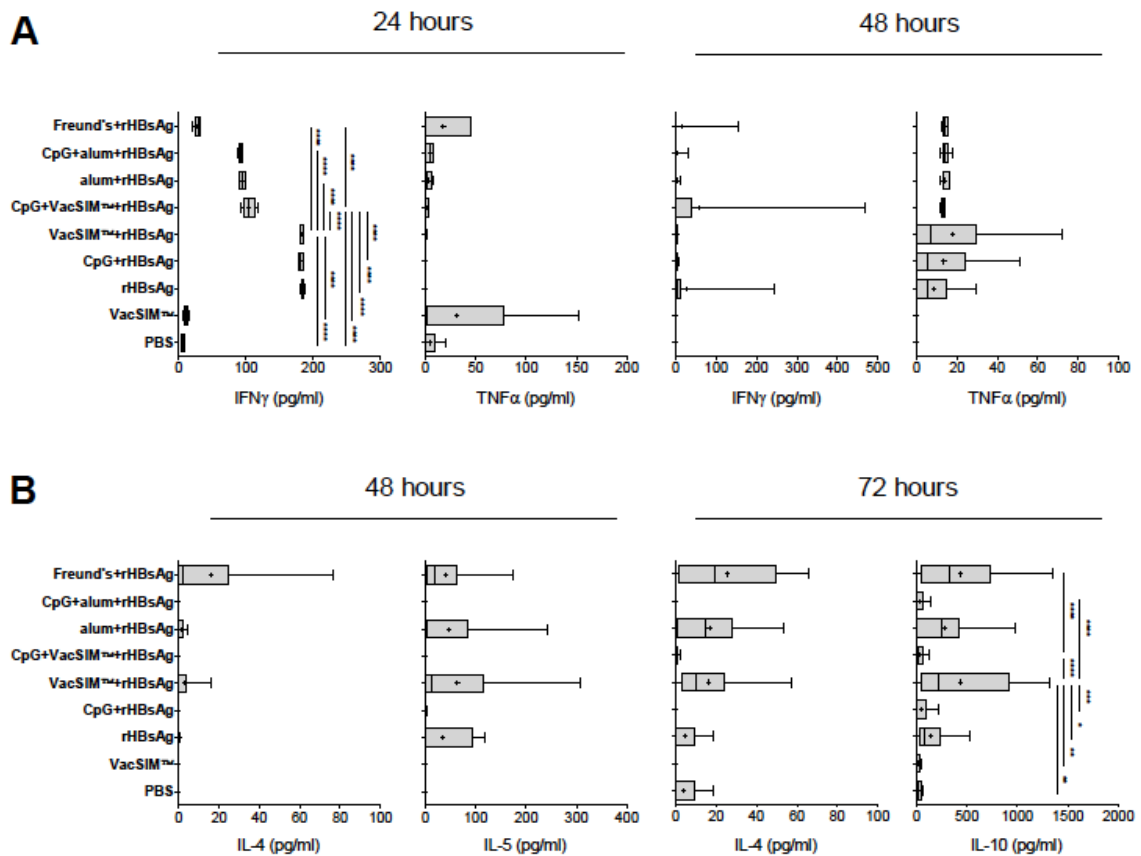


Figure A.3: VacSIM delivery produces a mixed Th1/Th2 type cellular response. Mice were immunized 4 weeks apart, and splenocytes were prepared from mice 2 weeks postboost. For rHBsAg-immunized mice, there are 10 mice per group and data were pooled from 2 independent experiments, whereas control groups (PBS- and VacSIM-immunized) had only 5 mice per group. Splenocytes were restimulated with 5 μ g/mL rHBsAg, and levels of proinflammatory (IFN- γ and TNF- α) (A) and anti-inflammatory (IL-4, IL-5, and IL-10) (B) cytokines were measured at 24, 48 or 72 h by ELISA. Statistical differences (*, $P < 0.05$; **, $P < 0.01$; ***, $P < 0.001$; ****, $P < 0.0001$) were determined by two-way ANOVA with Bonferroni posttest.

receptors specific for the immunodominant epitope. Responses in the group immunized with rHBsAg adjuvanted with alum were significantly higher than the others, but only after the boost.

We analyzed cytokine responses to rHBsAg at 2 weeks postboost. Splenocytes were stimulated with rHBsAg *ex vivo* for 24 to 72 h, and levels of Th1 and Th2 cytokines were determined as an estimate of the Th1/Th2 cytokine balance of the host. Figure 4A shows the levels of the proinflammatory cytokines IFN- γ and TNF- α , collected at 24 and 48 h after *ex vivo* rHBsAg restimulation of splenocytes. As expected, splenocytes from mice administered phosphate-buffered saline (PBS) or VacSIM, without rHBsAg coadministration, had minimal IFN- γ secretion, whereas immunization with rHBsAg alone resulted in a dramatic increase in IFN- γ at 24 h. Similarly, splenocytes from mice immunized via VacSIM™ without CpG made amounts of IFN- γ and TNF- α similar to those in splenocytes from mice immunized with only rHBsAg. Interestingly, splenocytes from mice immunized using Freund's adjuvant delivery of rHBsAg had the lowest levels of IFN- γ expression at 24 h, close to the amounts produced from splenocytes from PBS (sham)- or VacSIM only-immunized mice. Surprisingly, splenocytes from VacSIM with CpG-immunized mice had reduced IFN- γ expression at 24 h, compared to splenocytes from VacSIMrHBsAg, CpG-rHBsAg, and rHBsAg-alone groups. This result suggests that VacSIM does not cause an immediate proinflammatory

response in the host. All remaining comparisons were not significantly different from that obtained with antigen alone.

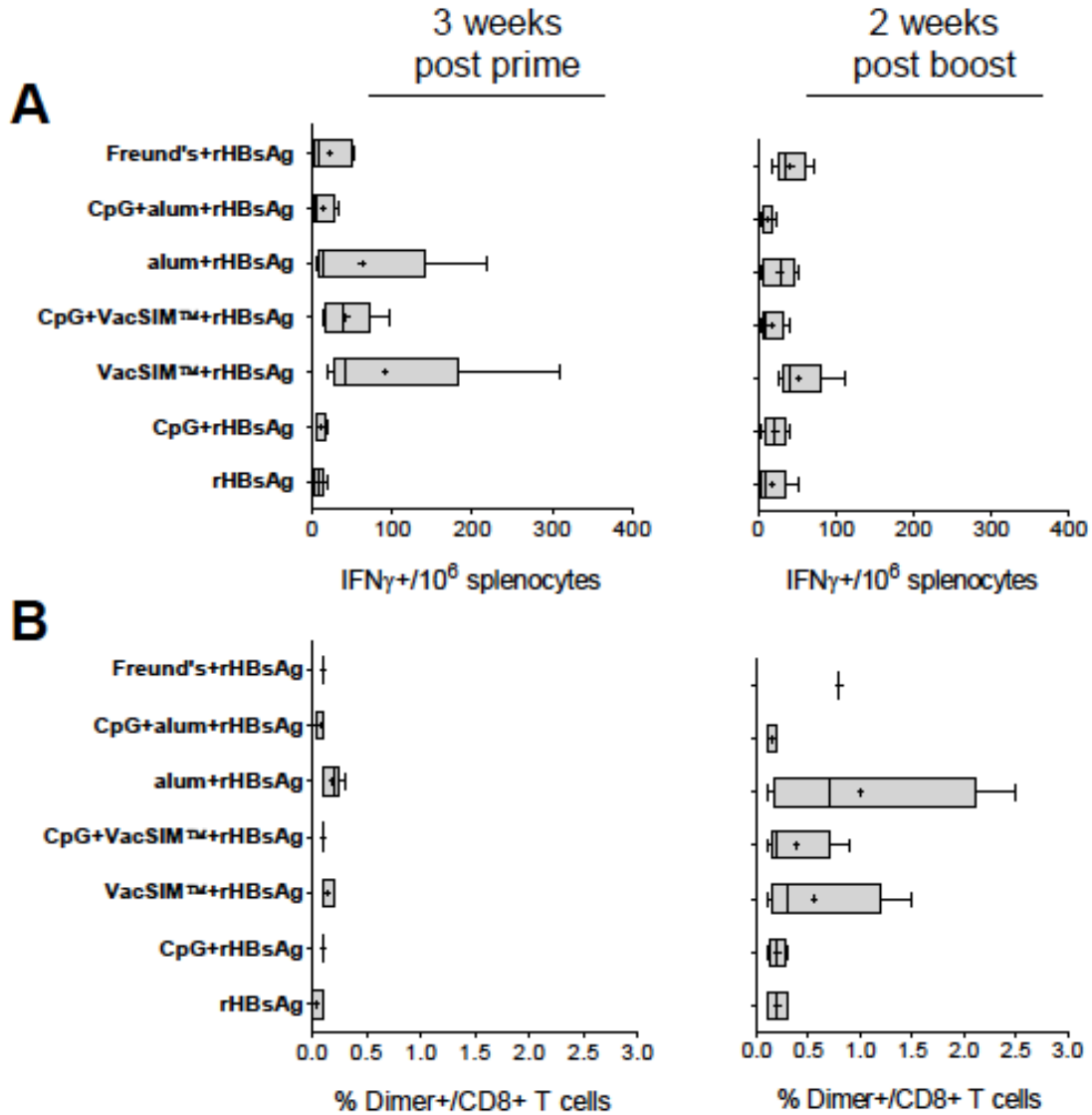


Figure A.4: Cell-mediated immunity is induced following immunization via VacSIM. Mice were immunized 4 weeks apart and rHBsAg-specific CD8_T cells were enumerated by IFN-_{ELISpot} (A) and flow cytometry (B) of splenocytes harvested from mice (n5, except n1 for rHBsAg_Freund's, due to lost samples) at 3 weeks postprime (left) and 2 weeks postboost (right).

We assayed for IL-4, IL-5, and IL-10 at 48 and 72 h after rHBsAg restimulation by ELISA (Fig. 4B). Cells from mice immunized with rHBsAg in VacSIM or Freund's adjuvant showed increased levels of anti-inflammatory cytokines at both time points, with significantly higher levels of IL-10 at 72 h than cells from rHBsAg-only mice. Immunization via alum also induced a not statistically significant increase in production of anti-inflammatory cytokines. Addition of CpG to the immunogens inhibited production of Th2 and anti-inflammatory cytokines.

Overall, these results suggest that VacSIM by itself is not proinflammatory and that it has significant potential to enhance immunogenicity and efficacy of various immunogens.

A.5 Discussion

Design and development of novel, nonreactogenic adjuvants, including synthetic LPS derivatives such as glucopyranosyl lipid A (GLA), are aimed at improving vaccine immunogenicity and efficacy (14). Candidate vaccines have been defined for a number of diseases that are currently unable to drive reasonable levels of efficacy. For example, vaccines that need to drive robust CTL responses to kill intracellular pathogens induce weak Th1-biased responses (39–41). Here, we compared a new delivery method (VacSIM) to alhydrogel and CFA delivery of the rHBsAg immunogen, to determine if VacSIM delivery would drive enhanced hepatitis B-specific humoral and cellular responses. For VacSIM, alum and rHBsAg alone, we also compared immunization plus or minus CpG as an adjuvant. The results demonstrate that delivery of rHBsAg with VacSIM with or without CpGs functioned to increase specific humoral (Fig. 1 and 2) and cellular (Fig. 3 and 4) responses. Alum has been considered a reasonable, nonreactogenic

adjuvant for years, promoting antigen presentation in a particulate form and enhancing internalization by APCs (42). The results presented here show that for the rHBsAg, VacSIM is superior to alum, significantly enhancing the humoral response postprime, by increasing antibody titers at earlier time points and maintaining them in a sustained manner (Fig. 1). The ability of VacSIM to increase early rHBsAg-specific adaptive immune responses may be due to the slow release of antigen from the gel depot, possibly enhancing antigen uptake by APCs compared to that seen when aluminum hydroxide particles or oil-in-water emulsions are used.

A major focus for enhancing immunogenicity is activation of the innate immune system by incorporating agents that ligate one or more innate immune pattern recognition receptors on antigenpresenting cells. Maturation of APCs is essential for priming antigen-specific naive T cells, influencing both the magnitude and the type of the T and B cell responses as well as the induction of memory cells (2). Furthermore, the interaction of T cells and APCs in the presence of immunomodulatory molecules (IL-4, IL-2, IFN- α , IL-12, TGF- β , and/or other cytokines) defines the lineage commitment of CD4⁺ T cells to Th1 and Th2 subtypes.

We examined the T helper biasing of the humoral response by evaluating IgG subtypes produced by the various immunization schemes. Immunization using VacSIM resulted in a mixed Th1/Th2 type antibody response, with more IgG1 than IgG2a. Adding CpG to VacSIM skewed the response toward Th1. We also tested biasing of cellular responses by analyzing antigen-specific restimulation of splenocytes after the boost. In that context, VacSIM induced a mixed Th1/Th2 type response, with high levels of all

cytokines. Interestingly, when CpG was added to rHBsAg and VacSIM, the levels of all cytokines were reduced.

A.6 Conclusions

The VacSIM delivery system tested in this study was superior to conventional delivery/adjuvants in driving early immune responses. Given the flexibility afforded by VacSIM, differential administration of adjuvants and delivery methods can be employed to produce a Th2 or mixed-type response, depending on the outcome desired for each vaccine target. In addition to our studies on VacSIM delivery of recombinant subunit vaccines, we are also evaluating VacSIM as a vaccine delivery method for parasitic and viral vaccines. In this regard, we are evaluating VacSIM™ for delivery of influenza vaccines, including both whole inactivated virus and subunit vaccines. A major goal of ongoing studies is to determine the mechanism(s) whereby VacSIM delivery of vaccines results in enhanced vaccine immunogenicity and efficacy. Lastly, we are working to define optimal parameters for VacSIM delivery, particularly the concentration of the (RADA)₄ peptide, as gel pore size will get smaller/larger with higher/lower (RADA)₄ concentration, respectively, altering the rate of antigen release from the gel depot. Because VacSIM delivery leads to release of antigen from the gel depot over time, we also need to optimize the interval between prime and boost and determine whether VacSIM will function to deliver mucosal vaccines. In summary, VacSIM delivery is a flexible “plug-and-play” platform technology, representing a new approach for delivery of vaccines.

A.7 Acknowledgements

This work was supported by NIH grants AI071883 and AI036657 awarded to D.A.H. and Coordination for the Improvement of Higher Level Education Personnel (CAPES) and The Council of the International Educational Exchange of Scholars (Fulbright, U.S. Department of State), both awarded to R.F.Q.G. We thank Cac Bui and Lindsay Nyhoff for technical assistance and the University of Georgia College of Veterinary Medicine Cytometry Core Facility. Patent applications have been filed on behalf of the authors for the use of the polypeptide matrix as a vaccine delivery system.

A.8 References

1. De Gregorio E, Tritto E, Rappuoli R. 2008. Alum adjuvanticity: unraveling a century old mystery. *Eur J Immunol* 38:2068–2071. <http://dx.doi.org/10.1002/eji.200838648>.
2. Miyaji EN, Carvalho E, Oliveira ML, Raw I, Ho PL. 2011. Trends in adjuvant development for vaccines: DAMPs and PAMPs as potential new adjuvants. *Braz J Med Biol Res* 44:500–513. <http://dx.doi.org/10.1590/S0100-879X2011007500064>.
3. Easterbrook JD, Schwartzman LM, Gao J, Kash JC, Morens DM, Couzens L, Wan H, Eichelberger MC, Taubenberger JK. 2012. Protection against a lethal H5N1 influenza challenge by intranasal immunization with virus-like particles containing 2009 pandemic H1N1 neuraminidase in mice. *Virology* 432:39–44. <http://dx.doi.org/10.1016/j.virol.2012.06.003>.
4. Deng MP, Hu ZH, Wang HL, Deng F. 2012. Developments of subunit and VLP vaccines against influenza A virus. *Virol Sin* 27:145–153. <http://dx.doi.org/10.1007/s12250-012-3241-1>.
5. Hossain MJ, Bourgeois M, Quan FS, Lipatov AS, Song JM, Chen LM, Compans RW, York I, Kang SM, Donis RO. 2011. Virus-like particle vaccine containing hemagglutinin confers protection against 2009 H1N1 pandemic influenza. *Clin Vaccine Immunol* 18:2010–2017. <http://dx.doi.org/10.1128/CVI.05206-11>.
6. Mooney AJ, Li Z, Gabbard JD, He B, Tompkins SM. 2013. Recombinant parainfluenza virus 5 vaccine encoding the influenza virus hemagglutinin protects against H5N1 highly pathogenic avian influenza virus infection following intranasal or intramuscular vaccination of BALB/c mice. *J Virol* 87:363–371. <http://dx.doi.org/10.1128/JVI.02330-12>.

7. Cornelissen LA, de Leeuw OS, Tacken MG, Klos HC, de Vries RP, de Boer-Luijze EA, van Zoelen-Bos DJ, Rigter A, Rottier PJ, Moormann RJ, de Haan CA. 2012. Protective efficacy of Newcastle disease virus expressing soluble trimeric hemagglutinin against highly pathogenic H5N1 influenza in chickens and mice. *PLoS One* 7:e44447. <http://dx.doi.org/10.1371/journal.pone.0044447>.
8. Hashem A, Jaentschke B, Gravel C, Tocchi M, Doyle T, Rosu-Myles M, He R, Li X. 2012. Subcutaneous immunization with recombinant adenovirus expressing influenza A nucleoprotein protects mice against lethal viral challenge. *Hum Vaccin Immunother* 8:425–430. <http://dx.doi.org/10.4161/hv.19109>.
9. Rosenkrands I, Vingsbo-Lundberg C, Bundgaard TJ, Lindenstrom T, Enouf V, van der Werf S, Andersen P, Agger EM. 2011. Enhanced humoral and cell-mediated immune responses after immunization with trivalent influenza vaccine adjuvanted with cationic liposomes. *Vaccine* 29:6283–6291. <http://dx.doi.org/10.1016/j.vaccine.2011.06.040>.
10. Even-Or O, Joseph A, Itskovitz-Cooper N, Samira S, Rochlin E, Eliyahu H, Goldwasser I, Balasingam S, Mann AJ, Lambkin-Williams R, Kedar E, Barenholz Y. 2011. A new intranasal influenza vaccine based on a novel polycationic lipid-ceramide carbamoyl-spermine (CCS). II. Studies in mice and ferrets and mechanism of adjuvanticity. *Vaccine* 29:2474–2486. <http://dx.doi.org/10.1016/j.vaccine.2011.01.009>.
11. Dong L, Liu F, Fairman J, Hong DK, Lewis DB, Monath T, Warner JF, Belser JA, Patel J, Hancock K, Katz JM, Lu X. 2012. Cationic liposome-DNA complexes (CLDC) adjuvant enhances the immunogenicity and crossprotective efficacy of a pre pandemic influenza A H5N1 vaccine in mice. *Vaccine* 30:254–264. <http://dx.doi.org/10.1016/j.vaccine.2011.10.103>.
12. Principi N, Esposito S. 2012. Adjuvanted influenza vaccines. *Hum Vaccin Immunother* 8:59–66. <http://dx.doi.org/10.4161/hv.8.1.18011>.
13. Zuccotti GV, Pariani E, Scaramuzza A, Santoro L, Giani E, Macedoni M, Gazzarri A, Anselmi G, Amendola A, Zanetti A. 2011. Long-lasting immunogenicity and safety of a 2009 pandemic influenza A(H1N1) MF59-adjuvanted vaccine when co-administered with a 2009-2010 seasonal influenza vaccine in young patients with type 1 diabetes mellitus. *Diabet Med* 28:1530–1536. <http://dx.doi.org/10.1111/j.1464-5491.2011.03449.x>.
14. Behzad H, Huckriede AL, Haynes L, Gentleman B, Coyle K, Wilschut JC, Kollmann TR, Reed SG, McElhaney JE. 2012. GLA-SE, a synthetic toll-like receptor 4 agonist, enhances T-cell responses to influenza vaccine in older adults. *J Infect Dis* 205:466–473. <http://dx.doi.org/10.1093/infdis/jir769>.
15. Clegg CH, Roque R, Van Hoeven N, Perrone L, Baldwin SL, Rininger JA, Bowen RA, Reed SG. 2012. Adjuvant solution for pandemic influenza vaccine

production. *Proc Natl Acad Sci U S A* 109:17585–17590.
<http://dx.doi.org/10.1073/pnas.1207308109>.

16. Coler RN, Baldwin SL, Shaverdian N, Bertholet S, Reed SJ, Raman VS, Lu X, DeVos J, Hancock K, Katz JM, Vedvick TS, Duthie MS, Clegg CH, Van Hoeven N, Reed SG. 2010. A synthetic adjuvant to enhance and expand immune responses to influenza vaccines. *PLoS One* 5:e13677.
<http://dx.doi.org/10.1371/journal.pone.0013677>.
17. Manon MJ, Cox PSC. 9 August 2012. Safety and immunogenicity of PanBlok influenza vaccine in healthy adults. *ClinicalTrials.gov*.
<http://clinicaltrials.gov/ct2/show/NCT01147068>. Accessed 29 October 2012.
18. Kisiday J, Jin M, Kurz B, Hung H, Semino C, Zhang S, Grodzinsky AJ. 2002. Self-assembling peptide hydrogel fosters chondrocyte extracellular matrix production and cell division: implications for cartilage tissue repair. *Proc Natl Acad Sci U S A* 99:9996-10001. <http://dx.doi.org/10.1073/pnas.142309999>.
19. Iwai Y, Matsuda Y, Nakatsuka M, Mikami Y, Kumabe S. 2012. A preliminary study of the dental implant therapy—initial osteogenesis of human mesenchymal stem (HMS0014) cells on titanium discs with different surface modifications. *Okajimas Folia Anat Jpn* 88:133–140. <http://dx.doi.org/10.2535/ofaj.88.133>.
20. Horii A, Wang X, Gelain F, Zhang S. 2007. Biological designer self assembling peptide nanofiber scaffolds significantly enhance osteoblast proliferation, differentiation and 3-D migration. *PLoS One* 2:e190.
<http://dx.doi.org/10.1371/journal.pone.0000190>.
21. Henriksson H, Hagman M, Horn M, Lindahl A, Brisby H. 2011. Investigation of different cell types and gel carriers for cell-based intervertebral disc therapy, in vitro and in vivo studies. *J Tissue Eng Regen Med* 6:738–747.
<http://dx.doi.org/10.1002/term.480>.
22. Zhang S. 2003. Fabrication of novel biomaterials through molecular self-assembly. *Nat Biotechnol* 21:1171–1178. <http://dx.doi.org/10.1038/nbt874>.
23. Kondo Y, Nagasaka T, Kobayashi S, Kobayashi N, Fujiwara T. 2014. Management of peritoneal effusion by sealing with a self-assembling nanofiber polypeptide following pelvic surgery. *Hepatogastroenterology* 61:349–353.
24. Rosa V, Zhang Z, Grande RH, Nor JE. 2013. Dental pulp tissue engineering in full-length human root canals. *J Dent Res* 92:970–975.
<http://dx.doi.org/10.1177/0022034513505772>.
25. Zhang S, Ellis-Behnke R, Zhao X, Spirio L. 2010. PuraMatrix: self-assembling peptide nanofiber scaffolds, p 217–240. In Ma PX, Elisseeff J (ed), *Scaffolding in tissue engineering*. CRC Press, Boca Raton, FL.

26. Zhang S, Holmes TC, DiPersio CM, Hynes RO, Su X, Rich A. 1995. Self-complementary oligopeptide matrices support mammalian cell attachment. *Biomaterials* 16:1385–1393. [http://dx.doi.org/10.1016/0142-9612\(95\)96874-Y](http://dx.doi.org/10.1016/0142-9612(95)96874-Y).
27. Nishimura A, Hayakawa T, Yamamoto Y, Hamori M, Tabata K, Seto K, Shibata N. 2012. Controlled release of insulin from self-assembling nanofibers hydrogel, PuraMatrix: application for the subcutaneous injection in rats. *Eur J Pharm Sci* 45:1–7. <http://dx.doi.org/10.1016/j.ejps.2011.10.013>.
28. Sacks DL. 2014. Vaccines against tropical parasitic diseases: a persisting answer to a persisting problem. *Nat Immunol* 15:403–405. <http://dx.doi.org/10.1038/ni.2853>.
29. Gray D, Skarvall H. 1988. B-cell memory is short-lived in the absence of antigen. *Nature* 336:70–73. <http://dx.doi.org/10.1038/336070a0>.
30. Ingavle GC, Gehrke SH, Detamore MS. 2014. The bioactivity of agarose-PEGDA interpenetrating network hydrogels with covalently immobilized RGD peptides and physically entrapped aggrecan. *Biomaterials* 35:3558–3570. <http://dx.doi.org/10.1016/j.biomaterials.2014.01.002>
31. Browning MB, Cereceres SN, Luong PT, Cosgriff-Hernandez EM. 2014. Determination of the in vivo degradation mechanism of PEGDA hydrogels. *J Biomed Mater Res A* 102:4244–4251. <http://dx.doi.org/10.1002/jbm.a.35096>.
32. Jose S, Hughbanks ML, Binder BY, Ingavle GC, Leach JK. 2014. Enhanced trophic factor secretion by mesenchymal stem/stromal cells with Glycine-Histidine Lysine (GHK)-modified alginate hydrogels. *Acta Biomater* 10:1955–1964. <http://dx.doi.org/10.1016/j.actbio.2014.01.020>.
33. Xiong Y, Yan K, Bentley WE, Deng H, Du Y, Payne GF, Shi XW. 2014. Compartmentalized multilayer hydrogel formation using a stimulus responsive self-assembling polysaccharide. *ACS Appl Mater Interfaces* 6:2948–2957. <http://dx.doi.org/10.1021/am405544r>.
34. Jorquera PA, Choi Y, Oakley KE, Powell TJ, Boyd JG, Palath N, Haynes LM, Anderson LJ, Tripp RA. 2013. Nanoparticle vaccines encompassing the respiratory syncytial virus (RSV) G protein CX3C chemokine motif induce robust immunity protecting from challenge and disease. *PLoS One* 8:e74905. <http://dx.doi.org/10.1371/journal.pone.0074905>.
35. Lee JW, Choi SO, Felner EI, Prausnitz MR. 2011. Dissolving microneedle patch for transdermal delivery of human growth hormone. *Small* 7:531–539. <http://dx.doi.org/10.1002/sml.201001091>.
36. Rudra JS, Tian YF, Jung JP, Collier JH. 2010. A self-assembling peptide acting as an immune adjuvant. *Proc Natl Acad Sci U S A* 107:622–627. <http://dx.doi.org/10.1073/pnas.0912124107>.

37. Chesson CB, Huelsmann EJ, Lacey AT, Kohlhapp FJ, Webb MF, Nabatiyan A, Zloza A, Rudra JS. 2014. Antigenic peptide nanofibers elicit adjuvant-free CD8 T cell responses. *Vaccine* 32:1174–1180. <http://dx.doi.org/10.1016/j.vaccine.2013.11.047>.
38. Rudra JS, Mishra S, Chong AS, Mitchell RA, Nardin EH, Nussenzweig V, Collier JH. 2012. Self-assembled peptide nanofibers raising durable antibody responses against a malaria epitope. *Biomaterials* 33:6476–6484. <http://dx.doi.org/10.1016/j.biomaterials.2012.05.041>.
39. Brandtzaeg P. 2007. Induction of secretory immunity and memory at mucosal surfaces. *Vaccine* 25:5467–5484. <http://dx.doi.org/10.1016/j.vaccine.2006.12.001>.
40. Roy MJ, Wu MS, Barr LJ, Fuller JT, Tussey LG, Speller S, Culp J, Burkholder JK, Swain WF, Dixon RM, Widera G, Vessey R, King A, Ogg G, Gallimore A, Haynes JR, Heydenburg Fuller D. 2000. Induction of antigen-specific CD8_T cells, T helper cells, and protective levels of antibody in humans by particle-mediated administration of a hepatitis B virus DNA vaccine. *Vaccine* 19:764–778. [http://dx.doi.org/10.1016/S0264-410X\(00\)00302-9](http://dx.doi.org/10.1016/S0264-410X(00)00302-9).
41. Wang R, Doolan DL, Le TP, Hedstrom RC, Coonan KM, Charoenvit Y, Jones TR, Hobart P, Margalith M, Ng J, Weiss WR, Sedegah M, de Taisne C, Norman JA, Hoffman SL. 1998. Induction of antigen-specific cytotoxic T lymphocytes in humans by a malaria DNA vaccine. *Science* 282:476–480. <http://dx.doi.org/10.1126/science.282.5388.476>.
42. Morefield GL, Sokolovska A, Jiang D, HogenEsch H, Robinson JP, Hem SL. 2005. Role of aluminum-containing adjuvants in antigen internalization by dendritic cells in vitro. *Vaccine* 23:1588–1595. <http://dx.doi.org/10.1016/j.vaccine.2004.07.050>.

APPENDIX B

CHAPTER 2 SUPPLEMENTARY DATA

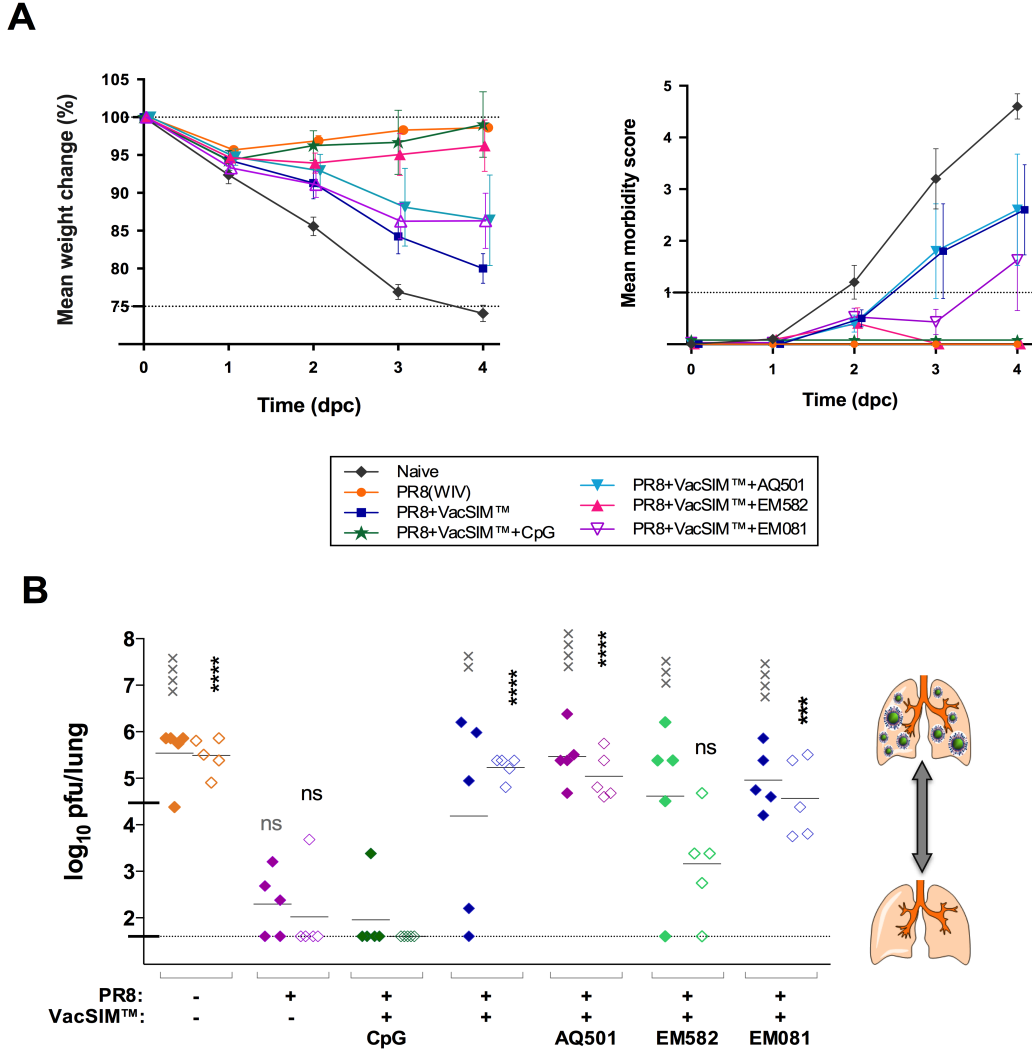


Figure B.1: Vaccine-induced morbidity and viral clearance from the lungs following influenza challenge. Mice were challenged at 4wpv with 1,000_{LD50} PR8 and monitored daily. Presented here are the mean changes in weight and symptom severity (morbidity scores) for each vaccine group post-challenge (A). A cohort of mice was sacrificed and lungs harvested to evaluate viral clearance, via plaque assay, at both 2 and 4dpc (B). Dashed lines indicate detection thresholds of the experiment. Results were replicated in a minimum of 2 separate experiments (n=5). Statistical significance was determined for the log-transformed values at 2 or 4dpc, compared to the PR8+VacSIM™+CpG vaccinated group at the same time point, using 2-way ANOVA and Dunnett's multiple comparisons test. Were (**p<0.01, ***p<0.001, ****p<0.0001) indicates statistical significance at 2dpc and (×p<0.01, ××p<0.001, ×××p<0.0001) indicates statistical significance at 4dpc (B).

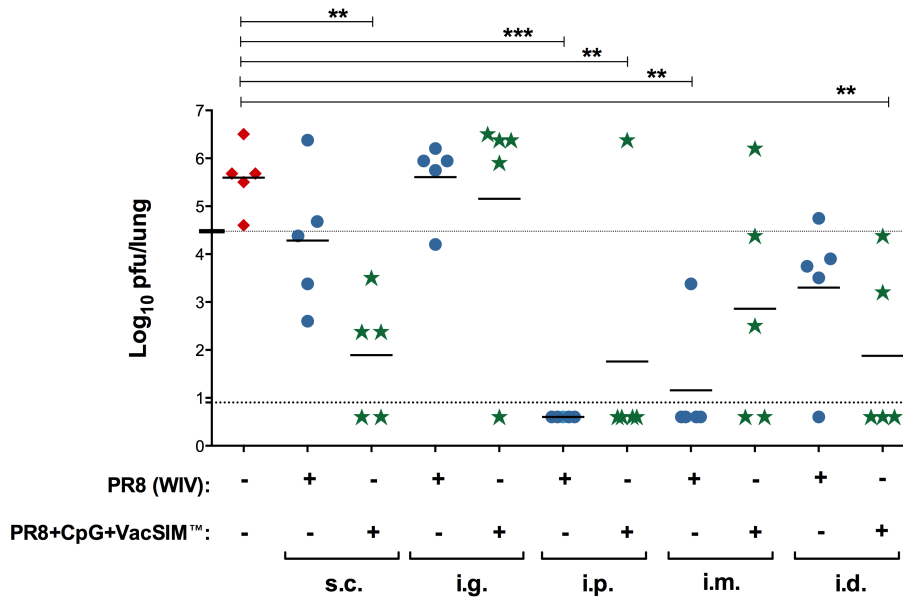
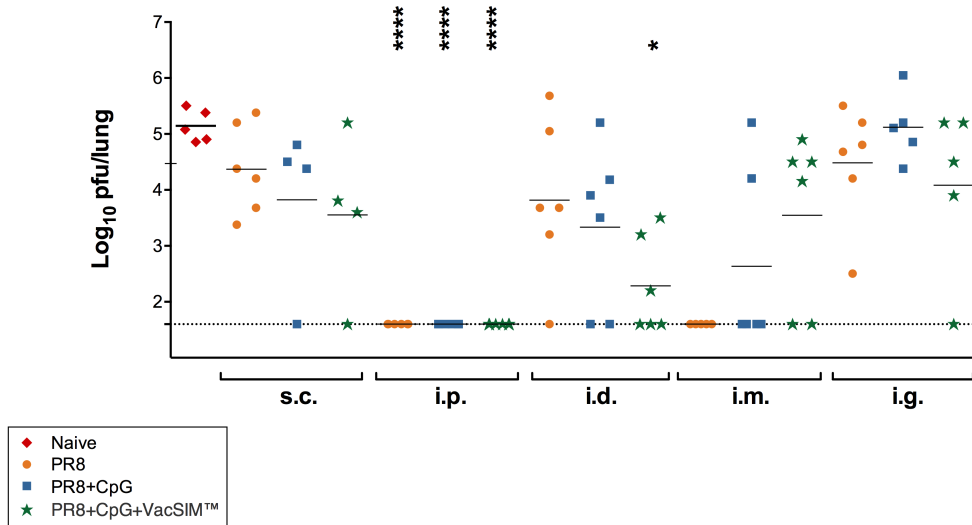
A**B**

Figure B.2: Route-dependent α -PR8 IgG sera levels and viral clearance from the lungs post challenge. All mice were bled prior to vaccination (baseline) with either PR8 in saline or PR8+CpG in VacSIM™ and again 4wpv, when α -PR8 IgG levels in the sera were detected by indirect ELISA (A). Viral clearance from the lungs was assessed 2 days post challenging with 1,000LD₅₀ live PR8, via plaque assay (B). Dotted lines indicate assay detection limits. Statistical significance between vaccine groups (**p<0.01, via a connecting bar) and statistical significance (×p<0.05, ××p<0.01, ×××p<0.001, ××××p<0.0001) compared to naive was determined by one-way ANOVA and Tukey's multiple comparisons test (A). Statistical significance (*p<0.05, **p<0.01, ***p<0.001, ****p<0.0001) of vaccine groups compared to naive was determined by one-way ANOVA and Dunnett's multiple comparisons test, on log-transformed data (B).

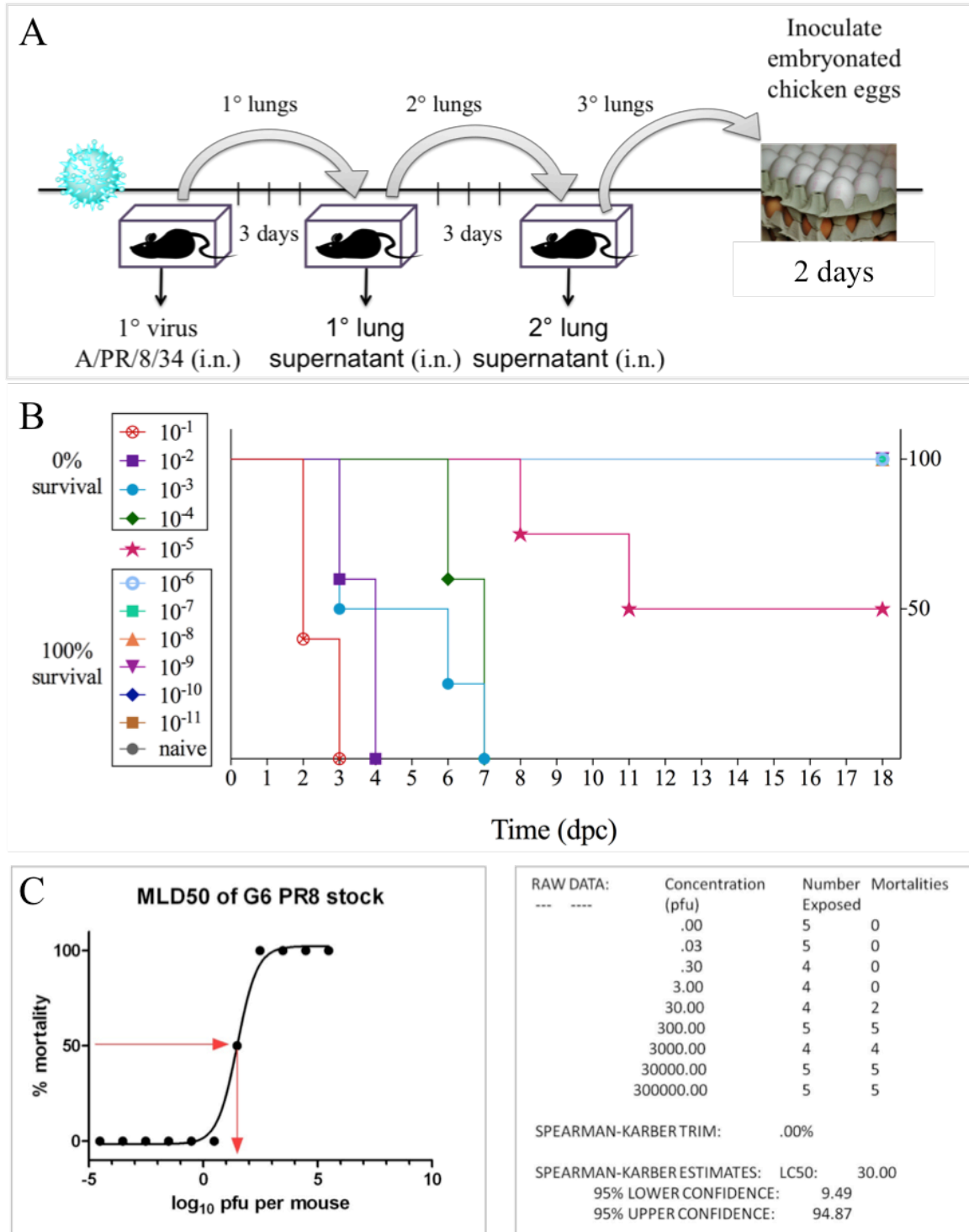


Figure B.3: Mouse lethal $\frac{1}{2}$ dose (MLD₅₀) determination for influenza A/Puerto Rico/08/34 challenge stock. Mouse-adapted influenza (PR8) challenge stock (coded “G6”) was generated through serial passage in C57Bl/6 mice prior to expansion in embryonated chicken eggs (A). The dose of virus at which 50% of the mice with succumb (MLD₅₀) was determined for C57BL/6 mice (B-C). A spearman-karber analysis was done on the MLD₅₀ results (C).

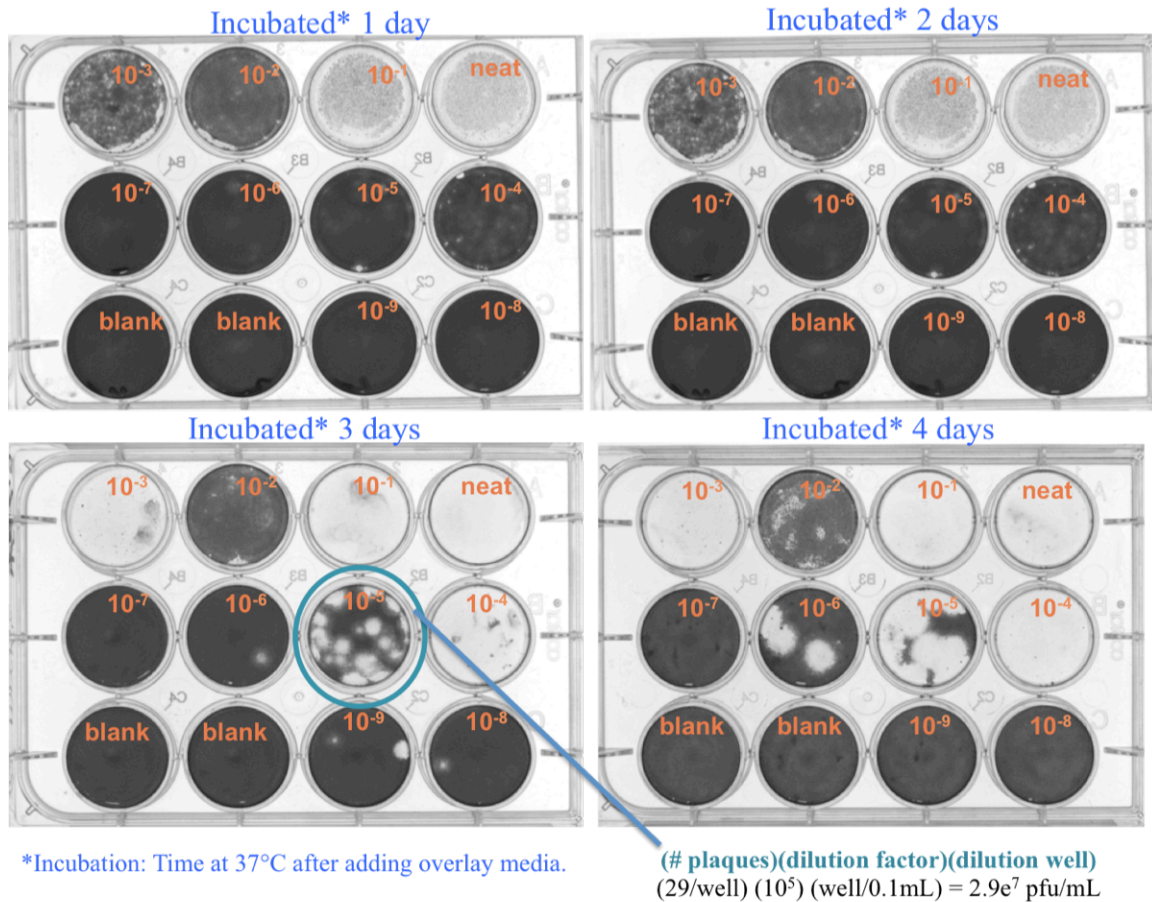
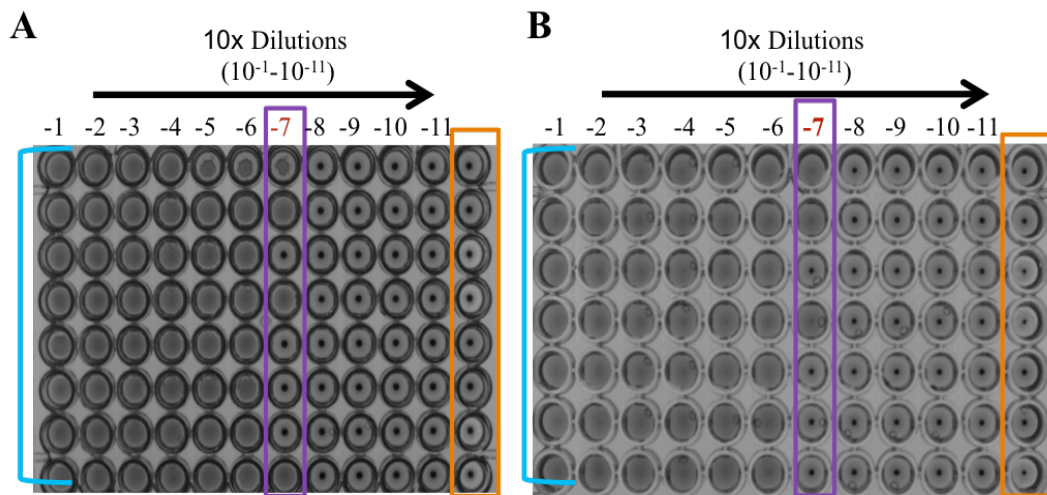


Figure B.4: Plaque assays to determine influenza PR8 challenge stock titer. Plaque assays are used to measure the quantity of live virus in a given sample. Virus titers are reported as plaque forming units or “pfu” (Table A.1).



G6 Challenge stock (replicates) = MDCKs in media + 10uL diluted G6 + Turkey RBCs

Control = MDCKs in media + 10uL PBS + Turkey RBCs

G6 Challenge stock = 10^7 TCID₅₀/0.01mL or 10^9 TCID₅₀/mL

Figure B.5: Tissue culture $\frac{1}{2}$ lethal dose (TCID₅₀) of influenza challenge stock. The TCID₅₀ was determined for influenza (PR8) challenge stock (G6) according with protocol in appendix D, utilizing epithelial Madin-Darby Canine Kidney (MDCK) cells (passage #30, viability 95%), along with freshly collected turkey red blood cells (RBCs) diluted prior to use.

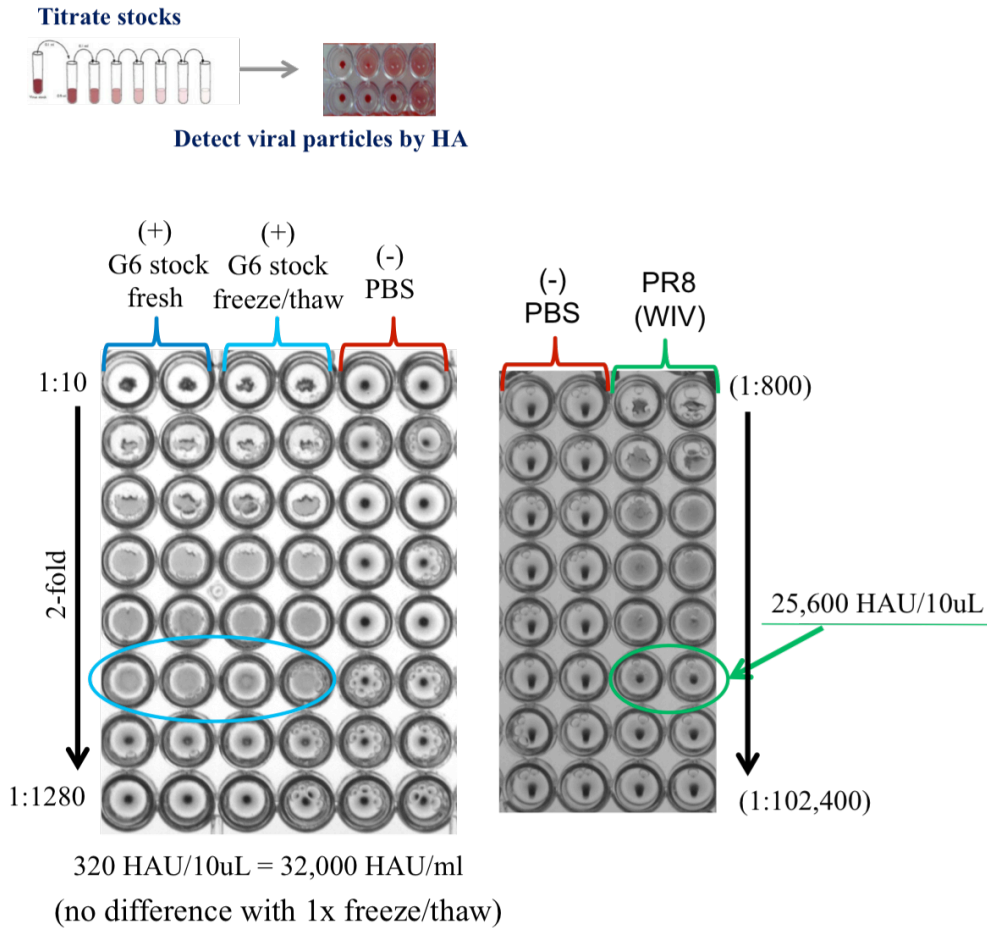


Figure B.6: Hemmagglutination unit (HAU) of influenza (PR8) challenge and vaccine stocks. The HAU titers were determined for the live and inactivated PR8 stocks according to standard methods (appendix D), utilizing freshly collected Turkey red blood cells (RBCs).

Table B.1: Lethality of influenza (A/Puerto Rico/08/34) challenge stock. This viral challenge stock was generated in February of 2012 and immediately titrated for lethality (coded “G6”).

Assay / Method	Acronym	<i>in vitro</i> / <i>in vivo</i>	Measures	Virus Stock
Plaque assay	na	<i>in vitro</i>	Live virus particles	3.0×10^7 pfu/mL
Tissue culture $\frac{1}{2}$ lethal dose	TCID ₅₀	<i>in vitro</i>	Live/dead virus particles	10^9 TCID ₅₀ /mL
Mouse $\frac{1}{2}$ lethal dose	MLD ₅₀	<i>in vivo</i>	Live virus particles	10^6 MLD ₅₀ /mL
Hemagglutination assay	HA	<i>in vitro</i>	Live/dead virus particles	HAU/mL

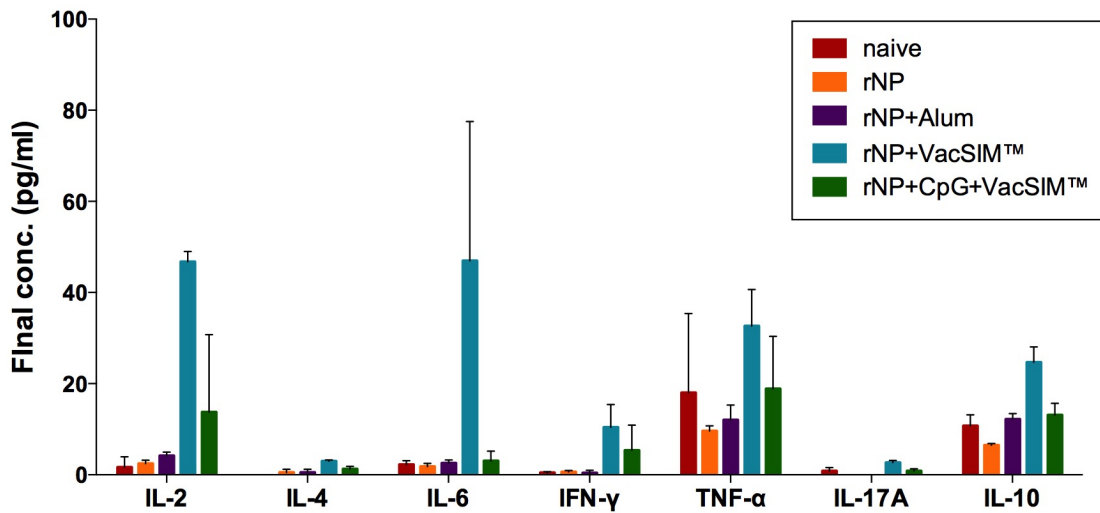


Figure B.7: Cytokine analysis on immunized mouse spleens. Spleens were harvested from C57BL/6 mice (28 dpv), processed and splenocytes re-stimulated (48 hrs) with 1ug/mL of rNP protein. Splenocytes were also re-stimulated with media or ConA as negative and positive re-stimulation controls (not plotted).

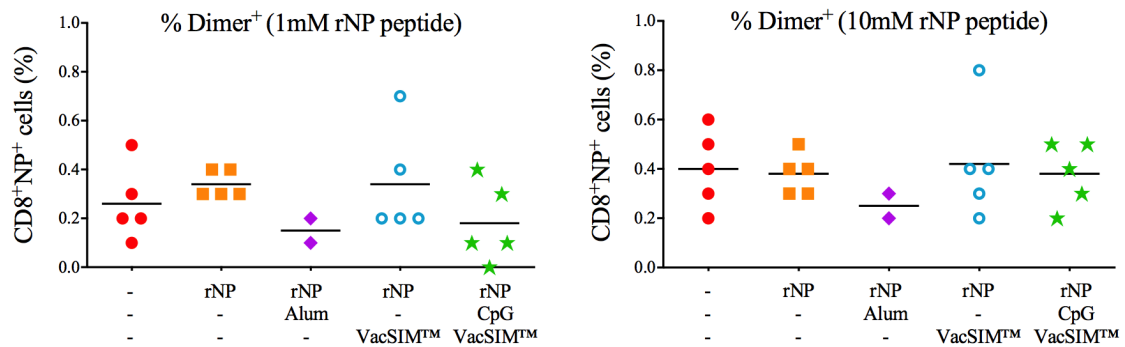


Figure B.8: Vaccine-specific CD8⁺ T cells in the spleens of immunized mice. Spleens were harvested from naïve and immunized mice (16-week old, C57BL/6), which had been vaccinated (s.c.) 6-weeks earlier with an internal recombinant influenza protein (rNP) ± Alum or CpG, delivered in saline or in VacSIM™. The frequency of CD8⁺NP⁺-dimer⁺ cells was determined via flow cytometry using a fluorescent antibody dimer kit (BD) previously conjugated with rNP (ASNENMETM). No significance difference between vaccination groups via one-way ANOVA and Bonferroni's multiple comparisons test.

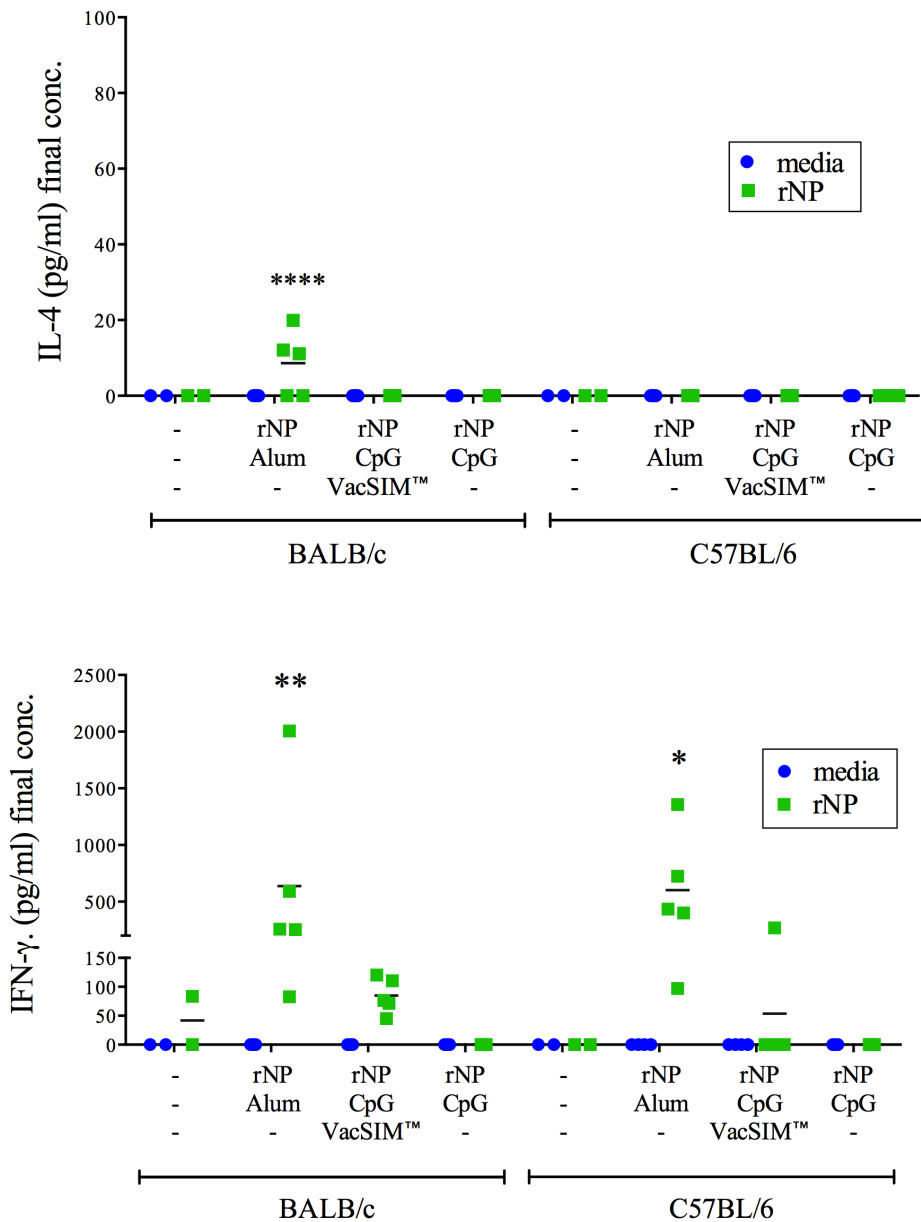


Figure B.9: IL-4 and IFN- γ levels in spleens of Th1- and Th2-biased, immunized mice. Cytokine levels were determined via ELISA using supernatants collected from splenocytes re-stimulated at 37C for 48-hours with r-NP (protein). Statistical significance over re-stimulation with media was determined by two-way ANOVA and Bonferroni's multiple comparisons test (n=5, only 2/5 samples run from unvaccinated).

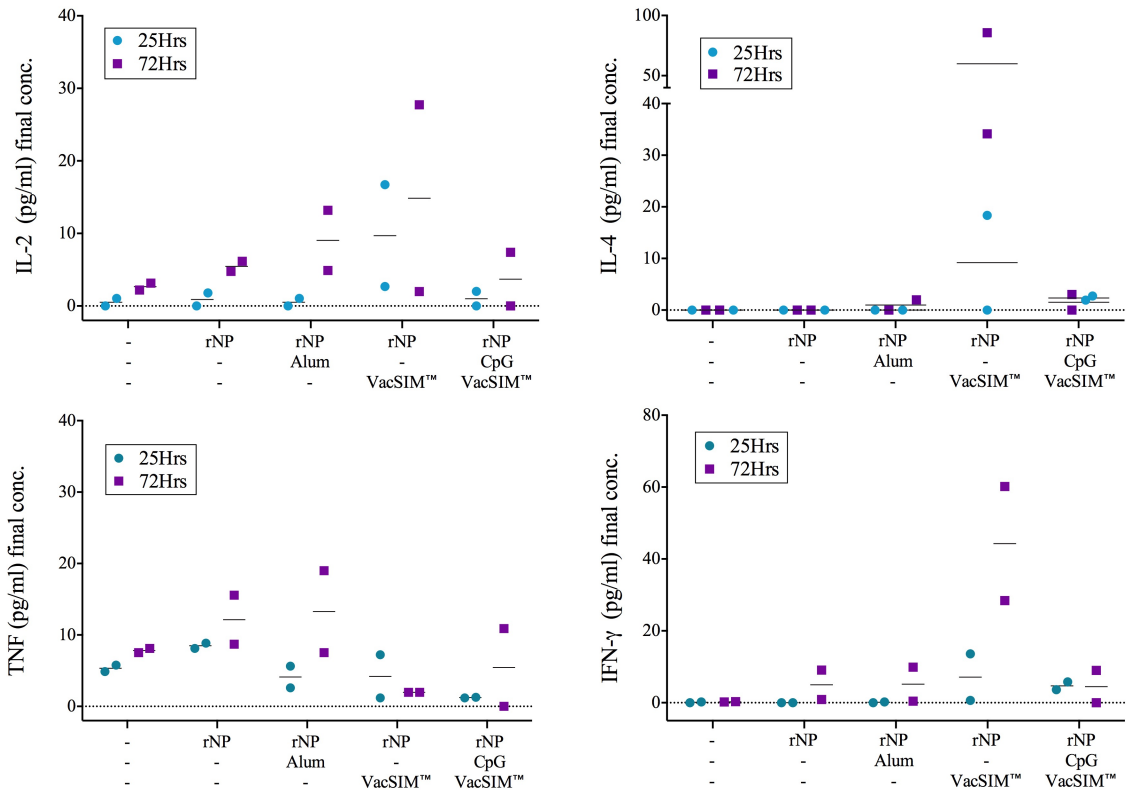


Figure B.10: Cytometric bead array (CBA) analysis on C57BL/6 spleens, naive or 28 days post vaccination (dpv). For immunized mice, spleens were harvested 28 days after a single vaccination (s.c.) with recombinant influenza protein (rNP) ± Alum, CpG or VacSIM™. Processed splenocytes were re-stimulated with rNP (protein) for either 25 or 72-hours, at which point supernatants were collected and 2 out of 5 mice samples were analyzed by flow, using the Th1/Th2/Th17 CBA kit from BD to evaluate cytokine levels. Performed but not included in this figure are the negative (media) and positive (ConA) re-stimulation controls.

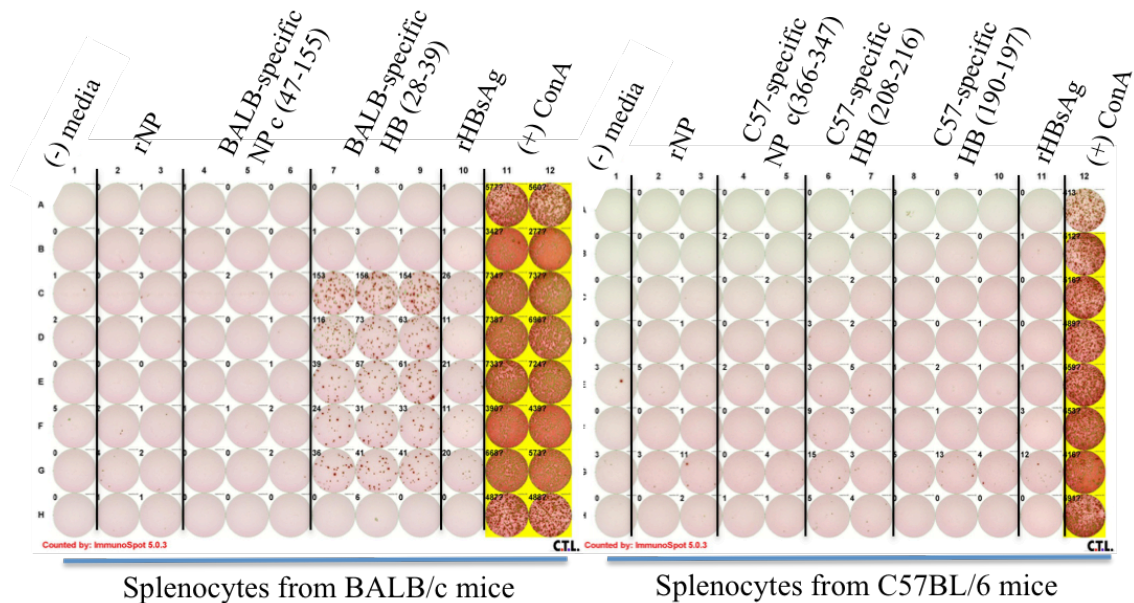


Figure B.11: Representative image of IFN- γ ELISpot plates. Splensens harvested from Th1- and Th2-biased mouse models 3-weeks post boost with a protein subunit antigen (rNP or rHBsAg) \pm Alum, CpG or VacSIMTM. Processed splenocytes were re-stimulated with rNP/rHB protein or peptides for 20-hours at 37°C (Figures A.12-A.13).

Table B.2: Summary of strain/virus-specific peptides. Peptides used, along with recombinant protein for 20-hour re-stimulation of splenocytes for to IFN- γ specific ELISpots (Figures A.11-A.13).

	Hepatitis B	Influenza
BALB/c	H2L ^d /S ₂₃₋₃₉ (surface)	H2K ^d /NP ₁₄₇₋₁₅₅ (internal)
C57BL/6	H2K ^b /S ₁₉₀₋₁₉₇ (surface) H2K ^b /S ₂₀₈₋₂₁₆ (surface)	H2D ^b /NP ₃₆₆₋₃₇₄ (internal)

BALB/c (Th2-biased)

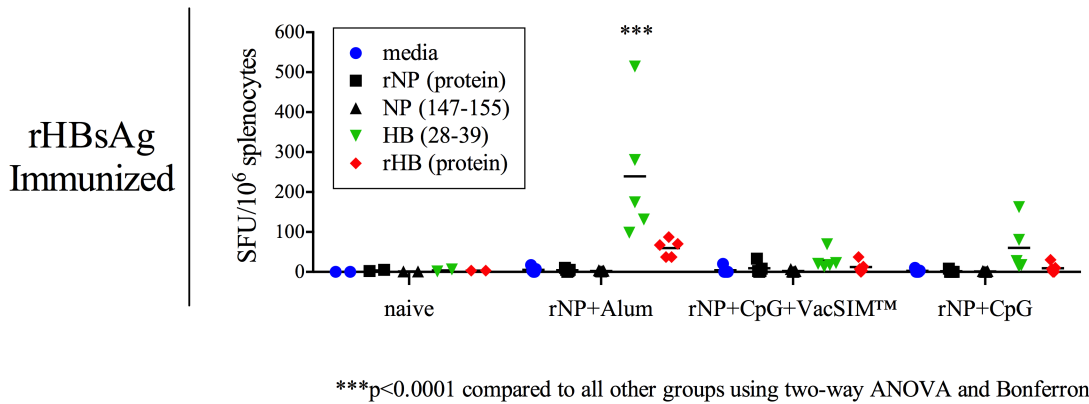
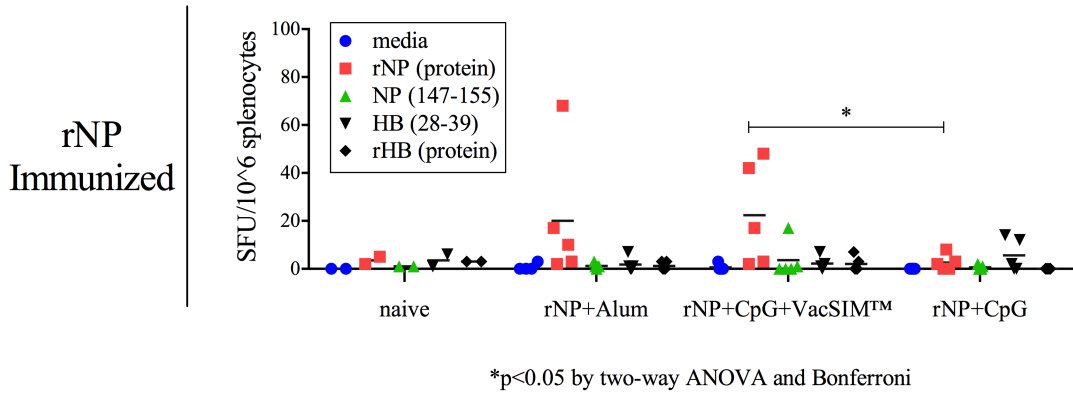


Figure B.12: IFN- γ specific ELISpot results from spleens of Th2-biased immunized mice. BALB/c mice were vaccinated (s.c.) 2x, 3-weeks apart with a 2 alternative protein subunit antigens (rNP or rHBsAg) \pm Alum, CpG and VacSIM™. Six weeks after their 1st vaccination, spleens were harvested and processed. Splenocytes were re-stimulated with either rNP/rHBsAg protein or peptides for 20-hours at 37° (Protocols in Appendix D). Splenocytes were also re-stimulated with ConA as a positive re-stimulation control (not plotted). Table A.2 contains specific peptide information. Statistics were calculated using two-way ANOVA and Bonferroni's multiple comparisons test.

C57BL/6 (Th1-biased)

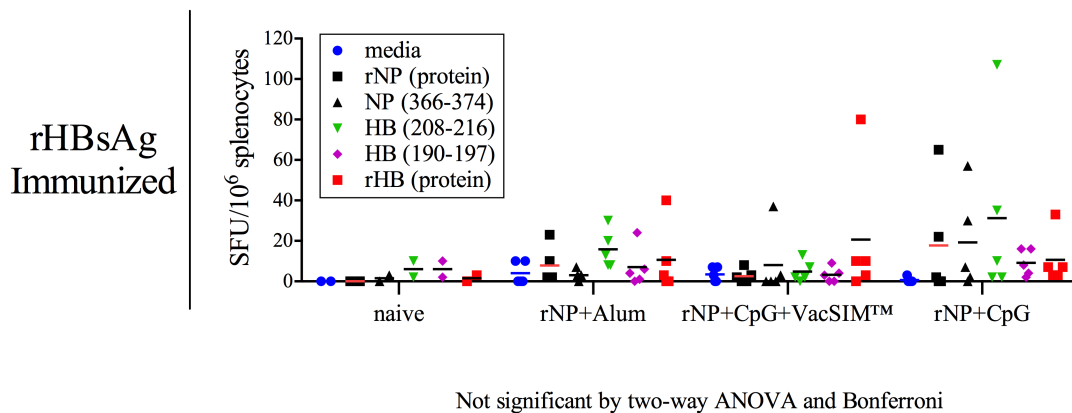
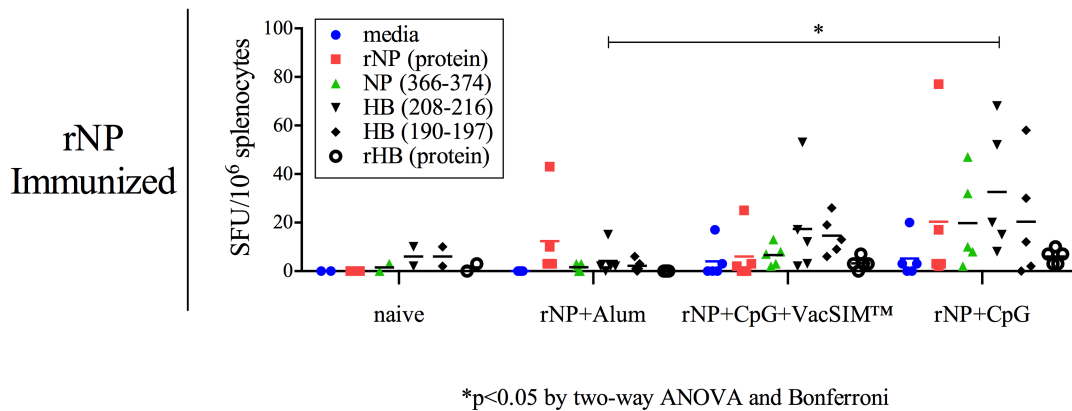


Figure B.13: IFN- γ specific ELISpot results from spleens of Th1-biased immunized mice. C57BL/6 mice were vaccinated (s.c.) 2x, 3-weeks apart with a 2 alternative protein subunit antigens (rNP or rHBsAg) \pm Alum, CpG and VacSIM[™]. Six weeks after their 1st vaccination, spleens were harvested and processed. Splenocytes were re-stimulated with either rNP/rHBsAg protein or peptides for 20-hours at 37^o (Protocols in Appendix D). Splenocytes were also re-stimulated with ConA as a positive re-stimulation control (not plotted). Table A.2 contains specific peptide information. Statistics were calculated using two-way ANOVA and Bonferroni's multiple comparisons test.

APPENDIX C

CHAPTER 4 SUPPLEMENTARY DATA

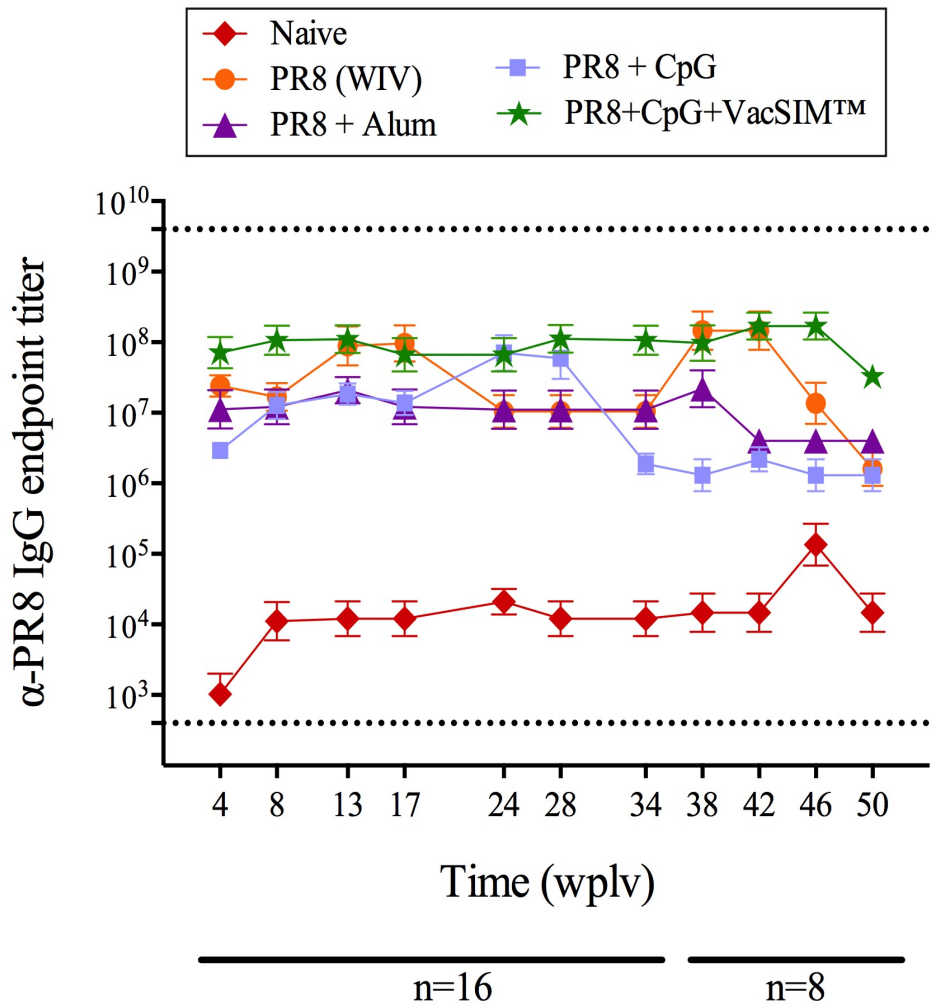


Figure C.1: PR8-specific IgG endpoint titers at various time points out to 50 wpv. Sera was collected from C57BL/6 mice prior to vaccinating and again at 8, 13, 17, 24, 28, 34, 38, 42, 46, and 50 weeks post-vaccination and PR8 (WIV) specific endpoint titers were determined by indirect ELISA. The mean values for each vaccine group at each time point following vaccination have been plotted with error bars (SD).

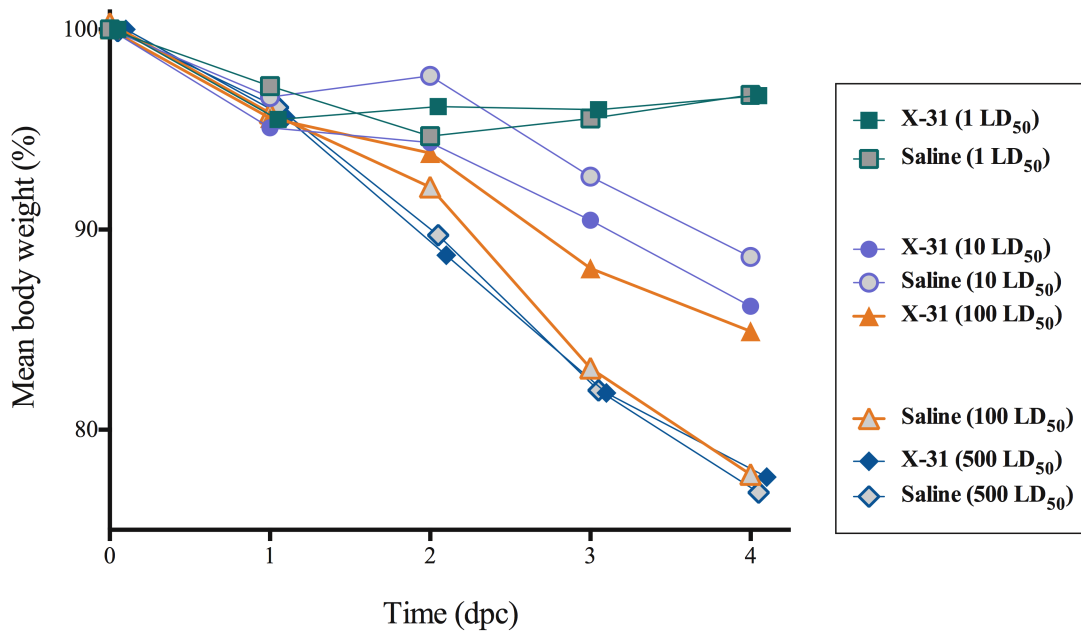


Figure C.2: Mean weight change at various heterologous (PR8) challenge doses. Pilot experiment in C57BL/6 mice (n=3) was used to select a PR8 challenge dose that would be lethal to unvaccinated and survivable (out to 4dpc) for mice immunized (s.c.) with 15ug of whole-inactivated X:31 in saline.

Table C.1: B cell epitopes on influenza hemagglutinin. Epitope information was obtained from the Immune Epitope Database (IEDB) version 3.0 (www.iedb.org). The italicized number within parentheses indicates the starting/ending position, specific to the alignment in Figure C.3.

Epitope ID	Antigen ID	Organism Name/ID	Epitope	Starting Position	Ending Position
178109	GI:223950 973	Influenza virus (B/Brisbane/60/2008), 604436	T52, K53, S54, H55, F56, K67, N74, T76, D77, H100		
225737	GI:223950 978	Influenza virus (B/Brisbane/60/2008), 604436	GKIPSARVSILH EVRPVTS	183 (199)	199 (215)
24012	GI:122884	Influenza A virus, 11320	HHPSTNQEQTSL YVQAS	154 (170)	168 (184)
570	GI:106907 813	Influenza virus (A/X:31(H3N2)), 132504	ACKRGP GSGFF SRLN	172 (188)	185 (201)

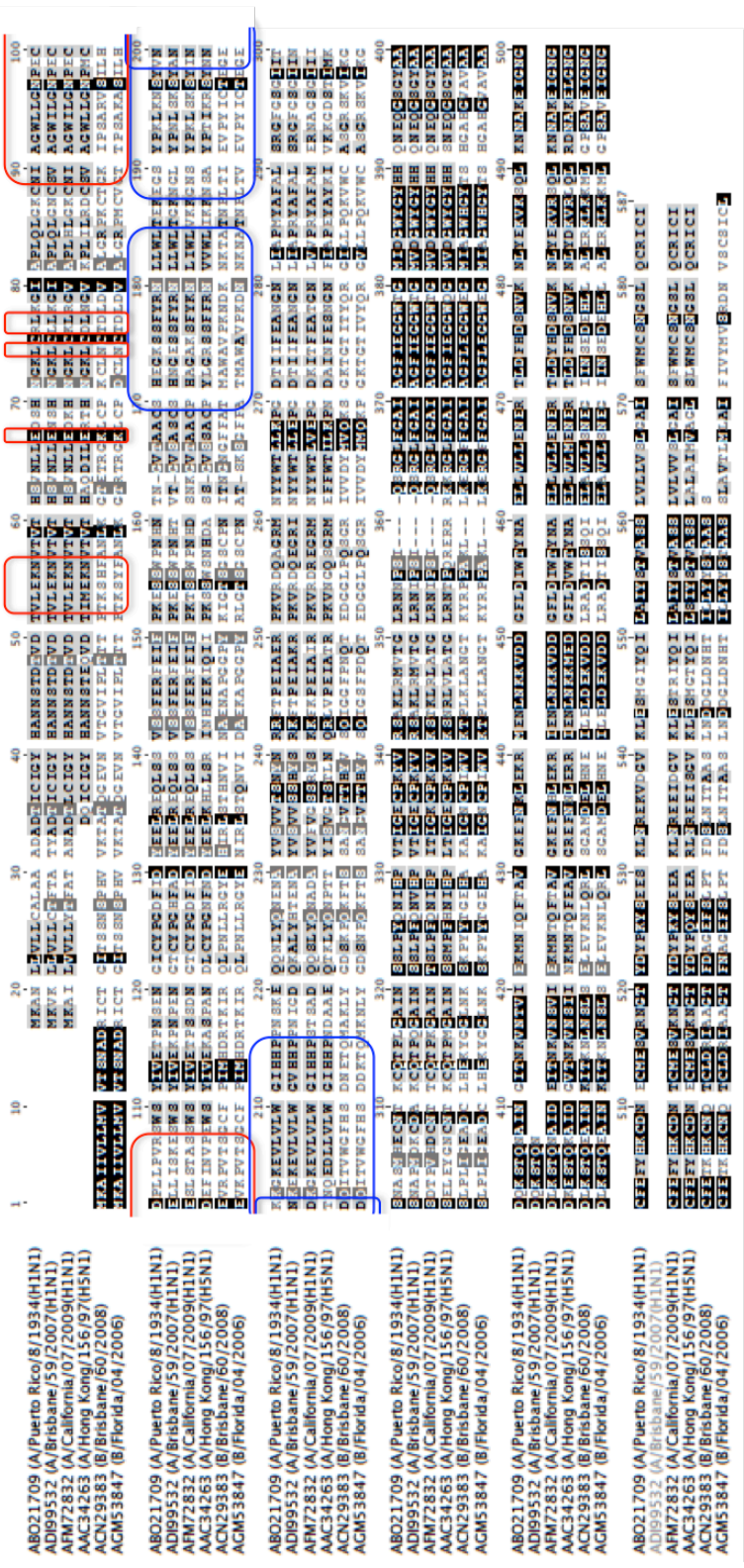


Figure C.3: B cell epitopes from hemagglutinin of various influenza viruses. B cell epitopes of either influenza A (blue) or influenza B viruses (red) have been marked via color-distinguishing boxes. Liner and discontinuous B cell epitopes included in this figure have been defined in Table C.1 and were obtained from the Immune Epitope Database (IEDB) version 3.0 (www.iedb.org). Hemagglutinin sequence alignment was generated using Geneious® version 8.1.4.

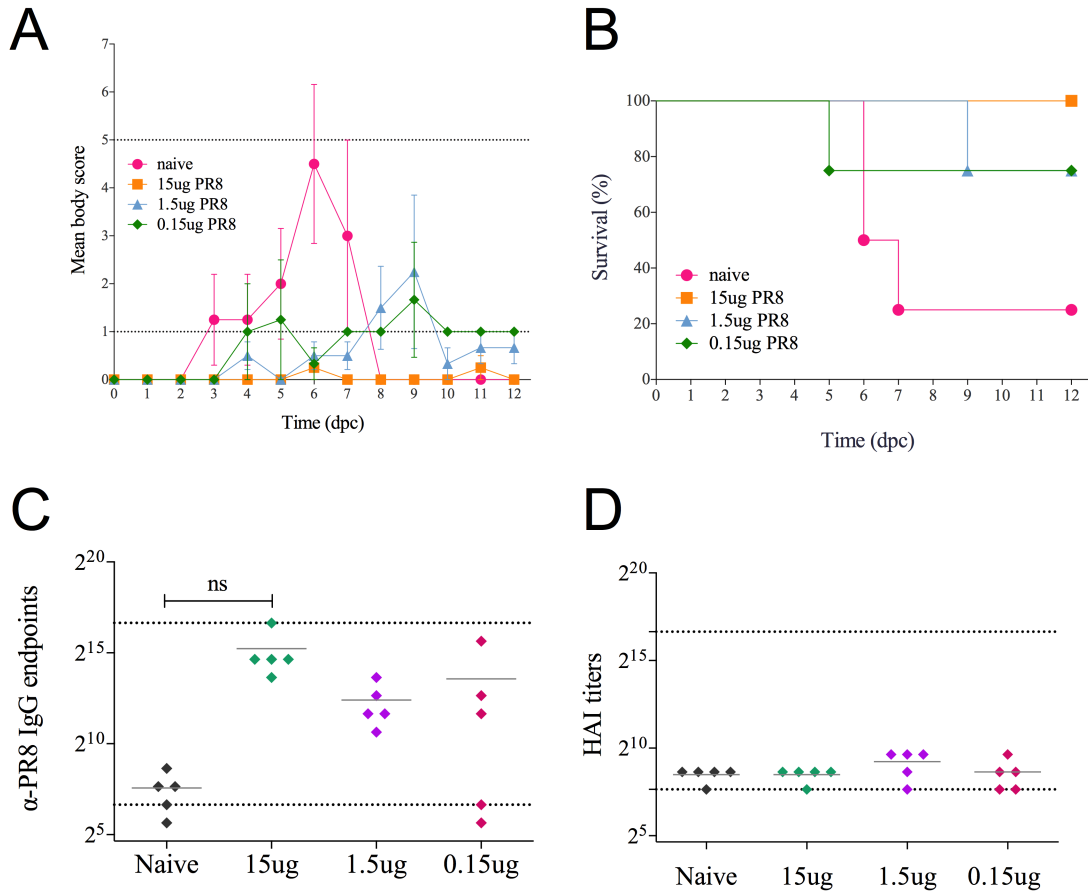


Figure C.4: Dose-sparing whole-inactivated virus in saline. C57BL/6 mice were utilized to establish a low-dose vaccine baseline (WIV (influenza A/PR/8/1934)) prior to incorporating additional vaccine delivery and/or adjuvanting agents. In this pilot study vaccine-induced immune responses (C-D) as well as protection following lethal challenge (A-B) was investigated.

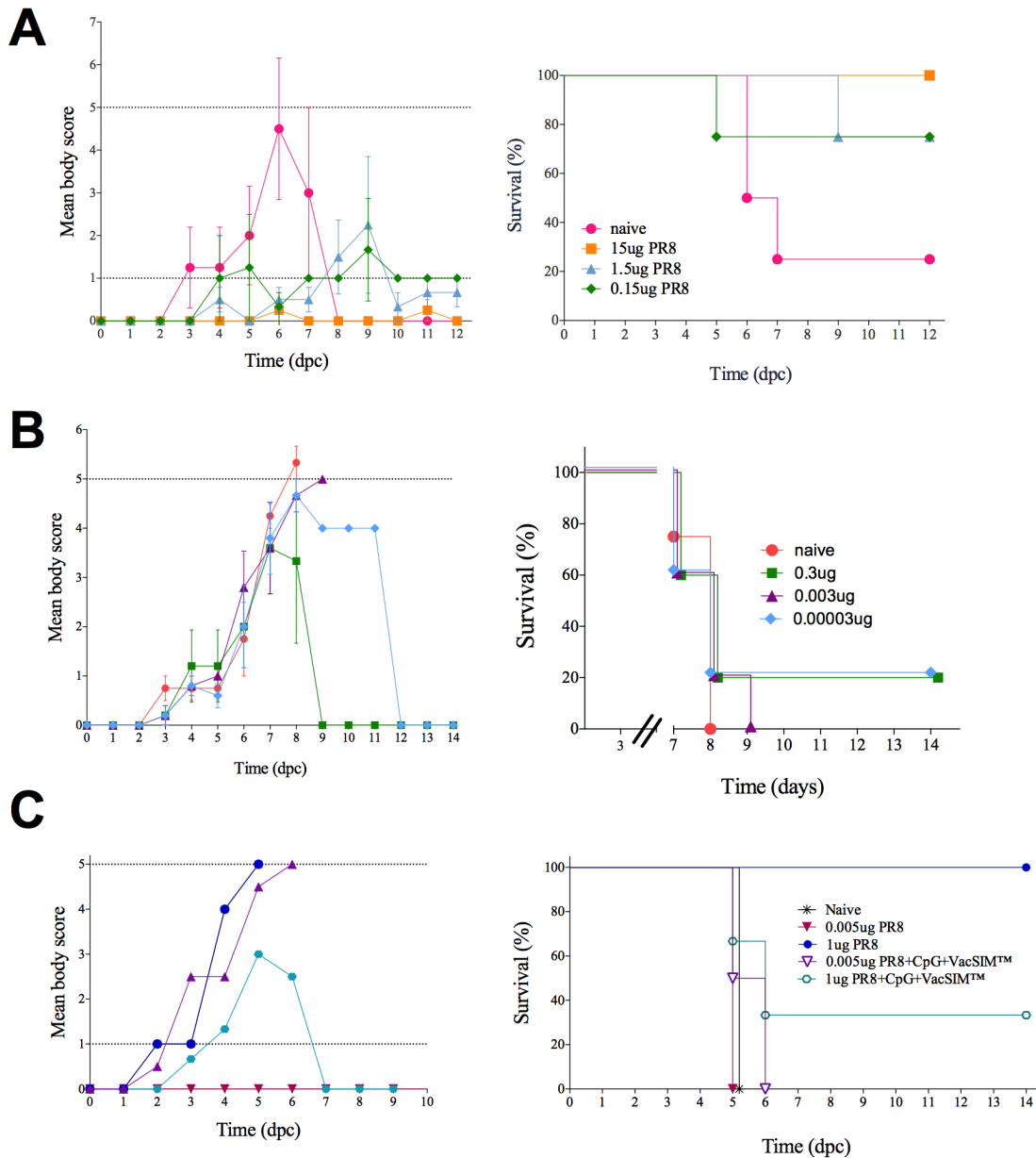


Figure C.5: Investigating low-dose vaccine-induced protection. All mice (C57BL/6) were challenged with 100 LD₅₀ of live PR8 at 5 wpv (C), 6 wpv (B) or 7 wpv (A). Immunized mice were given varying dose of PR8 (WIV) in saline (A-B) or in combination with CpG and delivered in VacSIM™.

APPENDIX D

CHAPTER 5 SUPPLEMENTARY DATA

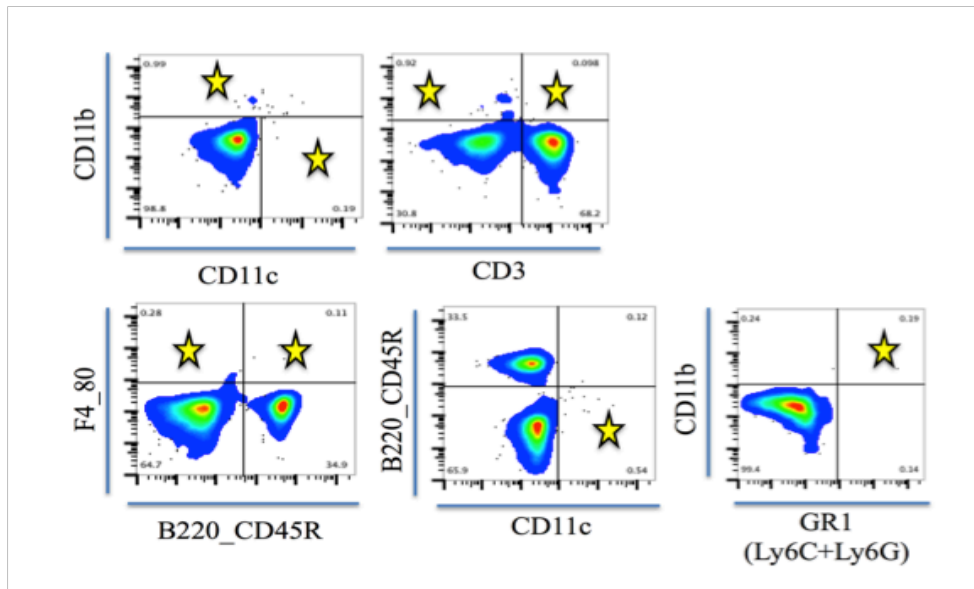


Figure D.1: Gating strategy for enumerating antigen presenting cells (APCs) in the draining and non-draining lymph nodes following immunization. An “or” gate was used to determine relative APC populations in the lymph nodes at 12, 24 or 36 hours post vaccination (h_{pv}). Cell population phenotypes included B220⁻CD45R⁻ and CD11b⁺, GR1⁺ and CD11b⁺, B220⁻CD45R⁻ and F4_80⁺. The representative flow panels were derived from an axillary draining lymph node (d-LN) sample, harvested at 12h_{pv} from a mouse receiving PR8+CpG delivered in saline.

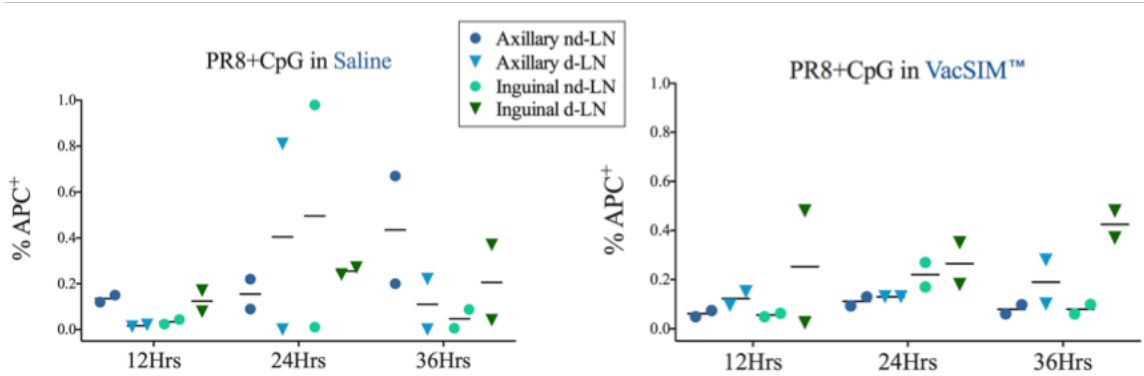


Figure D.2: Vaccine delivered in VacSIM™ may delay accumulation of antigen presenting cells (APCs) in the draining lymph nodes (d-LNs) versus the non-draining lymph nodes (nd-LNs), when compared to delivery in saline. APC⁺ populations were defined as live cells with any of following phenotypes; B220⁻CD45⁻ and CD11b⁺, GR1⁺ and CD11b⁺, B220⁻CD45⁻ and F4_80⁺ (Figure 5.3). The relative proportion of APC⁺ cells were determined by flow cytometry, using stained cells harvested from the d-LN or dn-LNs at 12, 24 or 36 hpv.

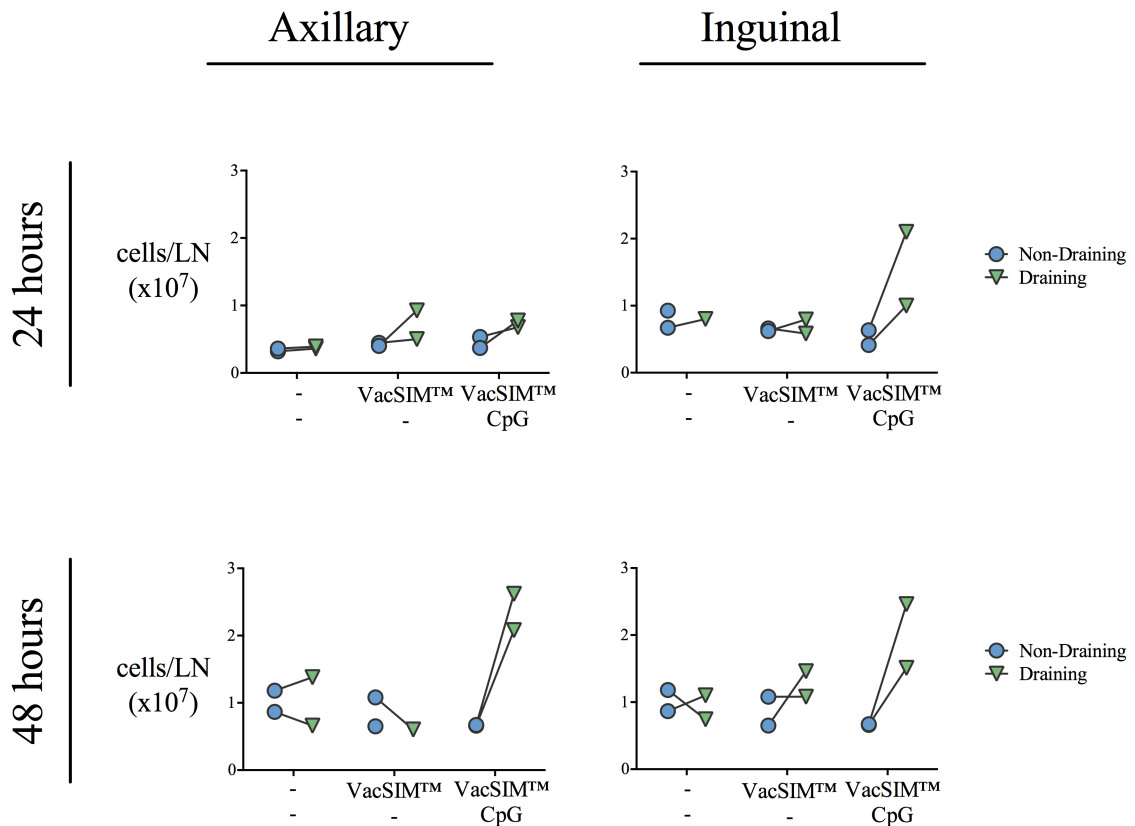


Figure D.3: In the absence of antigen VacSIM™ does not induce localized cell recruitment. Pilot study (n=2) in C57BL/6 mice vaccinated (s.c.) with VacSIM™ ± CpG. Total cell counts determined from draining and non-draining lymph nodes at 24 and 48 hours post vaccinations (hpv).

24Hpv

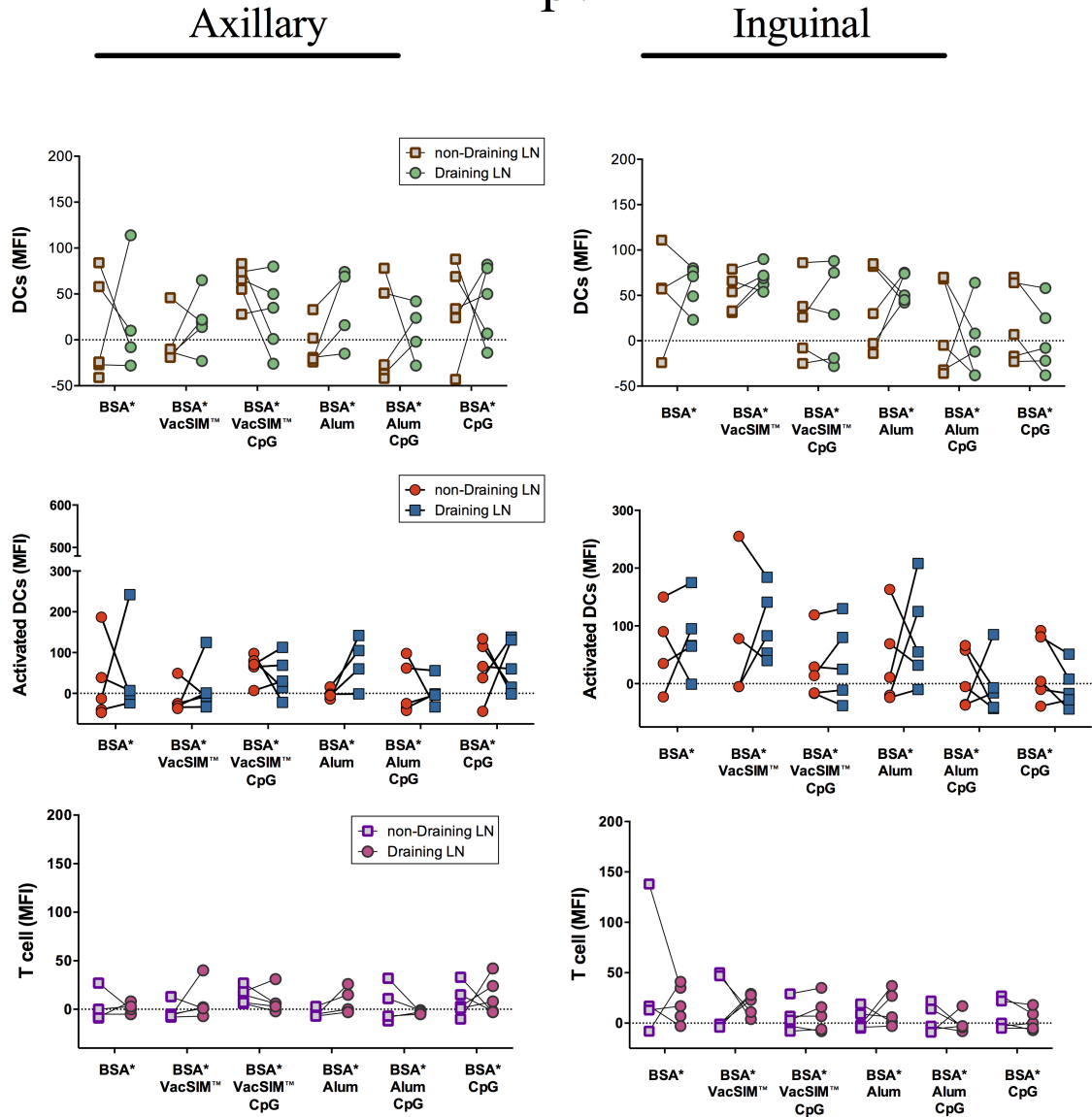


Figure D.4: Mean fluorescent intensity (MFI) of dendritic cells (DCs) and T cells in the non-draining/draining axillary and inguinal lymph nodes at 24 hpv (n=5 per time point). Corresponds with experiment described in Chapter 5 (subsection 5.2.3).

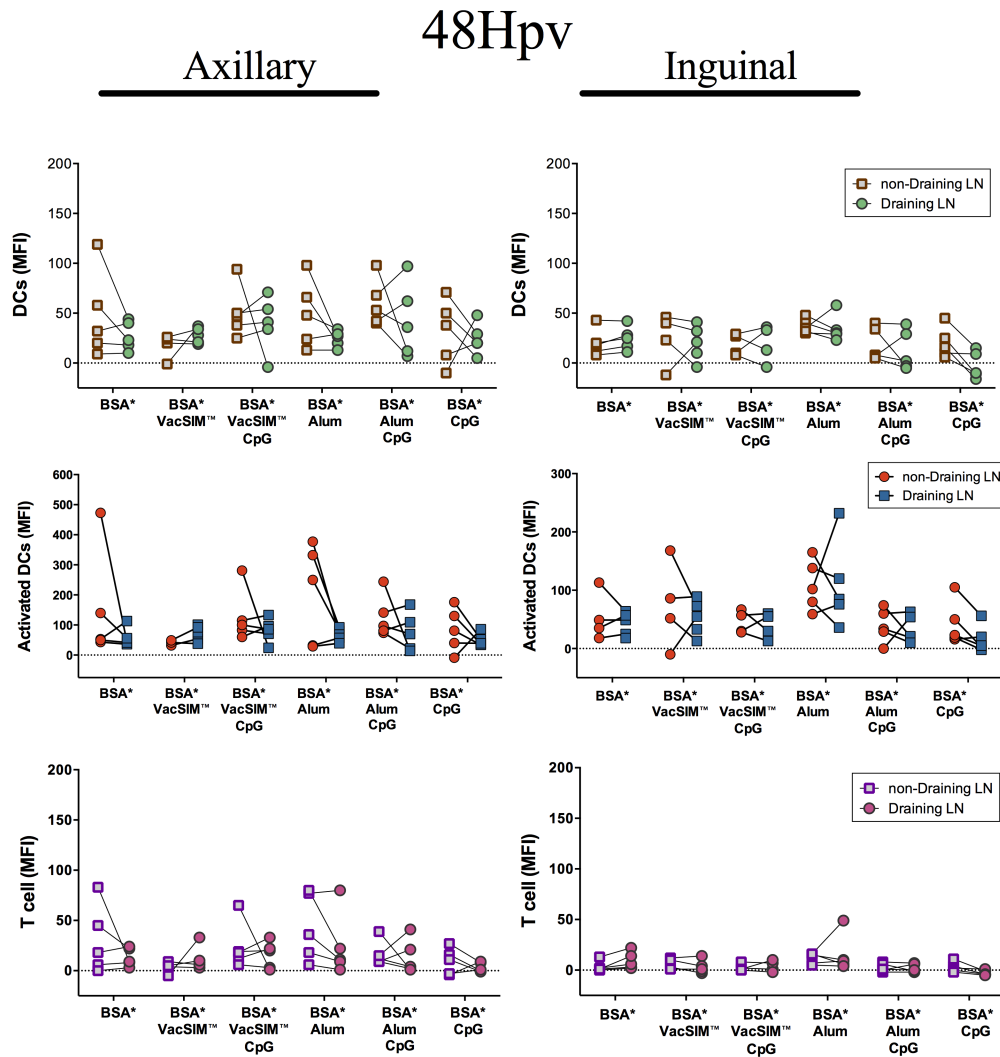


Figure D.5: Mean fluorescent intensity (MFI) of dendritic cells (DCs) and T cells in the non-draining/draining axillary and inguinal lymph nodes at 48 hpv (n=5 per time point). Corresponds with experiment described in Chapter 5 (subsection 5.2.3).

Phenotype Comparisons Pre- and Post-Challenge in Draining Lymph Nodes of Mice Vaccinated with CpG Adjuvanted PR8 (WIV) in VacSIM™.

Thus far, total cells and population frequency have been evaluated in the draining and/or non-draining lymph nodes, either at 1 and 2 days post-vaccination or 2 days post-viral challenge, across vaccine groups (Figures 5.3-5.7 and Appendix Figures C.2-C.7). The following study compares the specific cell totals and population frequencies of a single vaccine group, 4 wpv and either 1-day prior to challenge or 2-days following challenge (Figure 5.7). Two cohorts of mice (n=4-5) were vaccinated (s.c.) 4 weeks earlier with PR8+CPG in VacSIM™. Draining and non-draining lymph nodes from individual mice were pooled and processed and cells were stained as described in subsection 5.2.4 with one exception, which was the exclusion of cell marker NK1.1. The 6-different immune cell phenotypes (Table 5.2) were evaluated at day -1 and 2-days post challenge. Results from the population counts (Figure C.6) and relative frequencies (Figure C.7) indicated that following challenge all 6 populations maintained similar mean values, although individuals were spread across a tighter range. Small variations in specific cell frequency, although not statistically significant, were visible following challenge in all populations except in the CD3+,CD8+, CD44+ , NP-tet- and other (not CD3+/ CD4+/CD8+/NK1.1+) cell populations (Figure C.7).

PR8+CpG in VacSIM™

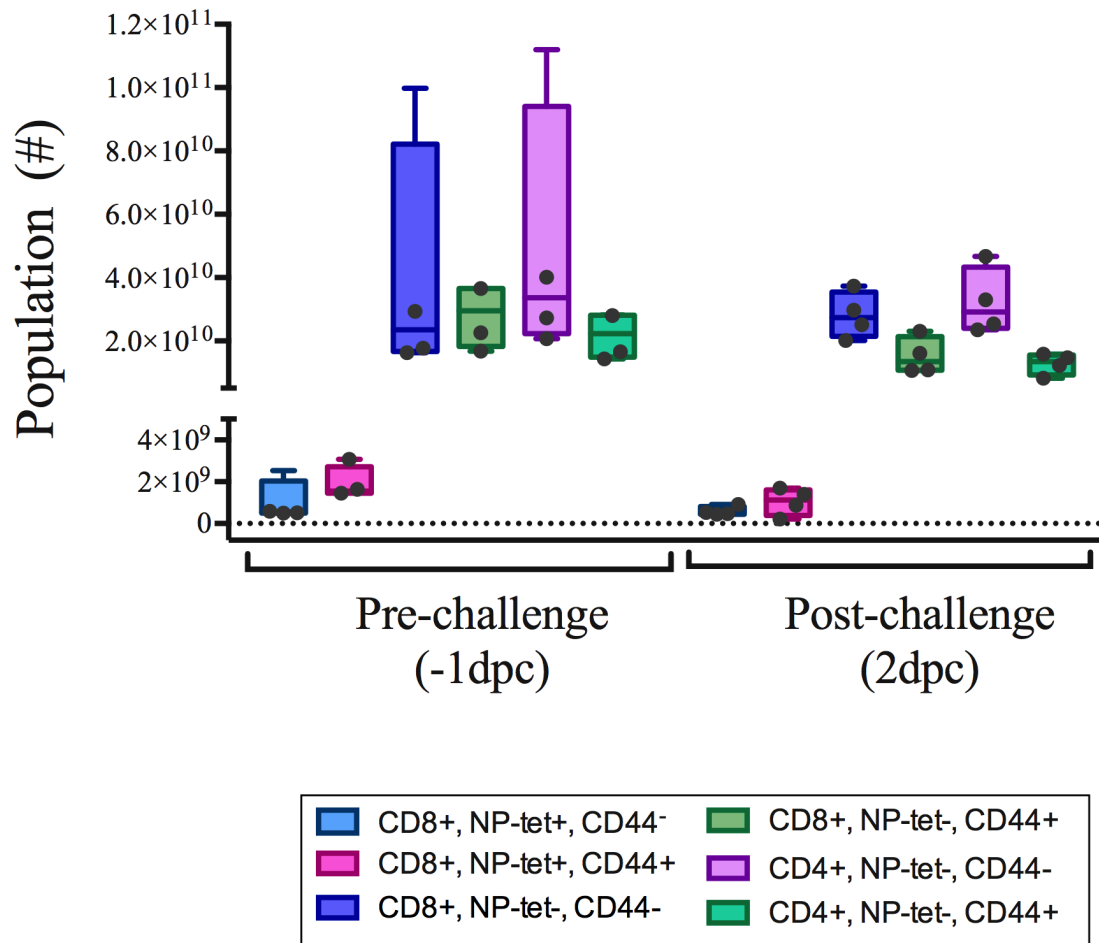


Figure D.6: Cell counts from lymph nodes of immunized mice pre/post-challenge. Mice were vaccinated (s.c.) with whole-inactivated PR8 and CpG in VacSIM™ (prime-only). At 5 wpv, 1 of 2 identically treated cohorts of mice was challenged with 1,000LD₅₀ PR8 virus (i.n.). This data was generated according with the methods detailed in chapter 5 and Figure 5.7.

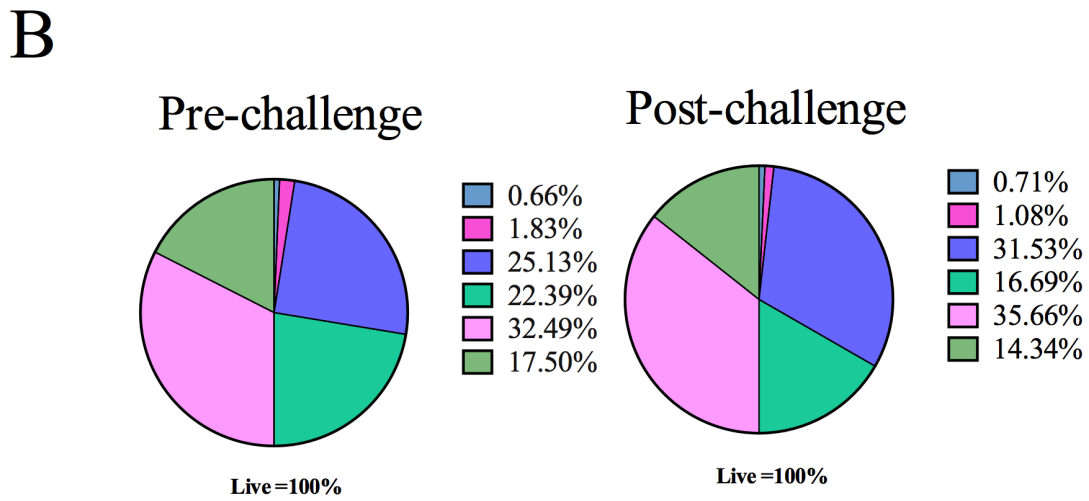
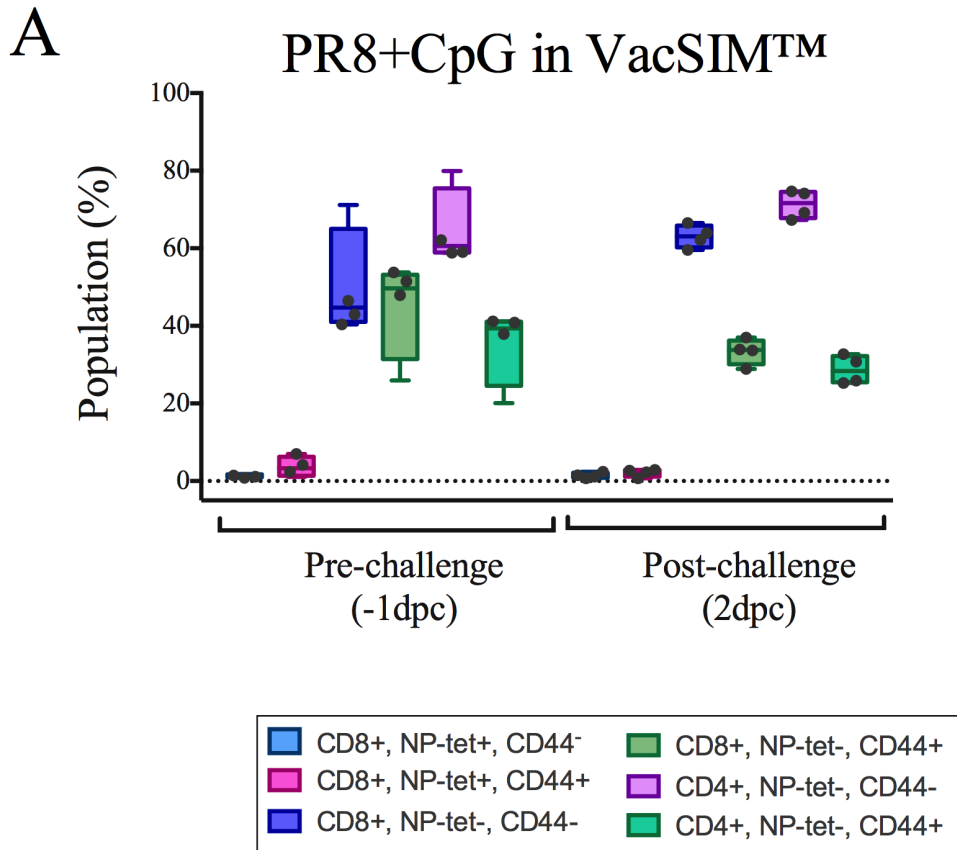


Figure D.7: Immune cell frequencies in lymph nodes of immunized mice pre/post-challenge. Mice were vaccinated (s.c.) with whole-inactivated PR8 and CpG in VacSIM™ (prime-only). At 5 wpv, 1 of 2 identically treated cohorts of mice was challenged with 1,000LD₅₀ PR8 virus (i.n.). This data was generated according with the methods detailed in chapter 5 and Figure 5.7.

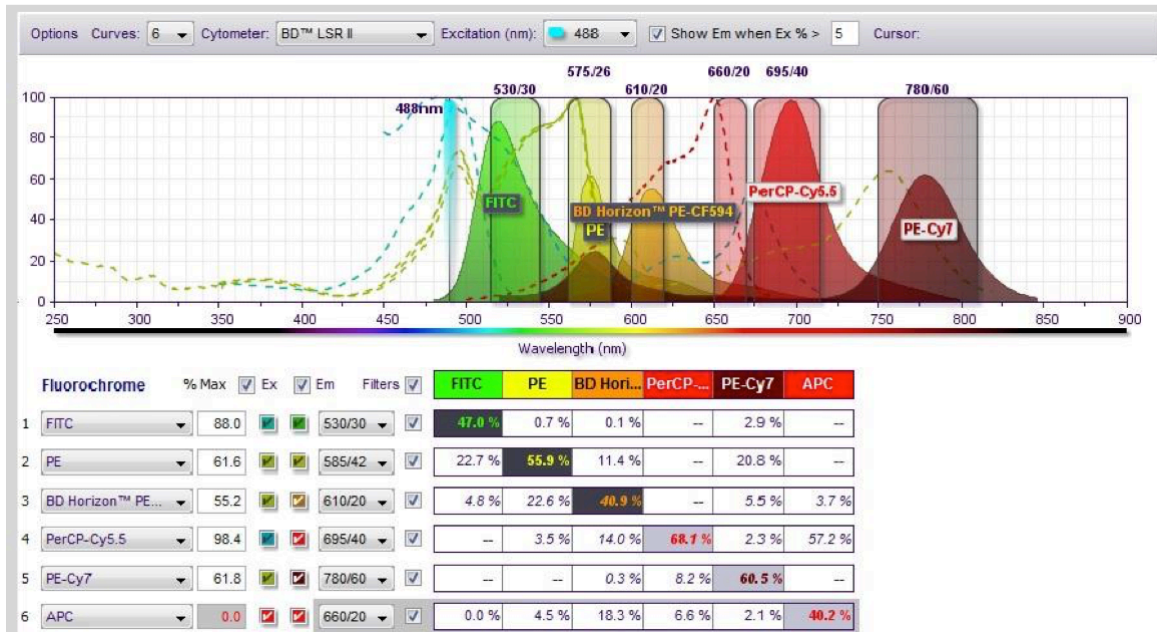


Figure D.8: Spectral overlap using BD's fluorescence spectral viewer. Corresponding to Figure 5.7, C4-C5.

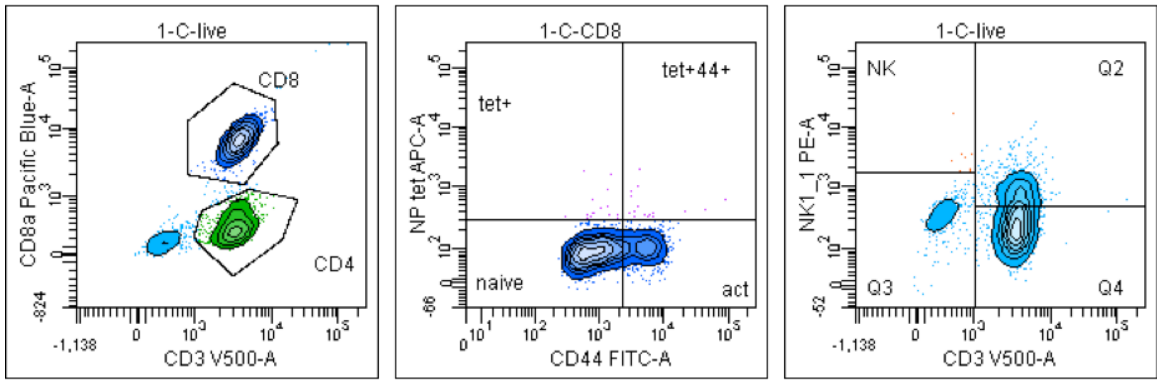


Figure D.9: Cell population gates corresponding to Figures 5.7, C4-C5.

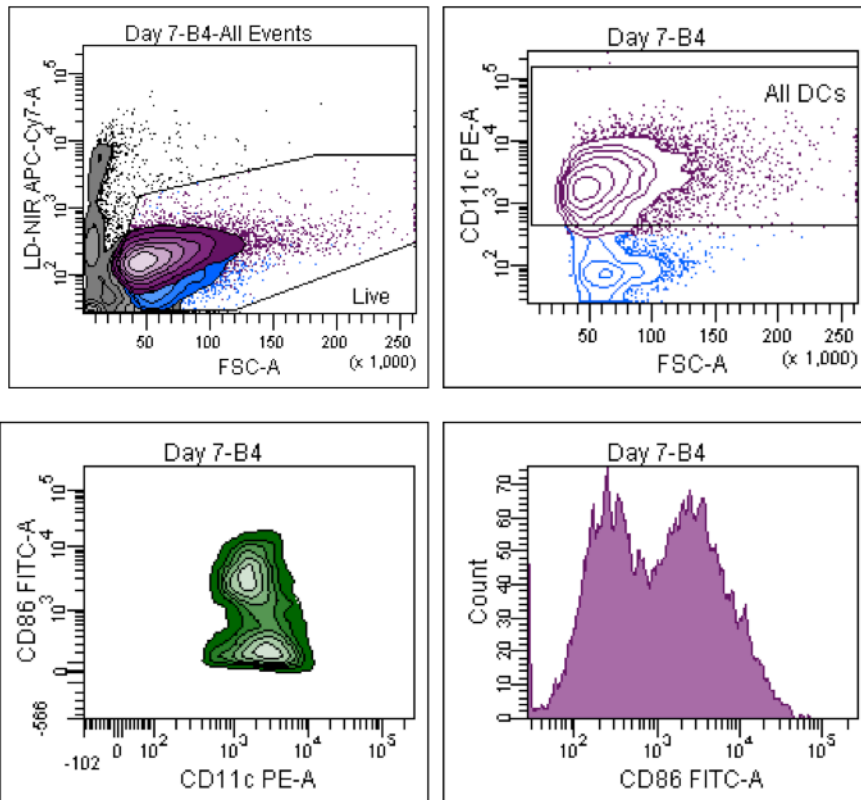


Figure D.10: Cell population gates corresponding to Figure 5.1.